2012 KRIBB Article Abstracts

First or corresponding articles indexed in SCIE, Scopus, and PubMed

2013. 5.

한국생명공학연구원
Korea Research Institute of Bioscience and Biotechnology

2012 KRIBB Article Abstracts

First or corresponding articles indexed in SCIE, Scopus, and PubMed

2013. 5.

한국생명공학연구원
Korea Research Institute of Bioscience and Biotechnology


KRIBB
www.kribb.re.kr

Contents

2012
KRIBB Article Abstracts : First or corresponding articles indexed in SCIE, Scopus, and PubMed

Bioconvergence Research Institute

- BioNanotechnology Research Center
- Super-Bacteria Research Center
- Biochemicals & Synthetic Biology Research Center

Korea Research Institute of Bioscience and Biotechnology

Article 1

Small-interfering RNA (siRNA)-based functional micro- and nanostructures for efficient and selective gene silencing

Acc Chem Res. 45(7):1014-25.

Lee SH, Chung BH, Park TG, Nam YS, Mok H*

*Co-corresponding:
BioNanotechnology Research Center

Because of RNA's ability to encode structure and functional information, researchers have fabricated diverse geometric structures from this polymer at the micro- and nanoscale. With their tunable structures, rigidity, and biocompatibility, novel two-dimensional and three-dimensional RNA structures can serve as a fundamental platform for biomedical applications, including engineered tissues, biosensors, and drug delivery vehicles. The discovery of the potential of small-interfering RNA (siRNA) has underscored the applications of RNA-based micro- and nanostructures in medicine. Small-interfering RNA (siRNA), synthetic double-stranded RNA consisting of approximately 21 base pairs, suppresses problematic target genes in a sequence-specific manner via inherent RNA interference (RNAi) processing. As a result, siRNA offers a potential strategy for treatment of many human diseases. However, due to inefficient delivery to cells and off-target effects, the clinical application of therapeutic siRNA has been very challenging. To address these issues, researchers have studied a variety of nanocarrier systems for siRNA delivery. In this Account, we describe several strategies for efficient siRNA delivery and selective gene silencing. We took advantage of facile chemical conjugation and complementary hybridization to design novel siRNA-based micro- and nanostructures. Using chemical crosslinkers and hydrophobic/hydrophilic polymers at the end of siRNA, we produced various RNA-based structures, including siRNA block copolymers, micelles, linear siRNA homopolymers, and microhydrogels. Because of their increased charge density and flexibility compared with conventional siRNA, these micro- and nanostructures can form polyelectrolyte complexes with poorly charged and biocompatible cationic carriers that are both more condensed and more homogenous than the complexes formed in other carrier systems. In addition, the fabricated siRNA-based structures are linked by cleavable disulfide bonds for facile generation of original siRNA in the cytosol and for target-specific gene silencing. These newly developed siRNA-based structures greatly enhance intracellular uptake and gene silencing both *in vitro* and *in vivo*, making them promising biomaterials for siRNA therapeutics.
PMID:22413937

Keywords : Biomaterial; Gene silencing; Nanostructure; RNAi processing; siRNA; Small-interfering RNA

Article 2

Color-tunable photoluminescent fullerene nanoparticles

Adv Mater. 24(15):1999-2003.

Jeong J, Jung J, Choi M, Kim JW, Chung SJ, Lim S, Lee H, Chung BH*

*Corresponding: chungbh@kribb.re.kr
BioNanotechnology Research Center

Highly water-soluble and color-tunable photoluminescent fullerene nanoparticles are synthesized by using tetraethylene glycol (TEG) and lithium hydroxide as a catalyst. The maximum PL emission changes depend on the contents of the remaining π-conjugation in oxidized C_{60}, which is partially covalently conjugated with TEG. The PL behavior is attributed to an electronic transition change due to the distortion of symmetrical C_{60}.
PMID: 22431377

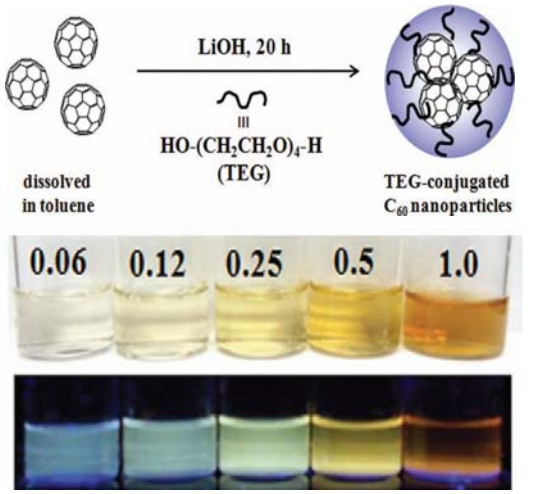

C_{60} concentration [mg/mL]	C=C-C [%] (284.05 eV)	C-O [%] (285.3 eV)	C=O [%] (287.7 eV)
0.06	40.05	41.15	17.59
0.12	45.19	40.89	13.83
0.25	49.93	34.79	15.23
0.50	49.22	34.87	15.91
1.00	55.16	30.56	14.28

Keywords : Color-tunable; Lithium hydroxide; Nanoparticle; Photoluminescent fullerene; Tetraethylene glycol

Article 3

Gold patterned biochips for on-chip immuno-MALDI-TOF MS: SPR imaging coupled multi-protein MS analysis

Analyst. 137(2):386-92.

Kim YE, Yi SY, Lee CS, Jung Y, Chung BH*

*Co-corresponding: chungbh@kribb.re.kr
BioNanotechnology Research Center

Matrix-assisted laser desorption/ionization time-of-flight mass spectrometry (MALDI-TOF-MS) analysis of immuno-captured target protein efficiently complements conventional immunoassays by offering rich molecular information such as protein isoforms or modifications. Direct immobilization of antibodies on MALDI solid support enables both target enrichment and MS analysis on the same plate, allowing simplified and potentially multiplexing protein MS analysis. Reliable on-chip immuno-MALDI-TOF MS for multiple biomarkers requires successful adaptation of antibody array biochips, which also must accommodate consistent reaction conditions on antibody arrays during immuno-capture and MS analysis. Here we developed a facile fabrication process of versatile antibody array biochips for reliable on-chip MALDI-TOF-MS analysis of multiple immuno-captured proteins. Hydrophilic gold arrays surrounded by super-hydrophobic surfaces were formed on a gold patterned biochip via spontaneous chemical or protein layer deposition. From antibody immobilization to MALDI matrix treatment, this hydrophilic/phobic pattern allowed highly consistent surface reactions on each gold spot. Various antibodies were immobilized on these gold spots both by covalent coupling or protein G binding. Four different protein markers were successfully analyzed on the present immuno-MALDI biochip from complex protein mixtures including serum samples. Tryptic digests of captured PSA protein were also effectively detected by on-chip MALDI-TOF-MS. Moreover, the present MALDI biochip can be directly applied to the SPR imaging system, by which antibody and subsequent antigen immobilization were successfully monitored.

PMID: 22087467

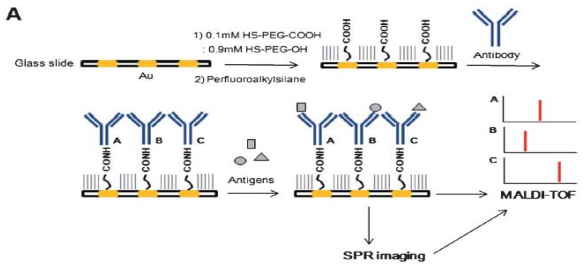

Keywords : Antibody; Biochip; Biomarker; MALDI-TOF-MS; Protein MS analysis; SPR imaging

Article 4

Hand-held syringe as a portable plastic pump for on-chip continuous-flow PCR: miniaturization of sample injection device

Analyst. 137(4):983-90.

Wu W*, Trinh KT, Lee NY

*First:
BioNanotechnology Research Center

On-chip continuous-flow polymerase chain reactions (PCRs) generally require peripheral apparatus such as a pump for injecting a sample liquid into the fluidic channel. This makes the overall instrumentation bulky, limiting integration. In this study, we propose a new scheme for injecting a sample employing a hand-held syringe as a portable plastic pump, and apply it to an on-chip continuous-flow PCR. In the proposed injection scheme, sample actuation was realized inside a highly gas-permeable and blunt-ended fluidic conduit connected to a hand-held plastic syringe filled with compressed air. In this system, the degree of air diffusion *via* the walls of the gas-permeable conduit becomes greater in the anterior (closer to the outlet) end of the sample plug than the posterior (closer to the inlet) end, because a relatively larger quantity of air is retained inside the syringe at the posterior end of the sample plug. This creates a pressure gradient at the inlet and outlet of the fluidic conduit and propels the sample forward toward the outlet. Preliminary experiments were performed for the quantitative analyses and evaluation of the proposed sample injection scheme using gas-permeable silicone tubes. As practical applications, a 230 bp gene fragment from a plasmid vector and the first 282 bp of the interferon-beta (IFN-β) promoter from a human genomic DNA were successfully amplified on a microdevice coupled with a hand-held syringe as a portable sample actuation device, greatly enhancing device portability for on-site analyses.

PMID: 22186958

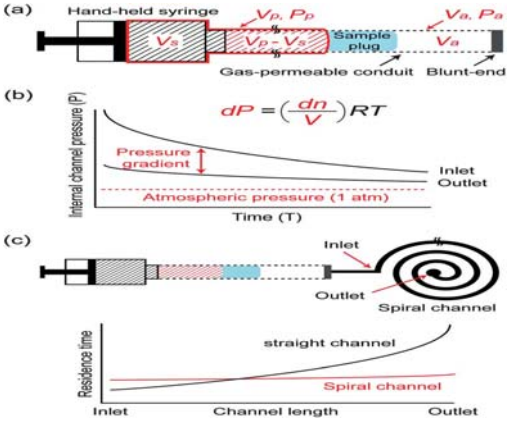

Keywords : Hand-held syringe; Microdevice; PCR; Portable plastic pump; Sample actuation device

Article 5

Active inclusion body formation using *Paenibacillus polymyxa* PoxB as a fusion partner in *Escherichia coli*

Anal Biochem. 426(1):63-5.

Park SY, Park SH, Choi SK*

*Corresponding: sookeun@kribb.re.kr
Super-Bacteria Research Center

Overexpression of *Paenibacillus polymyxa* PoxB in *Escherichia coli* induced the formation of inclusion bodies. An enzyme assay showed that the inclusion bodies exhibited PoxB activity, indicating that they were biologically active. Fusion of GFP and *Bacillus subtilis* AmyE to the C-terminus of the PoxB also induced the formation of biologically active aggregates when they were overexpressed in *E. coli*. Therefore, *P. polymyxa* PoxB can be used as a fusion partner to promote the formation of active inclusion bodies in *E. coli*.

PMID: 22490467

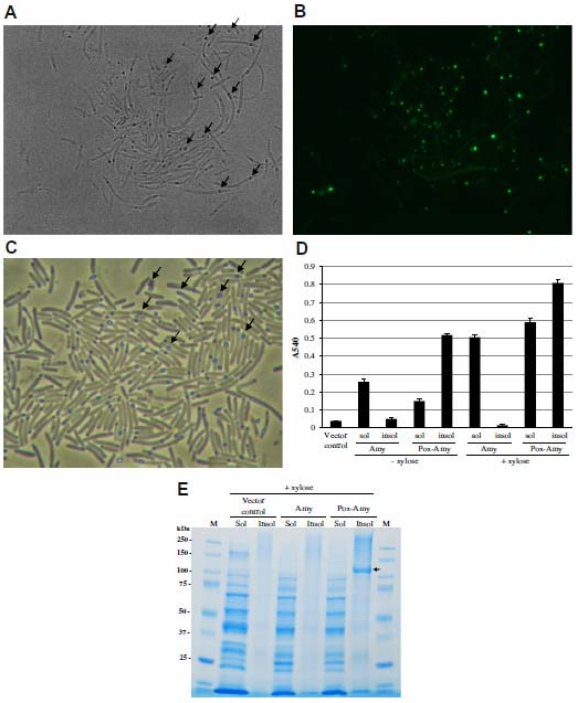

Keywords : Active inclusion body; *Paenibacillus polymyxa*; Poxb; Recombinant protein expression

Article 6

Foliar aphid feeding recruits rhizosphere bacteria and primes plant immunity against pathogenic and non-pathogenic bacteria in pepper

Ann Bot. 110(2):281-90.

Lee B, Lee S, Ryu CM*

*Corresponding: cmryu@kribb.re.kr
Super-Bacteria Research Center

BACKGROUND AND AIMS: Plants modulate defence signalling networks in response to different biotic stresses. The present study evaluated the effect of a phloem-sucking aphid on plant defence mechanisms in pepper (*Capsicum annuum*) during subsequent pathogen attacks on leaves and rhizosphere bacteria on roots.

METHODS: Plants were pretreated with aphids and/or the chemical trigger benzothiadiazol (BTH) 7 d before being challenged with two pathogenic bacteria, *Xanthomonas axonopodis* pv. *vesicatoria* (*Xav*) as a compatible pathogen and *X. axonopodis* pv. *glycines* (*Xag*) as an incompatible (non-host) pathogen.

KEY RESULTS: Disease severity was noticeably lower in aphid- and BTH + aphid-treated plants than in controls. Although treatment with BTH or aphids alone did not affect the hypersensitive response (HR) against *Xag* strain 8ra, the combination treatment had a synergistic effect on the HR. The aphid population was reduced by BTH pretreatment and by combination treatment with BTH and bacterial pathogens in a synergistic manner. Analysis of the expression of the defence-related genes *Capsicum annum pathogenesis-related gene 9* (*CaPR9*), *chitinase 2* (*CaCHI2*), *SAR8·2* and *Lipoxygenase1* (*CaLOX1*) revealed that aphid infestation resulted in the priming of the systemic defence responses against compatible and incompatible pathogens. Conversely, pre-challenge with the compatible pathogen *Xav* on pepper leaves significantly reduced aphid numbers. Aphid infestation increased the population of the beneficial *Bacillus subtilis* GB03 but reduced that of the pathogenic *Ralstonia solanacearum* SL1931. The expression of defence-related genes in the root and leaf after aphid feeding indicated that the above-ground aphid infestation elicited salicylic acid and jasmonic acid signalling throughout the whole plant.

CONCLUSIONS: The findings of this study show that aphid feeding elicits plant resistance responses and attracts beneficial bacterial populations to help the plant cope with subsequent pathogen attacks.

PMID: 22437662

Keywords : Aphid; *Capsicum annuum*; Foliar feeding; Pepper; PGPR; Plant defence; Plant resistance response; Rhizosphere bacteria; *Xanthomonas axonopodis*

Article 7

Roseovarius litoreus sp. nov., isolated from seawater of southern coast of Korean peninsula

Antonie Van Leeuwenhoek. 102(1):141-8.

Jung YT*, Park S, Yoon JH

*First:
Super-Bacteria Research Center

A gram-negative, non-flagellated and ovoid- to rod-shaped bacterial strain, designated GSW-M15^T, was isolated from seawater on the southern coast of South Korea. Strain GSW-M15^T grew optimally at 30 °C, at pH 7.0-7.5 and in the presence of 2 % (w/v) NaCl. The phylogenetic trees based on 16S rRNA gene sequences revealed that strain GSW-M15^T belonged to the genus *Roseovarius*. Strain GSW-M15^T exhibited highest 16S rRNA gene sequence similarity values (98.3 and 97.5 %) to *Roseovarius halotolerans* HJ50^T and *Roseovarius pacificus* 81-2^T and 92.8-96.2 % sequence similarity values to the type strains of the other *Roseovarius* species. Strain GSW-M15^T contained Q-10 as the predominant ubiquinone and $C_{18:1}$ ω7c and 11-methyl-$C_{18:1}$ ω7c as the major fatty acids. The major polar lipids detected in strain GSW-M15^T were phosphatidylcholine, phosphatidylglycerol, phosphatidyl-ethanolamine, one unidentified aminolipid and two unidentified lipids. The DNA G+C content of strain GSW-M15^T was 62.9 mol% and its mean DNA-DNA relatedness values with *R. halotolerans* KCTC 22224^T and *R. pacificus* LMG 24575^T were 33 and 18 %, respectively. Differential phenotypic properties of strain GSW-M15^T, together with the phylogenetic and genetic distinctiveness, demonstrated that this strain is distinguishable from other *Roseovarius* species. On the basis of the data presented here, strain GSW-M15^T (=KCTC 23897^T = CCUG 62218^T) represents a novel species of the genus *Roseovarius*, for which the name *Roseovarius litoreus* sp. nov. is proposed.
PMID: 22430766

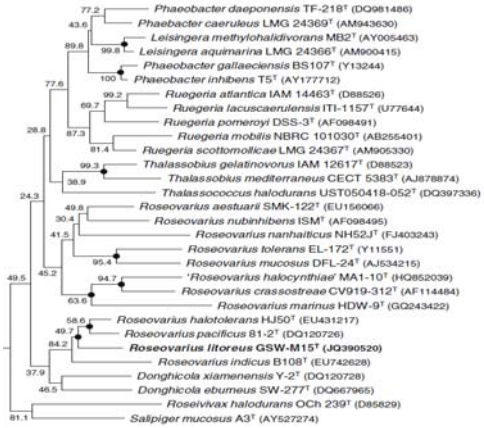

Keywords : *Alphaproteobacteria*; Novel species; *Roseovarius litoreus*; Seawater

Article 8

Efficient production of polymyxin in the surrogate host *Bacillus subtilis* by introducing a foreign *ectB* gene and disrupting the *abrB* gene

Appl Environ Microbiol. 78(12):4194-9.

Park SY, Choi SK, Kim J, Oh TK, Park SH*

*Corresponding: shpark@kribb.re.kr
Super-Bacteria Research Center

In our previous study, *Bacillus subtilis* strain BSK3S, containing a polymyxin biosynthetic gene cluster from *Paenibacillus polymyxa*, could produce polymyxin only in the presence of exogenously added L-2,4-diaminobutyric acid (Dab). The dependence of polymyxin production on exogenous Dab was removed by introducing an *ectB* gene encoding the diaminobutyrate synthase of *P. polymyxa* into BSK3S (resulting in strain BSK4). We found, by observing the complete inhibition of polymyxin synthesis when the *spo0A* gene was knocked out (strain BSK4-0A), that Spo0A is indispensable for the production of polymyxin. Interestingly, the *abrB-spo0A* double-knockout mutant, BSK4-0A-rB, and the single *abrB* mutant, BSK4-rB, showed 1.7- and 2.3-fold increases, respectively, in polymyxin production over that of BSK4. These results coincided with the transcription levels of *pmxA* in the strains observed by quantitative real-time PCR (qRT-PCR). The AbrB protein was shown to bind directly to the upstream region of *pmxA*, indicating that AbrB directly inhibits the transcription of polymyxin biosynthetic genes. The BSK4-rB strain, producing high levels of polymyxin, will be useful for the development and production of novel polymyxin derivatives.
PMID: 22467510

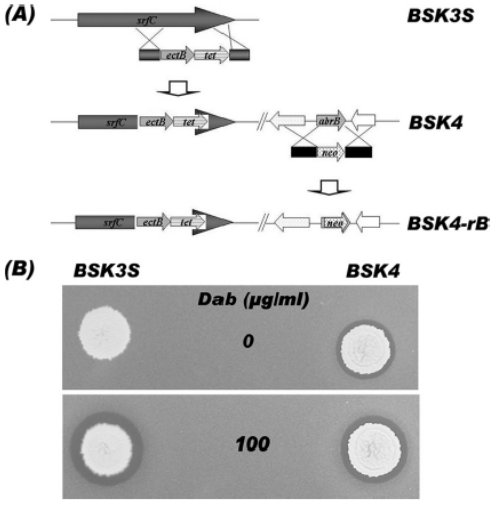

Keywords : Antibiotic-synthesis; Biosynthesis; Compatible solute ectoine; *Paenibacillus polymyxa*; Regulator abrb; Transcription

Article 9

Novel metagenome-derived, cold-adapted alkaline phospholipase with superior lipase activity as an intermediate between phospholipase and lipase

Appl Environ Microbiol. 78(14):4959-66.

Lee MH*, Oh KH, Kang CH, Kim JH, Oh TK, Ryu CM, Yoon JH

*First:
Super-Bacteria Research Center

A novel lipolytic enzyme was isolated from a metagenomic library obtained from tidal flat sediments on the Korean west coast. Its putative functional domain, designated MPlaG, showed the highest similarity to phospholipase A from *Grimontia hollisae* CIP 101886, though it was screened from an emulsified tricaprylin plate. Phylogenetic analysis showed that MPlaG is far from family I.6 lipases, including *Staphylococcus hyicus* lipase, a unique lipase which can hydrolyze phospholipids, and is more evolutionarily related to the bacterial phospholipase A_1 family. The specific activities of MPlaG against olive oil and phosphatidylcholine were determined to be 2,957 ± 144 and 1,735 ± 147 U mg^{-1}, respectively, which means that MPlaG is a lipid-preferred phospholipase. Among different synthetic esters, triglycerides, and phosphatidylcholine, purified MPlaG exhibited the highest activity toward p-nitrophenyl palmitate (C_{16}), tributyrin (C_4), and 1,2-dihexanoyl-phosphatidylcholine (C_8). Finally, MPlaG was identified as a phospholipase A_1 with lipase activity by cleavage of the *sn*-1 position of OPPC, interfacial activity, and triolein hydrolysis. These findings suggest that MPlaG is the first experimentally characterized phospholipase $A_1$with lipase activity obtained from a metagenomic library. Our study provides an opportunity to improve our insight into the evolution of lipases and phospholipases.
PMID: 22544255

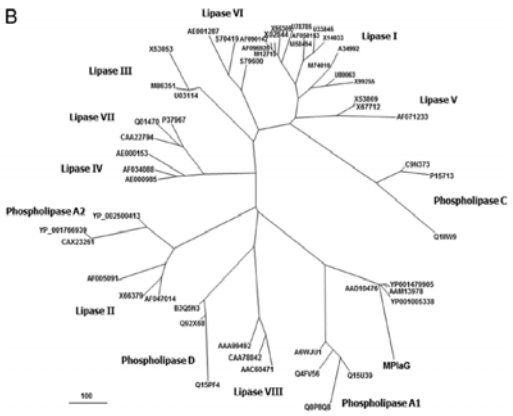

Keywords : Bacterial lipases; *Escherichia coli*; Lipolytic enzymes; Metagenomic library; Phospholipase; Staphylococcus hyicus lipase

Article 10

Development of fluorescent probes for the detection of fucosylated *N*-glycans using an *Aspergillus oryzae* lectin

Appl Microbiol Biotechnol. 93(1):251-60.

Mun JY, Lee KJ, Kim YJ, Kwon O, Kim SJ, Lee SG, Park WS, Heo WD, Oh DB*

*Corresponding: dboh@kribb.re.kr
Biochemicals & Synthetic Biology Research Center

The α(1,6)-fucose attached to the core N-glycan (core fucose) of glycoproteins has been known to play essential roles in various pathophysiological events, including oncogenesis and metastasis. *Aspergillus oryzae* lectin (AOL) encoded by the *fleA* gene has been reported to bind to N-glycans containing core fucose. The *fleA* gene encoding AOL was cloned into an *Escherichia coli* expression vector and then fused with genes of fluorescent proteins for production of fusion proteins. The resulting FleA-fluorescent fusion proteins were expressed well in *E. coli* and shown to detect glycoproteins containing *N*-glycans with core fucose by lectin blot assay. It was also shown to bind to the surface of cancer cells highly expressing the fucosyltransferase VIII for attachment of core fucose. Surprisingly, we found that FleA-fluorescent fusion proteins could be internalized into the intracellular compartment, early endosome, when applied to live cells. This internalization was shown to occur through a clathrin-mediated pathway by endocytosis inhibitor assay. Taken together, these results suggest that FleA-fluorescent fusion proteins can be employed as a valuable fluorescent probe for the detection of fucosylated glycans and/or a useful vehicle for delivery of substances to the inside of cells.
PMID: 21892597

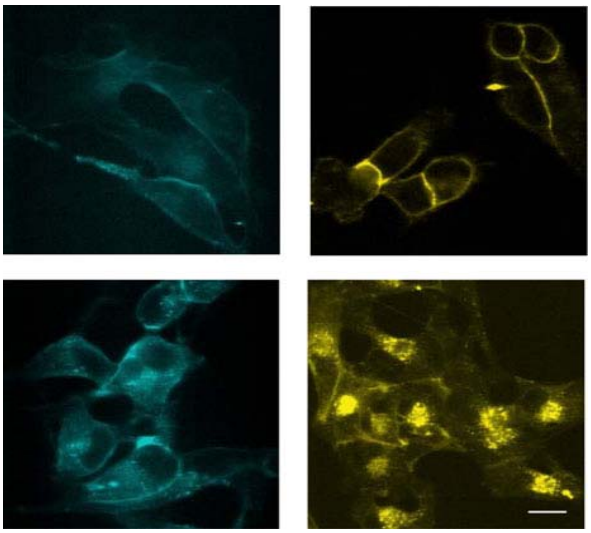

Keywords : AOL; Clathrin-mediated; Core fucose; Endocytosis; Fluorescent proteins

Article 11

Characterization of alcohol dehydrogenase 3 of the thermotolerant methylotrophic yeast *Hansenula polymorpha*

Appl Microbiol Biotechnol. 96(3):697-709.

Suwannarangsee S, Kim S, Kim OC, Oh DB, Seo JW, Kim CH, Rhee SK, Kang HA, Chulalaksananukul W, Kwon O*

*Corresponding: oskwon@kribb.re.kr
Biochemicals & Synthetic Biology Research Center

In this study, we identified and characterized mitochondrial alcohol dehydrogenase 3 from the thermotolerant methylotrophic yeast *Hansenula polymorpha* (HpADH3). The amino acid sequence of HpADH3 shares over 70% of its identity with the alcohol dehydrogenases of other yeasts and exhibits the highest similarity of 91% with the alcohol dehydrogenase 1 of *H. polymorpha*. However, unlike the cytosolic HpADH1, HpADH3 appears to be a mitochondrial enzyme, as a mitochondrial targeting extension exists at its N terminus. The recombinant HpADH3 overexpressed in *Escherichia coli* showed similar catalytic efficiencies for ethanol oxidation and acetaldehyde reduction. The HpADH3 displayed substrate specificities with clear preferences for medium chain length primary alcohols and acetaldehyde for an oxidation reaction and a reduction reaction, respectively. Although the *H. polymorpha ADH3* gene was induced by ethanol in the culture medium, both an ADH isozyme pattern analysis and an ADH activity assay indicated that HpADH3 is not the major ADH in *H. polymorpha* DL-1. Moreover, *HpADH3* deletion did not affect the cell growth on different carbon sources. However, when the *HpADH3* mutant was complemented by an *HpADH3* expression cassette fused to a strong constitutive promoter, the resulting strain produced a significantly increased amount of ethanol compared to the wild-type strain in a glucose medium. In contrast, in a xylose medium, the ethanol production was dramatically reduced in an HpADH3 overproduction strain compared to that in the wild-type strain. Taken together, our results suggest that the expression of HpADH3 would be an ideal engineering target to develop *H. polymorpha* as a substrate specific bioethanol production strain.
PMID:22249723

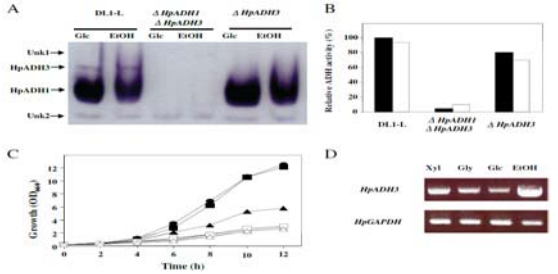

Keywords : *ADH3*; Alcohol dehydrogenase; Ethanol production; *Hansenula polymorpha*; Xylose fermentation

Article 12

Asymmetric liposome particles with highly efficient encapsulation of siRNA and without nonspecific cell penetration suitable for target-specific delivery

Biochim Biophys Acta. 1818(7):1633-41.

Mokhtarieh AA, Cheong S, Kim S, Chung BH, Lee MK*

*Corresponding: mklee@kribb.re.kr
BioNanotechnology Research Center

The discovery of siRNA has been an important step in gene therapy, but the problem of delivering siRNA to a target organ limits its use as a therapeutic drug. Liposomes can be used as a nonviral vector to deliver siRNA to target cells. In this study we developed a novel method of producing asymmetric liposome particles (ALPs) with highly efficient siRNA encapsulation. Two kinds of lipid inverted micelles were prepared for the purpose of obtaining ALPs. The inner one is composed of ionizable cationic 1,2-dioleoyl-3-dimethylammonium-propane (DODAP) and 1,2-dioleoyl-*sn*-glycero-3-phosphoethanolamine (DOPE), which entrap siRNA, and the outer one is composed of 1,2-distearoyl-sn-glycero-3-phosphocholine (DSPC), DOPE, polyethylene glycol-1,2-distearoyl-sn-glycero-3-phospha-tidylethanolamine (PEG-PE), and cholesterol. After mixing the inverted micelles, ALPs encapsulating siRNA were obtained by solvent evaporation and dialysis. This process allowed more than 90% siRNA encapsulation as well as the negatively charged surface. The ALPs protected siRNA from ribonuclease A degradation. ALPs without any surface modification elicited almost no uptake into cells, while the surface-modified ALPs with a polyarginine peptide (R12) induced nonspecific cell penetration. The conjugation of the anti-human epidermal growth factor receptor antibody (anti-EGFR) to ALPs induces an EGFR-mediated uptake into the non-small cell lung cancer cell lines but not into NIH-3T3 cells without the receptor. The siRNA encapsulated in ALPs showed the R12- or anti-EGFR-dependent target gene silencing in NCI-H322 cells. These properties of ALPs are useful for target-specific delivery of siRNA after modification of ALPs with a target-specific ligand.
PMID: 22465072

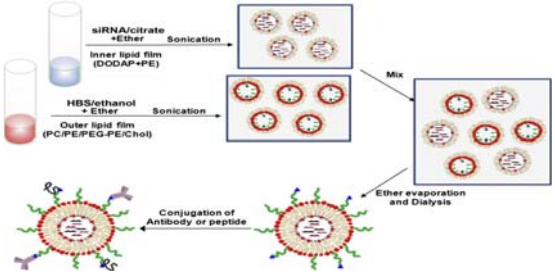

Keywords : anti-EGFR; Asymmetric liposome particles (ALPs); Cell penetration; siRNA encapsulation

Article 13

Hypoxia inhibition of camptothecin-induced apoptosis by Bax loss

Biologia. 67(3):616-21.

Park K, Woubit AS, Fermin CD, Reddy G, Habtemariam T, Chung JW, Park M, Seol D-W, Kim M*

*Corresponding: kimm@kribb.re.kr
BioNanotechnology Research Center

Tumor cell hypoxia is linked to the resistance of human solid tumors to the various anti-cancer therapies: thus, its exploitation has been considered to be a potential target for cancer treatment. Previously, we demonstrated for the first time that hypoxia inhibits apoptosis induced by tumor necrosis factor (TNF)-related apoptosis-inducing ligand (TRAIL) through blocking translocation of Bax, a pro-apoptotic protein, from the cytosol to the mitochondria. Nevertheless, the molecular mechanism coupling hypoxia to resistance for drugs, especially for anti-cancer chemotherapeutics, still remains to be elucidated. Here, we demonstrate that hypoxia attenuates camptothecin (CPT)-induced apoptosis by decreasing the protein levels of Bax, thereby leading to resistance to the drug. DNA damage after exposure to CPT resulted in an increase of p53, and a concomitant up-regulation of p21, regardless of oxygen content. Under normoxic condition, CPT induced expression of p53 and its down-stream target molecule Bax as well, in the presence of increased p21. In contrast, when preexposed to hypoxia, Bax-inducing activity of CPT was completely lost and the Bax level was even decreased, although CPT increased both p53 and p21 as observed under normoxic condition. Our data indicate that hypoxia attenuates apoptosis via Bax. Our data also suggest that hypoxia regulates tumor cell apoptosis differentially, through regulating Bax translocation or through down-regulating Bax levels, depending on death-inducing signals as shown by TRAIL- or CPT-induced apoptosis.

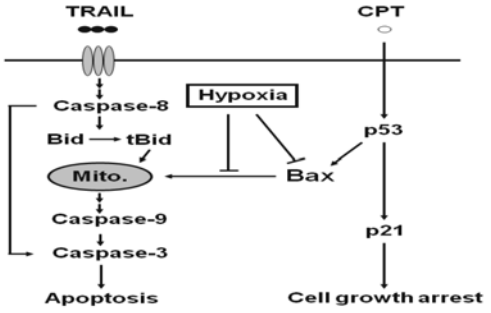

Keywords : Apoptosis; Bax; Camptothecin; Colon cancer; Hypoxia

Article 14

Chalcomoracin and moracin C, new inhibitors of *Staphylococcus aureus* enoyl-acyl carrier protein reductase from *Morus alba*

Biol Pharm Bull. 35(5):791-5.

Kim YJ, Sohn MJ, Kim WG*

*Corresponding: wgkim@kribb.re.kr
Super-Bacteria Research Center

Bacterial enoyl-acyl carrier protein (ACP) reductase has been confirmed as a novel target for antibacterial drug development. In the screening of inhibitors of *Staphylococcus aureus* enoyl-ACP reductase (FabI), we found that a methanol extract of leaves of *Morus alba* L. potently inhibited *S. aureus* FabI as well as growth of *S. aureus*. The active principles were identified as chalcomoracin and moracin C by MS and NMR analysis. Chalcomoracin and moracin C inhibited *S. aureus* FabI with IC_{50} of 5.5 and 83.8 μM, respectively. They also prevented the growth of *S. aureus* with minimum inhibitory concentration (MIC) of 4 and 32 μg/mL, respectively. Consistent with their inhibition against FabI and bacterial growth, they prevented [^{14}C]acetate incorporation into fatty acid in *S. aureus* while didn't affect protein synthesis. In this study, we reported that chalcomoracin and moracin C, potent antibacterial compounds from *Morus alba*, inhibited FabI and fatty acid synthesis.

PMID: 22687419

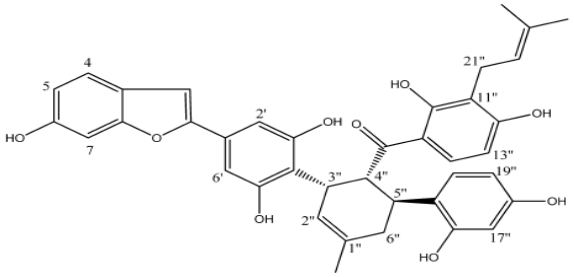

1

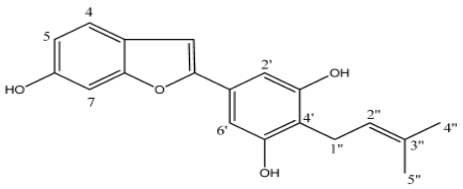

Keywords : Chalcomoracin; Enoyl-acyl carrier protein reductase; FabI; Fatty acid synthesis; Moracin C; *Staphylococcus aureus*

Article 15

Developing an antibody-binding protein cage as a molecular recognition drug modular nanoplatform

Biomaterials. 33(21):5423-30.

Kang HJ, Kang YJ, Lee YM, Shin HH, Chung SJ*, Kang S

*Co-corresponding:
BioNanotechnology Research Center

We genetically introduced the Fc-binding peptide (FcBP) into the loop of a self-assembled protein cage, ferritin, constituting four-fold symmetry at the surface to use it as a modular delivery nanoplatform. FcBP-presenting ferritin (FcBP-ferritin) formed very stable non-covalent complexes with both human and rabbit IgGs through the simple molecular recognition between the Fc region of the antibodies and the Fc-binding peptide clusters inserted onto the surface of FcBP-ferritin. This approach realized orientation-controlled display of antibodies on the surfaces of the protein cages simply by mixing without any complicated chemical conjugation. Using trastuzumab, a human anti-HER2 antibody used to treat patients with breast cancer, and a rabbit antibody to folate receptor, along with fluorescently labeled FcBP-ferritin, we demonstrated the specific binding of these complexes to breast cancer cells and folate receptor over-expressing cells, respectively, by fluorescent cell imaging. FcBP-ferritin may be potentially used as modular nanoplatforms for active targeted delivery vehicles or molecular imaging probes with a series of antibodies on demand.
PMID: 22542610

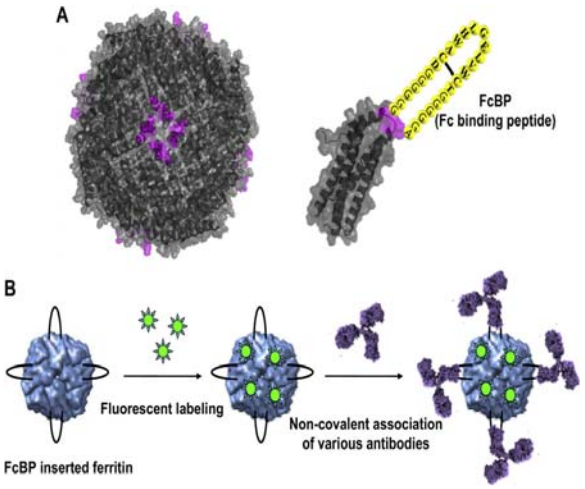

Keywords : Antibody-binding; Delivery platform; Fc-binding peptide; Molecular recognition; Protein cages

Article 16

Verrulactones A and B, new inhibitors of *Staphylococcus aureus* enoyl-ACP reductase produced by *Penicillium verruculosum* F375

Bioorg Med Chem Lett. 22(7):2503-6.

Kim N, Sohn MJ, Kim CJ, Kwon HJ, Kim WG*

*Corresponding: wgkim@kribb.re.kr
Super-Bacteria Research Center

New dimeric compounds of alternariol class, verrulactones A and B, were isolated from a culture broth of the fungal strain *Penicillium verruculosum* F375 and their structure were established by various spectral analysis. Verrulactones A and B strongly inhibited *Staphylococcus aureus* enoyl-ACP reductase with IC_{50} of 0.92 and 1.41 μM, respectively, and also showed antibacterial activity against *S. aureus* and MRSA with MICs of 8 and 16 μg/mL, respectively.
PMID: 22377515

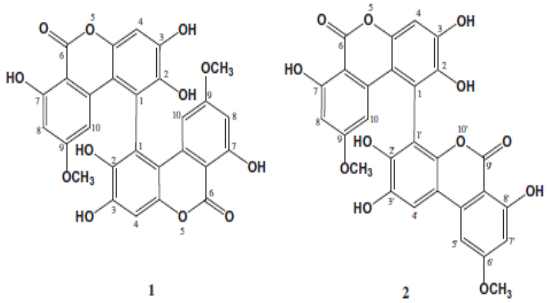

Keywords : Antibacterial activity; Enoyl-ACP reductase; FabI; Inhibitor; *Penicillium verruculosum*; *Staphylococcus aureus*; Verrulactones

Article 17

Direct lactic acid fermentation of Jerusalem artichoke tuber extract using *Lactobacillus paracasei* without acidic or enzymatic inulin hydrolysis

Bioresour Technol. 114:745-7.

Choi HY, Ryu HK, Park KM, Lee EG, Lee H, Kim SW, Choi ES*

*Corresponding: choi4162@kribb.re.kr
Biochemicals & Synthetic Biology Research Center

Lactic acid fermentation of Jerusalem artichoke tuber was performed with strains of *Lactobacillus paracasei* without acidic or enzymatic inulin hydrolysis prior to fermentation. Some strains of *L. paracasei*, notably KCTC13090 and KCTC13169, could ferment hot-water extract of Jerusalem artichoke tuber more efficiently compared with other Lactobacillus spp. such as L. casei type strain KCTC3109. The *L. paracasei* strains could utilize almost completely the fructo-oligosaccharides present in Jerusalem artichoke. Inulin-fermenting *L. paracasei* strains produced c.a. six times more lactic acid compared with L. casei KCTC3109. Direct lactic fermentation of Jerusalem artichoke tuber extract at 111.6g/L of sugar content with a supplement of 5 g/L of yeast extract by *L. paracasei* KCTC13169 in a 5L jar fermentor produced 92.5 ce:hsp sp="0.25"/>g/L of lactic acid with 16.8 g/L fructose equivalent remained unutilized in 72 h. The conversion efficiency of inulin-type sugars to lactic acid was 98% of the theoretical yield.
PMID: 22516247

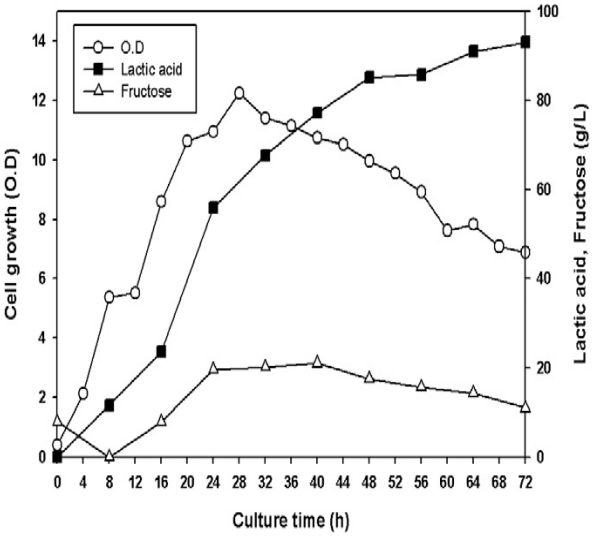

Keywords : Hydrolysis; Inulin; Jerusalem artichoke; Lactic acid; *Lactobacillus paracasei*

Article 18

Molecular insight into the role of the leucine residue on the L2 loop in the catalytic activity of caspases 3 and 7

Biosci Rep. 32(3):305-13.

Kang HJ, Lee YM, Jeong MS, Kim M, Bae KH, Kim SJ, Chung SJ*

*Corresponding:
BioNanotechnology Research Center

Various apoptotic signals can activate caspases 3 and 7 by triggering the L2 loop cleavage of their proenzymes. These two enzymes have highly similar structures and functions, and serve as apoptotic executioners. The structures of caspase 7 and procaspase 7 differ significantly in the conformation of the loops constituting the active site, indicating that the enzyme undergoes a large structural change during activation. To define the role of the leucine residue on the L2 loop, which shows the largest movement during enzyme activation but has not yet been studied, Leu^{168} of caspase 3 and Leu^{191} of caspase 7 were mutated. Kinetic analysis indicated that the mutation of the leucine residues sometimes improved the K_m but also greatly decreased the k_{cat}, resulting in an overall decrease in enzyme activity. The tryptophan fluorescence change at excitation/emission = 280/350 nm upon L2-L2' loop cleavage was found to be higher in catalytically active mutants, including the corresponding wild-type caspase, than in the inactive mutants. The crystal structures of the caspase 3 mutants were solved and compared with that of wild-type. Significant alterations in the conformations of the L1 and L4 loops were found. These results indicate that the leucine residue on the L2 loop has an important role in maintaining the catalytic activity of caspases 3 and 7.
PMID: 22304005

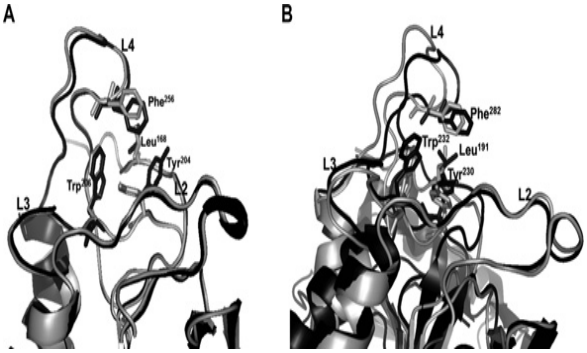

Keywords : Apoptosis; Caspase; Crystal structure; Fluorescence; Hydrophobic interaction; Proenzyme activation; Tryptophan

Article 19

Quantitative analyses of individual sugars in mixture using FRET-based biosensors

Biotechnol Prog. 28(5):1376-83.

Ha JS, Gam J, Choi SL, Oh KH, Ro HS, Song JJ, Shin CS, Lee SG*

*Corresponding: sglee@kribb.re.kr
Biochemicals & Synthetic Biology Research Center

Molecular biosensors were developed and applied to measure individual sugars in biological mixtures such as bacterial culture broths. As the sensing units, four sugar-binding proteins (SBPs for allose, arabinose, ribose, and glucose) were selected from the *Escherichia coli* genome and connected to a cyan fluorescent protein and yellow fluorescent protein via dipeptide linkers (CFP-L-SBP-YFP). The putative sensors were randomized in the linker region (L) and then investigated with regard to the intensity of fluorescence resonance energy transfer on the binding of the respective sugars. As a result, four representatives were selected from each library and examined for their specificity using 16 available sugars. The apparent dissociation constants of the allose, arabinose, ribose, and glucose sensors were estimated to be 0.35, 0.36, 0.17, and 0.18 μM. Finally, the sugar sensors were applied to monitor the consumption rate of individual sugars in an *E. coli* culture broth. The individual sugar profiles exhibited a good correlation with those obtained using an HPLC method, confirming that the biosensors offer a rapid and easy-to-use method for monitoring individual sugars in mixed compositions.
PMID: 22753346

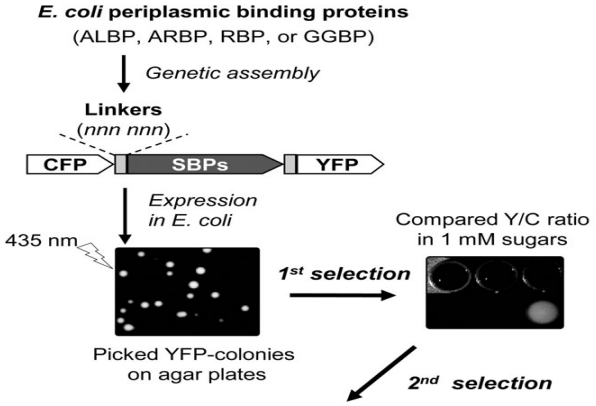

Sensors	Ligand	Linkers	ΔFRET*ratio*
ALBP-QV	Allose	Gln-Val	-0.21
ARBP-PR	Arabinose	Pro-Arg	0.29
RBP-ND	Ribose	Asn-Asp	-0.12
GGBP-SS	Glucose	Ser-Ser	-0.13

Keywords : Biomass; Fluorescence resonance energy transfer; Molecular biosensor; Protein; Sugar

Article 20

A selective Seoul-Fluor-based bioprobe, S*f*BP, for vaccinia H1-related phosphatase--a dual-specific protein tyrosine phosphatase

Chem Commun. 48(52):6553-5.

Jeong MS, Kim E, Kang HJ, Choi EJ, Cho AR, Chung SJ*, Park SB

*Co-corresponding:
BioNanotechnology Research Center

We report a Seoul-Fluor-based bioprobe, SfBP, for selective monitoring of protein tyrosine phosphatases (PTPs). A rational design based on the structures at the active site of dual-specific PTPs can enable S*f*BP to selectively monitor the activity of these PTPs with a 93-fold change in brightness. Moreover, screening results of S*f*BP against 30 classical PTPs and 35 dual-specific PTPs show that it is selective toward vaccinia H1-related (VHR) phosphatase, a dual-specific PTP (DUSP-3).
PMID: 22622190

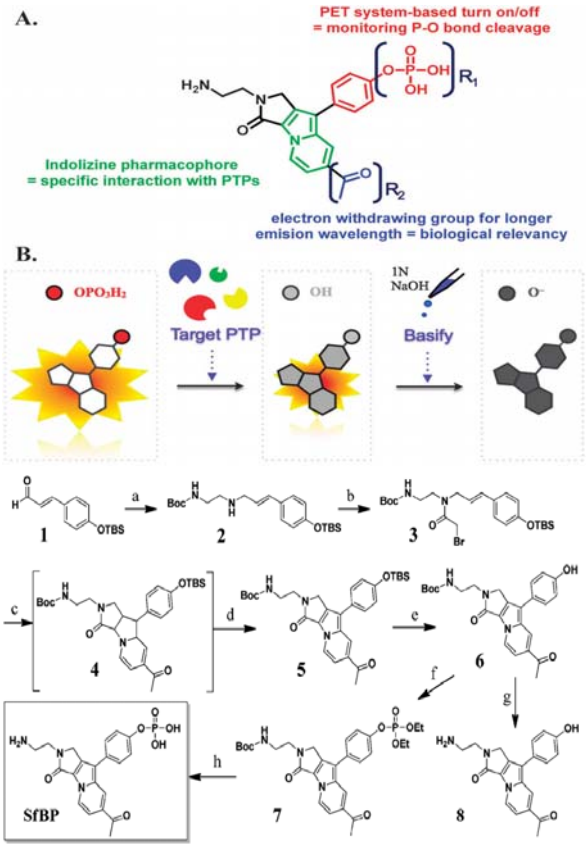

Keywords : Dual-specific PTPs; Protein tyrosine phosphatases; Seoul-Fluor-based bioprobe; Vaccinia H1-related

Article 21

Scanometric analysis of DNA microarrays using DNA intercalator-conjugated gold nanoparticles

Chem Commun. 48(61):7601-3.

Cho H, Jung J, Chung BH*

*Corresponding: chungbh@kribb.re.kr
BioNanotechnology Research Center

We introduce a scanometric detection method for the analysis of DNA microarrays using DNA intercalator-conjugated gold nanoparticles that can be analyzed with the naked eye or with an optical scanner after the enhancement of the AuNPs. Moreover, we successfully detected a hemagglutinin-subtyping DNA array using this method.
PMID: 22732710

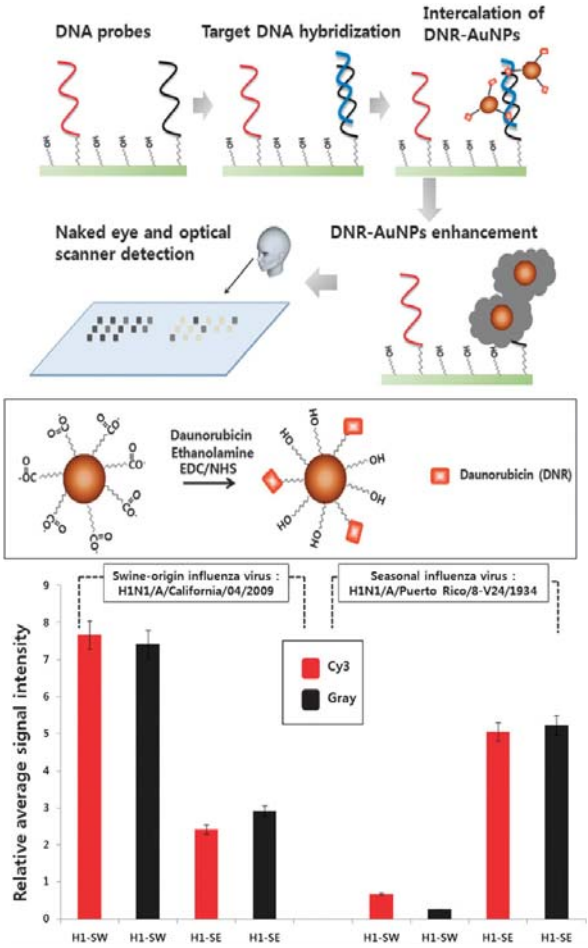

Keywords : DNA microarray; Gold nanoparticle; Hemagglutinin-subtyping DNA array; Scanometric detection method

Article 22

Indocyanine green encapsulated nanogels for hyaluronidase activatable and selective near infrared imaging of tumors and lymph nodes

Chem Commun. 48(69):8628-30.

Mok H, Jeong H, Kim SJ, Chung BH*

*Corresponding: chungbh@kribb.re.kr
BioNanotechnology Research Center

Indocyanine green (ICG) encapsulated hyaluronic acid (HA) nanogels were first studied for highly selective detection of specific cancers and lymph nodes *via* hyaluronidase sensitive switch-on of near infrared fluorescence as a long-lasting and stimuli-responsive imaging probe.
PMID: 22745939

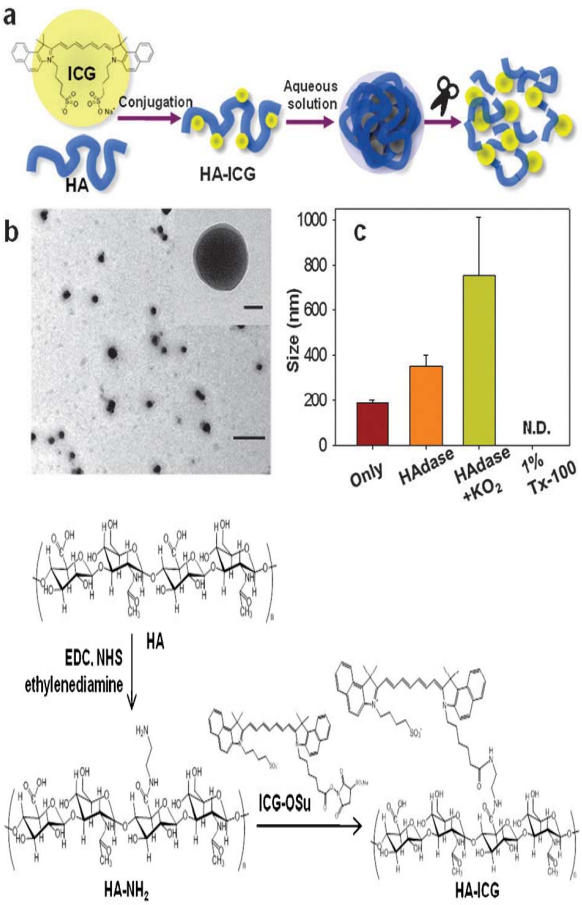

Keywords : Cancer; Encapsulated hyaluronic acid (HA); Fluorescence; Hyaluronidase sensitive switch; Indocyanine green (ICG); Nanogel

Article 23

Cascade imaging of proteolytic pathways in cancer cells using fluorescent protein-conjugated gold nanoquenchers

Chem Commun. 48(85):10547-9.

Park K, Jeong J, Chung BH*

*Corresponding: chungbh@kribb.re.kr
BioNanotechnology Research Center

The real-time monitoring of the caspase cascade in cancer cells during apoptosis was performed using various caspase substrate-linked fluorescent proteins-conjugated gold nanoparticles as a new imaging probe.
PMID: 22992541

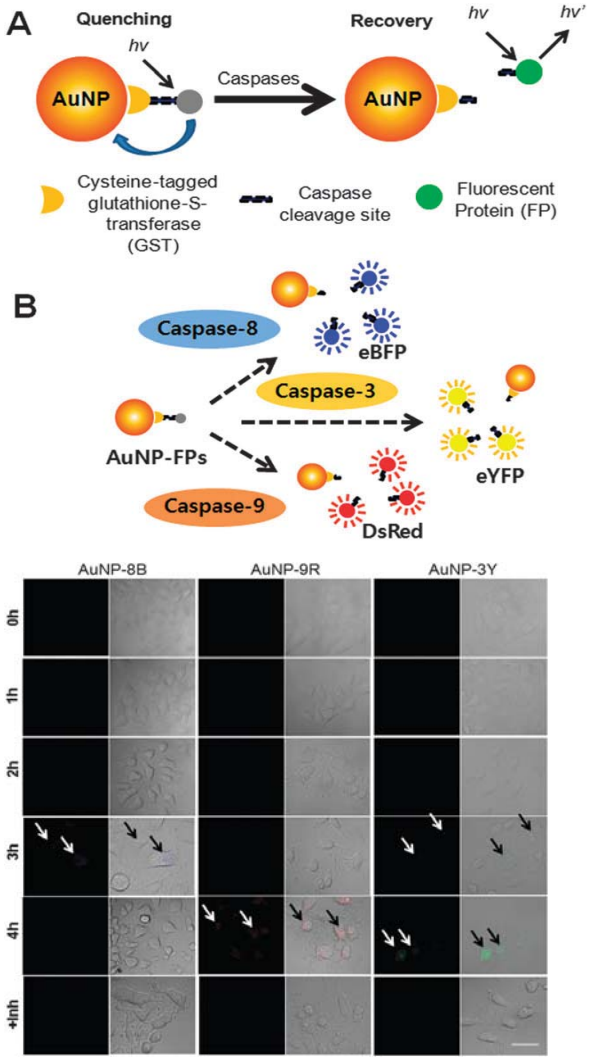

Keywords : Apoptosis; Cancer cell; Fluorescent proteins; Gold nanoparticle; Real-time monitoring

Article 24

A facile synthetic route to diazepinone derivatives *via* ring closing metathesis and its application for human cytidine deaminase inhibitors

Chem Commun. 48(93):11443-5.

Kim M, Gajulapati K, Kim C, Jung HY, Goo J, Lee K, Kaur N, Kang HJ, Chung SJ*, Choi Y

*Co-corresponding:
BioNanotechnology Research Center

A variety of diazepinone derivatives were prepared from α-amino acids and amino alcohols by a new synthetic methodology based on ring closing metathesis as a key step. The diazepinones were coupled with ribose derivatives to afford novel diazepinone nucleosides. Among them, (4*R*)-1-ribosyl-4-methyl-3,4-dihydro-1*H*-1,3-diazepin-2(7*H*)-one (3) showed a potent inhibitory effect (K_i = 145.97 ± 4.87 nM) against human cytidine deaminase.
PMID:23086289

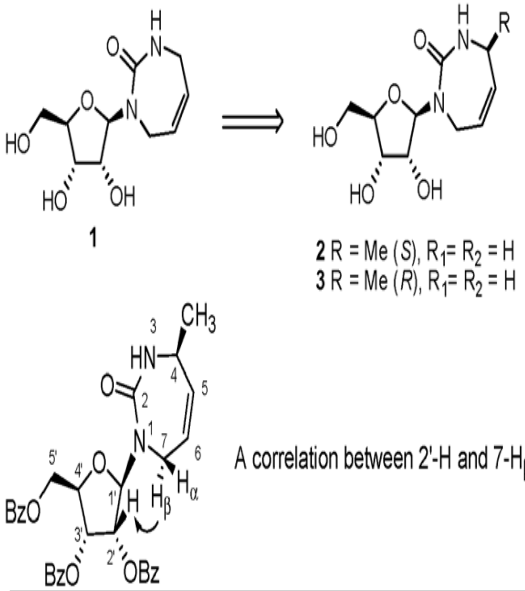

Inhibitor	1	2 (Me, *S*)	3 (Me, *R*)
K_i	35.3 ± 0.49 (nM)	2.56 ± 0.18 (μM)	146 ± 4.87 (nM)

[a] Human cytidine deaminase activity was determined by a direct spectrophotometric assay based on the decrease in absorbance at 282 nm upon cytidine deamination.

Keywords : Diazepinone derivative; Diazepinone nucleoside; Human cytidine deaminase; Inhibitory effect; Ring closing metathesis

Article 25

A novel fluorescent nanoparticle composed of fluorene copolymer core and silica shell with enhanced photostability

Colloids Surf B Biointerfaces. 91:219-25.

Lee CS, Chang HH, Jung J, Lee NA, Song NW, Chung BH*

*Corresponding: chungbh@kribb.re.kr
BioNanotechnology Research Center

A variety of fluorescent nanoparticles have been developed for demanding applications such as optical biosensing and fluorescence imaging in live cells. Silica-based fluorescent nanoparticles offer diverse advantages for biological applications. For example, they can be used as labeling probes due to their low toxicity, high sensitivity, resolution, and stability. In this research, a new class of highly fluorescent, efficient nanoparticles composed of a newly synthesized poly[di(2-methoxy-5-(2-ethylhexyloxy))-2,7-(9,9-dioctyl-9 H-fluorene)] (PDDF) core and a silica shell (designated as PDDF@SiO_2) were prepared using a simple reverse micelle method, and their fluorescent properties were evaluated using methods such as single-dot photoluminescence measurements. The enhanced photostability of the particles and their potential applications for bioanalysis are discussed in this article. The morphology, size, and fluorescent properties for prepared PDDF@SiO_2 nanoparticles were characterized using transmission electron microscopy (TEM), scanning electron microscopy (SEM) and photoluminescence spectroscopy. The prepared particles size, which was approximately 60 nm, resulted in an excellent colloidal stability in a physiological environment. The photobleaching dynamics, total numbers of emitted photons (TNEP) and statistical measurements of individual nanoparticles were observed using laser scanning fluorescence microscopy to assess the structure and photostability of PDDF@SiO_2 nanoparticles. Additionally, PDDF@SiO_2 nanoparticles were used in cell toxicity and permeation tests for biological analyses, demonstrating a great potential for use as powerful, novel materials within the emerging fields of biosensing and biomedical engineering.
PMID: 22138116

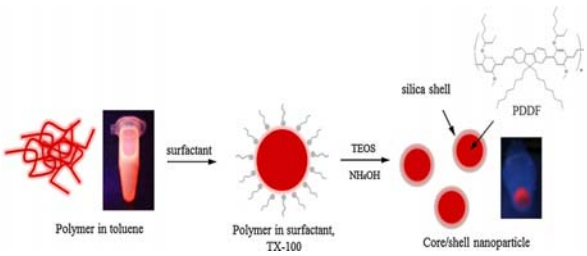

Keywords : Bioimaging; Biomedical engineering; Biosensing; Fluorescent nanoparticle; Fluorescent polymer; Photostability

Article 26

JNK/FOXO mediated *PeroxiredoxinV* expression regulates redox homeostasis during *Drosophila melanogaster* gut infection

Dev Comp Immunol. 38(3):466-73.

Ahn HM, Lee KS, Lee DS, Yu K*

*Co-corresponding: kweonyu@kribb.re.kr
BioNanotechnology Research Center

Innate immunity plays an important role in combating microbial infection in animals. During bacterial infection in *Drosophila melanogaster* gut, *Dual oxidase* (*Duox*) generates reactive oxygen species (ROS) to fight against the infected microbes. Concurrently, antioxidant systems eliminate residual ROS and protect the hosts. Here we found that *Drosophila melanogaster* Peroxiredoxin V (*dPrxV*) is an immune-related antioxidant enzyme which maintains intestinal redox homeostasis. *dPrxV* was highly expressed in gut and induced by the oral infection of *Erwinia carotovora carotovora*. *dPrxV* expression was increased by the gut-specific *Duox* overexpression but decreased by *Duox* inhibition. Moreover, *dPrxV* expression was mediated by the JNK/FOXO signaling and *dPrxV* mutant reduced survival after gut infection. These results suggest that JNK/FOXO mediated *dPrxV* expression plays a critical role in *Drosophila melanogaster* gut during bacterial infection in protecting the host gut epithelial cells from oxidative damage.
PMID: 22858408

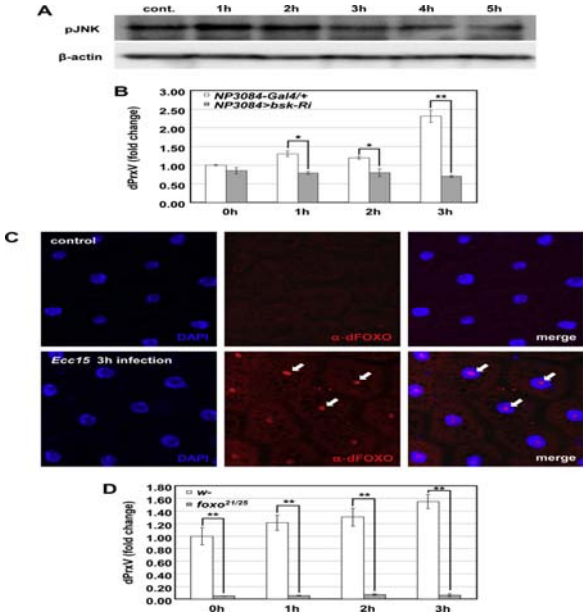

Keywords : *Drosophila melanogaster*; *Duox*; FOXO; Gut infection; JNK; Peroxiredoxin V; ROS

Article 27

Comparative multi-omics systems analysis of *Escherichia coli* strains B and K-12

Genome Biol. 13(5):R37.

Yoon SH*, Han MJ, Jeong H, Lee CH, Xia XX, Lee DH, Shim JH, Lee SY, Oh TK, Kim JF

*First: moncher@kribb.re.kr
Biochemicals & Synthetic Biology Research Center

BACKGROUND: Elucidation of a genotype-phenotype relationship is critical to understand an organism at the whole-system level. Here, we demonstrate that comparative analyses of multi-omics data combined with a computational modeling approach provide a framework for elucidating the phenotypic characteristics of organisms whose genomes are sequenced.
RESULTS: We present a comprehensive analysis of genome-wide measurements incorporating multifaceted holistic data - genome, transcriptome, proteome, and phenome - to determine the differences between *Escherichia coli* B and K-12 strains. A genome-scale metabolic network of *E. coli* B was reconstructed and used to identify genetic bases of the phenotypes unique to B compared with K-12 through *in silico* complementation testing. This systems analysis revealed that *E. coli* B is well-suited for production of recombinant proteins due to a greater capacity for amino acid biosynthesis, fewer proteases, and lack of flagella. Furthermore, *E. coli* B has an additional type II secretion system and a different cell wall and outer membrane composition predicted to be more favorable for protein secretion. In contrast, *E. coli* K-12 showed a higher expression of heat shock genes and was less susceptible to certain stress conditions.
CONCLUSIONS: This integrative systems approach provides a high-resolution system-wide view and insights into why two closely related strains of *E. coli*, B and K-12, manifest distinct phenotypes. Therefore, systematic understanding of cellular physiology and metabolism of the strains is essential not only to determine culture conditions but also to design recombinant hosts.
PMID: 22632713

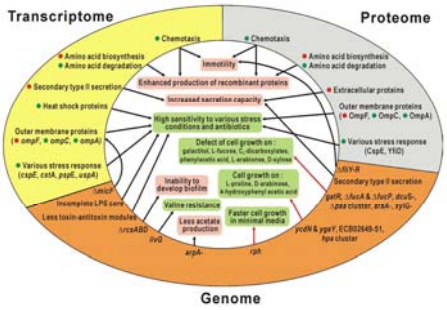

Keywords : Comparative analyses; Computational modeling; Heat shock gene; Multi-omics data

Article 28

Thalassobius maritimus sp. nov., isolated from seawater

Int J Syst Evol Microbiol. 62(Pt 1):8-12.

Park S*, Lee MH, Lee JS, Oh TK, Yoon JH

*First:
Super-Bacteria Research Center

A Gram-stain-negative, aerobic, motile, rod-shaped bacterial strain, GSW-M6^T, was isolated from seawater of Geoje island, Korea, and was subjected to a polyphasic taxonomic study. Strain GSW-M6^T grew optimally at pH 7.0-8.0, at 30 °C and in the presence of 2% (w/v) NaCl. In the neighbour-joining phylogenetic tree based on 16S rRNA gene sequences, strain GSW-M6^T clustered with *Thalassobius aestuarii*, *Thalassobius gelatinovorus* and *Thalassobius mediterraneus*. Strain GSW-M6^T exhibited 96.2-96.9% 16S rRNA gene sequence similarity to the type strains of these three *Thalassobius* species. Strain GSW-M6^T contained Q-10 as the predominant ubiquinone and $C_{18:1}\omega7c$ as the major fatty acid. The polar lipid profiles of strain GSW-M6^T and the type strains of the three *Thalassobius* species were similar, with phosphatidylcholine, phosphatidylglycerol, phosphatidylethanolamine and an unidentified lipid as common major components. The DNA G+C content of strain GSW-M6^T was 57 mol%. The mean level of DNA-DNA relatedness between strain GSW-M6^T and the type strain of *Thalassobius gelatinovorus* was 17%. Differential phenotypic properties, together with the phylogenetic and genetic distinctiveness, enabled strain GSW-M6^T to be differentiated from recognized species of the genus *Thalassobius*. On the basis of the data presented, strain GSW-M6^T is considered to represent a novel species of the genus *Thalassobius*, for which the name *Thalassobius maritimus* sp. nov. is proposed. The type strain is GSW-M6^T (=KCTC 23347^T =CCUG 60021^T).
PMID: 21257694

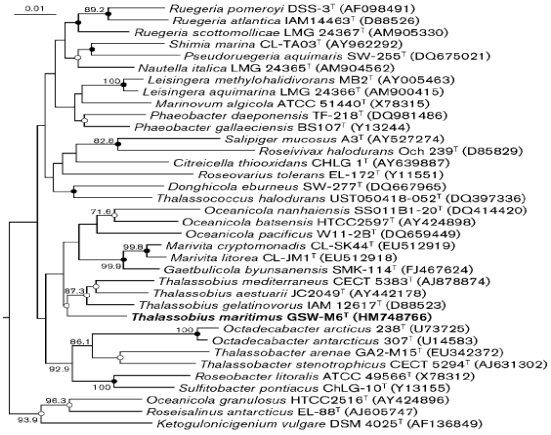

Keywords : Phylogenetic tree; Polyphasic taxonomic study; Seawater; *Thalassobius maritimus*

Article 29

Pedobacter boryungensis sp. nov., isolated from soil

Int J Syst Evol Microbiol. 62(Pt 1):13-7.

Jung YT*, Lee SY, Choi WC, Oh TK, Yoon JH

*First:
Super-Bacteria Research Center

A Gram-negative, non-sporulating, non-flagellated rod, designated BR-9^T, was isolated from soil collected on the Korean peninsula. Strain BR-9^T grew optimally at pH 6.0-7.0, at 30 °C and in the absence of NaCl. Phylogenetic analysis based on 16S rRNA gene sequences revealed that strain BR-9^T belonged to the genus *Pedobacter* and clustered with *Pedobacter insulae* DS-139^T and *Pedobacter koreensis* WPCB189^T. Strain BR-9^T exhibited 98.2 and 97.5% 16S rRNA gene sequence similarity with *P. insulae* DS-139^T and *P. koreensis* WPCB189^T, respectively, and <96.7% sequence similarity with the type strains of other species in the genus *Pedobacter*. Strain BR-9^T contained MK-7 as the predominant menaquinone and iso-$C_{15:0}$ and summed feature 3 ($C_{16:1}\omega7c$ and/or iso-$C_{15:0}$ 2-OH) as the major fatty acids. The DNA G+C content of strain BR-9^T was 38.5 mol%. DNA-DNA relatedness between strain BR-9^T and *P. insulae* DS-139^T and *P. koreensis* KCTC 12536^T was 3.4-4.2%, which indicated that the isolate was genetically distinct from these type strains. Strain BR-9^T was also distinguishable by differences in phenotypic properties. On the basis of the data presented, strain BR-9^T is considered to represent a novel species of the genus *Pedobacter*, for which the name *Pedobacter boryungensis* sp. nov. is proposed. The type strain is BR-9^T (=KCTC 23344^T =CCUG 60024^T).

PMID: 21257683

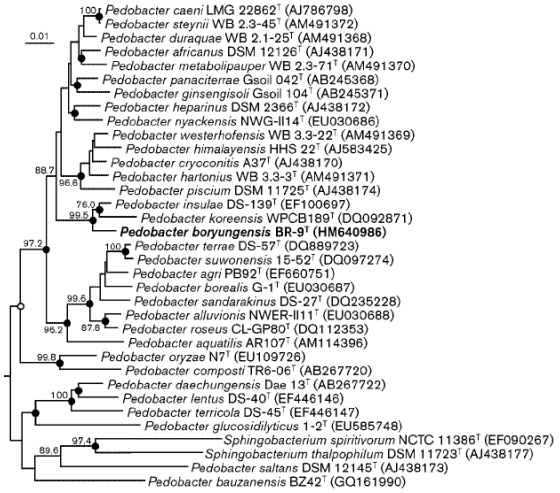

Keywords : *Pedobacter boryungensis*; Phenotypic property; Phylogenetic analysis; Soil

Article 30

Tenacibaculum geojense sp. nov., isolated from seawater

Int J Syst Evol Microbiol. 62(Pt 1):18-22.

Kang SJ*, Lee SY, Lee MH, Oh TK, Yoon JH

*First:
Super-Bacteria Research Center

A Gram-negative, non-flagellated, non-spore-forming bacterium, designated YCS-6^T, that was motile by gliding, was isolated from seawater on the southern coast of Korea. Strain YCS-6^T grew optimally at 30 °C and with 2% (w/v) NaCl. Phylogenetic analysis based on 16S rRNA gene sequences revealed that strain YCS-6^T fell within the genus *Tenacibaculum* and was most closely associated with *Tenacibaculum litopenaei* B-I^T, with which the isolate exhibited 95.9% 16S rRNA gene sequence similarity. Sequence similarity between strain YCS-6^T and other members of the genus *Tenacibaculum* was 93.8-95.7%. Strain YCS-6^T contained menaquinone-6 (MK-6) as the predominant respiratory quinone and iso-$C_{15:0}$, summed feature 3 (iso-$C_{15:0}$ 2-OH and/or $C_{16:1}\omega7c$), iso-$C_{15:0}$ 3-OH and iso-$C_{15:1}$ G as the major fatty acids. The DNA G+C content was 32.7 mol%. Differential phenotypic properties and phylogenetic distinctiveness distinguished strain YCS-6^T from all other members of the genus *Tenacibaculum*. On the basis of our phenotypic, chemotaxonomic and phylogenetic data, strain YCS-6^T is considered to represent a novel species of the genus *Tenacibaculum*, for which the name *Tenacibaculum geojense* sp. nov. is proposed. The type strain is YCS-6^T (=KCTC 23423^T =CCUG 60527^T).

PMID: 21257684

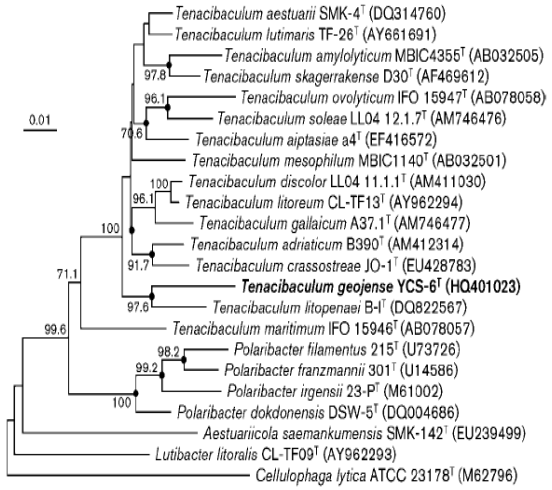

Keywords : Phenotypic property; Phylogenetic analysis; Seawater; *Tenacibaculum geojense*

Article 31

Pseudorhodobacter aquimaris sp. nov., isolated from seawater, and emended description of the genus *Pseudorhodobacter* Uchino *et al.* 2002

Int J Syst Evol Microbiol. 62(Pt 1):100-5.

Jung YT*, Oh KH, Oh TK, Yoon JH

*First:
Super-Bacteria Research Center

A Gram-stain-negative, aerobic, motile, ovoid bacterial strain, designated HDW-19^T, was isolated from seawater of the west coast of Korea and subjected to a polyphasic taxonomic study. Strain HDW-19^T grew optimally at pH 7.0-8.0, at 30 °C and in the presence of 2-3% (w/v) NaCl. Bacteriochlorophyll a was not produced by strain HDW-19^T. Neighbour-joining, maximum-likelihood and maximum-parsimony phylogenetic trees based on 16S rRNA gene sequences showed that strain HDW-19^T clustered with *Pseudorhodobacter ferrugineus* IAM 12616^T, with which it shared 96.4% similarity. A neighbour-joining phylogenetic tree based on *gyrB* gene sequences showed that strain HDW-19^T also clustered with the type strain of *P. ferrugineus*, sharing 83.0% similarity. Strain HDW-19^T contained Q-10 as the predominant ubiquinone and $C_{18:1}\omega7c$ as the major fatty acid. The major polar lipids were phosphatidylcholine, phosphatidylglycerol, three unidentified aminophospholipids and two unidentified aminolipids. The DNA G+C content of strain HDW-19^T was 60.9 mol%. Differential phenotypic properties, together with phylogenetic distinctiveness, showed that strain HDW-19^T can be differentiated from *P. ferrugineus*. On this basis, strain HDW-19^T is considered to represent a novel species of the genus *Pseudorhodobacter*, for which the name *Pseudorhodobacter aquimaris* sp. nov. is proposed. The type strain is HDW-19^T (=KCTC 23043^T =CCUG 58879^T).

PMID: 21335494

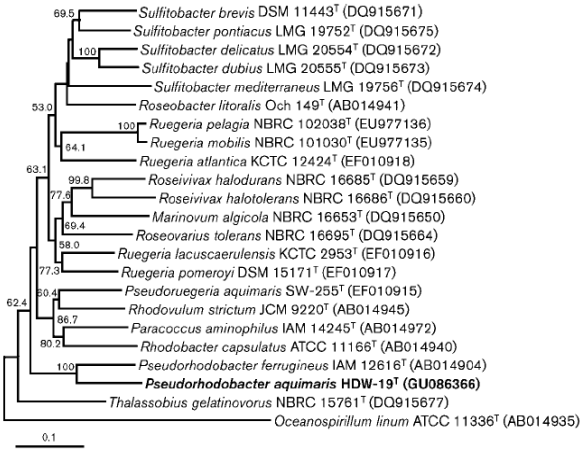

Keywords : Phenotypic property; Phylogenetic analysis; *Pseudorhodobacter aquimaris*; Seawater

Article 32

Virgibacillus campisalis sp. nov., from a marine solar saltern

Int J Syst Evol Microbiol. 62(Pt 2):347-51.

Lee SY*, Kang CH, Oh TK, Yoon JH

*First:
Super-Bacteria Research Center

A Gram-staining-variable, motile, endospore-forming and rod-shaped bacterial strain, IDS-20^T, was isolated from a marine solar saltern in Korea and subjected to a polyphasic taxonomic investigation. Strain IDS-20^T grew optimally at 37 °C, at pH 7.5-8.0 and in the presence of 4-5% (w/v) NaCl. Phylogenetic analysis based on 16S rRNA gene sequences revealed that strain IDS-20^T belongs to the genus *Virgibacillus*. Strain IDS-20^T exhibited 93.4-96.6% 16S rRNA gene sequence similarity to the type strains of species of the genus *Virgibacillus*. Strain IDS-20^T had MK-7 as the predominant menaquinone and a cell-wall peptidoglycan based on *meso*-diaminopimelic acid. The major fatty acids were anteiso-$C_{15:0}$ and anteiso-$C_{17:0}$ and major polar lipids were diphosphatidylglycerol, phosphatidylglycerol and two unidentified phospholipids. The DNA G+C content was 39.5 mol%. The phylogenetic distinctiveness and differential phenotypic characteristics of strain IDS-20^T demonstrated that this strain can be distinguished from recognized species of the genus *Virgibacillus*. On the basis of the data presented, strain IDS-20^T represents a novel species of the genus *Virgibacillus*, for which the name *Virgibacillus campisalis* sp. nov. is proposed. The type strain is IDS-20^T (=KCTC 13727^T =CCUG 59308^T).

PMID: 21441379

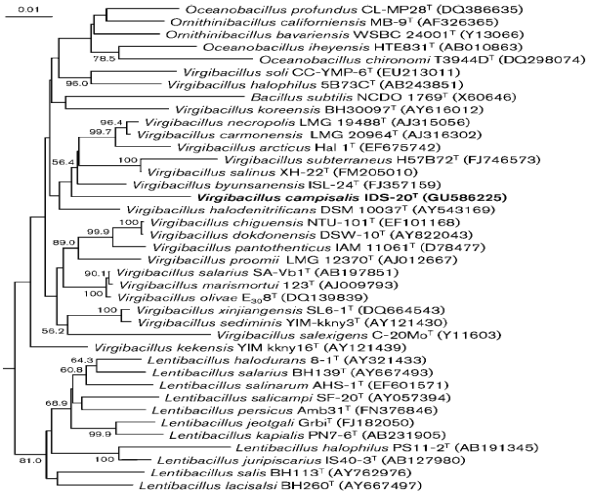

Keywords : Marine solar saltern; Phenotypic property; Phylogenetic analysis; *Virgibacillus campisalis*

Article 33

Lutibacter aestuarii sp. nov., isolated from a tidal flat sediment, and emended description of the genus *Lutibacter* Choi and Cho 2006

Int J Syst Evol Microbiol. 62(Pt 2):420-4.

Lee SY*, Lee MH, Oh TK, Yoon JH

*First:
Super-Bacteria Research Center

A gram-negative, non-spore-forming, non-motile rod, designated MA-My1^T, was isolated from a tidal flat sediment of the South Sea, Korea. Strain MA-My1^T grew optimally at pH 7.0-7.5, at 30 °C and with 2.0-3.0% (w/v) NaCl. Phylogenetic analysis based on 16S rRNA gene sequences revealed that strain MA-My1^T clustered with *Lutibacter litoralis* CL-TF09^T and *Lutibacter maritimus* S7-2^T, with which it exhibited 97.3 and 95.3% 16S rRNA gene sequence similarity, respectively. Strain MA-My1^T contained MK-6 as the predominant menaquinone and iso-$C_{15:0}$, iso-$C_{15:0}$ 3-OH and iso-$C_{16:0}$ 3-OH as the major fatty acids. The major polar lipids were phosphatidylethanolamine and two unidentified lipids. The DNA G+C content was 30.6 mol% and DNA-DNA relatedness between strain MA-My1^T and *L. litoralis* JCM 13034^T was 6.3±0.8%. The differential phenotypic properties, together with phylogenetic and genotypic distinctiveness, distinguished strain MA-My1^T from the members of the genus *Lutibacter*. On the basis of the data presented, strain MA-My1^T is considered to represent a novel species of the genus *Lutibacter*, for which the name *Lutibacter aestuarii* sp. nov. is proposed. The type strain is MA-My1^T (=KCTC 23499^T =CCUG 60022^T).
PMID: 21460139

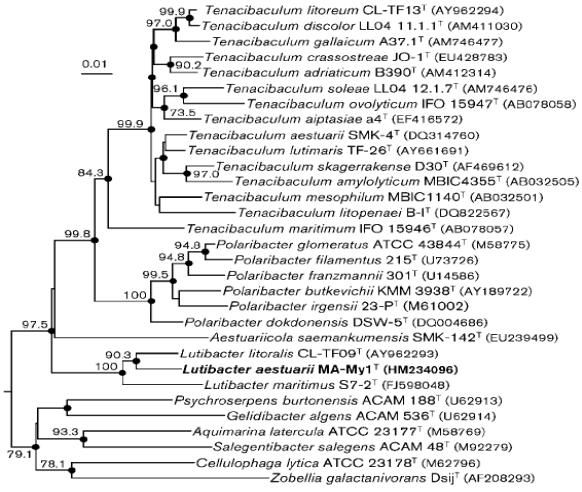

Keywords : *Lutibacter aestuarii*; Phenotypic property; Phylogenetic analysis; Tidal flat sediment

Article 34

Kangiella geojedonensis sp. nov., isolated from seawater

Int J Syst Evol Microbiol. 62(Pt 3):511-4.

Yoon JH*, Kang SJ, Lee SY, Lee JS, Oh TK

*Corresponding:
Super-Bacteria Research Center

A Gram-stain-negative, non-motile, non-spore-forming bacterial strain, YCS-5^T, was isolated from seawater off the southern coast of Korea. Strain YCS-5^T grew optimally at 30 °C and in the presence of 2% (w/v) NaCl. Phylogenetic analyses based on 16S rRNA gene sequences revealed that strain YCS-5^T fell within the clade comprising *Kangiella* species. Strain YCS-5^T exhibited 16S rRNA gene sequence similarity values of 96.6, 95.7 and 97.9% to the type strains of *Kangiella koreensis*, *Kangiella aquimarina* and *Kangiella japonica*, respectively, and less than 89.8% to strains of other species used in the phylogenetic analysis. Strain YCS-5^T contained Q-8 as the predominant ubiquinone and iso-$C_{15:0}$, iso-$C_{17:0}$, iso-$C_{11:0}$ 3-OH and iso-$C_{17:1}\omega9c$ as the major fatty acids. The polar lipid profile of strain YCS-5^T was similar to that of *K. koreensis* SW-125^T, with phosphatidylglycerol and an unidentified aminolipid as major polar lipids. The DNA G+C content was 47 mol%. The mean DNA-DNA relatedness value between strain YCS-5^T and *K. japonica* JCM 16211^T was 12%. Differential phenotypic properties and the phylogenetic and genetic distinctiveness of strain YCS-5^T demonstrated that this strain is distinguishable from other *Kangiella* species. On the basis of the data presented, strain YCS-5^T is considered to represent a novel species of the genus *Kangiella*, for which the name *Kangiella geojedonensis* sp. nov. is proposed; the type strain is YCS-5^T (=KCTC 23420^T=CCUG 60526^T).
PMID:21478391

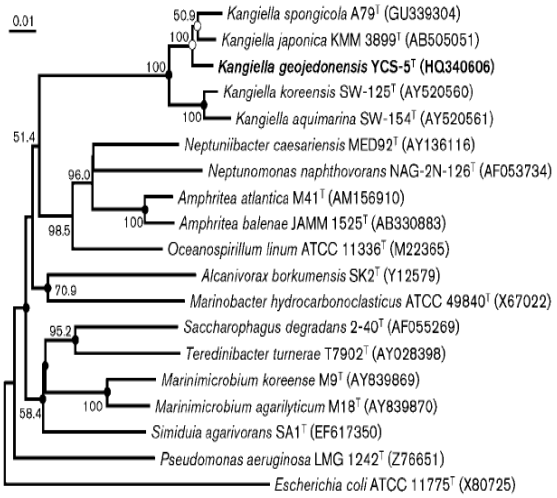

Keywords : *Kangiella geojedonensis*; Phenotypic property; Phylogenetic analysis; Seawater

Article 35

Mucilaginibacter lutimaris sp. nov., isolated from a tidal flat sediment

Int J Syst Evol Microbiol. 62(Pt 3):515-9.

Kim JH*, Kang SJ, Jung YT, Oh TK, Yoon JH

*First:
Super-Bacteria Research Center

A Gram-staining-negative, non-spore-forming, facultatively aerobic, non-motile, rod-shaped bacterial strain, BR-3^T, was isolated from a tidal flat on the western coast of Korea, and subjected to a polyphasic study. Strain BR-3^T grew optimally at 25 °C, at pH 6.5-7.0 and in the absence of NaCl. Phylogenetic analyses based on 16S rRNA gene sequences revealed that strain BR-3^T fell within the clade comprising species of the genus *Mucilaginibacter*, joining the type strain of *Mucilaginibacter rigui*, with which it exhibited highest 16S rRNA gene sequence similarity (98.2%). 16S rRNA gene sequence similarity values between strain BR-3^T and the type strains of the other species of the genus *Mucilaginibacter* were in the range 93.8-95.9%. A mean DNA-DNA relatedness value between strain BR-3^T and *M. rigui* KCTC 12534^T was 21%. Strain BR-3^T contained MK-7 as the predominant menaquinone and $C_{16:1}\omega7c$ and/or iso-$C_{15:0}$ 2-OH and iso-$C_{15:0}$ as the major fatty acids. The major polar lipids were phosphatidylethanolamine and an unidentified aminophospholipid. The DNA G+C content was 49.8 mol%. Differential phenotypic properties and phylogenetic and genetic distinctiveness of strain BR-3^T demonstrated that this strain is separate from *M. rigui* as well as the other species of the genus *Mucilaginibacter*. On the basis of the data presented, strain BR-3^T is considered to represent a novel species of the genus *Mucilaginibacter*, for which the name *Mucilaginibacter lutimaris* sp. nov. is proposed. The type strain is BR-3^T (=KCTC 23461^T =CCUG 60742^T).

PMID: 21478392

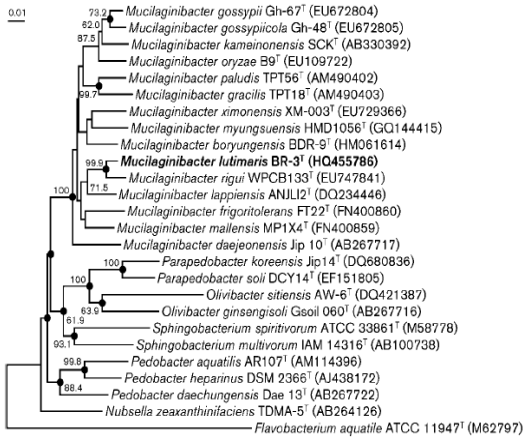

Keywords : *Mucilaginibacter lutimaris*; Phenotypic property; Phylogenetic analysis; Tidal flat

Article 36

Mariniflexile aquimaris sp. nov., isolated from seawater, and emended description of the genus *Mariniflexile* Nedashkovskaya *et al*. 2006

Int J Syst Evol Microbiol. 62(Pt 3):539-44.

Jung YT*, Kim JH, Oh TK, Yoon JH

*First:
Super-Bacteria Research Center

A Gram-staining-negative, non-flagellated, non-gliding and rod-shaped bacterial strain, designated HWR-17^T, was isolated from seawater of the Yellow Sea in Korea. Strain HWR-17^T grew optimally at pH 7.0-8.0, at 30 °C and in the presence of 2% (w/v) NaCl. Phylogenetic analyses based on 16S rRNA gene sequences showed that strain HWR-17^T clustered with the two *Mariniflexile* species in the family *Flavobacteriaceae*, exhibiting 16S rRNA gene sequence similarity of 97.1-97.2% to their type strains and less than 95.7% sequence similarity to other members of the family *Flavobacteriaceae*. Strain HWR-17^T contained MK-6 as the predominant menaquinone and iso-$C_{15:0}$ as the major fatty acid. The polar lipid profile of strain HWR-17^T contained phosphatidylethanolamine, an unidentified aminolipid and four unidentified lipids. The DNA G+C content of strain HWR-17^T was 35.7 mol% and it exhibited 11 and 10% DNA-DNA relatedness, respectively, with *Mariniflexile gromovii* KCTC 12570^T and *Mariniflexile fucanivorans* DSM 18792^T. The phylogenetic and genetic distinctiveness and differential phenotypic properties revealed that strain HWR-17^T is distinguishable from the two recognized *Mariniflexile* species. On the basis of the data presented, strain HWR-17^T is considered to represent a novel species of the genus *Mariniflexile*, for which the name *Mariniflexile aquimaris* sp. nov. is proposed. The type strain is HWR-17^T (=KCTC 23346^T =CCUG 60529^T). An emended description of the genus *Mariniflexile* is also proposed.

PMID: 21498661

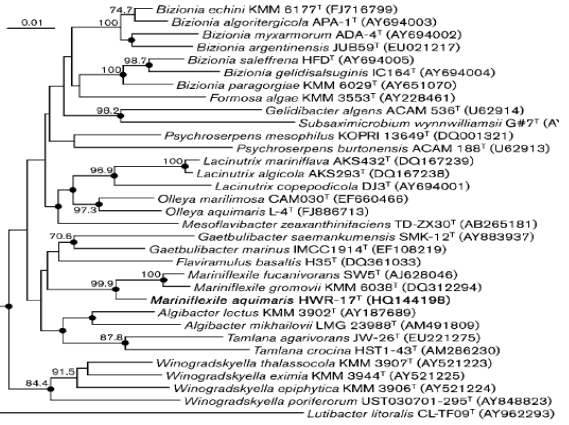

Keywords : *Mariniflexile aquimaris*; Phenotypic property; Phylogenetic analysis; Seawater

Article 37

Algoriphagus namhaensis sp. nov., isolated from seawater

Int J Syst Evol Microbiol. 62(Pt 3):575-9.

Oh KH*, Kang SJ, Lee SY, Park S, Oh TK, Yoon JH

*First:
Super-Bacteria Research Center

A Gram-staining-negative, non-motile, non-spore-forming bacterial strain, DPG-3^T, was isolated from seawater from the South Sea in Korea, and its taxonomic position was investigated using a polyphasic approach. Strain DPG-3^T grew optimally at 30 °C and in the presence of 2% (w/v) NaCl. In a neighbour-joining phylogenetic tree based on 16S rRNA gene sequences, strain DPG-3^T fell within a clade comprising *Algoriphagus* species and appeared most closely related to *Algoriphagus halophilus* JC 2051^T (96.1%16S rRNA gene sequence similarity) and *Algoriphagus lutimaris* S1-3^T (96.4%). The type strains of other *Algoriphagus* species showed 16S rRNA gene sequence similarities of 92.9-96.0% with strain DPG-3^T. The predominant menaquinone of strain DPG-3^T was MK-7. The major fatty acids were iso-$C_{15:0}$ and iso-$C_{15:0}$ 2-OH and/or $C_{16:1}\omega7c$ (summed feature 3). The major polar lipids detected in strain DPG-3^T were phosphatidylcholine, phosphatidylethanolamine and an unidentified lipid. The genomic DNA G+C content was 44.8 mol%. On the basis of phenotypic, chemotaxonomic and phylogenetic data, strain DPG-3^T is considered to represent a novel species of the genus *Algoriphagus*, for which the name *Algoriphagus namhaensis* sp. nov. is proposed. The type strain is DPG-3^T (=KCTC 23419^T=CCUG 60523^T).
PMID: 21515706

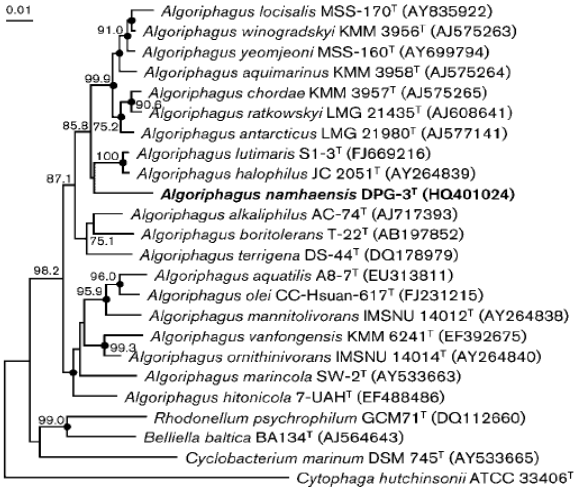

Keywords : *Algoriphagus namhaensis*; Phylogenetic analysis; Polyphasic approach; Seawater

Article 38

Tropicimonas aquimaris sp. nov., isolated from seawater, and emended description of the genus *Tropicimonas* Harwati *et al.* 2009

Int J Syst Evol Microbiol. 62(Pt 3):688-92.

Oh KH*, Choi WC, Jung YT, Kang SJ, Oh TK, Yoon JH

*First:
Super-Bacteria Research Center

A Gram-staining-negative, aerobic, non-motile and rod-shaped bacterial strain, designated DPG-21^T, was isolated from seawater from the South Sea in Korea, and investigated using a polyphasic taxonomic approach. Strain DPG-21^T grew optimally at pH 7.0-8.0, at 30 °C and in the presence of 2% (w/v) NaCl. In a neighbour-joining phylogenetic tree based on 16S rRNA gene sequences, strain DPG-21^T clustered with *Tropicimonas isoalkanivorans* B51^T (with a sequence similarity of 97.1%); the novel strain showed lower 16S rRNA gene sequence similarities (<95.4%) with the other species included in the tree. The mean DNA-DNA relatedness value between strain DPG-21^T and *T. isoalkanivorans* DSM 19548^T was 12%. The predominant ubiquinones of strain DPG-21^T were Q-10 and Q-9 while $C_{18:1}\omega7c$ was the strain's major fatty acid. The polar lipid profile of strain DPG-21^T was similar to that of *T. isoalkanivorans* DSM 19548^T. The genomic DNA G+C content of the novel strain was 69.6 mol%. Some phenotypic properties and the phylogenetic and genetic data indicated that strain DPG-21^T was distinct from *T. isoalkanivorans* and represents a novel species of the genus *Tropicimonas*, for which the name *Tropicimonas aquimaris* sp. nov. is proposed. The type strain is DPG-21^T (=KCTC 23424^T=CCUG 60524^T).
PMID: 21551334

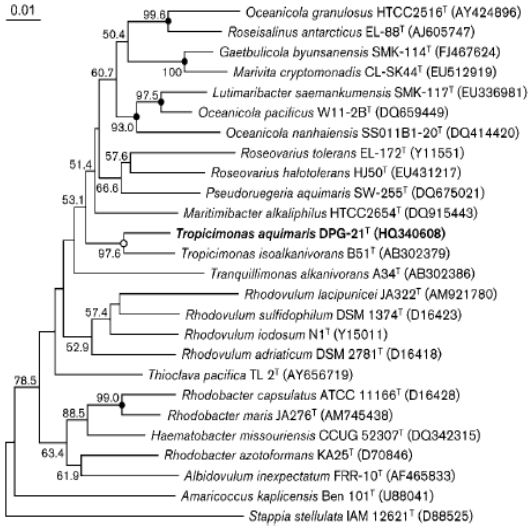

Keywords : Phenotypic property; Phylogenetic analysis; Seawater; *Tropicimonas aquimaris*

Article 39

Marivita hallyeonensis sp. nov., isolated from seawater, reclassification of *Gaetbulicola byunsanensis* as *Marivita byunsanensis* comb. nov. and emended description of the genus *Marivita* Hwang *et al.* 2009

Int J Syst Evol Microbiol. 62(Pt 4):839-43.

Yoon JH*, Kang SJ, Lee SY, Jung YT, Lee JS, Oh TK

*Corresponding:
Super-Bacteria Research Center

A Gram-stain-negative, non-motile, non-spore-forming, aerobic, rod-shaped bacterial strain, designated DPG-28T, was isolated from seawater on the southern coast of Korea. Strain DPG-28T grew optimally at 30 °C and in the presence of 2% (w/v) NaCl. Phylogenetic analysis based on 16S rRNA gene sequences revealed that strain DPG-28T formed a coherent cluster with members of the genera *Marivita* and *Gaetbulicola*, with which it exhibited sequence similarity values of 97.8-98.5%. The DNA G+C content of strain DPG-28T was 65.1 mol%. The predominant ubiquinone of strain DPG-28T was ubiquinone-10 (Q-10), consistent with data for the genera *Marivita* and Gaetbulicola. The cellular fatty acid profiles of strain DPG-28T and the type strains of *Marivita cryptomonadis*, *Marivita litorea* and *Gaetbulicola byunsanensis* were essentially similar in that the common predominant fatty acid was $C_{18:1}\omega7c$. Major polar lipids found in strain DPG-28T and the type strains of *M. cryptomonadis*, *M. litorea* and *G. byunsanensis* were phosphatidylcholine, phosphatidylglycerol, phosphatidylethanolamine and an unidentified aminolipid. From these data, it is proposed that *Gaetbulicola byunsanensis* be reclassified as a member of the genus *Marivita*, for which the name *Marivita byunsanensis* comb. nov. is proposed, with the type strain SMK-114T (=CCUG 57612T=KCTC 22632T), and that strain DPG-28T be classified in the genus *Marivita*. Differential phenotypic properties and genetic distinctiveness of strain DPG-28T demonstrated that this strain is distinguishable from *M. cryptomonadis*, *M. litorea* and *G. byunsanensis*. On the basis of the data presented, strain DPG-28T is considered to represent a novel species of the genus *Marivita*, for which the name *Marivita hallyeonensis* sp. nov. is proposed. The type strain is DPG-28T (=KCTC 23421T=CCUG 60522T). An emended description of the genus *Marivita* is also provided.
PMID: 21602362

Keywords : Cellular fatty acid profile; *Marivita hallyeonensis*; Phenotypic property; Phylogenetic analysis; Seawater

Article 40

Salinimicrobium gaetbulicola sp. nov., isolated from tidal flat sediment

Int J Syst Evol Microbiol. 62(Pt 5):1027-31.

Lee SY*, Park S, Oh TK, Yoon JH

*First:
Super-Bacteria Research Center

A Gram-stain-negative, aerobic, non-flagellated, non-gliding and short rod- or rod-shaped bacterial strain, designated BB-My20^T, was isolated from tidal flat sediment taken from the southern coast of Korea. Strain BB-My20^T grew optimally at 37 °C, at pH 7.0-7.5 and in the presence of 2% (w/v) NaCl. A phylogenetic tree based on 16S rRNA gene sequences showed that strain BB-My20^T fell within the clade comprising *Salinimicrobium* species, joining *Salinimicrobium catena* HY1^T, with which it had a 16S rRNA gene sequence similarity value of 97.4%. It exhibited 95.4-96.9% sequence similarity to the type strains of other members of the genus *Salinimicrobium*. Strain BB-My20^T contained MK-6 as the predominant menaquinone and iso-$C_{15:0}$, anteiso-$C_{15:0}$ and iso-$C_{17:0}$ 3-OH as the major fatty acids. The major polar lipids detected in strain BB-My20^T and *S. catena* JCM 14015^T were phosphatidylethanolamine and one unidentified lipid. The DNA G+C content of strain BB-My20^T was 45.1 mol% and its mean DNA-DNA relatedness value with *S. catena* JCM 14015^T was 4.5%. Differential phenotypic properties, together with its phylogenetic and genetic distinctiveness, revealed that strain BB-My20^T can be distinguished from the four recognized species of the genus *Salinimicrobium*. On the basis of the data presented, strain BB-My20^T is considered to represent a novel species of the genus *Salinimicrobium*, for which the name *Salinimicrobium gaetbulicola* sp. nov. is proposed; the type strain is BB-My20^T (=KCTC 23579^T=CCUG 60898^T).
PMID: 21685257

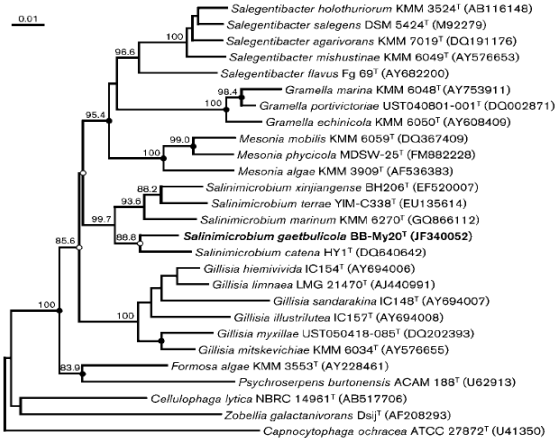

Keywords : Phenotypic property; Phylogenetic analysis; *Salinimicrobium gaetbulicola*; Tidal flat sediment

Article 41

Muricauda beolgyonensis sp. nov., isolated from a tidal flat

Int J Syst Evol Microbiol. 62(Pt 5):1134-9.

Lee SY*, Park S, Oh TK, Yoon JH

*First:
Super-Bacteria Research Center

The taxonomic position of a Gram-staining-negative, non-motile, rod-shaped bacterium, strain BB-My12^T, which was isolated from a sediment sample collected from a tidal flat in Korea, was investigated by using a polyphasic approach. Strain BB-My12^T grew optimally at 37 °C, at pH 7.0-7.5 and in the presence of 2-3% (w/v) NaCl. In phylogenetic analyses based on 16S rRNA gene sequences, strain BB-My12^T fell within the cluster comprising species of the genus *Muricauda* and appeared most similar to the type strains of *Muricauda aquimarina*, *Muricauda lutimaris* and *Muricauda ruestringensis* (97.5-97.6% sequence similarity). The DNA G+C content was 45.0 mol%. Strain BB-My12^T contained MK-6 as the predominant menaquinone and iso-$C_{15:1}$, iso-$C_{17:0}$ 3-OH and iso-$C_{15:0}$ as the major cellular fatty acids. The polar lipids of strain BB-My12^T were phosphatidylethanolamine and four unidentified lipids. The DNA-DNA relatedness values between strain BB-My12^T and the type strains of the three species of the genus *Muricauda* that appeared most closely related were in the range 5-7 %. The genetic distinctiveness and some phenotypic properties indicated that strain BB-My12^T did not belong to any established species of the genus *Muricauda*. Strain BB-My12^T is therefore considered to represent a novel species of the genus *Muricauda*, for which the name *Muricauda beolgyonensis* sp. nov. is proposed. The type strain is BB-My12^T (=KCTC 23501^T =CCUG 60800^T).
PMID: 21724956

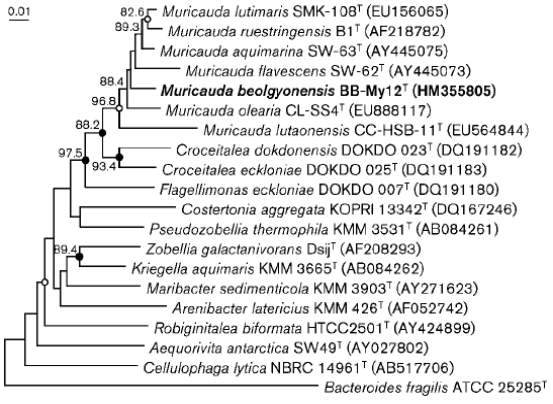

Keywords : *Muricauda beolgyonensis*; Phenotypic property; Phylogenetic analysis; Tidal flat sediment

Article 42

Cellulophaga geojensis sp. nov., a member of the family Flavobacteriaceae isolated from marine sand

Int J Syst Evol Microbiol. 62(Pt 6):1354-8.

Park S*, Oh KH, Lee SY, Oh TK, Yoon JH

*First:
Super-Bacteria Research Center

A Gram-stain-negative, aerobic, non-flagellated, non-spore-forming, motile (by gliding) bacterial strain, designated M-M6^T, was isolated from marine sand of Geoje island, Korea. Strain M-M6^T grew optimally at 25 °C, at pH 7.0-8.0 and in the presence of 2 % (w/v) NaCl. Phylogenetic analyses based on 16S rRNA gene sequences revealed that strain M-M6^T fell within the clade comprising *Cellulophaga* species, forming a coherent cluster with *Cellulophaga lytica* ATCC 23178^T and *Cellulophaga fucicola* NN015860^T, with which it shared 16S rRNA gene sequence similarities of 98.1 and 98.2 %, respectively. Sequence similarities between strain M-M6^T and the type strains of other recognized *Cellulophaga* species were in the range 92.4-93.8 %. Strain M-M6^T contained MK-6 as the predominant menaquinone and iso-$C_{15:0}$, iso-$C_{15:1}$ G, iso-$C_{17:0}$ 3-OH, and $C_{16:1}\omega7c$ and/or iso-$C_{15:0}$ 2-OH as the major fatty acids. The major polar lipids detected in strain M-M6^T and the type strains of *C. lytica* and *C. fucicola* were two unidentified lipids, one unidentified aminolipid and one unidentified aminophospholipid. The DNA G+C content of strain M-M6^T was 35.4 mol%. Levels of DNA-DNA relatedness between strain M-M6^T and *C. lytica* JCM 8516^T and *C. fucicola* JCM 21778^T were 33 and 35 %, respectively. Differential phenotypic properties and phylogenetic and genetic distinctiveness distinguished strain M-M6^T from all recognized *Cellulophaga* species. On the basis of the data presented, strain M-M6^T is considered to represent a novel species of the genus *Cellulophaga*, for which the name *Cellulophaga geojensis* sp. nov. is proposed. The type strain is M-M6^T (= KCTC 23498^T = CCUG 60801^T).
PMID: 21828016

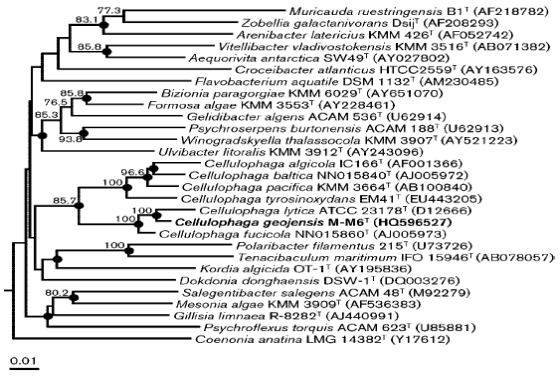

Keywords : *Cellulophaga geojensis*; Marine sand; Phenotypic property; Phylogenetic analysis

Article 43

Celeribacter baekdonensis sp. nov., isolated from seawater, and emended description of the genus *Celeribacter* Ivanova *et al.* 2010

Int J Syst Evol Microbiol. 62(Pt 6):1359-64.

Lee SY*, Park S, Oh TK, Yoon JH

*First:
Super-Bacteria Research Center

A Gram-stain-negative, non-motile, ovoid or rod-shaped bacterial strain, designated L-6^T, was isolated from seawater of Baekdo harbour of the East Sea in Korea and its taxonomic position was investigated by using a polyphasic study. Strain L-6^T grew optimally at 30 °C, at pH 7.5-8.0 and in the presence of 2 % (w/v) NaCl. In the neighbour-joining phylogenetic tree based on 16S rRNA gene sequences, strain L-6^T formed a cluster with the type strain of *Celeribacter neptunius* at a bootstrap resampling value of 100 %. Strain L-6^T exhibited 16S rRNA gene sequence similarity values of 97.7 % to *C. neptunius* H 14^T and of less than 96.2 % to the type strains of other species used in the phylogenetic analysis. The G+C content of the chromosomal DNA of strain L-6^T was 60.9 mol%. The predominant ubiquinone found in strain L-6^T and *C. neptunius* CIP 109922^T was ubiquinone-10 (Q-10). The predominant fatty acid of strain L-6^T and *C. neptunius* CIP 109922^T was $C_{18:1}\omega7c$. The major polar lipids of strain L-6^T were phosphatidylglycerol, one unidentified aminolipid and one unidentified lipid. The mean level of DNA-DNA relatedness between strain L-6^T and *C. neptunius* CIP 109922^T was 17 %. Differential phenotypic properties, together with phylogenetic and genetic distinctiveness, demonstrated that strain L-6^T is distinguishable from *C. neptunius*. On the basis of the data presented, strain L-6^T is considered to represent a novel species of the genus *Celeribacter*, for which the name *Celeribacter baekdonensis* sp. nov. is proposed. The type strain is L-6^T (= KCTC 23497^T = CCUG 60799^T).

PMID: 21828017

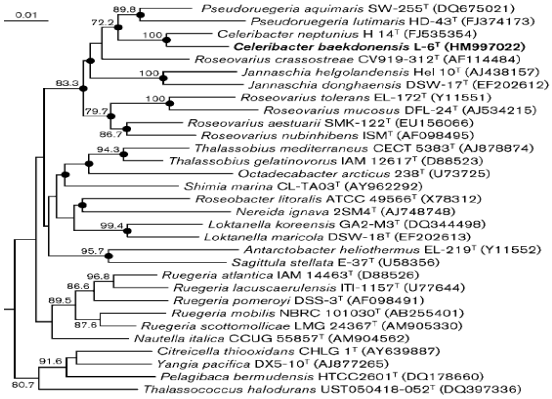

Keywords : *Celeribacter baekdonensis*; Phenotypic property; Phylogenetic analysis; Seawater

Article 44

Mesonia ostreae sp. nov., isolated from seawater of an oyster farm, and emended description of the genus *Mesonia*

Int J Syst Evol Microbiol. 62(Pt 8):1804-8.

Lee SY*, Lee MH, Yoon JH

*First:
Super-Bacteria Research Center

A Gram-negative, aerobic, non-flagellated, non-gliding rod, designated T-y2^T, was isolated from seawater of an oyster farm in the South Sea, Korea. Strain T-y2^T grew optimally at 25 °C, at pH 7.0-7.5 and with 2% (w/v) NaCl. Phylogenetic analysis based on 16S rRNA gene sequences showed that strain T-y2^T belonged to the genus *Mesonia* and exhibited 94.3-96.4% 16S rRNA gene sequence similarity with the type strains of species of the genus *Mesonia*. The DNA G+C content of strain T-y2^T was 42.1 mol%. Strain T-y2^T contained MK-6 as the predominant menaquinone and anteiso-$C_{15:0}$ and iso-$C_{15:0}$ as the major fatty acids. The only major phospholipid identified was phosphatidylethanolamine. The differential phenotypic properties and phylogenetic distinctiveness of strain T-y2^T revealed that it is distinguishable from recognized members of the genus *Mesonia*. On the basis of the data presented here, strain T-y2^T is considered to represent a novel species of the genus *Mesonia*, for which the name *Mesonia ostreae* sp. nov. is proposed. The type strain is T-y2^T (=KCTC 23500^T =CCUG 60802^T).

PMID: 21984667

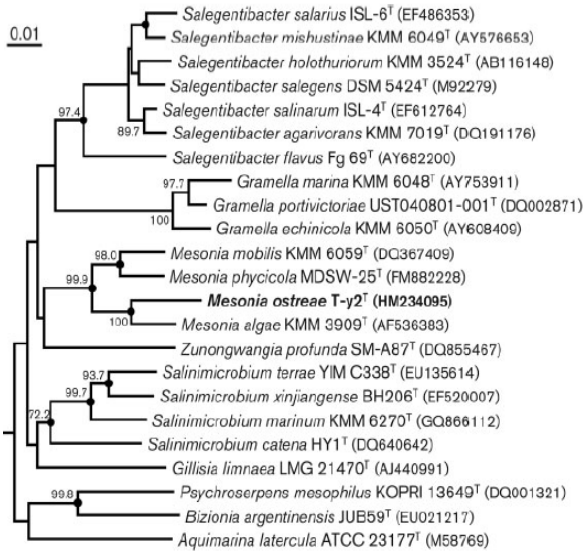

Keywords : *Mesonia ostreae* ; Phenotypic property; Phylogenetic analysis; Seawater

Article 45

Winogradskyella aquimaris sp. nov., isolated from seawater

Int J Syst Evol Microbiol. 62(Pt 8):1814-8.

Lee SY*, Park S, Oh TK, Yoon JH

*First:
Super-Bacteria Research Center

A Gram-negative, non-flagellated, motile by gliding, aerobic rod, designated DPG-24^T, was isolated from seawater of Geoje Island in the South Sea, Korea. Strain DPG-24^T grew optimally at 30-37 °C, at pH 7.0-7.5 and with 2% (w/v) NaCl. Phylogenetic analysis based on 16S rRNA gene sequences showed that strain DPG-24^T belonged to the genus *Winogradskyella* and clustered with *Winogradskyella poriferorum* UST030701-295^T and *Winogradskyella exilis* 022-2-26^T. Strain DPG-24^T exhibited 97.6 and 95.8% 16S rRNA gene sequence similarities with *W. poriferorum* UST030701-295^T and *W. exilis* 022-2-26^T, respectively, and 92.4-95.7% with other members of the genus *Winogradskyella*. Strain DPG-24^T contained MK-6 as the predominant menaquinone and iso-$C_{15:1}$ G, iso-$C_{15:0}$ and iso-$C_{17:0}$ 3-OH as the major fatty acids. The major polar lipids were phosphatidylethanolamine, one unidentified lipid, one unidentified aminolipid and one unidentified phospholipid. The DNA G+C content was 36.7 mol%. DNA-DNA relatedness between the isolate and *W. poriferorum* JCM 12885^T was 10.8%. The differential phenotypic properties and phylogenetic and genetic distinctiveness enabled strain DPG-24^T to be differentiated from recognized members of the genus *Winogradskyella*. On the basis of the data presented, strain DPG-24^T is considered to represent a novel species of the genus *Winogradskyella*, for which the name *Winogradskyella aquimaris* sp. nov. is proposed; the type strain is DPG-24^T (=KCTC 23502^T =CCUG 60798^T).
PMID: 21984672

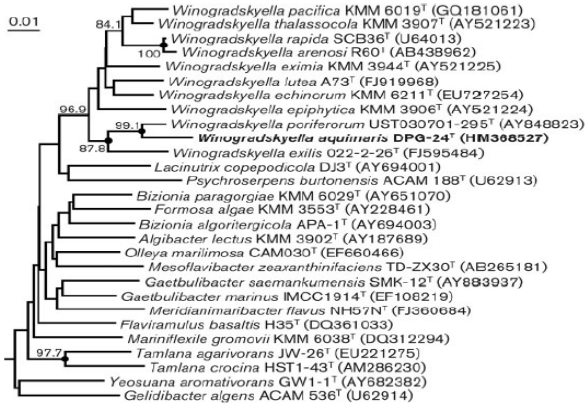

Keywords : Phenotypic property; Phylogenetic analysis; Seawater; *Winogradskyella aquimaris*

Article 46

Reclassification of the three species of the genus *Krokinobacter* into the genus *Dokdonia* as *Dokdonia genika* comb. nov., *Dokdonia diaphoros* comb. nov. and *Dokdonia eikasta* comb. nov., and emended description of the genus *Dokdonia* Yoon *et al.* 2005

Int J Syst Evol Microbiol. 62(Pt 8):1896-901.

Yoon JH*, Kang SJ, Park S, Oh TK

*Corresponding:
Super-Bacteria Research Center

The genera *Dokdonia* and *Krokinobacter*, members of the family *Flavobacteriaceae* in the phylum *Bacteroidetes*, were found to be phylogenetically closely related from the result of 16S rRNA gene sequence analysis. *Dokdonia donghaensis* DSW-1^T exhibited 16S rRNA gene sequence similarity values of 99.3, 98.1 and 98.1% to *Krokinobacter genikus* Cos-13^T, *Krokinobacter diaphorus* MSKK-32^T and *Krokinobacter eikastus* PMA-26^T, respectively. A taxonomic study of *D. donghaensis* DSW-1^T, *K. genikus* CIP 108744^T, *K. diaphorus* CIP 108745^T and *K. eikastus* CIP 108743^T was conducted using a polyphasic approach. The major fatty acids (>10% of the total fatty acids) in the four strains were iso-$C_{15:0}$, iso-$C_{15:1}$ G and iso-$C_{17:0}$ 3-OH, and their overall fatty acid profiles were essentially similar. The predominant menaquinone found in the type strains of the three species of the genus *Krokinobacter* was MK-6, in line with the genus *Dokdonia*. The polar lipid profiles of the type strains of the three species of the genus *Krokinobacter* were similar to that of *D. donghaensis* DSW-1^T in that phosphatidylethanolamine, one unidentified aminolipid and one unidentified lipid were the major polar lipids. In addition, one unidentified aminophospholipid was also present as a major polar lipid in *K. diaphorus* CIP 108745^T and *K. eikastus* CIP 108743^T. *D. donghaensis* DSW-1^T was distinguishable from *K. genikus* CIP 108744^T, *K. diaphorus* CIP 108745^T and *K. eikastus* CIP 108743^T by genetic relatedness and differential phenotypic properties. On the basis of these data, it is proposed that *K. genikus*, *K. diaphorus* and *K. eikastus* be reclassified into the genus *Dokdonia* as *Dokdonia genika* comb. nov. (type strain is Cos-13^T=NBRC 100811^T=CIP 108744^T), *Dokdonia diaphoros* comb. nov. (type strain is MSKK-32^T=NBRC 100817^T=CIP 108745^T), and *Dokdonia eikasta* comb. nov. (type strain is PMA-26^T=NBRC 100814^T =CIP 108743^T), respectively. An emended description of the genus *Dokdonia* is also presented.
PMID:21984677

Keywords : *Dokdonia diaphoros*; *Dokdonia eikasta*; *Dokdonia genika*; Phenotypic property; Phylogenetic analysis; Taxonomic study

Article 47

Erythrobacter marinus sp. nov., isolated from seawater

Int J Syst Evol Microbiol. 62(Pt 9):2050-5.

Jung YT*, Park S, Oh TK, Yoon JH

*First:
Super-Bacteria Research Center

A Gram-negative, non-motile, ovoid to rod-shaped bacterium, designated strain HWDM-33^T, was isolated from seawater of the Yellow Sea, Korea, and was subjected to a polyphasic taxonomic study. Strain HWDM-33^T grew optimally at pH 7-8, at 25 °C and in the presence of 2-3 % (w/v) NaCl. Neighbour-joining, maximum-likelihood and maximum-parsimony phylogenetic trees based on 16S rRNA gene sequences showed that strain HWDM-33^T clustered with *Erythrobacter gangjinensis* K7-2^T, with which it shared 96.9 % sequence similarity. Strain HWDM-33^T exhibited 94.2-95.8 % 16S rRNA gene sequence similarity to the type strains of other recognized species of the genus *Erythrobacter*. Strain HWDM-33^T contained Q-10 as the predominant ubiquinone and $C_{18:1}\omega7c$, $C_{17:1}\omega6c$, and $C_{16:1}\omega7c$ and/or iso-$C_{15:0}$ 2-OH as the major fatty acids. The major polar lipids were sphingoglycolipid, phosphatidylglycerol, phosphatidylcholine, phosphatidylethanolamine and an unidentified lipid. The DNA G+C content of strain HWDM-33^T was 66.1 mol%. Differential phenotypic properties and phylogenetic distinctiveness demonstrated that strain HWDM-33^T was separate from *E. gangjinensis* and other recognized species of the genus *Erythrobacter*. On the basis of the data presented here, strain HWDM-33^T represents a novel species of the genus *Erythrobacter*, for which the name *Erythrobacter marinus* sp. nov. is proposed. The type strain is HWDM-33^T (= KCTC 23554^T = CCUG 60528^T).

PMID: 22021578

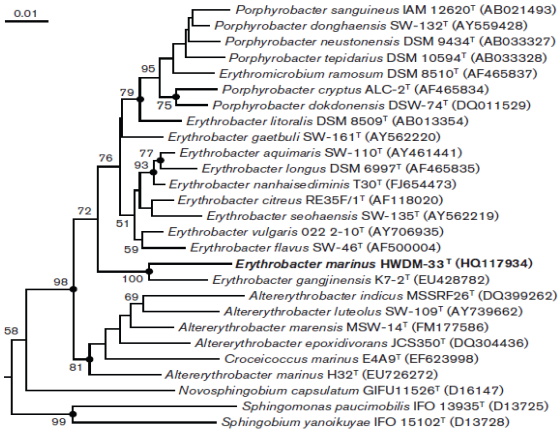

Keywords : *Erythrobacter marinus*; Phenotypic property; Phylogenetic analysis; Seawater

Article 48

Pseudahrensia aquimaris gen. nov., sp. nov., isolated from seawater

Int J Syst Evol Microbiol. 62(Pt 9):2056-61.

Jung YT*, Park S, Lee JS, Oh TK, Yoon JH

*First:
Super-Bacteria Research Center

A Gram-negative, non-motile, ovoid to rod-shaped bacterium, designated HDW-32^T, was isolated from seawater of the Yellow Sea, Korea. Strain HDW-32^T grew optimally at pH 7-8, at 30 °C and with 2-3 % (w/v) NaCl. Strain HDW-32^T exhibited 95.1 % 16S rRNA gene sequence similarity with *Nitratireductor basaltis* J3^T, 94.8 % sequence similarity with *Ahrensia kielensis* IAM 12618^T and <94.5 % with other members of the family *Phyllobacteriaceae*. In the neighbour-joining, maximum-likelihood and maximum-parsimony trees based on 16S rRNA gene sequences, strain HDW-32^T clustered with *A. kielensis* IAM 12618^T. Strain HDW-32^T contained Q-10 as the predominant ubiquinone and $C_{18:1}\omega7c$ as the major fatty acid. Differences in polar lipids, DNA G+C content and other phenotypic properties distinguished strain HDW-32^T from *A. kielensis* JCM 20689^T. Strain HDW-32^T could also be distinguished from representatives of the genera *Nitratireductor* and *Hoeflea* by differences in fatty acids and polar lipids. On the basis of phylogenetic, chemotaxonomic and phenotypic data, strain HDW-32^T represents a novel species belonging to a novel genus of the family *Phyllobacteriaceae* of the class *Alphaproteobacteria*, for which the name *Pseudahrensia aquimaris* gen. nov., sp. nov. is proposed. The type strain of the type species is HDW-32^T (= KCTC 23345^T = CCUG 60023^T).

PMID: 22021581

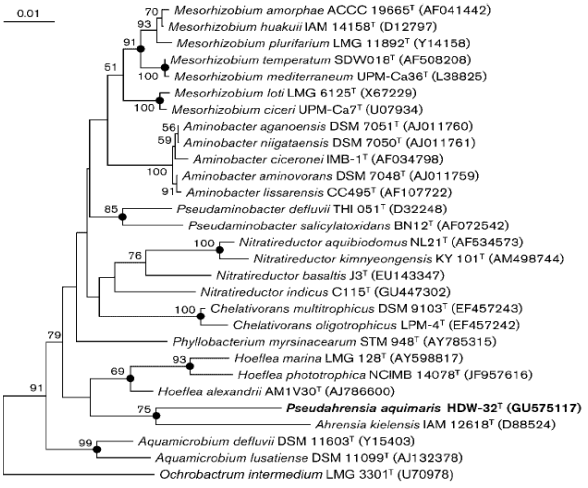

Keywords : Phenotypic property; Phylogenetic analysis; *Pseudahrensia aquimaris*; Seawater

Article 49

Marinomonas hwangdonensis sp. nov., isolated from seawater

Int J Syst Evol Microbiol. 62(Pt 9):2062-7.

Jung YT*, Oh TK, Yoon JH

*First:
Super-Bacteria Research Center

A Gram-negative, motile, rod-shaped bacterial strain, designated HDW-15^T, was isolated from seawater of the Yellow Sea, Korea, and subjected to a polyphasic taxonomic study. Strain HDW-15^T grew optimally at pH 7.0-8.0, at 25 °C and in the presence of 2 % (w/v) NaCl. Phylogenetic analyses based on 16S rRNA gene sequences revealed that strain HDW-15^T fell within the clade comprising *Marinomonas* species, joining the type strain of *Marinomonas arctica*, with which it exhibited highest 16S rRNA gene sequence similarity (97.7 %). The 16S rRNA gene sequence similarity values between strain HDW-15^T and the type strains of other *Marinomonas* species were in the range 93.7-97.2 %. Mean DNA-DNA relatedness values between strain HDW-15^T and the type strains of *M. arctica*, *Marinomonas polaris* and *Marinomonas pontica* were 5.0-9.9 %. The DNA G+C content of the isolate was 48.7 mol%. Strain HDW-15^T contained Q-8 as the predominant ubiquinone and $C_{18:1}\omega7c$, summed feature 3 ($C_{16:1}\omega7c$ and/or iso-$C_{15:0}$ 2-OH) and $C_{16:0}$ as the major fatty acids. The major polar lipids found in strain HDW-15^T were phosphatidylglycerol and phosphatidylethanolamine. Differential phenotypic properties, together with phylogenetic and genetic distinctiveness, showed that strain HDW-15^T can be differentiated from other *Marinomonas* species. On the basis of the data presented, strain HDW-15^T is considered to represent a novel species of the genus *Marinomonas*, for which the name *Marinomonas hwangdonensis* sp. nov. is proposed. The type strain is HDW-15^T (= KCTC 23661^T = CCUG 61321^T).
PMID: 22021582

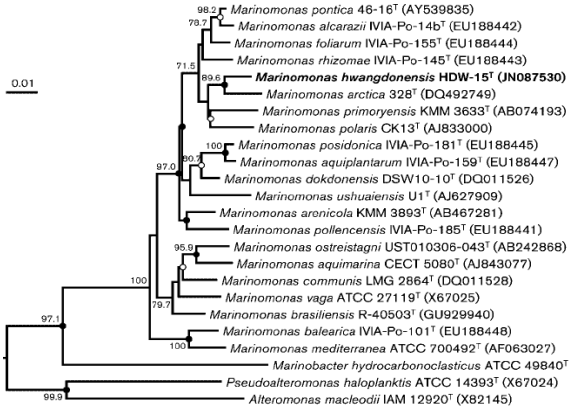

Keywords : *Marinomonas hwangdonensis*; Phenotypic property; Phylogenetic analysis; Seawater

Article 50

Namhaeicola litoreus gen. nov., sp. nov., a member of the family *Flavobacteriaceae* isolated from seawater

Int J Syst Evol Microbiol. 62(Pt 9):2163-8.

Jung YT*, Kim JH, Kang SJ, Oh TK, Yoon JH

*First:
Super-Bacteria Research Center

A Gram-staining-negative, non-flagellated, non-gliding and pleomorphic bacterial strain, designated DPG-25^T, was isolated from seawater in a seaweed farm in the South Sea in Korea and its taxonomic position was investigated by using a polyphasic approach. Strain DPG-25^T grew optimally at 25 °C, at pH 7.0-7.5 and in the presence of 2 % (w/v) NaCl. Flexirubin-type pigments were not produced. Phylogenetic analyses based on 16S rRNA gene sequences revealed that strain DPG-25^T formed a cluster with the type strains of *Actibacter sediminis*, *Aestuariicola saemankumensis* and *Lutimonas vermicola*. Strain DPG-25^T exhibited 16S rRNA gene sequence similarity values of 95.3, 93.1 and 93.6% to the type strains of *Actibacter sediminis*, *Aestuariicola saemankumensis* and *L. vermicola*, respectively. Strain DPG-25^T contained MK-6 as the predominant menaquinone and iso-$C_{15:0}$ and iso-$C_{17:0}$ 3-OH as the major fatty acids. The major polar lipids detected in strain DPG-25^T were phosphatidylethanolamine and one unidentified lipid. The DNA G+C content was 39.9 mol%. Differential phenotypic properties and the phylogenetic distinctiveness of strain DPG-25^T demonstrated that this strain is distinguishable from *Actibacter sediminis*, *Aestuariicola saemankumensis* and *L. vermicola*. On the basis of the data presented here, strain DPG-25^T represents a novel species in a novel genus of the family *Flavobacteriaceae*, for which the name *Namhaeicola litoreus* gen. nov., sp. nov. is proposed. The type strain of *Namhaeicola litoreus* is DPG-25^T (= KCTC 23702^T = CCUG 61485^T).
PMID: 22058323

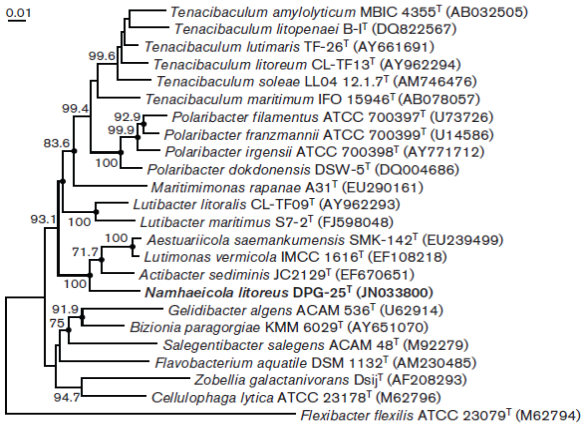

Keywords : *Namhaeicola litoreus*; Phenotypic property; Phylogenetic analysis; Seawater

Article 51

Distinct roles of β-galactosidase paralogues of the rumen bacterium *Mannheimia succiniciproducens*

J Bacteriol. 194(2):426-36.

Lee EG, Kim S, Oh DB, Lee SY, Kwon O*

*Corresponding: oskwon@kribb.re.kr
Biochemicals & Synthetic Biology Research Center

Mannheimia succiniciproducens, a rumen bacterium belonging to the family *Pasteurellaceae*, has two putative β-galactosidase genes, *bgaA* and *bgaB*, encoding polypeptides whose deduced amino acid sequences share 56% identity with each other and show approximately 30% identity to the *Escherichia coli* gene for LacZ. The *M. succiniciproducens bgaA* (*MsbgaA*) gene-deletion mutant was not able to grow on lactose as the sole carbon source, suggesting its essential role in lactose metabolism, whereas the *MsbgaB* gene-deletion mutant did not show any growth defect on a lactose medium. Furthermore, the expression of the *MsbgaA* gene was induced by the addition of lactose in the growth medium, whereas the *MsbgaB* gene was constitutively expressed independently of a carbon source. Biochemical characterization of the recombinant proteins revealed that MsBgaA is more efficient than MsbgaB in hydrolyzing o-nitrophenyl-β-d-galactopyranoside and *p*-nitrophenyl-β-d-galactopyranoside. MsBgaA was highly specific for the hydrolysis of lactose, with a catalytic efficiency of 46.9 s^{-1} mM^{-1}. However, MsBgaB was more efficient for the hydrolysis of lactulose than lactose, and the catalytic efficiency was 10.0 s^{-1} mM^{-1}. Taken together, our results suggest that the β-galactosidase paralogues of *M. succiniciproducens* BgaA and BgaB play a critical role in lactose metabolism and in an unknown but likely specific function for rumen bacteria, respectively.

PMID: 22081396

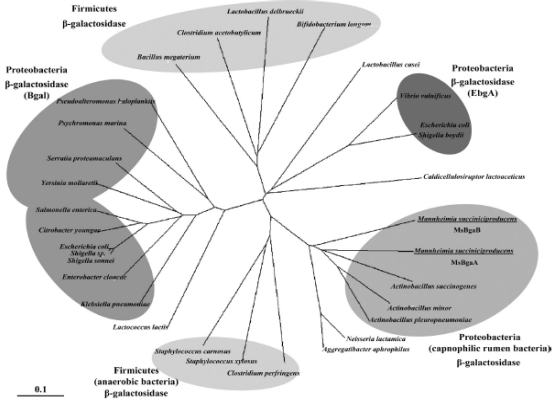

Keywords : Encoding polypeptide; Lactose metabolism; *Mannheimia succiniciproducens*;

Article 52

Genome sequence of enterohemorrhagic *Escherichia coli* NCCP15658

J Bacteriol. 194(14):3749-50.

Song JY*, Yoo RH, Jang SY, Seong WK, Kim SY, Jeong H, Kang SG, Kim BK, Kwon SK, Lee CH, Yu DS, Park MS, Cho SH, Kim JF

*First:
Super-Bacteria Research Center

Enterohemorrhagic *Escherichia coli* causes severe food-borne disease in the guts of humans and animals. Here, we report the high-quality draft genome sequence of *E. coli* NCCP15658 isolated from a patient in the Republic of Korea. Its genome size was determined to be 5.46 Mb, and its genomic features, including genes encoding virulence factors, were analyzed.

PMID:22740673

Keywords : Enterohemorrhagic *Escherichia coli*; Food-borne disease; Genome sequence

Article 53

Genome sequence of the Shiga toxin-producing *Escherichia coli* strain NCCP15657

J Bacteriol. 194(14):3751-2.

Kim BK*, Song GC, Hong GH, Seong WK, Kim SY, Jeong H, Kang SG, Kwon SK, Lee CH, Song JY, Yu DS, Park MS, Cho SH, Kim JF

*First:
Super-Bacteria Research Center

Shiga toxin-producing *Escherichia coli* causes bloody diarrhea and hemolytic-uremic syndrome and serious outbreaks worldwide. Here, we report the draft genome sequence of *E. coli* NCCP15657 isolated from a patient. The genome has virulence genes, many in the locus of enterocyte effacement (LEE) island, encoding a metalloprotease, the Shiga toxin, and constituents of type III secretion.

PMID:22740674

Keywords : Bloody diarrhea; Genome sequence; Shiga toxin-producing *Escherichia coli*

Article 54

Genome sequence of the leaf-colonizing Bacterium *Bacillus* sp. strain 5B6, isolated from a cherry tree

J Bacteriol. 194(14):3758-9.

Kim BK, Chung JH, Kim SY, Jeong H, Kang SG, Kwon SK, Lee CH, Song JY, Yu DS, Ryu CM*, Kim JF

*Corresponding: cmryu@kribb.re.kr
Super-Bacteria Research Center

Plant growth-promoting bacteria colonize various habitats, including the phyllosphere. Here, we present the high-quality draft genome sequence of *Bacillus* sp. strain 5B6, which was isolated from the leaf of a cherry tree. The 3.9-Mb genome uncovers its potential for understanding the nature of leaf colonization as well as antibiosis against plant pathogens.
PMID:22740678

Keywords : Antibiosis; Genome sequence; Leaf-colonizing bacterium *Bacillus*

Article 55

Genome sequence of an oligohaline hyperthermophilic archaeon, *Thermococcus zilligii* AN1, isolated from a terrestrial geothermal freshwater spring

J Bacteriol. 194(14):3765-6.

Kim BK*, Lee SH, Kim SY, Jeong H, Kwon SK, Lee CH, Song JY, Yu DS, Kang SG, Kim JF

*First:
Super-Bacteria Research Center

Thermococcus zilligii, a thermophilic anaerobe in freshwater, is useful for physiological research and biotechnological applications. Here we report the high-quality draft genome sequence of *T. zilligii* AN1^T. The genome contains a number of genes for an immune system and adaptation to a microbial biomass-rich environment as well as hydrogenase genes.
PMID:22740682

Keywords : Genome sequence; Immune system; *Thermococcus zilligii*; Thermophilic anaerobe

Article 56

Draft genome sequence of the plant growth-promoting bacterium *Bacillus siamensis* KCTC 13613T

J Bacteriol. 194(15):4148-9.

Jeong H, Jeong DE, Kim SH, Song GC, Park SY, Ryu CM, Park SH, Choi SK*

*Corresponding: sookeun@kribb.re.kr
Super-Bacteria Research Center

Bacillus siamensis KCTC 13613^T, a novel halophilic *Bacillus* species isolated from a salted Thai food, produced antimicrobial compounds against plant pathogens and promoted plant growth by volatile emission. We determined the 3.8-Mb genome sequence of *B. siamensis* KCTC 13613^T to reveal the plant-beneficial effect at the genomic level.
PMID: 22815459

Keywords : Antimicrobial compound; *Bacillus siamensis*; Genome sequence; Plant-beneficial effect

Article 57

Complete genome sequence of the endophytic bacterium *Burkholderia* sp. strain KJ006

J Bacteriol. 194(16):4432-3.

Kwak MJ, Song JY, Kim SY, Jeong H, Kang SG, Kim BK, Kwon SK, Lee CH, Yu DS, Park SH*, Kim JF

*Corresponding: shpark@kribb.re.kr
Super-Bacteria Research Center

Endophytes live inside plant tissues without causing any harm and may even benefit plants. Here, we provide the high-quality genome sequence of *Burkholderia* sp. strain KJ006, an endophytic bacterium of rice with antifungal activity. The 6.6-Mb genome, consisting of three chromosomes and a single plasmid, contains genes related to plant growth promotion or degradation of aromatic compounds.
PMID:22843575

Keywords : Endophytic bacterium *Burkholderia*; Genome sequence; Plant growth promotion

Article 58

Probing the ArcA regulon in the rumen bacterium *Mannheimia succiniciproducens* by genome-wide expression profiling

J Microbiol. 50(4):665-72.

Yun S, Shin JM, Kim OC, Jung YR, Oh DB, Lee SY, Kwon O*

*Corresponding: oskwon@kribb.re.kr
Biochemicals & Synthetic Biology Research Center

In this study, the putative target genes of the Arc two-component system of the rumen bacterium *Mannheimia succiniciproducens* were determined by analyzing the transcriptome of the ArcA overexpression strain and by the *in silico* scanning of the entire genome sequence with the position weight matrix of the ArcA binding sequence developed for *Escherichia coli*. The majority of 79 repressed genes were involved in energy metabolism and carbohydrate transport and metabolism, while the majority of 82 induced genes were involved in hypothetical or unknown functions. Our results suggest that the Arc system in *M. succiniciproducens* has a specific function that differs from that in *E. coli*.

PMID: 22923117

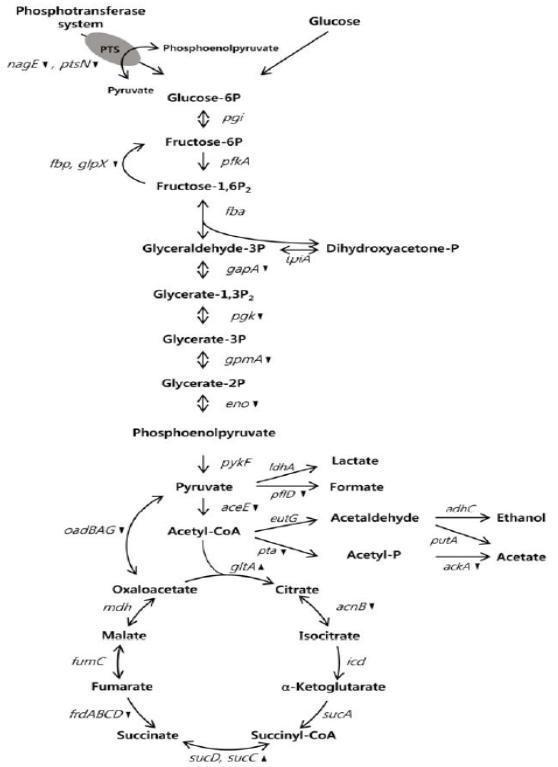

Keywords : ArcA response regulator; *Mannheimia succiniciproducens*; Target genes; Two-component signal transduction system

Article 59

Genome-wide enrichment screening reveals multiple targets and resistance genes for triclosan in *Escherichia coli*

J Microbiol. 50(5):785-91.

Yu BJ, Kim JA, Ju HM, Choi SK, Hwang SJ, Park S, Kim E, Pan JG*

*Corresponding: jgpan@kribb.re.kr
Super-Bacteria Research Center

Triclosan is a widely used biocide effective against different microorganisms. At bactericidal concentrations, triclosan appears to affect multiple targets, while at bacteriostatic concentrations, triclosan targets FabI. The site-specific antibiotic-like mode-of-action and a widespread use of triclosan in household products claimed to possibly induce cross-resistance to other antibiotics. Thus, we set out to define more systematically the genes conferring resistance to triclosan; A genomic library of *Escherichia coli* strain W3110 was constructed and enriched in a selective medium containing a lethal concentration of triclosan. The genes enabling growth in the presence of triclosan were identified by using a DNA microarray and confirmed consequently by ASKA clones overexpressing the selected 62 candidate genes. Among these, forty-seven genes were further confirmed to enhance the resistance to triclosan; these genes, including the FabI target, were involved in inner or outer membrane synthesis, cell-surface material synthesis, transcriptional activation, sugar phosphotransferase (PTS) systems, various transporter systems, cell division, and ATPase and reductase/dehydrogenase reactions. In particular, overexpression of *pgsA*, *rcsA*, or *gapC* conferred to *E. coli* cells a similar level of triclosan resistance induced by *fabI* overexpression. These results indicate that triclosan may have multiple targets other than well-known FabI and that there are several undefined novel mechanisms for the resistance development to triclosan, thus probably inducing cross antibiotic resistance.

PMID: 23124746

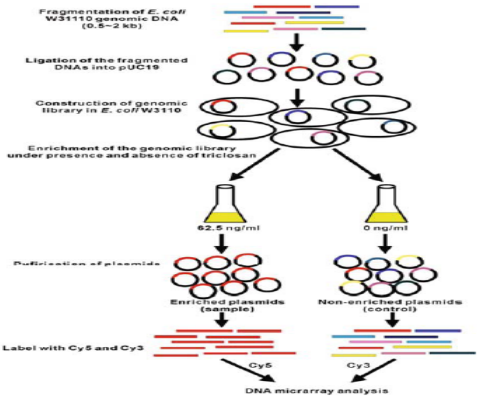

Keywords : *E. coli*; Genomic library; Multiple targets; Resistance; Triclosan

Article 60

Flavimycins A and B, dimeric 1,3-dihydroisobenzofurans with peptide deformylase inhibitory activity from *Aspergillus flavipes*

J Nat Prod. 75(2):271-4.

Kwon YJ, Sohn MJ, Kim CJ, Koshino H, Kim WG*

*Corresponding: wgkim@kribb.re.kr
Super-Bacteria Research Center

Flavimycins A (1) and B (2), novel dimeric 1,3-dihydroisobenzofurans, were isolated as inhibitors of peptide deformylase from cultures of *Aspergillus flavipes*. Their chemical structures were established by NMR and MS data analysis. Compounds 1 and 2 exist as epimeric mixtures at C-1 through fast hemiacetal-aldehyde tautomerism. Compounds 1 and 2 inhibited *Staphylococcus aureus* peptide deformylase with IC_{50} values of 35.8 and 100.1 μM, respectively. Consistent with their PDF inhibition, 1 showed two times stronger antibacterial activity than 2 on *S. aureus* including MRSA, with MIC values of 32-64 μg/mL.
PMID: 22329646

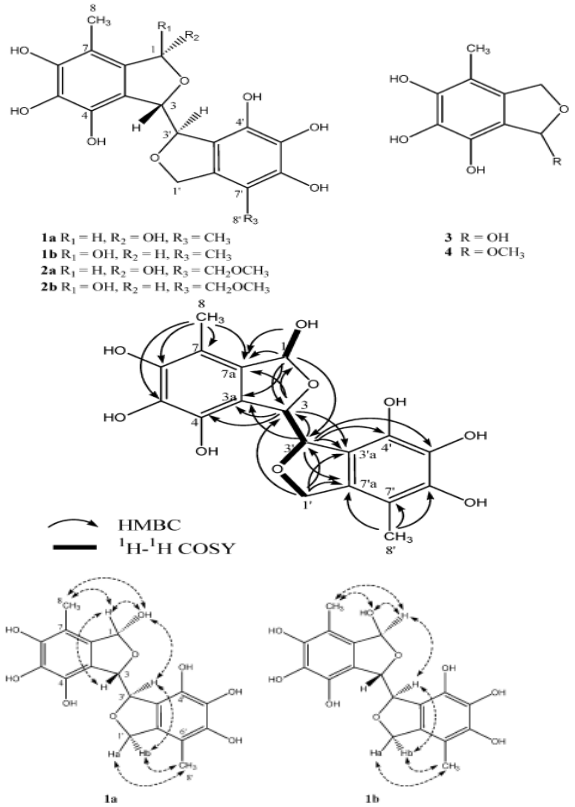

Keywords : Antibacterial activity; *Aspergillus flavipes*; Flavimycins; PDF inhibition; Peptide deformylase

Article 61

Mesh-integrated microdroplet array for simultaneous merging and storage of single-cell droplets

Lab Chip. 12(9):1594-7.

Um E, Rha E, Choi SL, Lee SG*, Park JK

*Co-corresponding: sglee@kribb.re.kr
Biochemicals & Synthetic Biology Research Center

We constructed a mesh-grid integrated microwell array which enables easy trapping and consistent addition of droplets. The grid acts as a microchannel structure to guide droplets into the microwells underneath, and also provides open access for additional manipulation in a high-throughput manner. Each droplet in the array forms a stable environment of pico-litre volume to implement a single-cell-based assay.
PMID:22422143

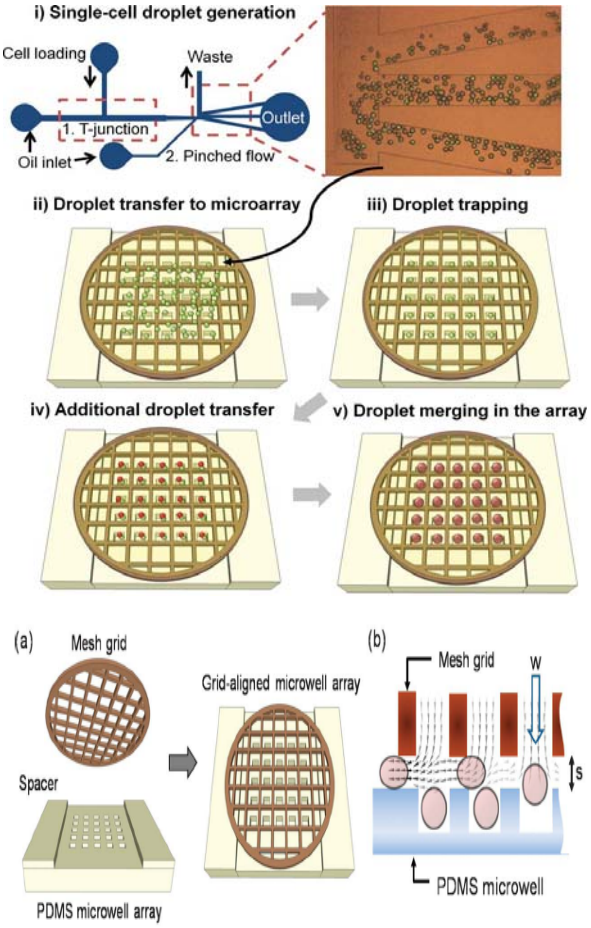

Keywords : Microchannel structure; Microdroplet array; Single-cell-based assay; Single-cell droplet

Article 62

Hybrid polymeric nanomaterials for siRNA delivery and imaging

Macromol Biosci. 12(1):40-8.

Mok H*, Park TG

*Corresponding:
BioNanotechnology Research Center

A combined nanomaterials-based approach for simultaneous therapy and molecular imaging has powerful potential for efficient treatment and monitoring the prognosis of incurable diseases such as malignant tumors or degenerative diseases. Recent developments of hybrid polymeric nanomaterials for siRNA delivery and imaging are highlighted. A particular focus is on various conjugation and formulation strategies of how to incorporate siRNA and imaging agents onto the surface of functionally active polymer-coated inorganic nanomaterials such as iron oxide, gold, and quantum-dot nanoparticles for theranostic applications. These multifunctional nanocarriers may allow real-time tracking of siRNA as well as visualization of its therapeutic effects *in vitro* and *in vivo*.

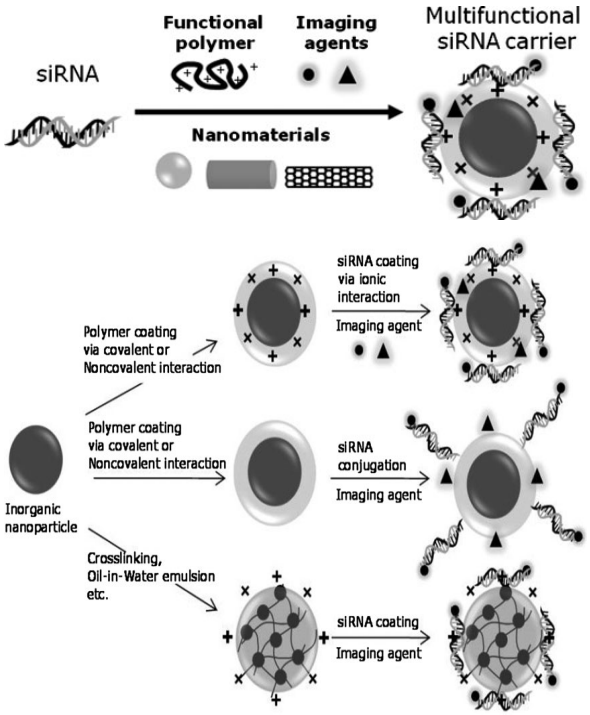

Keywords : Cancer therapy; Degenerative disease; Drug delivery; Imaging agent; Inorganic nanomaterials; Malignant tumors; Multi-functional nanocarriers; Nanomaterials; SiRNA

Article 63

Benzothiadiazole-elicited defense priming and systemic acquired resistance against bacterial and viral pathogens of pepper under field conditions

Plant Biotech Rep. 6(4):373-80.

Yi HS, Yang JW, Choi HK, Ghim SY, Ryu CM*

*Corresponding: cmryu@kribb.re.kr
Super-Bacteria Research Center

Like the innate immunity in mammals, plants have developed an induced resistance, referred to as systemic acquired resistance (SAR). Recently, defense priming that is not related to the direct activation of defenses, but instead elicits more rapid induction of resistance mechanisms following trigger application, has been proposed to explain the long-lasting effect of SAR. However, the majority of previous studies have focused on understanding the molecular mechanism underlying priming under *in vitro* and laboratory conditions. This study examined whether defense priming occurred and was detectable with SAR marker genes by a chemical elicitor, benzothiadiazole (BTH), under field conditions. Pepper seedling application of 0.5 mM BTH was sufficient to prime the *CaPR4* gene for 20 days as well as to induce SAR against bacterial spot caused by *Xanthomonas axonopodis*. Transcriptome analysis revealed to prime defense hormonal signaling and antimicrobial compound production genes. At the end of the season, when bacterial spot and *Cucumber mosaic virus* disease outbreaks naturally occurred, BTH-treated plants demonstrated less disease symptoms. Our results indicate that the priming of SAR genes plays a critical role in plant protection against pathogens under natural conditions.

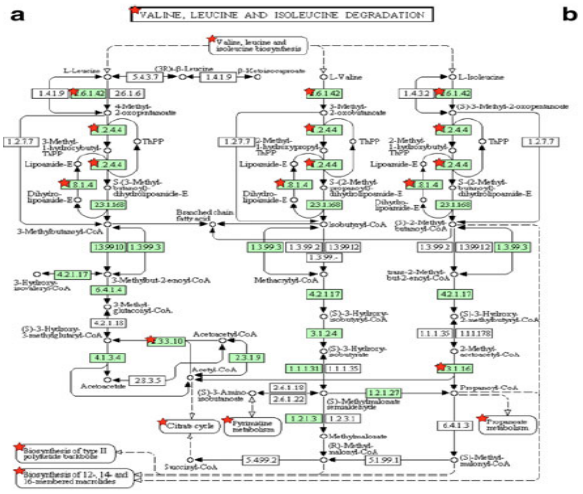

Keywords : BTH; Defense priming; ISR; Pepper; PGPR; Plant protection; SAR

Article 64

Minibrain/Dyrk1a regulates food intake through the Sir2-FOXO-sNPF/NPY pathway in *Drosophila* and mammals

PLoS Genet. 8(8):e1002857.

Hong SH, Lee KS, Kwak SJ, Kim AK, Bai H, Jung MS, Kwon OY, Song WJ, Tatar M, Yu K*

*Corresponding: kweonyu@kribb.re.kr
BioNanotechnology Research Center

Feeding behavior is one of the most essential activities in animals, which is tightly regulated by neuroendocrine factors. *Drosophila melanogaster* short neuropeptide F (sNPF) and the mammalian functional homolog neuropeptide Y (NPY) regulate food intake. Understanding the molecular mechanism of sNPF and NPY signaling is critical to elucidate feeding regulation. Here, we found that *minibrain* (*mnb*) and the mammalian ortholog *Dyrk1a*, target genes of sNPF and NPY signaling, [corrected] regulate food intake in *Drosophila melanogaster* and mice. In *Drosophila melanogaster* neuronal cells and mouse hypothalamic cells, sNPF and NPY modulated the *mnb* and *Dyrk1a* expression through the PKA-CREB pathway. Increased Dyrk1a activated Sirt1 to regulate the deacetylation of FOXO, which potentiated FOXO-induced *sNPF/NPY* expression and in turn promoted food intake. Conversely, AKT-mediated insulin signaling suppressed FOXO-mediated *sNPF/NPY* expression, which resulted in decreasing food intake. Furthermore, human *Dyrk1a* transgenic mice exhibited decreased FOXO acetylation and increased *NPY* expression in the hypothalamus, and [corrected] increased food intake. Our findings demonstrate that Mnb/Dyrk1a regulates food intake through the evolutionary conserved Sir2-FOXO-sNPF/NPY pathway in *Drosophila melanogaster* and mammals.
PMID: 22876196

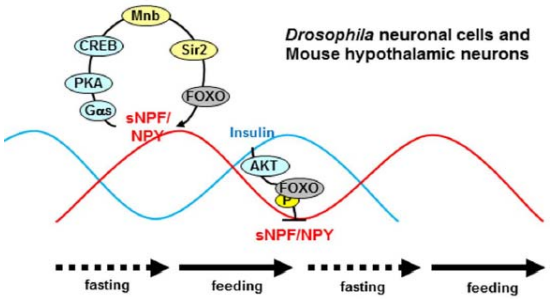

Keywords : AKT-mediated insulin; *Drosophila melanogaster* short neuropeptide F (sNPF); Food intake; Mammalian functional homolog neuropeptide Y (NPY)

Article 65

Induced resistance by a long-chain bacterial volatile: elicitation of plant systemic defense by a C13 volatile produced by *Paenibacillus polymyxa*

PLoS One. 7(11):e48744.

Lee B, Farag MA, Park HB, Kloepper JW, Lee SH, Ryu CM*

*Corresponding: cmryu@kribb.re.kr
Super-Bacteria Research Center

BACKGROUND: Some strains of plant growth-promoting rhizobacteria (PGPR) elicit induced systemic resistance (ISR) by emission of volatile organic compounds (VOCs) including short chain alcohols, acetoin, and 2,3-butanediol. The objective of this study was to evaluate whether species-specific VOCs from PGPR strain *Paenibacillus polymyxa* E681 can promote growth and induce resistance in *Arabidopsis*.
METHODOLOGY/PRINCIPAL FINDINGS: The efficacy of induction was strain-specific, with stronger protection against *Pseudomonas syringae* pv. maculicola ES4326 in plants exposed to VOCs from *P. polymyxa* E681 versus *Arabidopsis* plants exposed to VOCs from a reference strain *Bacillus subtilis* GB03, which was previously shown to elicit ISR and plant growth promotion. VOC emissions released from E681 primed transcriptional expression of the salicylic acid, jasmonic acid, and ethylene signaling marker genes *PR1*, *ChiB*, and *VSP2*, respectively. In addition, strain E681 produced more than thirty low molecular-weight VOCs, of which tridecane was only produced by E681 and not found in GB03 or IN937a volatile blends. These strain-specific VOCs induced *PR1* and *VSP2* genes.
CONCLUSIONS/SIGNIFICANCE: These results provide new insight into the existence of a long chain VOC signaling molecule produced by *P. polymyxa* that can serve as a bacterial trigger of induced systemic resistance *in planta*.
PMID: 23209558

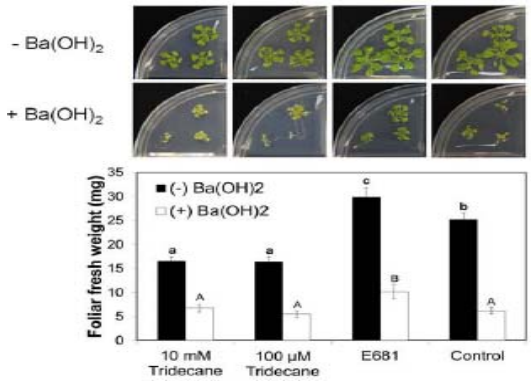

Keywords : Bacterial trigger; Induced systemic resistance (ISR); Plant growth-promoting rhizobacteria (PGPR); Volatile organic compounds (VOCs)

Article 66

High-throughput screening system based on phenolics-responsive transcription activator for directed evolution of organophosphate-degrading enzymes

Protein Eng Des Sel. 25(11):725-31.

Jeong YS, Choi SL, Kyeong HH, Kim JH, Kim EJ, Pan JG, Rha E, Song JJ, Lee SG*, Kim HS

*Co-corresponding: sglee@kribb.re.kr
Biochemicals & Synthetic Biology Research Center

Synthetic organophosphates (OPs) have been used as nerve agents and pesticides due to their extreme toxicity and have caused serious environmental and human health problems. Hence, effective methods for detoxification and decontamination of OPs are of great significance. Here we constructed and used a high-throughput screening (HTS) system that was based on phenolics-responsive transcription activator for directed evolution of OP-degrading enzymes. In the screening system, phenolic compounds produced from substrates by OP-degrading enzymes bind a constitutively expressed transcription factor DmpR, initiating the expression of enhanced green fluorescent protein located at the downstream of the DmpR promoter. Fluorescence intensities of host cells are proportional to the levels of phenolic compounds, enabling the screening of OP-degrading enzymes with high catalytic activities by fluorescence-activated cell sorting. Methyl parathion hydrolase from *Pseudomonas* sp. WBC-3 and *p*-nitrophenyl diphenylphosphate were used as a model enzyme and an analogue of G-type nerve agents, respectively. The utility of the screening system was demonstrated by generating a triple mutant with a 100-fold higher k_{cat}/K_m than the wild-type enzyme after three rounds of directed evolution. The contributions of individual mutations to the catalytic efficiency were elucidated by mutational and structural analyses. The DmpR-based screening system is expected to be widely used for developing OP-degrading enzymes with greater potential.

PMID:23077277

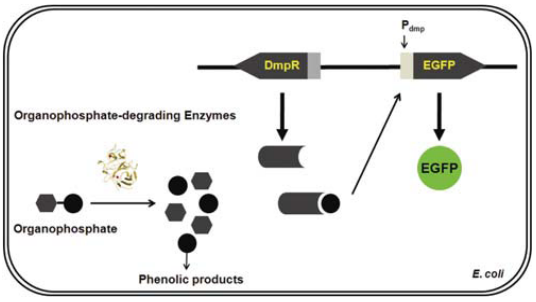

Keywords : Directed evolution; DmpR-based screening; High-throughput screening; Organophosphate-degrading enzymes; Transcription activator

Article 67

Characterization of sporulation histidine kinases of *Paenibacillus polymyxa*

Res Microbiol. 163(4):272-8.

Park SY, Park SH, Choi SK*

*Corresponding: sookeun@kribb.re.kr
Super-Bacteria Research Center

Sporulation histidine kinases, which sense sporulation-specific signals and initiate phosphorelay reactions, are poorly conserved among *Bacillus* species. We found several putative genes for sporulation histidine kinases in the genome sequence of *Paenibacillus polymyxa* E681 and assayed the genes for complementation of sporulation mutants of *Bacillus subtilis*. One of these genes, Kin1377, significantly restored the sporulation deficiency of *kinA kinB* double mutant of *B. subtilis*, but not of *B. subtilis spo0B* mutant. These results indicated that Kin1377 requires *B. subtilis* Spo0B and possibly Spo0F to transfer phosphate to *B. subtilis* Spo0A. Another putative kinase, Kin1038, slightly restored the sporulation deficiencies of both *kinA kinB* double mutant and *spo0B* mutant of *B. subtilis*. However the sporulation deficiency of the *B. subtilis spo0B* mutant was significantly restored in the presence of both Kin1038 and *P. polymyxa* Spo0A. These results indicate that the overexpressed Kin1038 is able to interact directly with and activate *P. polymyxa* Spo0A, and that Spo0A can support spore formation in *B. subtilis*.

PMID: 22391390

Strain	Relevant genotype	Sporulation[a] (%)
JH642	Wild type	61.00 (±1.62)
JHPP0A	*spo0A::erm, thr::spo0A*$_{pp}$	0.78 (±0.13)
JHKAB (pHCMC05)	*kinA kinB* pHCMC05	0
JHKAB (pMC99)	*kinA kinB* pMC99	0
JHKAB (pMC689)	*kinA kinB* pMC689	0
JHKAB (pMC1038)	*kinA kinB* pMC1038	1.27 (±0.23)
JHKAB (pMC1377)	*kinA kinB* pMC1377	39.05 (±5.03)
JHKAB (pMC3851)	*kinA kinB* pMC3851	0

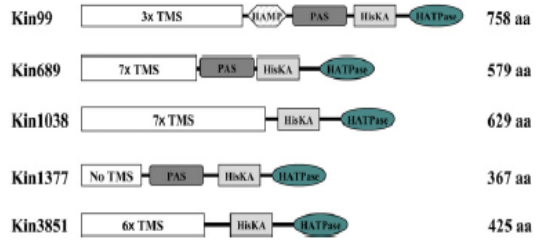

Keywords : *Bacillus*; Histidine kinase; *Paenibacillus polymyxa*; Phosphorelay; Sporulation

Article 68

A novel fluorescent reporter system for monitoring and identifying RNase III activity and its target RNAs

RNA Biol. 9(9):1167-76.

Kim KS*, Park S, Lee S, Kang SB, Lee J, Lee SG, Ryu CM

*Corresponding: sunny06@kribb.re.kr
Super-Bacteria Research Center

Bacteriophage vectors for achieving single-copy gene expression linked to a colorigenic reporter assay have been used successfully for genetic screening applications. However, the limited number of cloning sites in these vectors, combined with the requirement for *lac*- strains and the time- and/or media-dependence of the chemical-based colorimetric reaction, have limited the range of applications for these vectors. An alternative approach using a fluorescent reporter gene such as green fluorescent protein (GFP) or GFP derivatives could overcome some of these technical issues and facilitate real-time monitoring of promoter and/or protein activity. Here, we report the development of a novel translational bacteriophage fusion vector encoding enhanced GFP (eGFP) that can be incorporated into the chromosome as a single-copy gene. We identified a *Bacillus* promoter (BP) that is stably expressed in *Escherichia coli* and drives ~6-fold more expression of eGFP than the T7 promoter in the absence of inducer. Incorporating this BP and RNase III target signals into a single system enabled clear detection of the absence or downregulation of RNase III activity *in vivo*, thereby establishing a system for screening and identifying novel RNase III targets in a matter of days. An RNase III target signal identified in this manner was confirmed by post-transcriptional analysis. We anticipate that this novel translational fusion vector will be used extensively to study activity of both interesting RNases and related complex or to identify or validate targets of RNases that are otherwise difficult to study due to their sensitivity to environmental stresses and/or autoregulatory processes.
PMID: 22951591

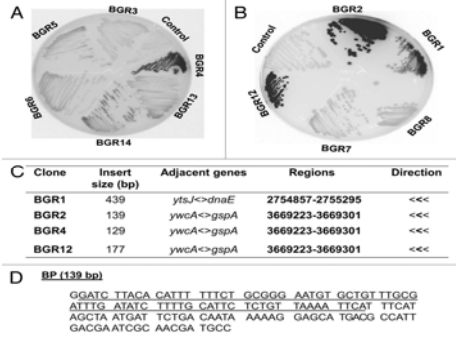

C	Clone	Insert size (bp)	Adjacent genes	Regions	Direction
	BGR1	439	*ytsJ<>dnaE*	2754857-2755295	<<<
	BGR2	139	*ywcA<>gspA*	3669223-3669301	<<<
	BGR4	129	*ywcA<>gspA*	3669223-3669301	<<<
	BGR12	177	*ywcA<>gspA*	3669223-3669301	<<<

D BP (139 bp)

GGATC TTACA CATTT TTTCT GCGGG AATGT GCTGT TTGCG
ATTTG ATATC TTTTG CATTC TCTGT TAAAA TTCAT TTCAT
AGCTA ATGAT TCTGA CAATA AAAAG GAGCA TGACG CCATT
GACGA ATCGC AACGA TGCC

Keywords : Bacteriophage vector; Fluorescent protein; Reporter system; RNase III; Translational fusion

Article 69

Bacillus spore display

Trends Biotechnol. 30(12):610-2.

Pan JG*, Kim EJ, Yun CH

*Corresponding: jgpan@kribb.re.kr
Super-Bacteria Research Center

Many surface proteins have been used for displaying target proteins, such as antigens, enzymes, and bioadsorbents. we discuss the unique molecular display system of Bacillus spores: (i) the spore is the most resilient life form; (ii) no secretion is required for the display; and (iii) the foreign proteins can be displayed in their native forms, thus obviating the need to produce fusion proteins. Surface-displayed enzymes streamline the enzyme production and downstream immobilization. Spores are excellent vehicles to present heterologous antigens because they are heat stable and enable needlefree mucosal or oral immunization. Although fusion of the target protein to the display motif is a prerequisite for protein display, foreign proteins expressed at the late sporulation phase are found to be displayed in their native form on the spore surface. Spores can also be used as an adsorption support. Phytase adsorbs to *Bacillus polyfermenticus* spores and is stabilized. There are more ways that spore display can be improved. Spores displaying foreign proteins maintain the original robustness of the spore, which would be useful in developing robust biocatalysts and vaccines.
PMID:23084844

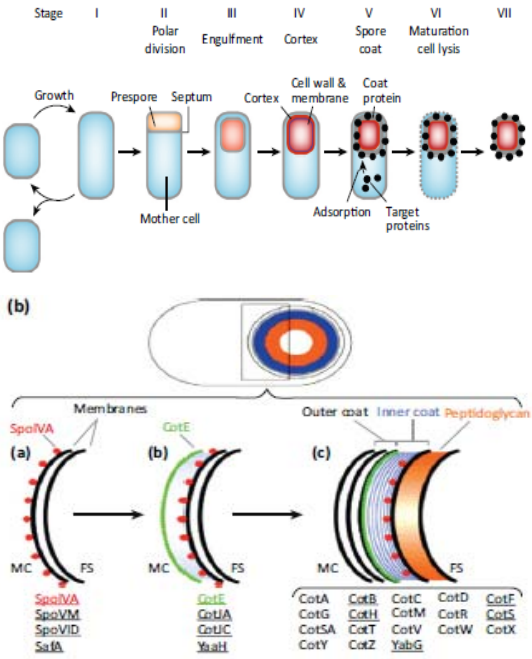

Keywords : *Bacillus*; Molecular display; Robust biocatalysts; Surface protein; Vaccines

Article 70

HpYPS1 and *HpYPS7* encode functional aspartyl proteases localized at the cell surface in the thermotolerant methylotrophic yeast *Hansenula polymorpha*

Yeast. 29(1):1-16.

Sohn MJ, Oh DB*, Kim EJ, Cheon SA, Kwon O, Kim JY, Lee SY, Kang HA

*Co-first: dboh@kribb.re.kr
Biochemicals & Synthetic Biology Research Center

In the present study, we functionally analysed two yapsin genes of the thermotolerant methylotrophic yeast *Hansenula polymorpha*, *HpYPS1* and *HpYPS7*, for their roles in maintaining cell wall integrity and proteolytic processing. Both *HpYPS1* and *HpYPS7* proteins were shown to largely localize on the cell wall via glycosylphosphatidylinositol anchor. Heterologous expression of *HpYPS1* completely restored all of the growth defects of the *Saccharomyces cerevisiae yps1*-deletion strains, while *HpYPS7* expression exhibited a limited complementation effect on the *S. cerevisiae yps7*-deletion strain. However, different from *S. cerevisiae*, deletion of the *HpYPS* genes generated only minor influence on the sensitivity to cell wall stress. Likewise, *HpYPS1* expression was significantly induced only by a subset of stressor agents, such as sodium dodecyl sulphate and tunicamycin. HpYps1p was shown to consist of two subunits, whereas HpYps7p comprises a single long polypeptide chain. Biochemical analysis revealed that HpYps1p has much stronger proteolytic cleavage activity at basic amino acids, compared to HpYps7p. Consistent with the much higher proteolytic activity and expression level of HpYps1p compared to HpYps7p, the sole disruption of *HpYPS1* was sufficient in eliminating the aberrant proteolytic cleavage of recombinant proteins secreted by *H. polymorpha*. The results indicate that, although their roles in the maintenance of cell wall integrity are not critical, HpYps1p and HpYps7p are functional aspartic proteases at the cell surface of *H. polymorpha*. Furthermore, our data present the high biotechnological potential of *H. polymorpha yps1*-mutant strains as hosts useful for the production of secretory recombinant proteins.

PMID:22162039

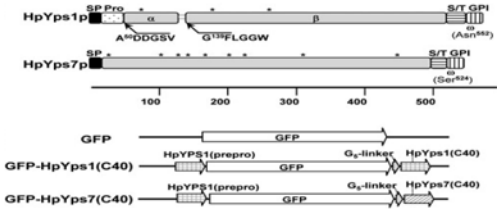

Keywords : Aspartyl protease; Cell wall stress; Glycosylphosphatidylinositol anchor; *Hansenula polymorpha*; *Pichia angusta*; Proteolytic activity; Yapsin


KRIBB
www.kribb.re.kr

2012
KRIBB Article Abstracts : First or corresponding articles indexed in SCIE, Scopus, and PubMed

Biomedical Science Institute

- Aging Research Center
- Infection and Immunity Research Center
- Immunotherapy Research Center
- Stem Cell Research Center

Korea Research Institute of Bioscience and Biotechnology

Article 71

A novel small molecule facilitates the reprogramming of human somatic cells into a pluripotent state and supports the maintenance of an undifferentiated state of human pluripotent stem cells

Angew Chem Int Ed Engl. 51(50):12509-13.

Lee J, Xia Y, Son MY, Jin G, Seol B, Kim MJ, Son MJ, Do M, Lee M, Kim D, Lee K, Cho YS*

*Corresponding: june@kribb.re.kr
Stem Cell Research Center

Booster of pluripotency: RSC133, a new synthetic derivative of indoleacrylic acid/indolepropionic acid, exhibits dual activity by inhibiting histone deacetylase and DNA methyltransferase. Furthermore it potently improves the reprogramming of human somatic cells into a pluripotent state and aids the growth and maintenance of human pluripotent stem cells (hPSCs).
PMID: 23125037

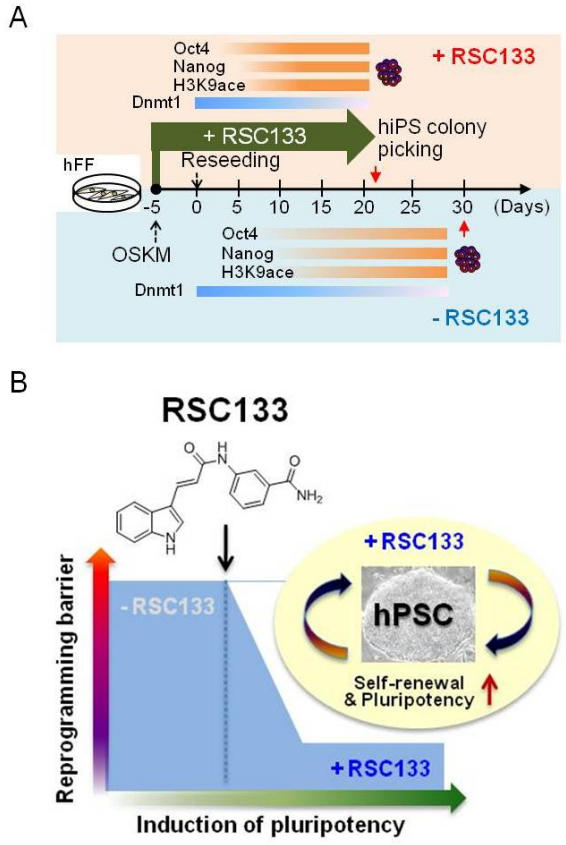

Keywords : Pluripotency; Reprogramming; Small molecules; Stem cells

Article 72

Homologous Alkalophilic and Acidophilic L-Arabinose isomerases reveal region-specific contributions to the pH dependence of activity and stability

Appl Environ Microbiol. 78(24):8813-6.

Lee SJ, Lee SJ*, Lee YJ, Kim SB, Kim SK, Lee DW

*Co-first: leesj@kribb.re.kr
Infection and Immunity Research Center

To study the pH dependence of l-arabinose isomerase (AI) activity and stability, we compared homologous AIs with their chimeras. This study demonstrated that an ionizable amino acid near the catalytic site determines the optimal pH (pH_{opt}) for activity, whereas the N-terminal surface R residues play an important role in determining the pH_{opt} for stability.
PMID:23001647

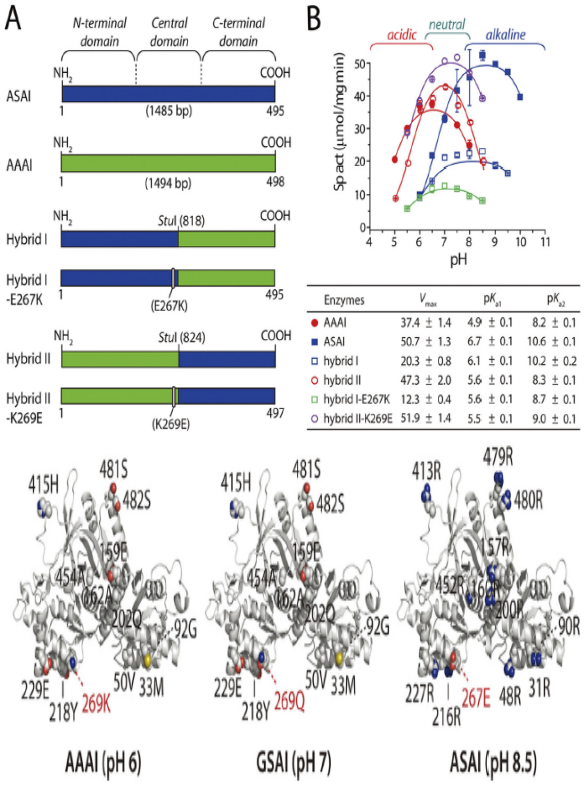

Keywords : l-arabinose isomerase; Homologous AIs; Ionizable amino acid; pH dependence

Article 73

Reactive oxygen species mediated DNA damage is essential for abnormal erythropoiesis in peroxiredoxin II$^{-/-}$ mice

Biochem Biophys Res Commun. 424(1):189-95.

Kwon TH, Han YH, Hong SG, Lee DJ, Ha HL, Kang SW, Li W, Yoon do Y, Yu DY*

*Corresponding: dyyu10@kribb.re.kr
Aging Research Center

Erythroid cells are highly prone to oxidative damage generated during erythropoiesis and thus are well equipped with antioxidant defense systems. However, their roles have been poorly characterized. Here, we investigated the role of peroxiredoxin II in mouse erythropoiesis. Loss of Prx II significantly increased apoptosis and cell cycle arrest leading to abnormal erythropoiesis at 3 weeks of age when erythropoietin levels were almost same between wild type and Prx II$^{-/-}$. In Prx II$^{-/-}$ bone marrow cells, DNA tail length as an indicator of the oxidative damage was greatly increased and mRNAs of the molecules associated with DNA damage and repair and transcription regulators of antioxidant enzymes were also significantly increased. In addition, *N*-Acetyl-L-Cysteine treatment significantly decreased immature erythroblasts and apoptotic cells increased in Prx II$^{-/-}$ BMCs. These results strongly demonstrate that Prx II plays an essential role in maintaining normal erythropoiesis by protecting DNA damage.

PMID: 22749995

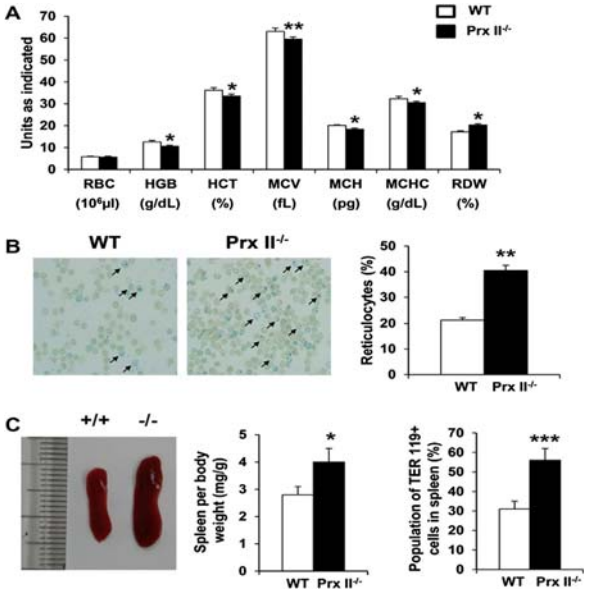

Keywords : Apoptosis; Cell cycle arrest; DNA damage; Erythropoiesis; Knockout mouse; Peroxiredoxin II

Article 74

CDK2 differentially controls normal cell senescence and cancer cell proliferation upon exposure to reactive oxygen species

Biochem Biophys Res Commun. 425(1):94-9.

Hwang CY, Lee SM, Park SS, Kwon KS*

*Corresponding: kwonks@kribb.re.kr
Aging Research Center

Reactive oxygen species modulate cell fate in a context-dependent manner. Sublethal doses of H_2O_2 decreased the level of proliferating cell nuclear antigen (PCNA) in normal cells (including primary human dermal fibroblasts and IMR-90 cells) without affecting cyclin-dependent kinase 2 (CDK2) activity, leading to cell cycle arrest and subsequent senescence. In contrast, exposure of cancer cells (such as HeLa and MCF7 cells) to H_2O_2 increased CDK2 activity with no accompanying change in the PCNA level, leading to cell proliferation. A CDK2 inhibitor, CVT-313, prevented H_2O_2-induced cancer cell proliferation. These results support the notion that the cyclin/CDK2/p21^{Cip1}/PCNA complex plays an important role as a regulator of cell fate decisions.

PMID: 22819841

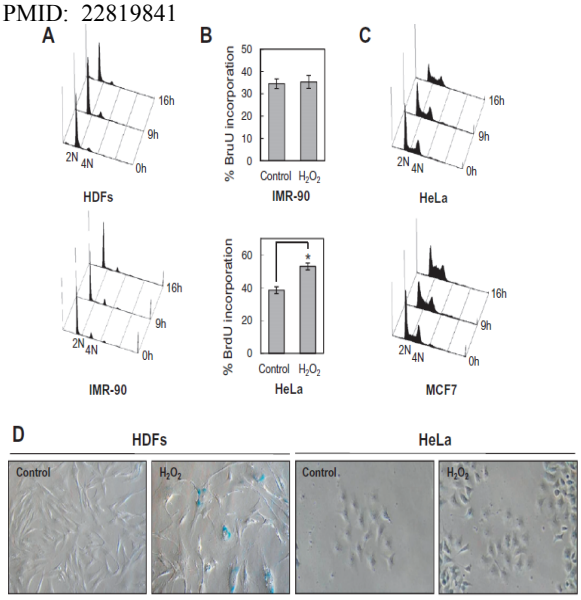

Keywords : CDK2; H_2O_2; p21^{Cip1}; PCNA; Proliferation; Senescence

Article 75

Cryptotanshinone and tanshinone IIA enhance IL-15-induced natural killer cell differentiation

Biochem Biophys Res Commun. 425(2):340-7.

Kim WS, Kim DO, Yoon SJ, Kim MJ, Yoon SR, Park YJ, Jung H, Kim TD, Kwon BM, Choi I*

*Corresponding: ipchoi@kribb.re.kr
Immunotherapy Research Center

Natural killer (NK) cells are a subset of lymphocytes crucial for innate and adaptive immune responses. Here we show a stimulatory effect of cryptotanshinone (CTS) and tanshinone IIA (TS), isolated from *Salvia miltiorrhiza Bunge*, on the differentiation of NK cells. In the presence of IL-15, tanshinones increased NK cell maturation, NK cell differentiation and the expression of several transcription factors, including Id2, GATA3, T-bet, and Ets-1. Additionally, tanshinones increased p38 MAPK phosphorylation during NK cell differentiation. Furthermore, the p38 inhibitor SB203580 blocked the developmental effects of the tanshinones and suppressed Id2, T-bet, and Ets-1 expression during NK cell differentiation. These results suggest that tanshinones significantly increased IL-15-induced NK cell differentiation via enhancing the p38 phosphorylation and the expression of transcription factors.
PMID: 22842576

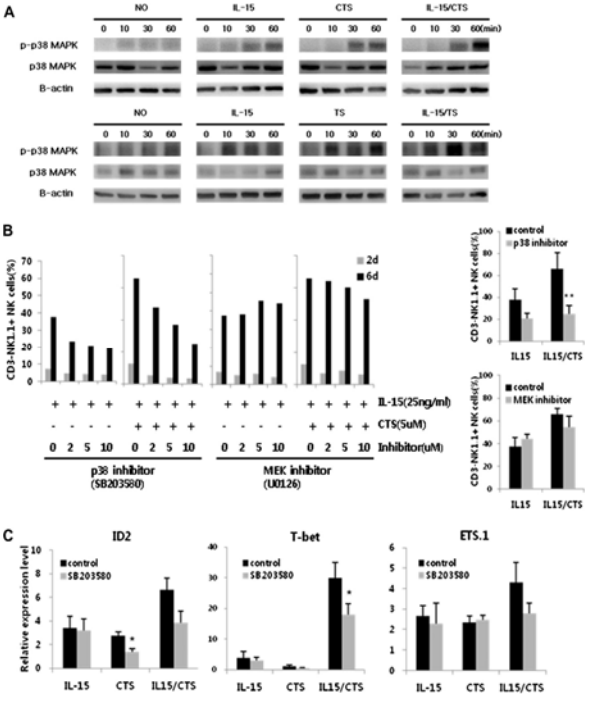

Keywords : Cryptotanshinone; Differentiation; Id2; IL-15; NK cells; Tanshinone IIA

Article 76

Peroxiredoxin II is essential for preventing hemolytic anemia from oxidative stress through maintaining hemoglobin stability

Biochem Biophys Res Commun. 426(3):427-32.

Han YH, Kim SU, Kwon TH, Lee DS, Ha HL, Park DS, Woo EJ, Lee SH, Kim JM, Chae HB, Lee SY, Kim BY, Yoon do Y, Rhee SG, Fibach E, Yu DY*

*Corresponding: dyyu10@kribb.re.kr
Aging Research Center

The pathophysiology of oxidative hemolytic anemia is closely associated with hemoglobin (Hb) stability; however, the mechanism of how Hb maintains its stability under oxidative stress conditions of red blood cells (RBCs) carrying high levels of oxygen is unknown. Here, we investigated the potential role of peroxiredoxin II (Prx II) in preventing Hb aggregation induced by reactive oxygen species (ROS) using Prx II knockout mice and RBCs of patients with hemolytic anemia. Upon oxidative stress, ROS and Heinz body formation were significantly increased in Prx II knockout RBCs compared to wild-type (WT), which ultimately accelerated the accumulation of hemosiderin and heme-oxygenase 1 in the Prx II knock-out livers. In addition, ROS-dependent Hb aggregation was significantly increased in Prx II knockout RBCs. Interestingly, Prx II interacted with Hb in mouse RBCs, and their interaction, in particular, was severely impaired in RBCs of patients with thalassemia (THAL) and sickle cell anemia (SCA). Hb was bound to the decameric structure of Prx II, by which Hb was protected from oxidative stress. These findings suggest that Prx II plays an important role in preventing hemolytic anemia from oxidative stress by binding to Hb as a decameric structure to stabilize it.
PMID: 22960070

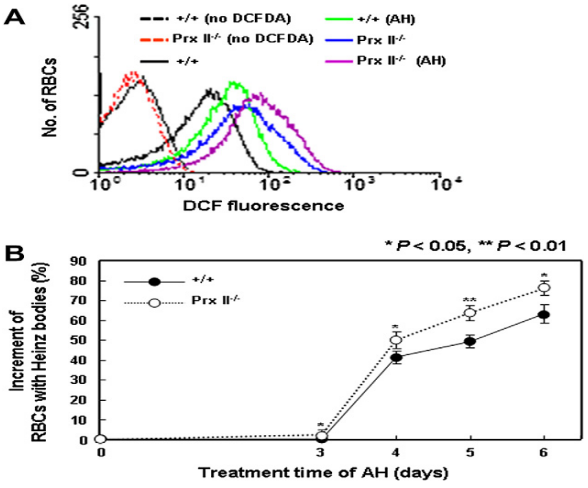

Keywords : Heme-oxygenase 1; Hemoglobin; Reactive oxygen species; Red blood cells; Peroxiredoxin II

Article 77

Cytosolic malate dehydrogenase regulates senescence in human fibroblasts

Biogerontology. 13(5):525-36.

Lee SM, Dho SH, Ju SK, Maeng JS, Kim JY, Kwon KS*

*Corresponding: kwonks@kribb.re.kr
Aging Research Center

Carbohydrate metabolism changes during cellular senescence. Cytosolic malate dehydrogenase (MDH1) catalyzes the reversible reduction of oxaloacetate to malate at the expense of reduced nicotinamide adenine dinucleotide (NADH). Here, we show that MDH1 plays a critical role in the cellular senescence of human fibroblasts. We observed that the activity of MDH1 was reduced in old human dermal fibroblasts (HDFs) [population doublings (PD) 56], suggesting a link between decreased MDH1 protein levels and aging. Knockdown of MDH1 in young HDFs (PD 20) and the IMR90 human fibroblast cell line resulted in the appearance of significant cellular senescence features, including senescence-associated β-galactosidase staining, flattened and enlarged morphology, increased population doubling time, and elevated $p16^{INK4A}$ and $p21^{CIP1}$ protein levels. Cytosolic NAD/NADH ratios were decreased in old HDFs to the same extent as in MDH1 knockdown HDFs, suggesting that cytosolic NAD depletion is related to cellular senescence. We found that AMP-activated protein kinase, a sensor of cellular energy, was activated in MDH1 knockdown cells. We also found that sirtuin 1 (SIRT1) deacetylase, a controller of cellular senescence, was decreased in MDH1 knockdown cells. These results indicate that the decrease in MDH1 and subsequent reduction in NAD/NADH ratio, which causes SIRT1 inhibition, is a likely carbohydrate metabolism-controlled cellular senescence mechanism.

PMID: 22971926

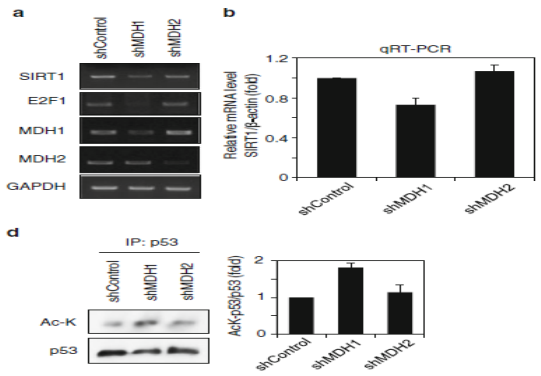

Keywords : AMPK; MDH1; NAD/NADH; Senescence; SIRT1

Article 78

Peroxiredoxin I deficiency attenuates phagocytic capacity of macrophage in clearance of the red blood cells damaged by oxidative stress

BMB Rep. 45(10):560-4.

Han YH, Kwon T, Kim SU, Ha HL, Lee TH, Kim JM, Jo EK, Kim BY, Yoon do Y, Yu DY*

*Corresponding: dyyu10@kribb.re.kr
Aging Research Center

The role of peroxiredoxin (Prx) I as an erythrocyte antioxidant defense in red blood cells (RBCs) is controversial. Here we investigated the function of Prx I by using Prx $I^{-/-}$ and Prx $I/II^{-/-}$ mice. Prx $I^{-/-}$ mice exhibited a normal blood profile. However, Prx $I/II^{-/-}$ mice showed more significantly increased Heinz body formation as compared with Prx $II^{-/-}$ mice. The clearance rate of Heinz body-containing RBCs in Prx $I^{-/-}$ mice decreased significantly through the treatment of aniline hydrochloride (AH) compared with wild-type mice. Prx I deficiency decreased the phagocytic capacity of macrophage in clearing Heinz body-containing RBCs. Our data demonstrate that Prx I deficiency did not cause hemolytic anemia, but showed that further increased hemolytic anemia symptoms in Prx $II^{-/-}$ mice by attenuating phagocytic capacity of macrophage in oxidative stress damaged RBCs, suggesting a novel role of Prx I in phagocytosis of macrophage.

PMID: 23101509

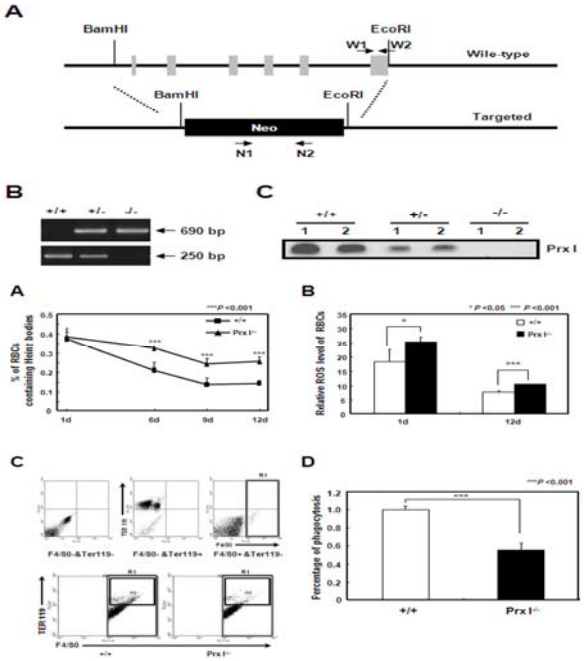

Keywords : Aniline hydrochloride; Erythrocyte antioxidant defense; Peroxiredoxin (Prx); Red blood cells

Article 79

Upregulation of CD9 in ovarian cancer is related to the induction of TNF-α gene expression and constitutive NF-κB activation

Carcinogenesis. 33(1):77-83.

Hwang JR, Jo K, Lee Y, Sung BJ, Park YW*, Lee JH

*Co-corresponding: ywpark@kribb.re.kr
Aging Research Center

Ovarian cancer is a gynecological cancer with a high death rate. We utilized global gene expression profiles of ovarian carcinomas obtained by complementary DNA (cDNA) microarray to identify ovarian cancer-specific proteins. *CD9* was upregulated in ovarian carcinomas, and overexpression of the CD9 protein was detected in ovarian carcinomas by immunohistochemistry. CD9 was also overexpressed in several cancer cell lines, including ovarian cancer cells. In order to elucidate the biological significance of highly expressed CD9 in cancer cells, functional studies of CD9 were performed by ectopic expression, knockdown of CD9 using small interfering RNA (siRNA) and blockage of CD9 activity using the CD9-specific monoclonal antibody ALB6. Ectopic CD9 induced cell survival. In order to identify signaling pathways related to CD9, the gene expressions of CD9/SKOV3 cells were analyzed by cDNA microarray. Among the many upregulated genes, *tumor necrosis factor* (*TNF*)-α was induced in CD9/SKOV3 cells. The effect of overexpressed CD9 on the downstream signaling events of TNF-α was further investigated. In CD9/SKOV3 cells, the nuclear factor-kappaB (NF-κB)-signaling pathway was constitutively activated. Knockdown of CD9 by siRNA and blockage of CD9 activity by ALB6 in ovarian cancer cells demonstrated that constitutive activation of NF-κB is CD9 dependent and that CD9 is involved in anti-apoptosis. A CD9 functional study was performed in an ovarian cancer-xenograft mouse by injecting ALB6 into the peritoneum. ALB6 resulted in reduced tumor weight compared with that of control IgG(1). Collectively, these results demonstrate that CD9 functions as an oncogene and represents a target for the development of cancer-specific therapeutics.

PMID:22095071

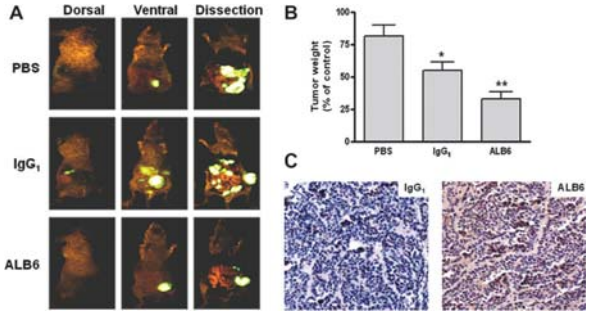

Keywords : Anti-apoptosis; Biological significance; Cancer-specific therapeutics; Ovarian cancer

Article 80

ZEB2 upregulates integrin α5 expression through cooperation with Sp1 to induce invasion during epithelial-mesenchymal transition of human cancer cells

Carcinogenesis. 33(3):563-71.

Nam EH, Lee Y, Park YK, Lee JW, Kim S*

*Corresponding: semikim@kribb.re.kr
Immunotherapy Research Center

Epithelial-mesenchymal transition (EMT) is a process implicated in tumor invasion, metastasis, embryonic development and wound healing. ZEB2 is a transcription factor involved in EMT that represses E-cadherin transcription. Although E-cadherin downregulation is a major event during EMT and tumor progression, E-cadherin reduction is probably not sufficient for full invasiveness. The mechanisms by which E-cadherin transcriptional repressors induce mesenchymal genes during EMT remain largely unknown. Here, we investigated the role of ZEB2 in the induction of integrin α5 during cancer EMT and its underlying mechanism. In human cancer cells, ZEB2 was found to directly upregulate integrin α5 transcription in a manner that is independent of the regulation of E-cadherin expression. Conversely, depletion of ZEB2 by small interfering RNA suppressed integrin α5 expression, leading to reduced invasion. Suppression of integrin α5 inhibited cancer cell invasion, suggesting an important role for integrin α5 in cancer progression. Furthermore, ZEB2 was found to activate the integrin α5 and vimentin promoters by interacting with and activating the transcription factor Sp1, suggesting that cooperation between ZEB2 and Sp1 represents a novel mechanism of mesenchymal gene activation during EMT. These findings increase our understanding of the pathways beyond E-cadherin reduction that regulate mesenchymal gene expression during EMT and cancer progression.

PMID: 22227038

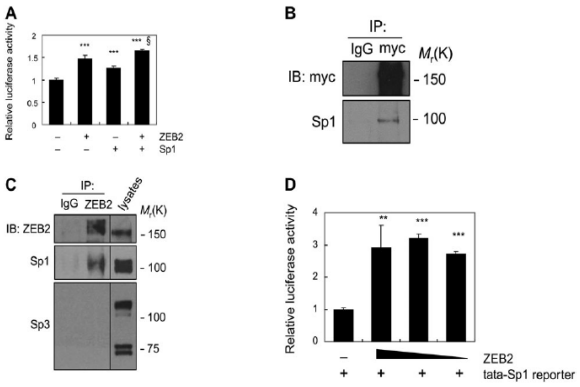

Keywords : Cancer cell; Epithelial-mesenchymal transition; E-cadherin reduction; Transcriptional repressors

Article 81

VDUP1 exacerbates bacteremic shock in mice infected with *Pseudomonas aeruginosa*

Cell Immunol. 280(1):1-9.

Piao ZH, Kim MS, Jeong M, Yun S, Lee SH, Sun HN, Song HY, Suh HW, Jung H, Yoon SR, Kim TD, Lee YH, Choi I*

*Corresponding: ipchoi@kribb.re.kr
Immunotherapy Research Center

Vitamin-D3 upregulated protein-1 (VDUP1) is a stress response protein. *Pseudomonas aeruginosa* (*P. aeruginosa*) infection is a leading cause of death. Mice infected with live *P. aeruginosa* exhibit significantly decreased VDUP1 expression. However, the function of VDUP1 during *P. aeruginosa*-induced mouse bacteremic shock is unknown. To address the function of VDUP1 in *P. aeruginosa*-infected mice, we constructed a bacteremic shock model wherein both wild-type and VDUP1-deficient mice were infected intra-peritoneally with live *P. aeruginosa*. We found that VDUP1-deficient mice were more resistant to *P. aeruginosa*-induced bacteremic shock than wild-type mice, as shown by the increased survival, accelerated bacterial clearance and suppression of cytokine overproduction of the VDUP1-deficient mice. VDUP1 promoted the recruitment of neutrophils into the peritoneal cavities of infected mice. VDUP1 impeded the phagocytosis of non-opsonized *P. aeruginosa* via phosphatidylinositide 3-kinase (PI3K) pathway in macrophages. *P. aeruginosa* infection induced the generation of reactive oxygen species (ROS), and the increased production of ROS by the peritoneal cells of VDUP1-deficient mice was advantageous in clearing the bacteria. Overall, VDUP1 aggravates bacteremic shock; thus, VDUP1 can be considered a target molecule for the inhibition of *P. aeruginosa*-induced bacteremic shock.

PMID: 23246829

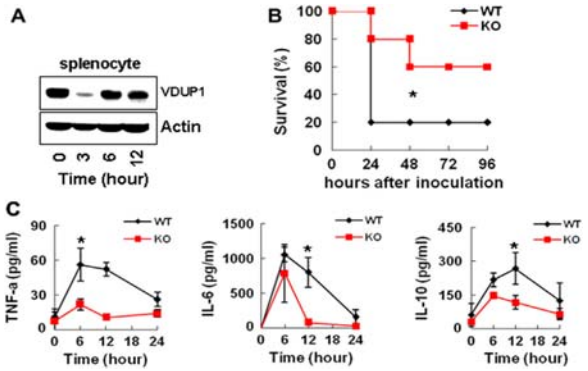

Keywords : Bacteremic shock; *P. aeruginosa*; ROS; VDUP1

Article 82

XAGE-1a and XAGE-1d are potential biomarkers of lung squamous cell carcinoma

Clin Chim Acta. 413(15-16):1226-31.

Ha JS, Sung HY, Kim SY, Lim HM, Kim HK, Park SS*

*Co-corresponding: sspark@kribb.re.kr
Aging Research Center

BACKGROUND: Lung cancer is the leading cause of cancer deaths worldwide. We evaluated the diagnostic potential of sera XAGE-1a and XAGE-1d in lung cancer, both of which are variants of the X antigen family, member 1.
METHODS: The expression levels of XAGE-1a and XAGE-1d in cell lines were determined using western blot analysis. Competitive ELISA was used to analyze XAGE-1a and XAGE-1d levels in culture supernatants and sera from 194 lung cancer patients and 194 healthy sex- and age-group-matched controls. To evaluate the diagnostic performance of these proteins, we also analyzed carcinoembryonic antigen (CEA) and cytokeratin 19 fragment (CYFRA 21-1) in culture supernatants and 388 sera using commercial ELISA kits.
RESULTS: XAGE-1a and XAGE-1d proteins were expressed in both breast cancer and lung cancer cell lines, but they were only secreted by the latter. The areas under the curves (AUCs) for XAGE-1a and XAGE-1d were 0.787 and 0.806, respectively. The cutoff values (sensitivity, specificity) for XAGE-1a and XAGE-1d were 1.62 ng/ml (0.866, 0.572) and 2.51 ng/ml (0.871, 0.613), respectively. The diagnostic performance was improved for patients with squamous cell carcinoma. The AUC values for XAGE-1a and XAGE-1d for patients with squamous cell carcinoma versus a group containing all healthy participants and patients with any illness other than squamous cell carcinoma were similar to those for CEA and CYFRA 21-1. Better performance (AUC: 0.914) for all patients was obtained when using a combination of four markers (Random Forest).
CONCLUSIONS: Sera XAGE-1a and XAGE-1d are potential biomarkers for lung cancer; they display a diagnostic performance comparable to that of CEA or CYFRA 21-1. Further studies are needed to evaluate the diagnostic and prognostic potential of XAGE-1a and XAGE-1d in lung cancer.

PMID: 22515959

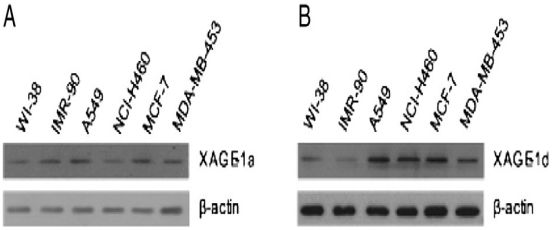

Keywords : Biomarker validation; Lung cancer; Serum biomarkers; XAGE-1a; XAGE-1d

Article 83

Direct lineage reprogramming to neural cells

Curr Opin Neurobiol. 22(5):778-84.

Kim J*, Ambasudhan R, Ding S

*First: janghwan@kribb.re.kr
Stem Cell Research Center

Recently we have witnessed an array of studies on direct reprogramming that describe induced inter conversion of mature cell types from higher organisms including human. While these studies reveal an unexpected level of plasticity of differentiated somatic cells, they also provide unprecedented opportunities to develop regenerative therapies for many debilitating disorders and model these 'diseases-in-a-dish' for studying their pathophysiology. Here we review the current state of the art in direct lineage reprogramming to neural cells, and discuss the challenges that need to be addressed toward achieving the full potential of this exciting new technology.
PMID: 22652035

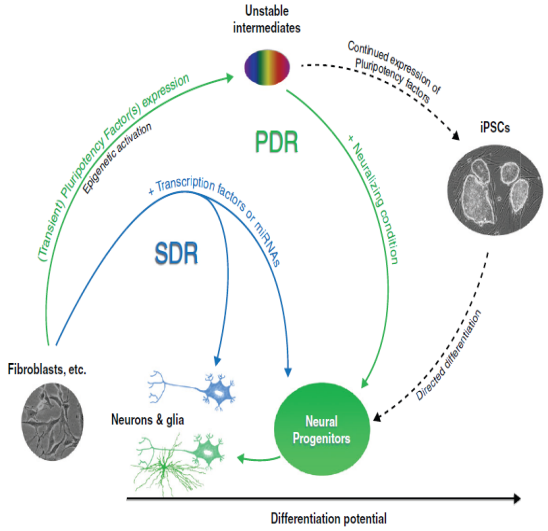

Keywords : Differentiated somatic cells; Direct lineage reprogramming; Inter conversion; Regenerative therapy

Article 84

Draft genome sequence of *Bacillus oceanisediminis* 2691

J Bacteriol. 194(22):6351-2.

Lee YJ, Lee SJ, Jeong H, Kim HJ, Ryu N, Kim BC, Lee HS, Lee DW, Lee SJ*

*Corresponding: leesj@kribb.re.kr
Infection and Immunity Research Center

Bacillus oceanisediminis 2691 is an aerobic, Gram-positive, spore-forming, and moderately halophilic bacterium that was isolated from marine sediment of the Yellow Sea coast of South Korea. Here, we report the draft genome sequence of *B. oceanisediminis* 2691 that may have an important role in the bioremediation of marine sediment.
PMID: 23105082

Keywords : *Bacillus oceanisediminis*; Bioremediation; Genome sequence

Article 85

Role of Junctin protein interactions in cellular dynamics of calsequestrin polymer upon calcium perturbation

J Biol Chem. 287(3):1679-87.

Lee KW, Maeng JS, Choi JY, Lee YR, Hwang CY, Park SS, Park HK, Chung BH, Lee SG, Kim YS, Jeon H, Eom SH, Kang C, Kim do H, Kwon KS*

*Corresponding: kwonks@kribb.re.kr
Aging Research Center

Calsequestrin (CSQ), the major intrasarcoplasmic reticulum calcium storage protein, undergoes dynamic polymerization and depolymerization in a Ca^{2+}-dependent manner. However, no direct evidence of CSQ depolymerization *in vivo* with physiological relevance has been obtained. In the present study, live cell imaging analysis facilitated characterization of the *in vivo* dynamics of the macromolecular CSQ structure. CSQ2 appeared as speckles in the presence of normal sarcoplasmic reticulum (SR) Ca^{2+} that were decondensed upon Ca^{2+} depletion. Moreover, CSQ2 decondensation occurred only in the stoichiometric presence of junctin (JNT). When expressed alone, CSQ2 speckles remained unchanged, even after Ca^{2+} depletion. FRET analysis revealed constant interactions between CSQ2 and JNT, regardless of the SR Ca^{2+} concentration, implying that JNT is an essential component of the CSQ scaffold. *In vitro* solubility assay, electron microscopy, and atomic force microscopy studies using purified recombinant proteins confirmed Ca^{2+} and JNT-dependent disassembly of the CSQ2 polymer. Accordingly, we conclude that reversible polymerization and depolymerization of CSQ are critical in SR Ca^{2+} homeostasis.
PMID: 22123818

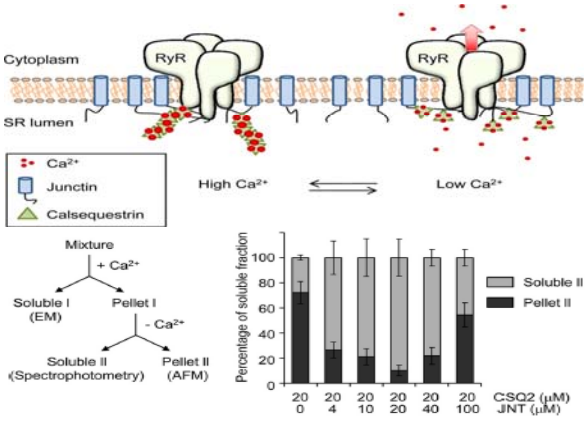

Keywords : Calsequestrin polymer; CSQ depolymerization; FRET analysis; Live cell imaging analysis; Reversible polymerization

Article 86

Diet-induced obesity dramatically reduces the efficacy of a 2009 pandemic H1N1 vaccine in a mouse model

J Infect Dis. 205(2):244-51.

Kim YH, Kim JK, Kim DJ, Nam JH, Shim SM, Choi YK, Lee CH, Poo H*

*Corresponding: haryoung@kribb.re.kr
Infection and Immunity Research Center

BACKGROUND: Obesity, a risk factor for increased severity of diverse diseases, is believed to have negative impact on vaccine efficacy. Recently, mortality has emerged as an outcome of pandemic influenza A virus subtype H1N1, necessitating development of effective vaccine strategies. Here we investigated effects of diet-induced obesity on vaccine-induced immune responses and protective efficacy against pandemic H1N1 influenza virus.
METHODS: Diet-induced obese and lean C57BL/6J mice were immunized with commercial monovalent 2009 H1N1 vaccine, and antigen-specific antibody responses and neutralizing activities were observed. Following vaccination, mice were challenged with homologous H1N1 virus, and pathogenesis and mortality were examined.
RESULTS: Vaccine-induced H1N1-specific antibody responses and neutralizing activities were markedly reduced in obese mice. Consistent with antibody responses, lung virus titers were significantly higher in obese mice than in lean controls after challenge. In addition, obese group showed greatly increased expression of proinflammatory cytokines and chemokines in lung tissue, severe lung inflammation, and higher eventual mortality rate (100%) compared with that among lean control mice (14%).
CONCLUSIONS: Our results show that prophylactic immune responses and protectiveness induced by 2009 H1N1 vaccine could be extremely compromised in diet-induced obesity. These results suggest that novel vaccination strategies for high-risk groups, including the obese population, are required.
PMID:22147801

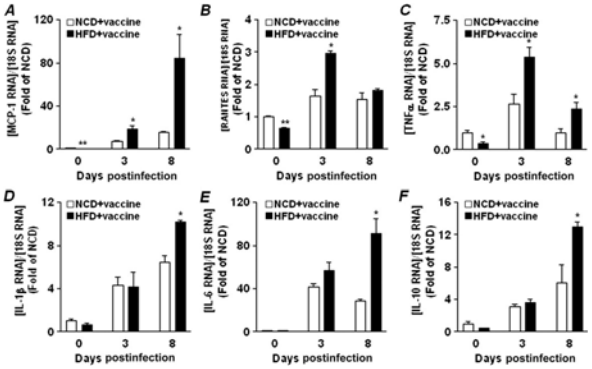

Keywords : Antibody responses; H1N1; Novel vaccination strategies; Pandemic influenza A virus

Article 87

Complete genome sequence of a mammalian species-infectious and -pathogenic H6N5 avian influenza virus without evidence of adaptation

J Virol. 86(22):12459-60.

Park SJ, Park BK, Song DS*, Poo H*

*Corresponding: sds1@kribb.re.kr haryoung@kribb.re.kr
Infection and Immunity Research Center

An H6N5 avian influenza virus (AIV) strain, designated A/aquatic bird/Korea/CN5/2009 (H6N5), was isolated from fecal swabs of aquatic birds in 2009, and surprisingly, it showed infectivity and pathogenicity in mammalian species without evidence of adaptation. In this study, we report the first complete genome sequence containing 3' and 5' noncoding regions (NCRs) of a mammalian species-infectious and pathogenic H6N5 AIV, which will help provide important insights into the molecular basis of pathogenesis, transmission, and evolution of AIV.
The complete genome sequence of the A/AB/Kor/CN5/09 (H6N5) has been deposited in GenBank under accession numbers JX465637 to JX465644 for Seg-1 to Seg-8.
PMID: 23087119

Keywords : Aquatic birds; Evolution; Genome sequence; H6N5 avian influenza virus (AIV); Pathogenesis; Transmission

Article 88

PI3K-ERK1/2 activation contributes to extracellular H_2O_2 generation in amyloid β toxicity

Neurosci Lett. 526(2):112-7.

Ha JS, Sung HY, Lim HM, Kwon KS, Park SS*

*Corresponding: kwonks@kribb.re.kr
Aging Research Center

Amyloid β peptide (Aβ) induces hydrogen peroxide (H_2O_2) and superoxide generation, leading to neuronal death. Many studies have shown the involvement of NADPH oxidase, but the isotype-specific role was not assessed. Moreover, the activation status of phosphoinositide 3-kinase (PI3K) and extracellular signal-regulated kinase (ERK) 1/2 is unclear in extracellular H_2O_2 generation. In this paper, we showed that Aβ1-42 induced extracellular H_2O_2 generation and the resulting cytotoxicity in a concentration-dependent manner. Nox2- and Nox4-specific siRNAs suppressed H_2O_2 and superoxide generation. LY294002 and U0126, inhibitors of PI3K and ERK1/2, respectively, reduced H_2O_2 generation in concentration-dependent manners. Furthermore, PI3K activation is responsible for ERK1/2 phosphorylation. An additional increase in H_2O_2 generation and corresponding cytotoxicity was observed after treatment with Aβ1-42 and glutamate. These results suggest that Aβ1-42 enhances the neuronal vulnerability to oxidative injury in Alzheimer's disease (AD) by increasing H_2O_2 generation.
PMID: 22925659

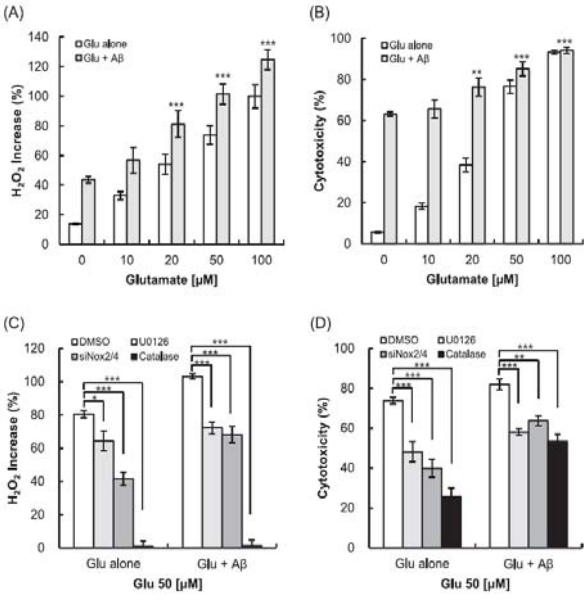

Keywords : Alzheimer's disease; Amyloid β peptide; ERK1/2; NADPH oxidase; Oxidative stress; PI3K

Article 89

A novel gibberellin 2-oxidase gene *CaGA2ox1* in pepper is specifically induced by incompatible plant pathogens

Plant Biotech Rep. 6(4):381-90.

Lee Y, Kim YC, Kim SY, Lee IJ, Choi D, Paek KH, Cho HS, Kweon SY, Park JM*

*Corresponding: jmpark@kribb.re.kr
Infection and Immunity Research Center

Phytohormone balance is increasingly recognized as central to the outcome of plant-pathogen interactions. Differential screening for genes induced by a non-host pathogen in pepper plants (*Capsicum annuum*) identified a putative gibberellin 2-oxidase gene, *CaGA2ox1*. Analysis of the deduced amino acid sequence of CaGA2ox1 showed 53 and 50 % amino acid identity to *Pisum sativum* PsGA2ox2 and *Arabidopsis* AtGA2ox6, respectively. Expression in pepper plants of *CaGA2ox1* was preferentially increased in response to non-host pathogen inoculation and during the host resistance response. *CaGA2ox1* expression increased following treatment with salicylic acid and ethephon (albeit with different induction patterns), but remained unchanged following treatment with methyl jasmonate and abscisic acid. The gene product of *CaGA2ox1* is predicted to catalyze the metabolism of GA 4, and does so in recombinant *E. coli* extracts. Further PEG-mediated transient expression studies showed that CaGA2ox1 fused with soluble modified green fluorescent protein localized to the cytosol in chili pepper protoplasts. Interestingly, the transcript level of *CaGA2ox1* was not affected by treatments of either pepper with bioactive GA_{4+7} or paclobutrazol, an inhibitor of GA biosynthesis. Taken together, these results provide the first evidence that a GA 2-oxidase, which is important in GA metabolism, may also play a role in plant defense signaling and plant-microbe interactions.

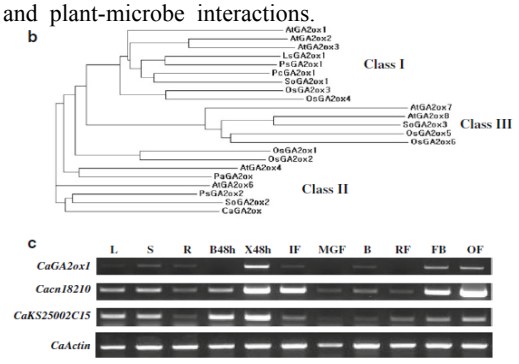

Keywords : *CaGA2ox1*; Capsicum frutescens; Chili pepper (*Capsicum annum*); Gibberellin (GA); Non-host pathogen; *Pisum sativum*

Article 90

Oral administration of HPV-16 L2 displayed on *Lactobacillus casei* induces systematic and mucosal cross-neutralizing effects in Balb/c mice

Vaccine. 30(22):3286-94.

Yoon SW, Lee TY, Kim SJ, Lee IH, Sung MH, Park JS, Poo H*

*Corresponding: haryoung@kribb.re.kr
Infection and Immunity Research Center

The human papillomavirus (HPV) minor capsid protein, L2, is a good candidate for prophylactic vaccine development because L2-specific antibodies have cross-neutralizing activity against diverse HPV types. Here, we developed a HPV mucosal vaccine candidate using the poly-γ-glutamic acid synthetase A (pgsA) protein to display a partial HPV-16 L2 protein (N-terminal 1-224 amino acid) on the surface of *Lactobacillus casei* (*L. casei*). The oral immunization with *L. casei*-L2 induced productions of L2-specific serum IgG and vaginal IgG and IgA in Balb/c mice. To examine cross-neutralizing activity, we used a sensitive high-throughput neutralization assay based on HPV-16, -18, -45, -58, and bovine papillomavirus 1 (BPV1) pseudovirions. Our results revealed that mice vaccinated with *L. casei*-L2 not only generated neutralizing antibodies against HPV-16, but they also produced antibodies capable of cross-neutralizing the HPV-18, -45, and -58 pseudovirions. Consistent with previous reports, vaccination with HPV-16 L1 virus-like particles (VLPs) failed to show cross-neutralizing activity. Finally, we found that oral administration of *L. casei*-L2 induced significant neutralizing activities against genital infection by HPV-16, -18, -45, and -58 pseudovirions encoding a fluorescence reporter gene. These results collectively indicate that oral administration of L2 displayed on *L. casei* induces systemic and mucosal cross-neutralizing effects in mice.

PMID: 22426329

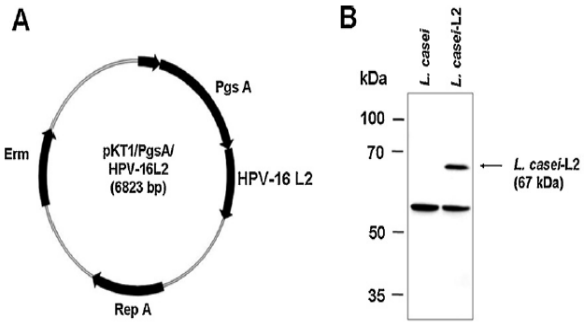

Keywords : Cross-neutralization; HPV-16 L2; *Lactobacillus casei*; Mucosal immunity


KRIBB
www.kribb.re.kr

2012
KRIBB Article Abstracts : First or corresponding articles indexed in SCIE, Scopus, and PubMed

Division of Biomedical Research

- BioMedical Genomics Research Center
- BioMedical Proteomics Research Center
- BioMedical Translational Research Cente
- Research Center of Integrative Cellulomics

Korea Research Institute of Bioscience and Biotechnology

Article 91

High-contrast reversible fluorescence photoswitching of dye-crosslinked dendritic nanoclusters in living vertebrates

Angew Chem Int Ed Engl. 51(12):2878-82.

Kim Y*, Jung HY, Choe YH, Lee C, Ko SK, Koun S, Choi Y, Chung BH, Park BC, Huh TL, Shin I, Kim E

*Corresponding: ykim@kribb.re.kr
BioMedical Proteomics Research Center

Reversibly photoswitchable dendritic nanoclusters for *in vivo* fluorescence imaging were developed using the diarylethene derivative as a crosslinker, which showed high on-off contrast (6.0-19.1 folds) in living systems. Moreover, to our best knowledge, this is the first biocompatible fluorescent nanostructure that has internalized effectively into a living zebrafish via two independent routes—permeation and microinjection—for the imaging of interior organs and blood vessels, respectively. Unlike the recently reported photoswitchable GFP-like proteins, our biocompatible dendritic nanoclusters for high-contrast reversible photoswitching do not require complex biological manipulations such as genetic encoding and protein expression, and can be simply treated or injected to living cells and organisms like small molecule fluorophores. Additional functional units such as targeting groups can be attached to the surface of these nanoclusters to accomplish multiple goals simultaneously. Furthermore, with proper structural modification of the diarylethene component, the spectroscopic properties can be tuned for photoswitching at a desired wavelength. We envision that our relatively nontoxic and water-soluble dendritic nanoclusters may facilitate fluorescence imaging *in vivo* by enhancing its resolution through the reversibly controlled exhibition of high on-off contrast.

PMID: 22307986

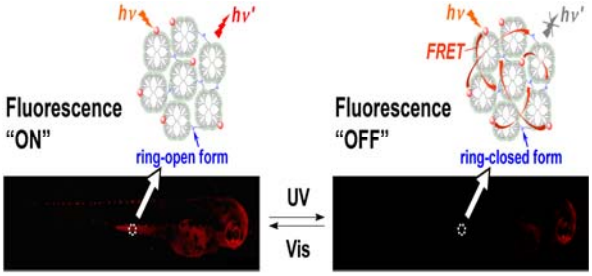

Keywords : Biocompatible fluorescent nanostructure; Diarylethene derivative; Fluorescence imaging; Photoswitchable dendritic nanoclusters;

Article 92

Mechanisms to prevent caspase activation in rotenone-induced dopaminergic neurodegeneration: role of ATP depletion and procaspase-9 degradation

Apoptosis. 17(5):449-62.

Kang H, Han BS*, Kim SJ, Oh YJ

*Co-first: bshan@kribb.re.kr
Research Center of Integrative Cellulomics

The evidence implicating a mode of cell death that either favors or argues against caspase-dependent apoptosis is available in studies that used experimental models of Parkinson's disease. We sought to investigate the mechanisms by which release of cytochrome c is not linked to caspase activation during rotenone-induced dopaminergic (DA) neurodegeneration. Unlike caspase activation in 6-hydroxydopamine-treated cells, both MN9D DA neuronal cells and primary cultures of mesencephalic neurons showed no obvious signs of caspase activation upon exposure to rotenone. We found that intracellular levels of ATP significantly decreased at the early phase of neurodegeneration (<~24 h) and therefore external addition of ATP to the lysates obtained at this stage reconstituted caspase-3 activity. At a later phase of cell death (>~24 h), both decreased levels of ATP and procaspase-9 contributed to the lack of caspase-3 activation. Under this condition, calpain and the proteasome system were responsible for the degradation of procaspase-9. Consequently, external addition of ATP and procaspase-9 to the lysates harvested at the later phase was required for activation of caspase-3. Similarly, caspase-3 activity was also reconstituted in the lysates harvested from cells co-treated with inhibitors of these proteases and incubated in the presence of external ATP. Taken together, our findings provided a sequential mechanism underlying how DA neurons may undergo caspase-independent cell death, even in the presence of cytoplasmic cytochrome *c* following inhibition of mitochondrial complex I.

PMID:22289916

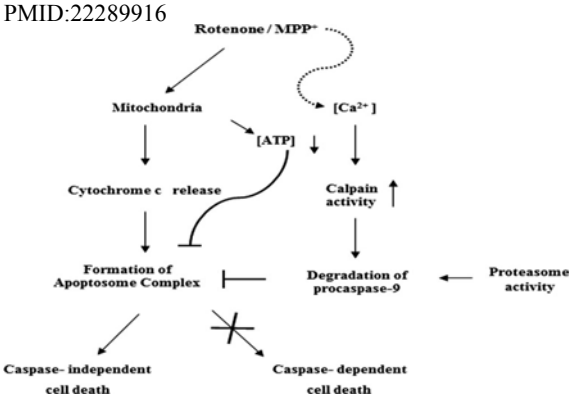

Keywords : Calpain; Mitochondrial complex I inhibitor; Neurodegeneration; Proteasome

Article 93

Small heat-shock protein Hsp9 has dual functions in stress adaptation and stress-induced G2-M checkpoint regulation via Cdc25 inactivation in *Schizosaccharomyces pombe*

Biochem Biophys Res Commun. 417(1):613-8.

Ahn J, Won M, Choi JH, Kyun ML, Cho HS, Park HM, Kang CM, Chung KS*

*Co-corresponding: kschung@kribb.re.kr
BioMedical Genomics Research Center

The small heat-shock protein Hsp9 from *Schizosaccharomyces pombe* was previously reported to be a homologue of *Saccharomyces cerevisiae* HSP12. Although Hsp9 is expressed in response to heat shock and nutritional limitation, its function is still not completely understood. Here, we explored the biological function of Hsp9 in *S. pombe*. The *hsp9* gene might play a role in stress adaptation; *hsp9* deletion caused heat sensitivity and overexpression induced heat tolerance. In addition, Hsp9 also contribute to cell cycle regulation in the nucleus. Δ*hsp9* cells grew more quickly and were shorter in length than wild-type cells. Moreover, Δ*hsp9* cells did not achieve checkpoint arrest under stress conditions, leading to cell death, and exhibited a short doubling time and short G2 phase. Overexpression of *hsp9* induced cell cycle delay, increased the population of G2 phase cells, and rescued the phenotypes of *cdc2-33*, *cdc25-22*, Δ*rad24*, and Δ*rad25* mutants, suggesting that Hsp9 probably regulates Cdc2 phosphorylation by modulating the Cdc25 activity. Indeed, immunoprecipitation experiments revealed that Hsp9 is associated with 14-3-3 and Cdc25. In Δ*hsp9* cells, the association of 14-3-3 with Cdc25 was weakened and Cdc2 phosphorylaton was reduced. Together, our data suggest that Hsp9 has dual functions in stress adaptation and regulating a G2-M checkpoint by the Cdc25 inactivation; this differs from *S. cerevisiae* HSP12, which maintains cell membrane stability under stress conditions.
PMID: 22182414

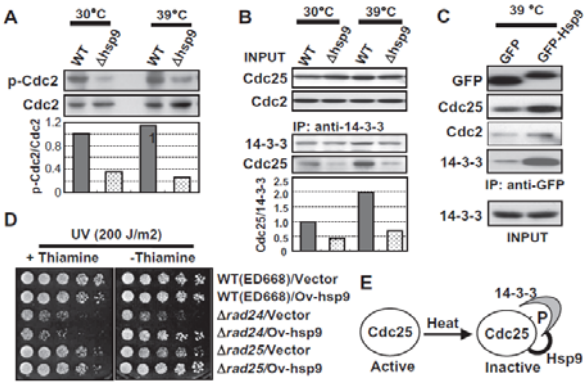

Keywords : Cdc25; G2-M checkpoint; Hsp9; Small heat shock protein; Stress

Article 94

Structural insights into the dual-targeting mechanism of Nutlin-3

Biochem Biophys Res Commun. 420(1):48-53.

Shin JS, Ha JH, He F, Muto Y, Ryu KS, Yoon HS, Kang S, Park SG, Park BC, Choi SU, Chi SW*

*Co-corresponding: swchi@kribb.re.kr
BioMedical Proteomics Research Center

Multi-targeting therapy is an emerging strategy of drug discovery to improve therapeutic efficacy, safety and resistance profiles. In this study, we monitored the binding of a potent MDM2 inhibitor Nutlin-3 with anti-apoptotic Bcl-2 family proteins using NMR spectroscopy. Our results showed the universal binding of Nutlin-3 with diverse anti-apoptotic Bcl-2 family proteins. Taken together with the binding data for Nutlin-3 analogs, the structural model of the Bcl-X_L/Nutlin-3 complex showed that the binding mode of Nutlin-3 resembles that of the Bcl-X_L/Bcl-2 inhibitors, suggesting the molecular mechanism of transcription-independent mitochondrial apoptosis by Nutlin-3. Finally, our structural comparison provides structural insights into the dual-targeting mechanism of how Nutlin-3 can bind to two different target proteins, MDM2 and anti-apoptotic Bcl-2 family proteins in a similar manner.
PMID: 22402281

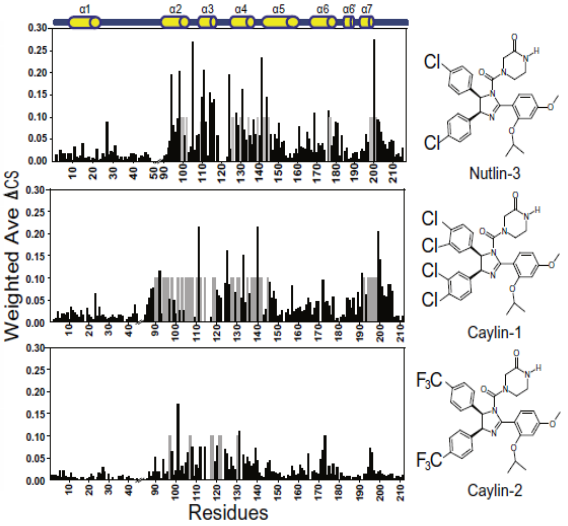

Keywords : Apoptosis; Bcl-2 family proteins; Multi-targeting drug; NMR; Nutlin-3

Article 95

Pyruvate kinase M2 promotes the growth of gastric cancer cells via regulation of Bcl-xL expression at transcriptional level

Biochem Biophys Res Commun. 423(1):38-44.

Kwon OH, Kang TW, Kim JH, Kim M, Noh SM, Song KS, Yoo HS, Kim WH, Xie Z, Pocalyko D, Kim SY*, Kim YS*

*Co-corresponding: kimsy@kribb.re.kr yongsung@kribb.re.kr
BioMedical Genomics Research Center

PKM2 is an isoenzyme of the glycolytic enzyme pyruvate kinase that promotes aerobic glycolysis. Here, we describe an important role for PKM2 in regulating the survival of gastric cancer (GC) cells. We showed that PKM2 was overexpressed in gastric tumor tissues compared to normal tissues and its expression level was associated with poor survival of gastric cancer patients. We also showed that PKM2 affected cell survival by regulating Bcl-xL at the transcriptional level. PKM2 knockdown partially affected the stability of NF-kB subunit p65, suggesting that post-translational regulation of p65 by PKM2 is one of plausible mechanisms for the increased cell growth. Therefore, PKM2 may function as an upstream molecule that regulates p65 function and thus enhances the growth of tumor cells.

PMID: 22627140

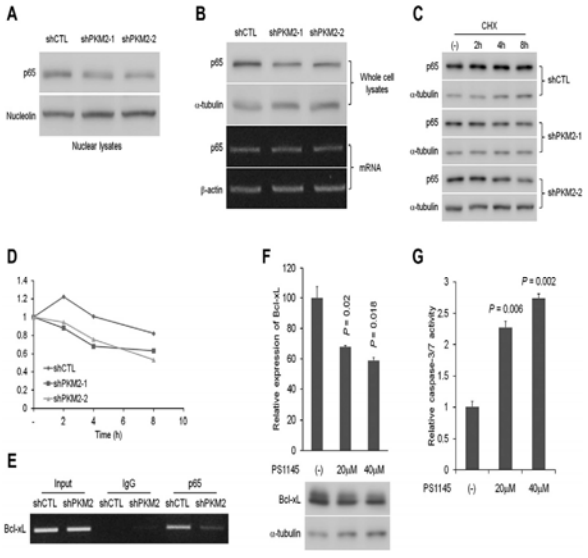

Keywords : Aerobic glycolysis; Bcl-xL; Gastric cancer; NF-kB; PKM2; Transcriptional level

Article 96

Confirmation of Frm2 as a novel nitroreductase in *Saccharomyces cerevisiae*

Biochem Biophys Res Commun. 423(4):638-41.

Bang SY, Kim JH, Lee PY, Bae KH, Lee JS, Kim PS, Lee do H, Myung PK, Park BC, Park SG*

*Corresponding: sgpark@kribb.re.kr
BioMedical Proteomics Research Center

Nitroreductases comprise a group of FMN- or FAD-dependent enzymes that reduce nitrosubstituted compounds by using NAD(P)H, and are found in bacterial species and yeast. Although there is little information on the biological functions of nitroreductases, some studies suggest their possible involvement in oxidative stress responses. In the yeast *Saccharomyces cerevisiae*, a putative nitroreductase protein, Frm2, has been identified based on its sequence similarity with known bacterial nitroreductases. Frm2 has been reported to function in the lipid signaling pathway. To study the functions of Frm2, we measured the nitroreductase activity of purified Frm2 on 4-nitroquinoline-N-oxide (4-NQO) using NADH. LC-MS analysis of the reaction products revealed that Frm2 reduced NQO into 4-aminoquinoline-N-oxide (4-AQO) via 4-hydroxyaminoquinoline (4-HAQO). An Frm2 deletion mutant exhibited growth inhibition in the presence of 4-NQO. Thus, in this study, we demonstrate a novel nitroreductase activity of Frm2 and its involvement in the oxidative stress defense system.

PMID: 22687599

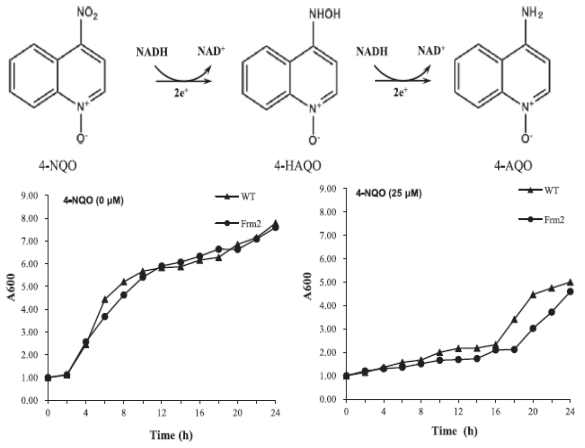

Keywords : 4-AQO; 4-NQO; Frm2; Nitroreductase; Oxidative stress

Article 97

Inheritance of mitochondrial DNA in serially recloned pigs by somatic cell nuclear transfer (SCNT)

Biochem Biophys Res Commun. 424(4):765-70.

Do M, Jang WG, Hwang JH, Jang H, Kim EJ, Jeong EJ, Shim H, Hwang SS, Oh KB, Byun SJ, Kim JH, Lee JW*

*Corresponding: jwlee@kribb.re.kr
Research Center of Integrative Cellulomics

Somatic cell nuclear transfer (SCNT) has been established for the transmission of specific nuclear DNA. However, the fate of donor mitochondrial DNA (mtDNA) remains unclear. Here, we examined the fate of donor mtDNA in recloned pigs through third generations. Fibroblasts of recloned pigs were obtained from offspring of each generation produced by fusion of cultured fibroblasts from a Minnesota miniature pig (MMP) into enucleated oocytes of a Landrace pig. The D-loop regions from the mtDNA of donor and recipient differ at nucleotide sequence positions 16050 (A→T), 16062 (T→C), and 16135 (G→A). In order to determine the fate of donor mtDNA in recloned pigs, we analyzed the D-loop region of the donor's mtDNA by allele-specific PCR (AS-PCR) and real-time PCR. Donor mtDNA was successfully detected in all recloned offspring (F1, F2, and F3). These results indicate that heteroplasmy that originate from donor and recipient mtDNA is maintained in recloned pigs, resulting from SCNT, unlike natural reproduction.
PMID: 22809505

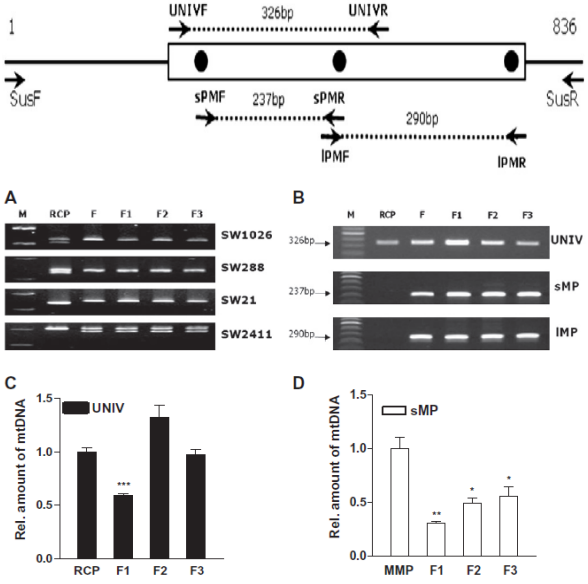

Keywords : Heteroplasmy; Mitochondrial DNA; Recloned pig; Somatic cell nuclear transfer

Article 98

2'-Benzoyloxycinnamaldehyde-mediated DJ-1 upregulation protects MCF-7 cells from mitochondrial damage

Biol Pharm Bull. 35(6):895-902.

Ismail IA, Kang HS, Lee HJ, Kwon BM*, Hong SH

*Co-corresponding: kwonbm@kribb.re.kr
BioMedical Genomics Research Center

2'-Benzoyloxycinnamaldehyde (BCA) is a promising antitumor agent which induces cancer cells apoptosis *via* reactive oxygen species (ROS) generation. BCA shows more effective antiproliferation in MDA-MB-435 than in MCF-7 breast cancer cells. DJ-1 has been known to protect cells against oxidative stress as an antioxidant because of its cysteine residues sensitive to oxidative stress. In the present study, we evaluated the mechanism of DJ-1 for cell protection from oxidative stress after BCA treatment in MCF-7 cell. BCA upregulates the expression of DJ-1 in MCF-7 cells. However, DJ-1 expression decreased continuously for 24 h after BCA treatment in MDA-MB-435 cells. DJ-1 knockdown sensitized MCF-7 cells to BCA, on the contrary, DJ-1 overexpression induced MDA-MB-435 cells less sensitive to BCA. Confocal microscopic observation showed that only in MCF-7 cells BCA increased the overlapped signal between mitochondria and DJ-1 protein. Mitochondrial membrane potential (MMP) was decreased in MDA-MB-435 cells by BCA, and DJ-1 overexpression inhibited BCA-induced MMP decrease in these cells. On the contrary, DJ-1 knockdown in MCF-7 induced MMP perturbation by BCA. These findings suggest that DJ-1 upregulation protects MCF-7 cells from BCA *via* inhibiting mitochondrial damage.
PMID:22687481

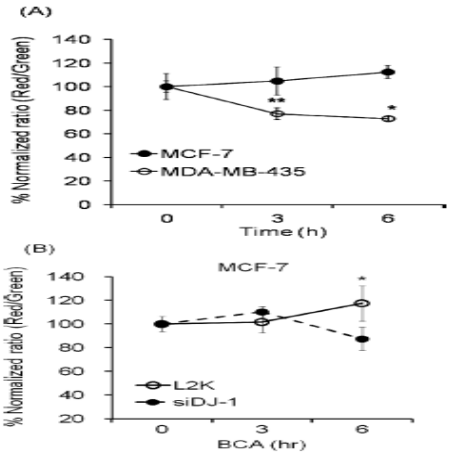

Keywords : 2-benzoyloxycinnamaldehyde; Breast cancer cell; DJ-1; Mitochondrial membrane potential

Article 99

Emodin inhibits migration and invasion of DLD-1 (PRL-3) cells via inhibition of PRL-3 phosphatase activity

Bioorg Med Chem Lett. 22(1):323-6.

Han YM, Lee SK, Jeong DG, Ryu SE, Han DC, Kim DK, Kwon BM*

*Co-corresponding: kwonbm@kribb.re.kr
BioMedical Genomics Research Center

Anthraquinones have been reported as phosphatase inhibitors. Therefore, anthraquinone derivatives were screened to identify a potent phosphatase inhibitor against the phosphatase of regenerating liver-3 (PRL-3). Emodin strongly inhibited phosphatase activity of PRL-3 with IC_{50} values of 3.5μM and blocked PRL-3-induced tumor cell migration and invasion in a dose-dependent manner. Emodin rescued the phosphorylation of ezrin, which is a known PRL-3 substrate. The results of this study reveal that emodin is a PRL-3 inhibitor and a good lead molecule for obtaining a selective PRL-3 inhibitor.

PMID: 22137788

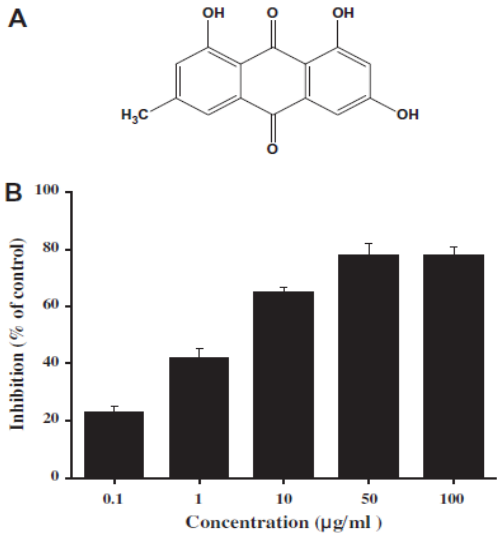

Keywords : Emodin; Invasion; Metastasis; Migration; PRL-3

Article 100

Structure-based virtual screening approach to the discovery of novel PTPMT1 phosphatase inhibitors

Bioorg Med Chem Lett. 22(2):1271-5.

Park H, Kim SY, Kyung A, Yoon TS, Ryu SE, Jeong DG*

*Corresponding: dgjeong@kribb.re.kr
BioMedical Proteomics Research Center

Dual-specificity protein tyrosine phosphatase localized to mitochondrion 1 (PTPMT1) has recently proved to be a promising therapeutic target for the treatment of type II diabetes. Herein we report the first example for a successful application of the structure-based virtual screening to identify the novel inhibitors of human PTPMT1. These inhibitors were computationally screened for having desirable physicochemical properties as a drug candidate and reveal a high potency with IC_{50} values ranging from 0.7 to 17.3μM. Therefore, they deserve consideration for further development by structure-activity relationship studies to optimize the antidiabetic activities. Structural features relevant to the stabilization of the newly identified inhibitors in the active site of PTPMT1 are addressed in detail.

PMID:22115589

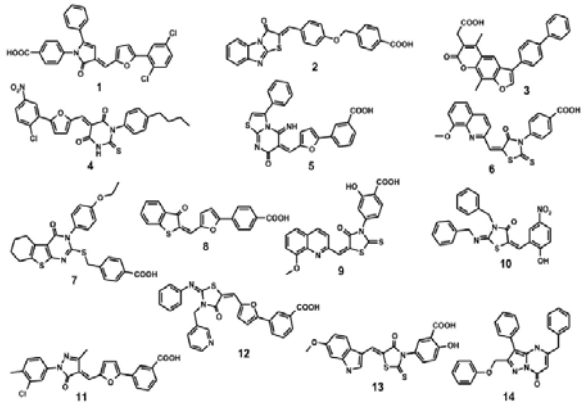

Keywords : Antidiabetic agents; Docking; Inhibitor; PTPMT1; Virtual screening

Article 101

Identification of 3-acyl-2-phenylamino-1,4-dihydroquinolin-4-one derivatives as inhibitors of the phosphatase SerB653 in *Porphyromonas gingivalis*, implicated in periodontitis

Bioorg Med Chem Lett. 22(5):2084-8.

Jung SK, Ko Y, Yu KR, Kim JH, Lee JY, Chae CH, Ji S, Kim CH, Lee HK, Choi EB, Kim BY, Erikson RL, Chung SJ, Kim SJ*

*Co-corresponding: ksj@kribb.re.kr
BioMedical Proteomics Research Center

The serine phosphatase SerB653 plays a crucial role in the infection of *Porphyromonas gingivalis*, which contributes to the pathogenesis of periodontitis, an inflammatory disease of teeth-supporting tissues. Because functional loss of SerB653 eliminates the virulence of *P. gingivalis*, SerB653 inhibitors are considered potential periodontitis therapeutic or preventive agents. To identify SerB653 inhibitors with potent anti-periodontitis activity, we conducted a high-throughput screen of a representative 6800-compound subset of a synthetic chemical library of the Korea Chemical Bank (KCB) for compounds with activity against SerB653. The primary screening yielded 150 hits, and subsequent confirmatory studies identified eight compounds, mainly within a single cluster of 3-acyl-2-phenylamino-1,4-dihydroquinolin-4-one derivatives, that showed greater than 50% inhibition of SerB653 activity at a concentration of 50μM. A second screening with a focused library identified 10 compounds with IC_{50} values less than 10μM. In antibacterial tests, three of these compounds showed a minimum inhibitory concentration against *P. gingivalis* growth of 5-50nM.

PMID: 22326397

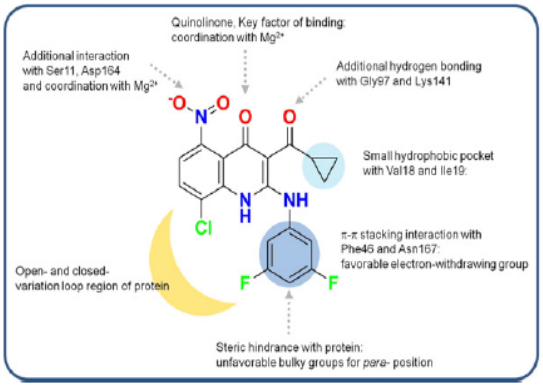

Keywords : Competitive inhibitor; Gram-negative anaerobe; Haloacid dehalogenase; HTS; Malachite green colorimetric method; Periodontitis

Article 102

Crystal structure of xenotropic murine leukaemia virus-related virus (XMRV) ribonuclease H

Biosci Rep. 32(5):455-63.

Kim JH, Kang S, Jung SK, Yu KR, Chung SJ, Chung BH, Erikson RL, Kim BY*, Kim SJ*

*Co-corresponding: bykim@kribb.re.kr ksj@kribb.re.kr
BioMedical Proteomics Research Center

RNase H (retroviral ribonuclease H) cleaves the phosphate backbone of the RNA template within an RNA/DNA hybrid to complete the synthesis of double-stranded viral DNA. In the present study we have determined the complete structure of the RNase H domain from XMRV (xenotropic murine leukaemia virus-related virus) RT (reverse transcriptase). The basic protrusion motif of the XMRV RNase H domain is folded as a short helix and an adjacent highly bent loop. Structural superposition and subsequent mutagenesis experiments suggest that the basic protrusion motif plays a role in direct binding to the major groove in RNA/DNA hybrid, as well as in establishing the co-ordination among modules in RT necessary for proper function.

PMID: 22724525

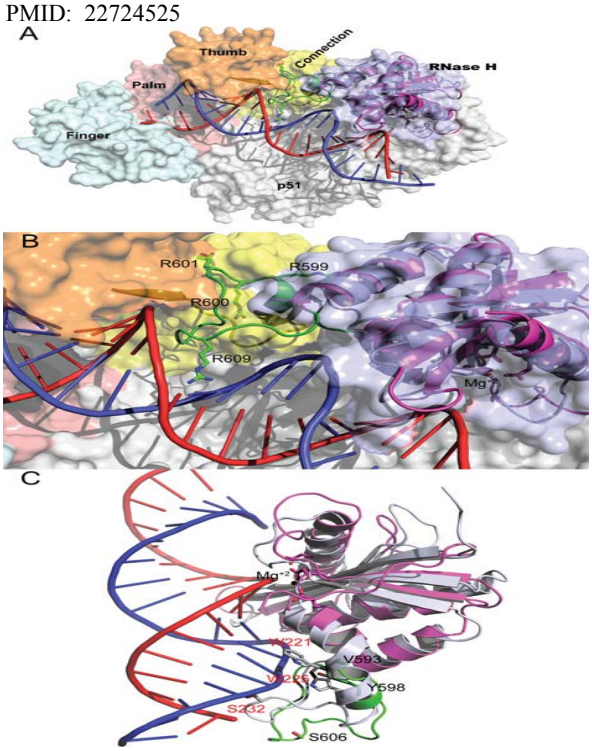

Keywords : *Escherichia coli*; Leukaemia virus-related virus (XMRV); Murine leukaemia virus; Reverse transcriptase; Ribonuclease H; Xenotropic murine

Article 103

Molecular docking study on the α3β2 neuronal nicotinic acetylcholine receptor complexed with α-conotoxin GIC

BMB Rep. 45(5):275-80.

Lee C, Lee SH, Kim DH, Han KH*

*Corresponding: khhan600@kribb.re.kr
BioMedical Translational Research Center

Nicotinic acetylcholine receptors (nAChRs) are a diverse family of homo- or heteropentameric ligand-gated ion channels. Understanding the physiological role of each nAChR subtype and the key residues responsible for normal and pathological states is important. α-Conotoxin neuropeptides are highly selective probes capable of discriminating different subtypes of nAChRs. In this study, we performed homology modeling to generate the neuronal α3, β2 and β4 subunits using the x-ray structure of the α1 subunit as a template. The structures of the extracellular domains containing ligand binding sites in the α3β2 and α3β4 nAChR subtypes were constructed using MD simulations and ligand docking processes in their free and ligand-bound states using α-conotoxin GIC, which exhibited the highest α3β2 vs. α3β4 discrimination ratio. The results provide a reasonable structural basis for such a discriminatory ability, supporting the idea that the present strategy can be used for future investigations on nAChR-ligand complexes.
PMID: 22617450

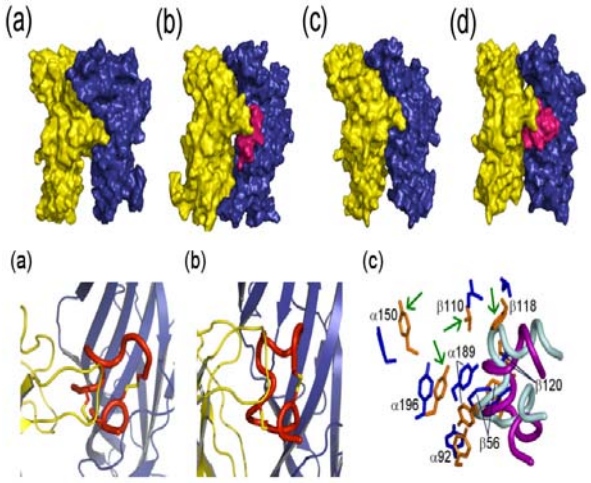

Keywords : α-Conotoxin GIC; Homology modeling; Ligand-docking; Molecular dynamics simulations; Nicotinic acetylcholine receptors (nAChRs)

Article 104

Expression level and glycan dynamics determine the net effects of TIMP-1 on cancer progression

BMB Rep. 45(11):623-8.

Kim YS, Kim SH, Kang JG, Ko JH*

*Corresponding: jhko@kribb.re.kr
BioMedical Translational Research Center

Tissue inhibitor of metalloproteinases (TIMPs; TIMP-1, -2, -3 and -4) are endogenous inhibitor for matrix metalloproteinases (MMPs) that are responsible for remodeling the extracellular matrix (ECM) and involved in migration, invasion and metastasis of tumor cells. Unlike under normal conditions, the imbalance between MMPs and TIMPs is associated with various diseased states. Among TIMPs, TIMP-1, a 184-residue protein, is the only N-linked glycoprotein with glycosylation sites at N30 and N78. The structural analysis of the catalytic domain of human stromelysin-1 (MMP-3) and human TIMP-1 suggests new possibilities of the role of TIMP-1 glycan moieties as a tuner for the proteolytic activities by MMPs. Because the TIMP-1 glycosylation participate in the interaction, aberrant glycosylation of TIMP-1 presumably affects the interaction, thereby leading to pathogenic dysfunction in cancer cells. TIMP-1 has not only the cell proliferation activities but also anti-oncogenic properties. Cancer cells appear to utilize these bilateral aspects of TIMP-1 for cancer progression; an elevated TIMP-1 level exerts to cancer development via MMP-independent pathway during the early phase of tumor formation, whereas it is the aberrant glycosylation of TIMP-1 that overcome the high anti-proteolytic burden. The aberrant glycosylation of TIMP-1 can thus be used as staging and/or prognostic biomarker in colon cancer.
PMID: 23187000

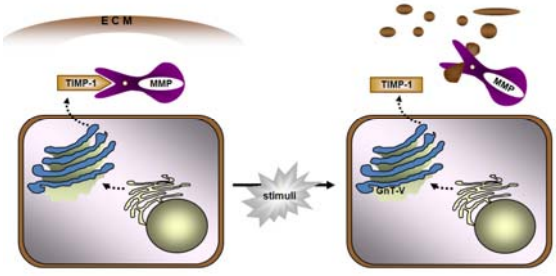

Keywords : Aberrant glycosylation; Cancer progression; MMP; TIMP-1; Tumor microenvironment

Article 105

Tumor-associated autoantibodies as diagnostic and prognostic biomarkers

BMB Rep. 45(12):677-85.

Heo CK, Bahk YY, Cho EW*

*Corresponding: ewcho@kribb.re.kr
BioMedical Translational Research Center

In the process of tumorigenesis, normal cells are remodeled to cancer cells and protein expression patterns are changed to those of tumor cells. A newly formed tumor microenvironment elicits the immune system and, as a result, a humoral immune response takes place. Although the tumor antigens are undetectable in sera at the early stage of tumorigenesis, the nature of an antibody amplification response to antigens makes tumor-associated autoantibodies as promising early biomarkers in cancer diagnosis. Moreover, the recent development of proteomic techniques that make neo-epitopes of tumor-associated autoantigens discovered concomitantly has opened a new area of 'immuno-proteomics', which presents tumor-associated autoantibody signatures and confers information to redefine the process of tumorigenesis. In this article, the strategies recently used to identify and validate serum autoantibodies are outlined and tumor-associated antigens suggested until now as diagnostic/prognostic biomarkers in various tumor types are reviewed. Also, the meaning of autoantibody signatures and their clinical utility in personalized medicine are discussed.

PMID: 23261052

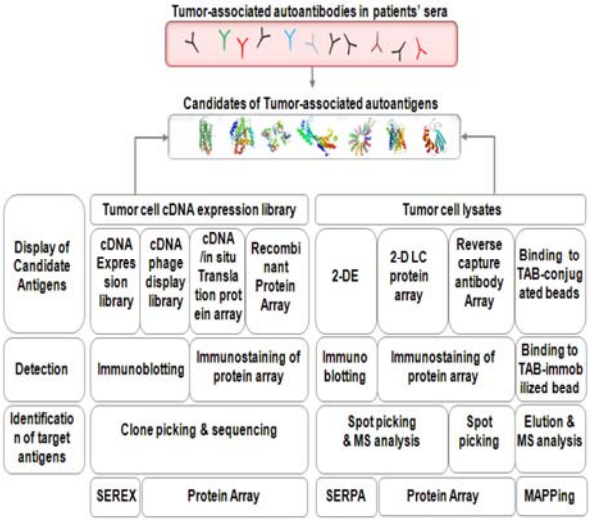

Keywords : Biomarker; Diagnostic; Prognostic; Tumor-associated autoantibody; Tumor-associated autoantigen

Article 106

Structure and catalytic mechanism of human protein tyrosine phosphatome

BMB Rep. 45(12):693-9.

Kim SJ*, Ryu SE

*Corresponding: ksj@kribb.re.kr
BioMedical Proteomics Research Center

Together with protein tyrosine kinases (PTKs), protein tyrosine phosphatases (PTPs) serve as hallmarks in cellular signal transduction by controlling the reversible phosphorylation of their substrates. The human genome is estimated to encode more than 100 PTPs, which can be divided into eleven sub-groups according to their structural and functional characteristics. All the crystal structures of catalytic domains of sub-groups have been elucidated, enabling us to understand their precise catalytic mechanism and to compare their structures across all sub-groups. In this review, I describe the structure and mechanism of catalytic domains of PTPs in the structural context.

PMID: 23261054

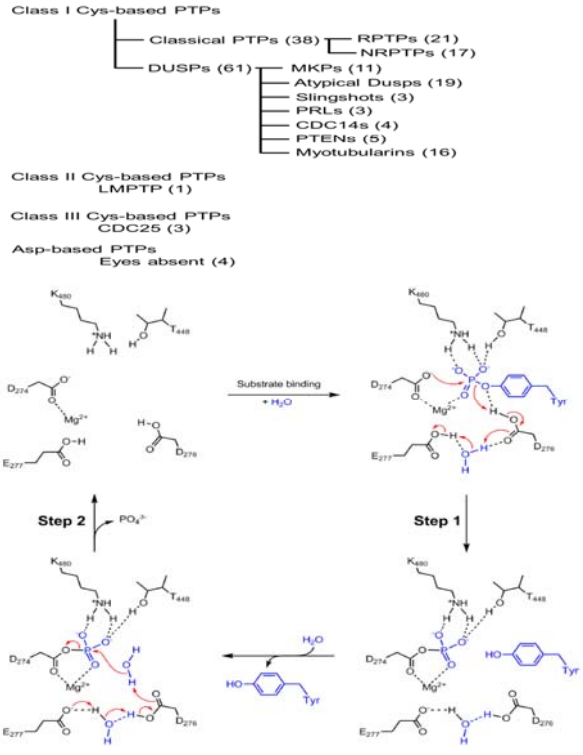

Keywords : Classical PTP; Crystal structure; Dual specificity PTP; Eyes absent; Protein tyrosine phosphatase (PTP)

Article 107

Involvement of protein tyrosine phosphatases in adipogenesis: new anti-obesity targets?

BMB Rep. 45(12):700-6.

Bae KH, Kim WK, Lee SC*

*Corresponding: lesach@kribb.re.kr
Research Center of Integrative Cellulomics

Obesity is a worldwide epidemic as well as being a major risk factor for diabetes, cardiovascular diseases and several types of cancers. Obesity is mainly due to the overgrowth of adipose tissue arising from an imbalance between energy intake and energy expenditure. Adipose tissue, primarily composed of adipocytes, plays a key role in maintaining whole body energy homeostasis. In view of the treatment of obesity and obesity-related diseases, it is critical to understand the detailed signal transduction mechanisms of adipogenic differentiation. Adipogenic differentiation is tightly regulated by many key signal cascades, including insulin signaling. These signal cascades generally transfer or amplify the signal by using serial tyrosine phosphorylations. Thus, protein tyrosine kinases and protein tyrosine phosphatases are closely related to adipogenic differentiation. Compared to protein tyrosine kinases, protein tyrosine phosphatases have received little attention in adipogenic differentiation. This review aims to highlight the involvement of protein tyrosine phosphatases in adipogenic differentiation and the possibility of protein tyrosine phosphatases as drugs to target obesity.

PMID: 23261055

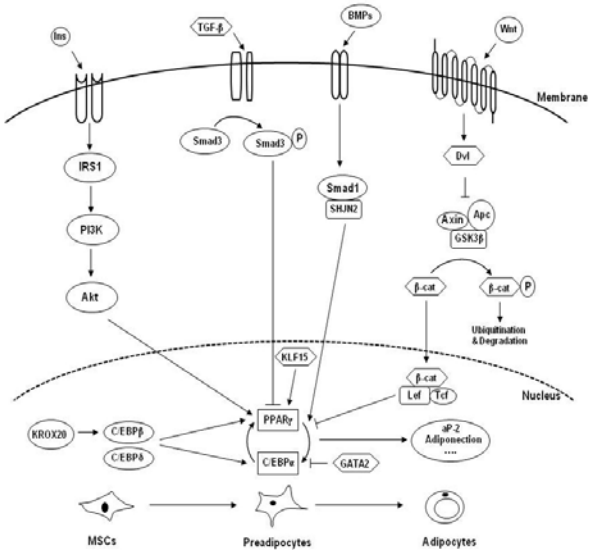

Keywords : Adipocyte; Adipogenesis; Obesity; Phosphorylation; Protein tyrosine phosphatase

Article 108

Ganglioside GM1 influences the proliferation rate of mouse induced pluripotent stem cells

BMB Rep. 45(12):713-8.

Ryu JS, Chang KT, Lee JT, Lim MU, Min HK, Na YJ, Lee SB, Moussavou G, Kim SU, Kim JS, Ko K, Ko K, Hwang KA, Jeong EJ, Lee JW*, Choo YK

*Co-corresponding: jwlee@kribb.re.kr
Research Center of Integrative Cellulomics

Gangliosides play important roles in the control of several biological processes, including proliferation and transmembrane signaling. In this study, we demonstrate the effect of ganglioside GM1 on the proliferation of mouse induced pluripotent stem cells (miPSCs). The proliferation rate of miPSCs was lower than in mouse embryonic stem cells (mESCs). Fluorescence activated cell sorting analysis showed that the percentage of cells in the G2/M phase in miPSCs was lower than that in mESCs. GM1 was expressed in mESCs, but not miPSCs. To confirm the role of GM1 in miPSC proliferation, miPSCs were treated with GM1. GM1-treated miPSCs exhibited increased cell proliferation and a larger number of cells in the G2/M phase. Furthermore, phosphorylation of mitogen-activated protein kinases was increased in GM1- treated miPSCs.

PMID:23261057

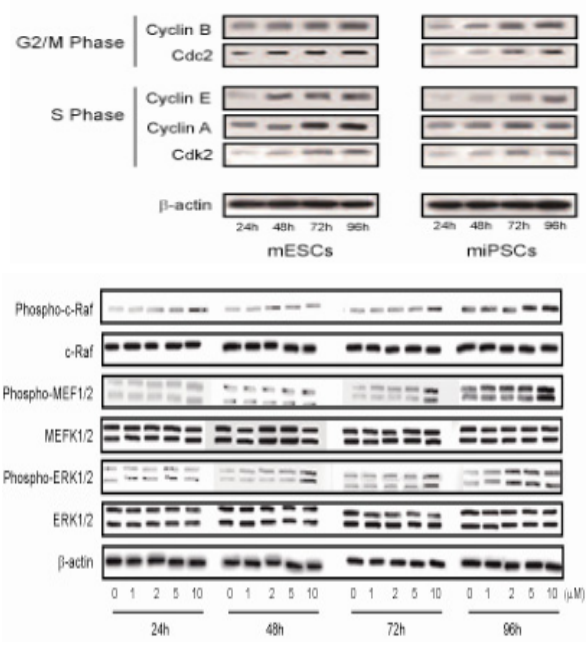

Keywords : Cell cycle; Ganglioside GM1; MAP kinase; Mouse induced pluripotent stem cells (miPSCs); Proliferation

Article 109

An efficient strategy for cell-based antibody library selection using an integrated vector system

BMC Biotechnol. 12:62.

Yoon H, Song JM, Ryu CJ, Kim YG, Lee EK, Kang S, Kim SJ*

*Corresponding: sjick@kribb.re.kr
Research Center of Integrative Cellulomics

BACKGROUND: Cell panning of phage-displayed antibody library is a powerful tool for the development of therapeutic and imaging agents since disease-related cell surface proteins in native complex conformation can be directly targeted. Here, we employed a strategy taking advantage of an integrated vector system which allows rapid conversion of scFv-displaying phage into scFv-Fc format for efficient cell-based scFv library selection on a tetraspanin protein, CD9.
RESULTS: A mouse scFv library constructed by using a phagemid vector, pDR-D1 was subjected to cell panning against stable CD9 transfectant, and the scFv repertoire from the enriched phage pool was directly transferred to a mammalian cassette vector, pDR-OriP-Fc1. The resulting constructs enabled transient expression of enough amounts of scFv-Fcs in HEK293E cells, and flow cytometric screening of binders for CD9 transfectant could be performed simply by using the culture supernatants. All three clones selected from the screening showed correct CD9-specificity. They could immunoprecipitate CD9 molecules out of the transfectant cell lysate and correctly stain endogenous CD9 expression on cancer cell membrane. Furthermore, competition assay with a known anti-CD9 monoclonal antibody (mAb) suggested that the binding epitopes of some of them overlap with that of the mAb which resides within the large extracellular loop of CD9.
CONCLUSIONS: This study demonstrates that scFv-Fc from mammalian transient expression can be chosen as a reliable format for rapid screening and validation in cell-based scFv library selection, and the strategy described here will be applicable to efficient discovery of antibodies to diverse cell-surface targets.
PMID: 22989299

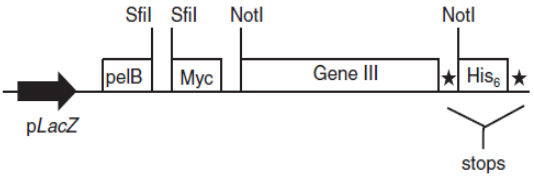

Keywords : Antibody library; CD9; Cell panning; Phage display; scFv-Fc

Article 110

The functional and structural characterization of a novel oncogene GIG47 involved in the breast tumorigenesis

BMC Cancer. 12:274.

Han KH*, Lee SH*, Ha SA, Kim HK, Lee C, Kim DH, Gong KH, Yoo J, Kim S, Kim JW

*Co-first: khhan600@kribb.re.kr shlee@kribb.re.kr
BioMedical Translational Research Center

BACKGROUND: A candidate oncogene GIG47, previously known as a neudesin with a neurotrophic activity, was identified by applying the differential expression analysis method.
METHODS: As a first step to understand the molecular role of GIG47, we analyzed the expression profile of GIG47 in multiple human cancers including the breast cancer and characterized its function related to human carcinogenesis. Based on this oncogenic role of GIG47, we then embarked on determining the high-resolution structure of GIG47. We have applied multidimensional heteronuclear NMR methods to GIG47.
RESULTS: GIG47 was over-expressed in primary breast tumors as well as other human tumors including carcinomas of the uterine cervix, malignant lymphoma, colon, lung, skin, and leukemia. To establish its role in the pathogenesis of breast cancer in humans, we generated stable transfectants of MCF7 cells. The ectopic expression of GIG47 in MCF7 cells promoted the invasiveness in the presence of 50% serum. In addition, it also resulted in the increased tumorigenicity in *in vivo* tumor formation assay. The tumorigenesis mechanism involving GIG47 might be mediated by the activation of MAPK and PI3K pathways. These results indicate that GIG47 plays a role in the breast tumorigenesis, thus representing a novel target for the treatment of breast cancer. To facilitate the development of GIG47-targeted therapeutics, we determined the structural configuration of GIG47. The high-resolution structure of GIG47 was obtained by combination of NMR and homology modeling. The overall structure of GIG47 has four α-helices and 6 β-strands, arranged in a β1-α1-β2-β3-α2-β4-α3-α4-β5-β6 topology. There is a potential heme/steroid binding pocket formed between two helices α2 and α3.
CONCLUSION: The determined three-dimensional structure of GIG47 may facilitate the development of potential anti-cancer agents.
PMID: 22748190

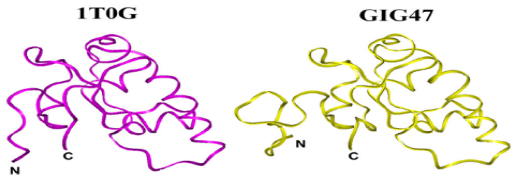

Keywords : Anti-cancer agents; Breast cancer; GIG47; Oncogene; Three-dimensional structure

Article 111

Elevated fibroblast growth factor-inducible 14 expression promotes gastric cancer growth via nuclear factor-κB and is associated with poor patient outcome

Cancer Lett. 314(1):73-81.

Kwon OH, Park SJ, Kang TW, Kim M, Kim JH, Noh SM, Song KS, Yoo HS, Wang Y, Pocalyko D, Paik SG, Kim YH, Kim SY*, Kim YS*

*Co-corresponding: kimsy@kribb.re.kr yongsung@kribb.re.kr
BioMedical Genomics Research Center

The fibroblast growth factor-inducible 14 (Fn14) gene encodes a type I transmembrane protein that belongs to the tumor necrosis factor receptor superfamily and regulates multiple cellular processes in diverse physiological and pathological conditions, including cancer. Here, we describe an important role for Fn14 in regulating the growth of gastric cancer cells. Previous gene expression data analysis demonstrated that Fn14 was up-regulated in various tumor tissues, including gastric cancer. Using qRT-PCR, we showed that Fn14 was overexpressed in gastric tumor tissues compared to normal tissues. Furthermore, Fn14 expression levels were inversely correlated with gastric cancer patient survival. Using ectopic overexpression and shRNA-mediated knockdown of Fn14, we demonstrated that the expression level of Fn14 affected cell growth in gastric cancer. The effect of Fn14 on cell growth was mediated by the NF-κB activity and eventually by the transcriptional regulation of the anti-apoptotic Bcl-2 family gene (Bcl-xL). These results suggest that Fn14 may play an important role in gastric tumor growth by regulating NF-κB-mediated anti-apoptosis and that Fn14 may be a useful prognostic marker for gastric cancer.

PMID: 21993017

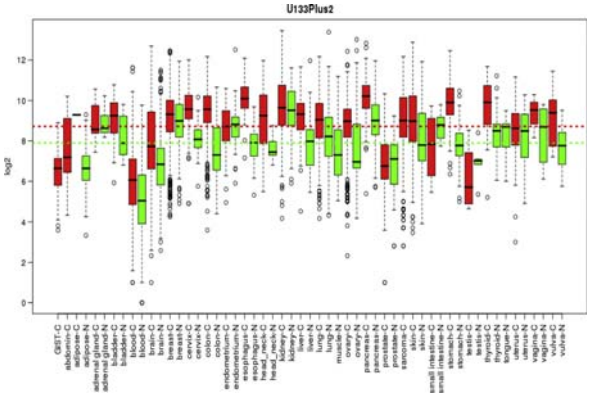

Keywords : Anti-apoptosis; Cell growth; Fn14; Gastric cancer; NF-jB

Article 112

L1 cell adhesion molecule and epidermal growth factor receptor activation confer cisplatin resistance in intrahepatic cholangiocarcinoma cells

Cancer Lett. 316(1):70-6.

Yoon H*, Min JK, Lee DG, Kim DG, Koh SS, Hong HJ

*First:
Research Center of Integrative Cellulomics

Intrahepatic cholangiocarcinoma (ICC) is refractory to conventional chemotherapy. We previously generated chemoresistant ICC (SCK^R) cells and showed that AKT and ERK signaling conferred cisplatin resistance. Here, we report that epidermal growth factor receptor (EGFR) signaling and L1 cell adhesion molecule (L1CAM) conferred cisplatin resistance in SCK^R cells in an additive fashion. Activation of EGFR connected to AKT and ERK signaling pathways may induce anti-apoptosis and promote cell proliferation, while L1CAM promoted cell proliferation by mainly activating ERK signaling. Inhibition of EGFR activation or L1ACM greatly sensitized the cells to cisplatin. EGFR and L1CAM may be important targets for ICC therapy.

PMID: 22088438

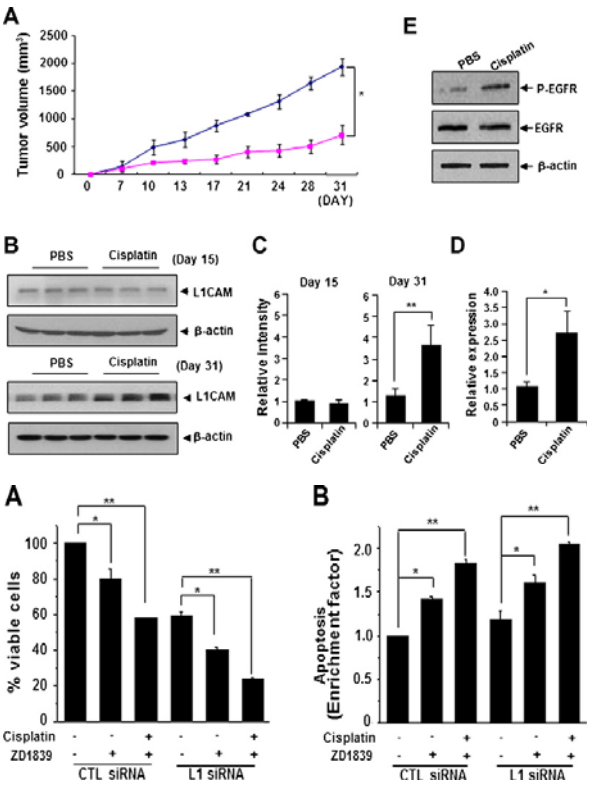

Keywords : Cisplatin resistance; EGFR; Intrahepatic cholangiocarcinoma; L1CAM

Article 113

Dysregulation of overexpressed IL-32α in hepatocellular carcinoma suppresses cell growth and induces apoptosis through inactivation of NF-κB and Bcl-2

Cancer Lett. 318(2):226-33.

Kang YH*, Park MY, Yoon DY, Han SR, Lee CI, Ji NY, Myung PK, Lee HG, Kim JW, Yeom YI, Jang YJ, Ahn DK, Kim JW, Song EY

*First: yhkang@kribb.re.kr
BioMedical Genomics Research Center

IL-32 is a newly discovered cytokine. Recently, various reports suggest that it plays a role as a proinflammatory mediator and may be involved in several cancer carcinogenesis. However, IL-32 expression in hepatocellular carcinoma (HCC) remains unclear. In this study, we investigated the expression and role of IL-32α in hepatocellular carcinoma, because IL-32 was identified as an upregulated gene in hepatocellular carcinoma tissues compared to nontumorous regions using DNA microarray. IL-32α was overexpressed in tissue and serum from patients with HCC and localized in the cytoplasm and nucleus of hepatocellular carcinoma tumor cells. Moreover, secreted IL-32α concentration in the serum of patients with hepatocellular carcinoma was elevated as compared with those in the normal serum using a developed sandwich ELISA. Furthermore, IL-32α suppression in hepatocellular carcinoma decreased expression of phospho-p38 MAPK, NF-κB, and antiapoptotic protein Bcl-2 and induced expression of proapoptotic proteins as well as p53 and PUMA resulting in the suppression of cell growth and induction of intrinsic apoptosis. Based on our results, we suggest that IL-32α is involved in the progression of hepatocellular carcinoma and may be a useful biomarker for diagnosis and therapeutic target of hepatocellular carcinoma.

PMID:22198481

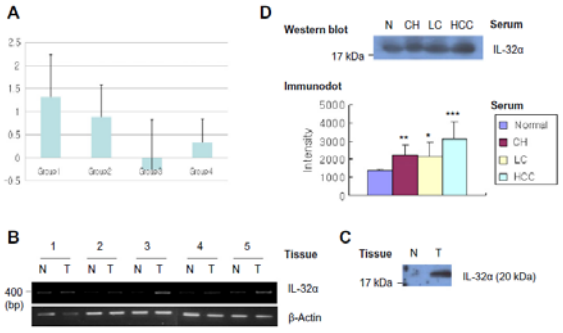

Keywords : Apoptosis; Cell growth; Diagnostic marker; Hepatocellular carcinoma; IL-32a

Article 114

Epigenetic alteration of *CCDC67* and its tumor suppressor function in gastric cancer

Carcinogenesis. 33(8):1494-501.

Park SJ, Jang HR, Kim M, Kim JH, Kwon OH, Park JL, Noh SM, Song KS, Kim SY*, Kim YH, Kim YS*

*Co-corresponding: kimsy@kribb.re.kr yongsung@kribb.re.kr
BioMedical Genomics Research Center

In this study, the promoter of the gene *coiled-coil domain-containing 67* (*CCDC67*) was found to be frequently methylated in gastric cancer cell lines and in primary gastric tumors, as examined by restriction landmark genomic scanning. In addition, *CCDC67* expression was down-regulated in 72.7% of gastric cancer cell lines tested. In most cases, gene down-regulation was associated with CpG hypermethylation in the *CCDC67* promoter. Treatment with 5-aza-2'-deoxycytidine and/or trichostatin A restored *CCDC67* expression in down-regulated cell lines. Pyrosequencing analysis of 150 paired primary gastric cancer samples revealed that promoter CpG methylation was increased in 74% of tested tumors compared with paired adjacent normal tissues, and this hypermethylation correlated significantly with down-regulation of *CCDC67*. CCDC67 protein was localized to the cell membrane by immunocytochemistry. Stable transfection of a *CCDC67* gene in one gastric cancer cell line inhibited adhesion-dependent and -independent colony formation, and *CCDC67* expression suppressed tumorigenesis in nude mice. We suggest that *CCDC67* is a putative tumor suppressor gene that is silenced in gastric cancers by promoter CpG methylation and that it may play an important role in cell signaling and migration related to tumorigenesis.

PMID: 22610074

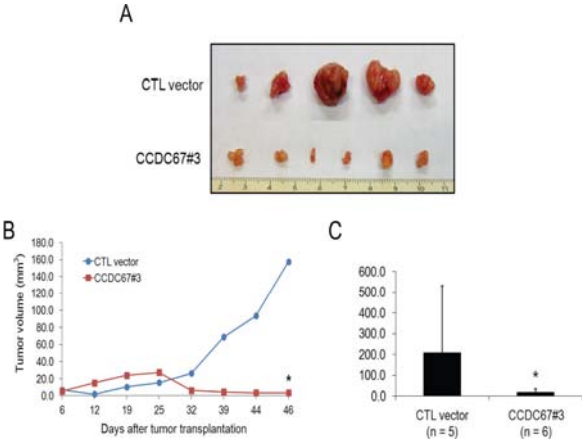

Keywords : CpG hypermethylation; Gastric cancer cell; Pyrosequencing analysis; Putative tumor suppressor

Article 115

Receptor activator of nuclear factor-κB ligand is a novel inducer of myocardial inflammation

Cardiovasc Res. 94(1):105-14.

Ock S, Ahn J, Lee SH, Park H, Son JW, Oh JG, Yang DK, Lee WS, Kim HS, Rho J, Oh GT, Abel ED, Park WJ, Min JK*, Kim J

*Co-corresponding: jekmin@kribb.re.kr
Research Center of Integrative Cellulomics

AIMS: Although increased levels of myocardial receptor activator of nuclear factor (NF)-κB ligand (RANKL) have been reported in heart failure, the role of this pathway in mediating activation of inflammatory pathways during myocardial remodelling is less well understood. This study sought to determine the role of myocardial RANKL in regulating cytokine expression.
METHODS AND RESULTS: A marked increase in RANKL expression occurred as early as 6h following transverse aortic constriction (TAC) in mouse hearts and persisted at 3 and 17 days. An increase in tumour necrosis factor-α (TNF-α), interleukin (IL)-1α, and IL-1β was observed in the hypertrophied hearts only at 3 or 17 days after TAC. Treatment with losartan significantly attenuated TAC-induced cardiac hypertrophy, in parallel with decreased expression of RANKL, TNF-α, IL-1α, and IL-1β. Furthermore, injection of a RANKL-neutralizing monoclonal antibody attenuated RANKL-induced cytokine expression. RANKL stimulated expression of TNF-α, IL-1α, and IL-1β in neonatal rat cardiomyocytes via activation of NF-κB. RANKL-induced NF-κB activation and expression of these cytokines were both attenuated when RANK, receptor for RANKL, or TRAF2 or TRAF6, adaptors for RANK, was silenced by siRNA. Furthermore, inhibitors of phospholipase C (PLC), protein kinase C (PKC), and inhibitor of κB kinase also significantly inhibited RANKL-induced cellular activities, but inhibitors of phosphatidylinositol 3-kinase, extracellular signal-regulated kinase, or p38 mitogen-activated protein kinase were without effect.
CONCLUSION: Our data demonstrate for the first time that the pressure-overloaded myocardium generates RANKL, which induces TNF-α, IL-1α, and IL-1β production via a RANK-TRAF2/TRAF6-PLC-PKC-NF-κB-mediated autocrine mechanism.
PMID:22298642

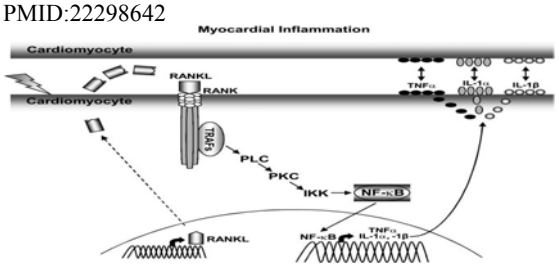

Keywords : Cardiomyocytes; NF-kB; Proinflammatory cytokine; RANKL

Article 116

A critical step for JNK activation: isomerization by the prolyl isomerase Pin1

Cell Death Differ. 19(1):153-61.

Park JE, Lee JA, Park SG, Lee DH, Kim SJ, Kim HJ, Uchida C, Uchida T, Park BC*, Cho S

*Co-corresponding: parkbc@kribb.re.kr
BioMedical Proteomics Research Center

c-Jun N-terminal kinase (JNK) is activated by dual phosphorylation of both threonine and tyrosine residues in the phosphorylation loop of the protein in response to several stress factors. However, the precise molecular mechanisms for activation after phosphorylation remain elusive. Here we show that Pin1, a peptidyl-prolyl isomerase, has a key role in the JNK1 activation process by modulating a phospho-Thr-Pro motif in the phosphorylation loop. Pin1 overexpression in human breast cancer cell lines correlates with increased JNK activity. In addition, small interfering RNA (siRNA) analyses showed that knockdown of Pin1 in a human breast cancer cell line decreased JNK1 activity. Pin1 associates with JNK1, and then catalyzes prolyl isomerization of the phospho-Thr-Pro motif in JNK1 from trans- to cis-conformation. Furthermore, Pin1 enhances the association of JNK1 with its substrates. As a result, *Pin1*$^{-/-}$ cells are defective in JNK activation and resistant to oxidative stress. These results provide novel insights that, following stress-induced phosphorylation of Thr in the Thr-Pro motif of JNK1, JNK1 associates with Pin1 and undergoes conformational changes to promote the binding of JNK1 to its substrates, resulting in cellular responses from extracellular signals.
PMID: 21660049

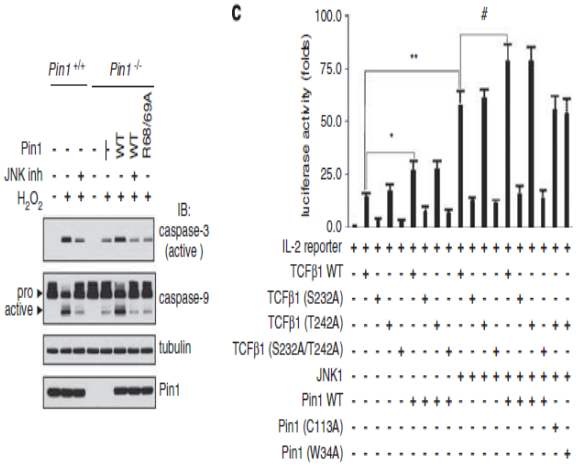

Keywords : Apoptosis; c-Jun N-terminal kinase; Peptidyl-prolyl cis/trans-isomerase

Article 117

ESM-1 regulates cell growth and metastatic process through activation of NF-κB in colorectal cancer

Cell Signal. 24(10):1940-9.

Kang YH, Ji NY, Han SR, Lee CI, Kim JW, Yeom YI, Kim YH, Chun HK, Kim JW, Chung JW, Ahn DK, Lee HG*, Song EY

*Co-corresponding: hglee@kribb.re.kr
BioMedical Genomics Research Center

In our previous study, we reported that endothelial cell specific molecule-1 (ESM-1) was increased in tissue and serum from colorectal cancer patients and suggested that ESM-1 can be used as a potential serum marker for early detection of colorectal cancer. The aim of this study was to evaluate the role of ESM-1 as an intracellular molecule in colorectal cancer. ESM-1 expression was knocked down by small interfering RNA (siRNA) in colorectal cancer cells. Expression of ESM-1 siRNA decreased cell survival through the Akt-dependent inhibition of NF-κB/IκB pathway and an interconnected reduction in phospho-Akt, -p38, -ERK1, -RSK1, -GSK-3α/β and -HSP27, as determined by a phospho-MAPK array. ESM-1 silencing induced G_1 phase cell cycle arrest by induction of PTEN, resulting in the inhibition of cyclin D1 and inhibited cell migration and invasion of COLO205 cells. Consistently, ESM-1 overexpression in HCT-116 cells enhanced cell proliferation through the Akt-dependent activation of NF-κB pathway. In addition, ESM-1 interacted with NF-κB and activated NF-κB promoter. This study demonstrates that ESM-1 is involved in cell survival, cell cycle progression, migration, invasion and EMT during tumor invasion in colorectal cancer. Based on our results, ESM-1 may be a useful therapeutic target for colorectal cancer.

PMID: 22735811

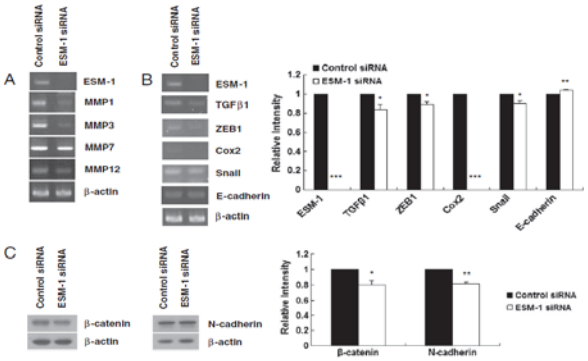

Keywords : Cell growth; Colorectal cancer; ESM-1; Metastatic process; NF-κB activation

Article 118

Identification of potential serum biomarkers for gastric cancer by a novel computational method, multiple normal tissues corrected differential analysis

Clin Chim Acta. 413(3-4):428-33.

Kim M, Kim HJ, Choi BY, Kim JH, Song KS, Noh SM, Kim JC, Han DS, Kim SY*, Kim YS*

*Co-corresponding: kimsy@kribb.re.kr yongsung@kribb.re.kr
BioMedical Genomics Research Center

BACKGROUND: Genes specifically expressed in one or a few tissues and upregulated in tumors are potentially good serum biomarkers.
METHODS: By applying a recently developed computational method, called multiple normal tissues corrected differential analysis (MNTDA), we identified genes that are likely to be upregulated in the blood of gastric cancer patients as compared to normal controls.
RESULTS: We identified four genes (MMP-1, MMP-3, MMP-12, and CXCL5) as potential serum biomarkers for gastric cancer. Of these four genes, only MMP-1 was significantly upregulated in the sera of 40 gastric cancer patients, as compared to 40 control sera. The same pattern was observed in the second cohort of 80 gastric cancer patients and 80 controls. In a combined analysis, the level of serum MMP-1 in gastric cancer patients was significantly higher than the level in control samples (P<0.0001). The use of MMP-1 was 62.5% sensitive and 62.5% specific in detecting gastric cancer patients. Patients with high serum levels of MMP-1 had a significantly worse outcome than patients with low serum MMP-1 levels. Finally, we determined that preoperative serum MMP-1 levels were prognostic, independent of tumor stage.
CONCLUSIONS: MMP-1 is a potential prognostic marker for gastric cancer patients after gastrectomy.

PMID: 22057037

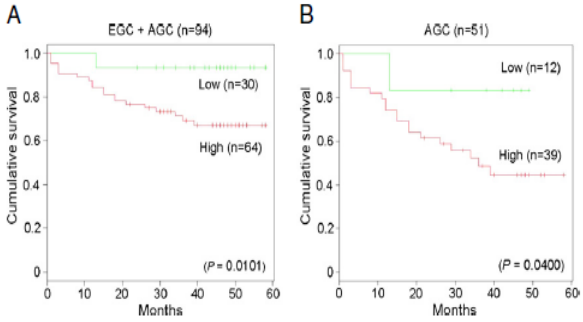

Keywords : Computational method; Gastric cancer; MMP-1; Prognostic biomarker

Article 119

Aberrant l1 cell adhesion molecule affects tumor behavior and chemosensitivity in anaplastic thyroid carcinoma

Clin Cancer Res. 18(11):3071-8.

Kim KS, Min JK*, Liang ZL, Lee K, Lee JU, Bae KH, Lee MH, Lee SE, Ryu MJ, Kim SJ, Kim YK, Choi MJ, Jo YS, Kim JM, Shong M

*Co-first: jekmin@kribb.re.kr
Research Center of Integrative Cellulomics

PURPOSE: Anaplastic thyroid carcinoma (ATC) is one of the most invasive human cancers and has a poor prognosis. Molecular targets of ATC that determine its highly aggressive nature remain unidentified. This study investigated L1 cell adhesion molecule (L1CAM) expression and its role in tumorigenesis of ATCs.
EXPERIMENTAL DESIGN: Expression of L1CAM in thyroid cancer was evaluated by immunohistochemical analyses of tumor samples from patients with thyroid cancer. We investigated the role of L1CAM in proliferation, migration, invasion, and chemoresistance using short hairpin RNA (shRNA) knockdown experiments in human ATC cell lines. Finally, we evaluated the role of L1CAM on tumorigenesis with ATC xenograft assay in a nude mouse model.
RESULTS: L1CAM expression was not detectable in normal follicular epithelial cells of the thyroid or in differentiated thyroid carcinoma. In contrast, analysis of ATC samples showed specifically higher expression of L1CAM in the invasive area of the tumor. Specific knockdown of L1CAM in the ATC cell lines, FRO and 8505C, caused a significant decrease in the proliferative, migratory, and invasive capabilities of the cells. Suppression of L1CAM expression in ATC cell lines increased chemosensitivity to gemcitabine or paclitaxel. Finally, in an ATC xenograft model, depletion of L1CAM markedly reduced tumor growth and increased the survival of tumor-bearing mice.
CONCLUSIONS: We report that L1CAM is highly expressed in the samples taken from patients with ATCs. L1CAM plays an important role in determining tumor behavior and chemosensitivity in cell lines derived from ATCs. Therefore, we suggest that L1CAM may be an important therapeutic target in patients with ATCs.
PMID:22472175

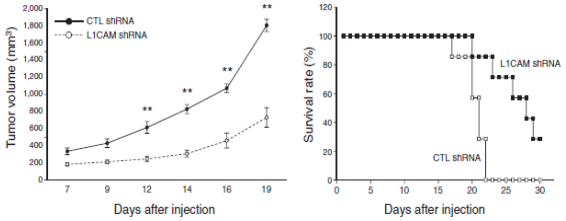

Keywords : Anaplastic thyroid carcinoma; ATC xenograft model; L1 cell adhesion molecule; Thyroid cancer

Article 120

Chemokine (C-X-C motif) ligand 12 is associated with gallbladder carcinoma progression and is a novel independent poor prognostic factor

Clin Cancer Res. 18(12):3270-80.

Lee HJ, Lee K, Lee DG, Bae KH, Kim JS, Liang ZL, Huang SM, Suk Oh Y, Kim HY, Jo DY, Min JK*, Kim JM, Lee HJ

*Co-corresponding: jekmin@kribb.re.kr
Research Center of Integrative Cellulomics

PURPOSE: Although recent studies have suggested that chemokine (C-X-C motif) ligand 12 (CXCL12) is important in the progression of various malignancies, its role in gallbladder carcinoma (GBC) remains unknown. We investigated CXCL12 expression in GBC and its biologic and prognostic role in GBC tumorigenesis.
EXPERIMENTAL DESIGN: We examined CXCL12 expression in tumor specimens from 72 patients with GBC by immunohistochemistry and analyzed the correlation between CXCL12 expression and clinicopathologic factors or survival. The functional significance of CXCL12 expression was investigated by CXCL12 treatment and suppression of CXCR4, a major receptor of CXCL12, as well as by CXCL12 overexpression in *in vitro* and *in vivo* studies.
RESULTS: CXCL12 was differentially expressed in GBC tissues. CXCL12 expression was significantly associated with a high histologic grade (P = 0.042) and nodal metastasis (P = 0.015). Multivariate analyses showed that CXCL12 expression (HR, 8.675; P = 0.014) was an independent risk factor for patient survival. CXCL12 significantly increased anchorage-dependent and -independent growth, migration, invasion, adhesiveness, and survival of GBC cells *in vitro*, and these effects were dependent on CXCR4. Consistent with these results, overexpression of CXCL12 significantly promoted GBC tumorigenicity in a xenograft model.
CONCLUSIONS: Our results indicate that GBC cells express both CXCL12 and its receptor CXCR4, and CXCL12 may have a role in GBC progression through an autocrine mechanism. In addition, CXCL12 is a novel independent poor prognostic factor in patients with GBCs. Thus, targeting CXCL12 and CXCR4 may provide a novel therapeutic strategy for GBC treatment.
PMID:22553346

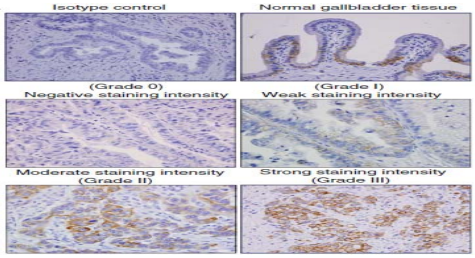

Keywords : Chemokine ligand 12; Clinicopathologic factors; Gallbladder carcinoma; Xenograft model

Article 121

Understanding pre-structured motifs (PreSMos) in intrinsically unfolded proteins

Curr Protein Pept Sci. 13(1):34-54.

Lee SH, Kim DH, Han JJ, Cha EJ, Lim JE, Cho YJ, Lee C, Han KH*

*Corresponding: khhan600@kribb.re.kr
BioMedical Translational Research Center

Intrinsically unfolded proteins (IUPs) do not obey the golden rule of structural biology, 3D structure = function, as they manifest their inherent functions without resorting to three-dimensional structures. Absence of a compact globular topology in these proteins strongly implies that their ligand recognition processes should involve factors other than spatially well-defined binding pockets. Heteronuclear multidimensional (HetMulD) NMR spectroscopy assisted with a stable isotope labeling technology is a powerful tool for quantitatively investigating detailed structural features in IUPs. In particular, it allows us to delineate the presence and locations of pre-structured motifs (PreSMos) on a per-residue basis. PreSMos are the transient local structural elements that presage target-bound conformations and act as specificity determinants for IUP recognition by target proteins. Here, we present a brief chronicle of HetMulD NMR studies on IUPs carried out over the past two decades along with a discussion on the functional significance of PreSMos in IUPs.
PMID: 22044148

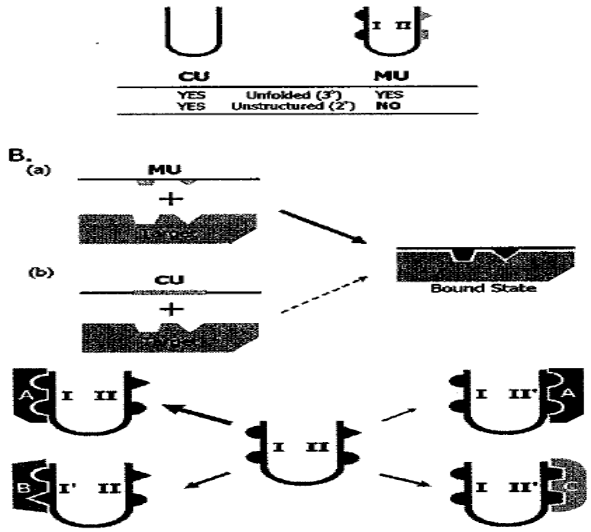

Keywords : Completely unstructured; Intrinsically Dirsordered Region (IDR); Intrinsically Unfolder Proteins (IUPs); Mostly unstructured; NMR; Pre-Structured Motifs (PreSMos)

Article 122

Over-expression of extracellular superoxide dismutase in mouse synovial tissue attenuates the inflammatory arthritis

Exp Mol Med. 44(9):529-35.

Yu DH, Yi JK, Yuh HS, Park Sj, Kim HJ, Bae KB, Ji YR, Kim NR, Park SJ, Kim do H, Kim SH, Kim MO, Lee JW*, Ryoo ZY

*Co-corresponding: jwlee@kribb.re.kr
Research Center of Integrative Cellulomics

Oxidative stress such as reactive oxygen species (ROS) within the inflamed joint have been indicated as being involved as inflammatory mediators in the induction of arthritis. Correlations between extracellular- superoxide dismutase (EC-SOD) and inflammatory arthritis have been shown in several animal models of RA. However, there is a question whether the over-expression of EC-SOD on arthritic joint also could suppress the progression of disease or not. In the present study, the effect on the synovial tissue of experimental arthritis was investigated using EC-SOD over-expressing transgenic mice. The over-expression of EC-SOD in joint tissue was confirmed by RT-PCR and immunohistochemistry. The degree of the inflammation in EC-SOD transgenic mice was suppressed in the collagen-induced arthritis model. In a cytokine assay, the production of pro-inflammatory cytokines such as, IL-1β, TNFα, and matrix metalloproteinases (MMPs) was decreased in fibroblast-like synoviocyte (FLS) but not in peripheral blood. Histological examination also showed repressed cartilage destruction and bone in EC-SOD transgenic mice. In conclusion, these data suggest that the over-expression of EC-SOD in FLS contributes to the activation of FLS and protection from joint destruction by depressing the production of the pro-inflammatory cytokines and MMPs. These results provide EC-SOD transgenic mice with a useful animal model for inflammatory arthritis research.
PMID:22718219

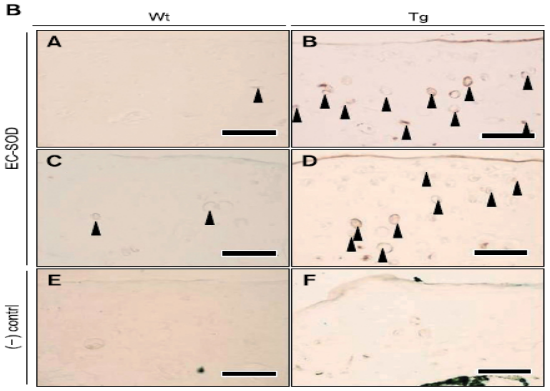

Keywords : Arthritis; Reactive oxygen species; Rheumatoid arthritis; Superoxide dismutase; Synovial membrane

Article 123

NDRG2 and PRA1 interact and synergistically inhibit T-cell factor/β-catenin signaling

FEBS Lett. 586(22):3962-8.

Kim JT, Kim JW, Kang YH, Kim KD, Lee SJ, Choi SC, Kim KS, Chae SK, Kim JW, Lim JS, Lee HG*

*Co-corresponding: hglee@kribb.re.kr
BioMedical Genomics Research Center

NDRG2 is a member of the N-myc downstream regulated gene (NDRG) family, implicated in cell growth and differentiation. Investigation of NDRG2 molecular interactions by yeast two-hybrid screening identified prenylated Rab acceptor-1 (PRA1), involved in vesicle trafficking and protein transport, as binding partner. Binding of NDRG2 (and NDRG1-4) with PRA1 *in vitro* was confirmed by GST pull-down assay and immunoprecipitation, and colocalization was verified by confocal microscopy in HCT116 cells. Intracellular coexpression showed that NDRG2 and PRA1 synergistically downregulate T-cell factor (TCF) promoter activity and GSK3β phosphorylation. Results suggest that NDRG2 and PRA1 might act synergistically to prevent signaling of TCF/β-catenin.

PMID: 23068607

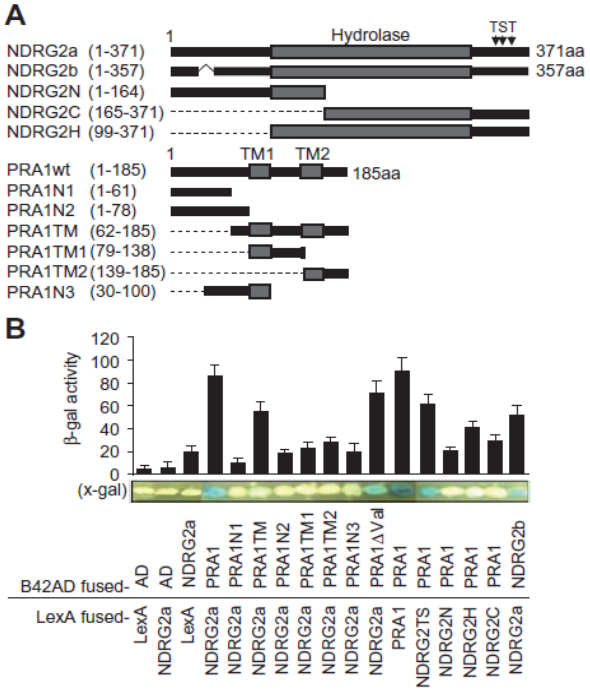

Keywords : Cell proliferation; NDRG; PRA1; Promoter inhibition; Protein–protein interaction; Yeast two-hybrid screen

Article 124

Inhibition of MKK7-JNK by the TOR signaling pathway regulator-like protein contributes to resistance of HCC cells to TRAIL-induced apoptosis

Gastroenterology. 143(5):1341-51.

Song IS, Jun SY, Na HJ, Kim HT, Jung SY, Ha GH, Park YH, Long LZ, Yu DY, Kim JM, Kim JH, Ko JH, Kim CH, Kim NS*

*Co-corresponding: nskim37@kribb.re.kr
BioMedical Genomics Research Center

BACKGROUND & AIMS: The TOR signaling pathway regulator-like (TIPRL) protein, the mammalian ortholog of yeast TIP41, was identified in an expression profiling screen for factors that regulate human liver carcinogenesis. We investigated the role of human TIPRL protein in hepatocellular carcinoma (HCC).
METHODS: We measured the level of TIPRL in HCC and adjacent nontumor tissues from patients. We used small interfering RNAs and zebrafish to study the function of TIPRL. We used annexin V propidium iodide staining and immunoblot analyses to measure apoptosis and activation of apoptotic signaling pathways. We used confocal microscopy, coimmunoprecipitation, and glutathione-S transferase pull-down analyses to determine interactions among mitogen-activated protein kinase kinase 7 (MKK7 or MAP2K7), TIPRL, and the protein phosphatase type 2A (PP2Ac). We studied the effects of TIPRL in tumor xenografts in mice. RESULTS: Levels of TIPRL were higher in HCC tissues and cell lines than nontumor tissues and primary hepatocytes. Knockdown of tiprl expression in zebrafish led to large amounts of apoptosis throughout the embryos. Incubation of HCC cells, but not primary human hepatocytes, with small interfering RNA against TIPRL (siTIPRL) and tumor necrosis factor-related apoptosis-inducing ligand (TRAIL) caused prolonged activation (phosphorylation) of MKK7 and c-Jun N-terminal kinase (JNK) and led to apoptosis, indicated by cleavage of procaspase-8,-3 and of poly-(adenosine diphosphate-ribose) polymerase. TIPRL bound to MKK7 and PP2Ac and promoted the interaction between MKK7 and PP2Ac. In mice, injection of HCC xenograft tumors with siTIPRL and TRAIL led to tumor apoptosis and regression.
CONCLUSIONS: TIPRL is highly up-regulated in human HCC samples and cell lines, compared with noncancerous liver tissues. TIPRL prevents prolonged activation of MKK7 and JNK and TRAIL-induced apoptosis by mediating the interaction between MKK7 and PP2Ac.

PMID: 22841785

Keywords : Chemotherapy resistance mechanisms; Liver cancer; TRAIL-induced apoptosis; Tumor cell death

Article 125

Dynamics of Setdb1 expression in early mouse development

Gene Expr Patterns. 12(5-6):213-8.

Cho S, Park JS, Kwon S, Kang YK*

*Corresponding: ykkang@kribb.re.kr
BioMedical Translational Research Center

Setdb1/Eset, a histone lysine methyltransferase, is recruited by various transcription factors to modify local chromatin. The observation that *Setdb1*-null blastocysts fail to produce epiblast-lineage cells suggests a role for Setdb1 in generating mouse embryonic stem cells (mESCs). When examined in mouse zygotes, Setdb1 proteins appeared as dots at perinucleolar rims of pronuclei, with the dot-shaped signals more prominent in male pronuclei. Setdb1 signals were observed diffusely in the nucleus from the two-cell stage onward and, by the blastocyst, took a punctate form, away from nucleolus. Such varying expression patterns suggest its involvement in diverse biological processes at preimplantation stage. Setdb1 appeared in Oct4-positive cells of inner-cell-mass origin but not in trophectoderm-lineage cells in blastocyst outgrowths. Setdb1 co-immunoprecipitated with Oct4 in mESCs, and Setdb1 expression was markedly reduced upon retinoic acid-induced differentiation. These observations suggest that Setdb1 has an important role in maintaining the self-renewal of mESCs through collaboration with Oct4.

PMID: 22504302

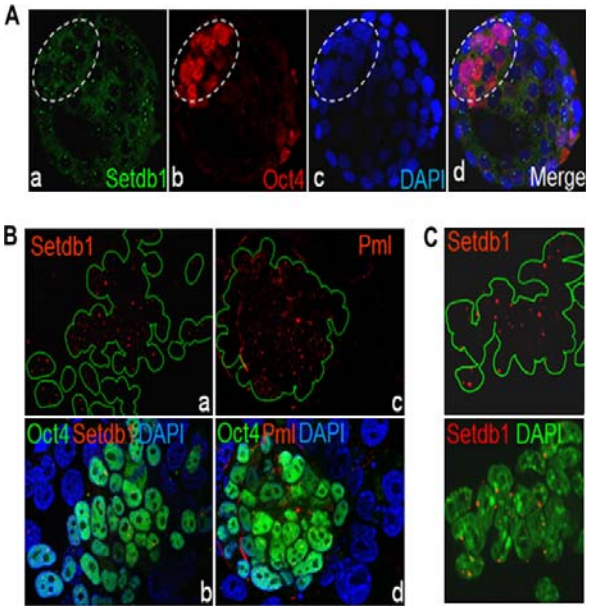

Keywords : Blastocyst outgrowth; Embryonic stem cell; Histone methylation; Mouse embryo; Setdb1/Eset

Article 126

CaGe: a web-based cancer gene annotation system for cancer genomics

Genomics Inform. 10(1):33-9.

Park YK, Kang TW, Baek SJ, Kim KI, Kim SY, Lee D, Kim YS*

*Co-corresponding: yongsung@kribb.re.kr
BioMedical Genomics Research Center

High-throughput genomic technologies (HGTs), including next-generation DNA sequencing (NGS), microarray, and serial analysis of gene expression (SAGE), have become effective experimental tools for cancer genomics to identify cancer-associated somatic genomic alterations and genes. The main hurdle in cancer genomics is to identify the real causative mutations or genes out of many candidates from an HGT-based cancer genomic analysis. One useful approach is to refer to known cancer genes and associated information. The list of known cancer genes can be used to determine candidates of cancer driver mutations, while cancer gene-related information, including gene expression, protein-protein interaction, and pathways, can be useful for scoring novel candidates. Some cancer gene or mutation databases exist for this purpose, but few specialized tools exist for an automated analysis of a long gene list from an HGT-based cancer genomic analysis. This report presents a new web-accessible bioinformatic tool, called CaGe, a cancer genome annotation system for the assessment of candidates of cancer genes from HGT-based cancer genomics. The tool provides users with information on cancer-related genes, mutations, pathways, and associated annotations through annotation and browsing functions. With this tool, researchers can classify their candidate genes from cancer genome studies into either previously reported or novel categories of cancer genes and gain insight into underlying carcinogenic mechanisms through a pathway analysis. We show the usefulness of CaGe by assessing its performance in annotating somatic mutations from a published small cell lung cancer study.

PMID: 23105926

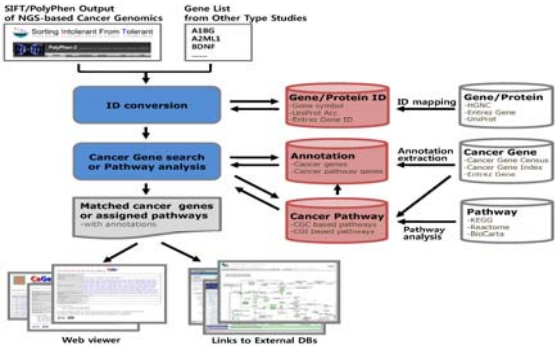

Keywords : Annotation; Cancer gene; High-throughput genomic technology; Mutation; Next-generation sequencing; Pathway

Article 127

Anti-allergic effect of lambertianic acid from Thuja orientalis in mouse bone marrow-derived mast cells

Immunopharmacol Immunotoxicol. 34(2):250-5.

Chae HS*, Chin YW

*First:
BioMedical Genomics Research Center

Lambertianic acid is a bioactive diterpene found in the leaves of Thuja orientalis. Its effect on the bone marrow-derived mast cell (BMMC) mediated allergy and inflammation mechanism remains unknown. In this study, lambertianic acid was evaluated for its effect on the allergic mediators, including prostaglandin D_2 (PGD_2), leukotriene C_4 (LTC_4), β-hexosaminidase (β-Hex) and cyclooxygenase-2 (COX-2) protein, in phorbol 12-myristate 13-acetate (PMA) plus calcimycin-stimulated BMMCs. The results revealed that lambertianic acid inhibited the production of interleukin-6 (IL-6), PGD_2 and LTC_4, the expression of COX-2 and the degranulation of β-hexosaminidase in the PMA plus calcimycin-induced BMMCs. Taken together, these findings implied that lambertianic acid may possess the potential in the treatment of allergy.
PMID:21854102

Keywords : Allergy; Bioactive diterpene; Bone marrow-derived mast cell (BMMC); Inflammation; Lambertianic acid; Thuja orientalis

Article 128

Myostatin inhibits brown adipocyte differentiation via regulation of Smad3-mediated β-catenin stabilization

Int J Biochem Cell Biol. 44(2):327-34.

Kim WK, Choi HR, Park SG, Ko Y, Bae KH*, Lee SC*

*Co-corresponding: khbae@kribb.re.kr lesach@kribb.re.kr
Research Center of Integrative Cellulomics

Brown adipocytes play an important role in regulating energy balance, and there is a good correlation between obesity and the amount of brown adipose tissue. Although the molecular mechanism of white adipocyte differentiation has been well characterized, brown adipogenesis has not been studied extensively. Moreover, extracellular factors that regulate brown adipogenic differentiation are not fully understood. Here, we assessed the mechanism of the regulatory action of myostatin in brown adipogenic differentiation using primary brown preadipocytes. Our results clearly showed that differentiation of brown adipocytes was significantly inhibited by myostatin treatment. In addition, myostatin-induced suppression of brown adipogenesis was observed during the early phase of differentiation. Myostatin induced the phosphorylation of Smad3, which led to increased β-catenin stabilization. These effects were blocked by treatment with a Smad3 inhibitor. Expression of brown adipocyte-related genes, such as PPAR-γ, UCP-1, PGC-1α, and PRDM16, were dramatically down-regulated by treatment with myostatin, and further down-regulated by co-treatment with a β-catenin activator. Taken together, the present study demonstrated that myostatin is a potent negative regulator of brown adipogenic differentiation by modulation of Smad3-induced β-catenin stabilization. Our findings suggest that myostatin could be used as an extracellular factor in the control of brown adipocyte differentiation.
PMID: 22094186

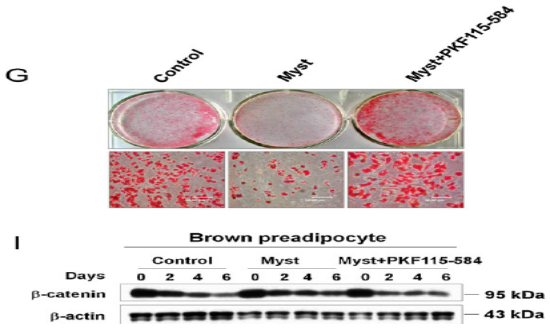

Keywords : Adipogenesis; β-Catenin; Brown adipocytes; Myostatin; Smad3

Article 129

Phosphatase of regenerating liver-3 promotes migration and invasion by upregulating matrix metalloproteinases-7 in human colorectal cancer cells

Int J Cancer. 131(3):E190-203.

Lee SK, Han YM, Yun J, Lee CW, Shin DS, Ha YR, Kim J, Koh JS, Hong SH, Han DC*, Kwon BM*

*Co-corresponding: dchan@kribb.re.kr kwonbm@kribb.re.kr
BioMedical Genomics Research Center

Phosphatase of regenerating liver (PRL)-3, a member of a subgroup of protein tyrosine phosphatases that can stimulate the degradation of the extracellular matrix, is over-expressed in metastatic colorectal cancer (CRC) relative to primary tumors. To determine whether PRL-3-induced enhancement of migration and invasion is dependent on the expression of matrix metalloproteinases (MMPs), PRL-3 was expressed in DLD-1 human CRC cells. The motility, migration and invasion characteristics of the cells were examined, and metastasis to the lung was confirmed in a nude mouse using PRL-3-overexpressing DLD-1 cells [DLD-1 (PRL-3)]. Migration and invasion of the cells were inhibited by phosphatase and farnesyltransferase inhibitors. Expression of MMPs was enhanced 3- to 10-fold in comparison to control cells, and migration and invasion were partially inhibited by small interfering RNA (siRNA) knockdown of MMP-2, -13 or -14. Importantly, siRNA knockdown of MMP-7 completely inhibited the migration and invasion of DLD-1 (PRL-3) cells, whereas overexpression of MMP-7 increased migration. The expression of MMP-7 was also downregulated by phosphatase and farnesyltransferase inhibitors. It was found that PRL-3 induced MMP-7 through oncogenic pathways including PI3K/AKT and ERK and that there is a relationship between the expression of PRL-3 and MMP-7 in human tumor cell lines. The expression of MMP-13 and -14 was very sensitive to the inhibition of farnesyltransferase; however, the migration and invasion of DLD-1 (PRL-3) cells did not strongly depend on the expression of MMP-13 or -14. These results suggest that the migration and invasion of PRL-3-expressing CRC cells depends primarily on the expression of MMP-7.

PMID: 22131018

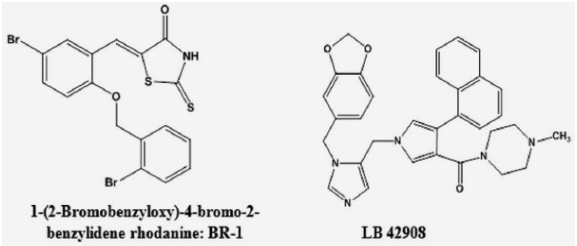

Keywords : Invasion; Matrix metalloproteinases; Migration; Phosphatase of regenerating liver-3

Article 130

Fibulin-3 promoter methylation alters the invasive behavior of non-small cell lung cancer cell lines via MMP-7 and MMP-2 regulation

Int J Oncol. 40(2):402-8.

Kim EJ, Lee SY, Woo MK, Choi SI, Kim TR, Kim MJ, Kim KC, Cho EW*, Kim IG

*Co-corresponding: ewcho@kribb.re.kr
BioMedical Translational Research Center

Fibulin-3, an extracellular glycoprotein, has been suggested as having functions in tissue regeneration and organogenesis. However, its role in cancer remains unclear. We show here that fibulin-3 was silenced by hypermethylation of the promoter region in the relatively invasive A549 non-small cell lung cancer (NSCLC) cells compared with less invasive H460 NSCLC cells. Enforced expression of fibulin-3 in A549 cells down-regulated cellular MMP-7 and MMP-2, which was followed by inhibition of cell invasiveness. Conversely, suppression of fibulin-3 expression with siRNA in H460 cells showed the opposite effect. These results indicate that fibulin-3 is a negative regulator of invasiveness in NSCLC and further studies are needed for its therapeutic applications in treatment of NSCLC.

PMID:21901248

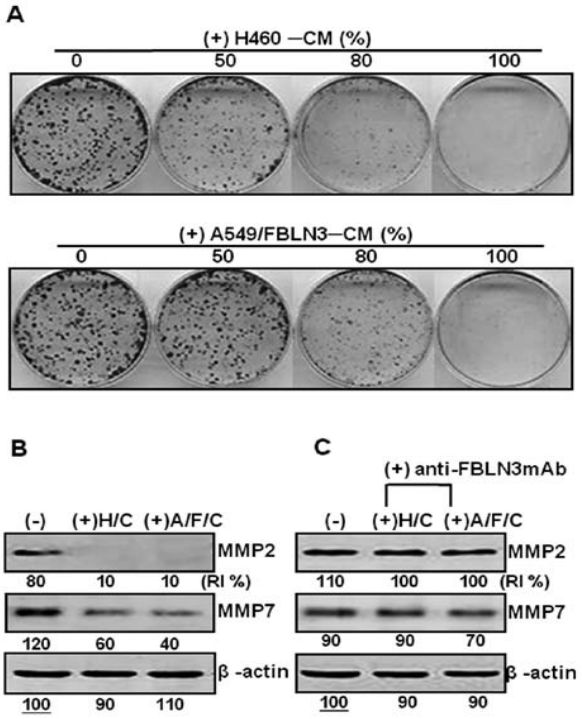

Keywords : Fibulin-3; Invasion; Lung cancer; Methylation; MMP-7; Tumour suppressor

Article 131

Ion yields for some salts in MALDI: mechanism for the gas-phase ion formation from preformed ions

J Am Soc Mass Spectrom. 23(1):162-70.

Moon JH*, Shin YS, Bae YJ, Kim MS

*First: jhdal@kribb.re.kr
BioMedical Proteomics Research Center

Preformed ion emission is the main assumption in one of the prevailing theories for peptide and protein ion formation in matrix-assisted laser desorption ionization (MALDI). Since salts are in preformed ion forms in the matrix-analyte mixture, they are ideal systems to study the characteristics of preformed ion emission. In this work, a reliable method to measure the ion yield (IY) in MALDI was developed and used for a solid salt benzyltriphenylphosphonium chloride and two room-temperature ionic liquids 1-butyl-3-methylimidazolium hexafluorophosphate and trihexyltetradecylphosphonium bis(2,4,4-trimethylpentyl)phosphinate. IY for the matrix (α-cyano-4-hydroxycinnamic acid, CHCA) was also measured. Taking 1 pmol salts in 25 nmol CHCA as examples, IYs for three salts were similar, (4-8) × 10^{-4}, and those for CHCA were (0.8-1.2) × 10^{-7}. Even though IYs for the salts and CHCA remained virtually constant at low analyte concentration, they decreased as the salt concentrations increased. Two models, Model 1 and Model 2, were proposed to explain low IYs for the salts and the concentration dependences. Both models are based on the fact that the ion-pair formation equilibrium is highly shifted toward the neutral ion pair. In Model 1, the gas-phase analyte cations were proposed to originate from the same cations in the solid that were dielectrically screened from counter anions by matrix neutrals. In Model 2, preformed ions were assumed to be released from the solid sample in the form of neutral ion pairs and the anions in the ion pairs were assumed to be eliminated via reactions with matrix-derived cations.
PMID: 22048904

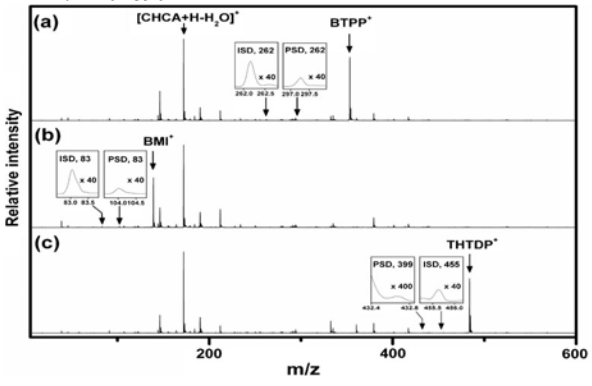

Keywords : Ion formation mechanism; Ion pair; Ion yield; MALDI; Preformed ion

Article 132

Association of novel domain in active site of archaic hyperthermophilic maltogenic amylase from *Staphylothermus marinus*

J Biol Chem. 287(11):7979-89.

Jung TY, Li D, Park JT, Yoon SM, Tran PL, Oh BH, Janeček Š, Park SG, Woo EJ*, Park KH

*Co-corresponding: ejwoo@kribb.re.kr
BioMedical Proteomics Research Center

Staphylothermus marinus maltogenic amylase (SMMA) is a novel extreme thermophile maltogenic amylase with an optimal temperature of 100 °C, which hydrolyzes α-(1-4)-glycosyl linkages in cyclodextrins and in linear malto-oligosaccharides. This enzyme has a long N-terminal extension that is conserved among archaic hyperthermophilic amylases but is not found in other hydrolyzing enzymes from the glycoside hydrolase 13 family. The SMMA crystal structure revealed that the N-terminal extension forms an N' domain that is similar to carbohydrate-binding module 48, with the strand-loop-strand region forming a part of the substrate binding pocket with several aromatic residues, including Phe-95, Phe-96, and Tyr-99. A structural comparison with conventional cyclodextrin-hydrolyzing enzymes revealed a striking resemblance between the SMMA N' domain position and the dimeric N domain position in bacterial enzymes. This result suggests that extremophilic archaea that live at high temperatures may have adopted a novel domain arrangement that combines all of the substrate binding components within a monomeric subunit. The SMMA structure provides a molecular basis for the functional properties that are unique to hyperthermophile maltogenic amylases from archaea and that distinguish SMMA from moderate thermophilic or mesophilic bacterial enzymes.
PMID: 22223643

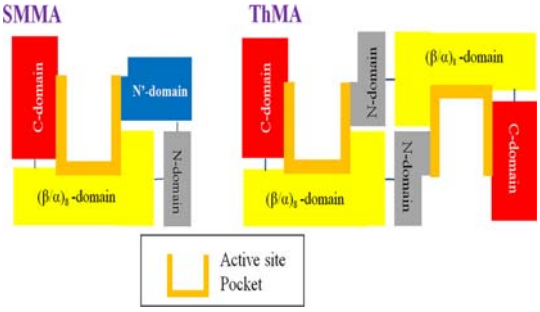

Keywords : Bacterial enzymes; Hyperthermophile maltogenic amylases; *Staphylothermus marinus* maltogenic amylase; Starch-binding domain

Article 133

Overexpression and β-1,6-N-acetylglucosaminylation-initiated aberrant glycosylation of TIMP-1: a "double whammy" strategy in colon cancer progression

J Biol Chem. 287(39):32467-78.

Kim YS, Ahn YH, Song KJ, Kang JG, Lee JH, Jeon SK, Kim HC, Yoo JS, Ko JH*

*Corresponding: jhko@kribb.re.kr
BioMedical Translational Research Center

There has been ongoing debate over whether tissue inhibitor of metalloproteinase-1 (TIMP-1) is pro- or anti-oncogenic. We confirmed that TIMP-1 reinforced cell proliferation in an αvβ3 integrin-dependent manner and conferred resistance against cytotoxicity triggered by TNF-α and IL-2 in WiDr colon cancer cells. The cell-proliferative effects of TIMP-1 contributed to clonogenicity and tumor growth during the onset and early phase of tumor formation *in vivo* and *in vitro*. However, mass-produced TIMP-1 impeded further tumor growth by tightly inhibiting the activities of collagenases, which are critical for tumor growth and malignant transformation. Tumor cells could overcome this impasse by overexpression of N-acetylglucosaminyltransferase V, which deteriorates TIMP-1 into an aberrant glycoform. The aberrant glycoform of TIMP-1 was responsible for the mitigated inhibition of collagenases. The outbalanced activities of collagenases can degrade the basement membrane and the interstitial matrix, which act as a physical barrier for tumor growth and progression more efficiently. The concomitant overexpression of TIMP-1 and N-acetylglucosaminyltransferase V enabled WiDr cells to show a higher tumor growth rate as well as more malignant behaviors in a three-dimensional culture system.

PMID: 22859303

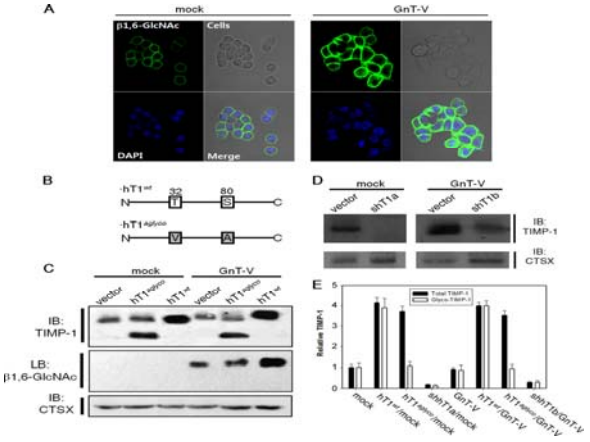

Keywords : Lung cancer; Metastasis; Tissue inhibitor of metalloproteinase-1; Tumor-necrosis-factor

Article 134

Enforced expression of roquin protein in T cells exacerbates the incidence and severity of experimental arthritis

J Biol Chem. 287(50):42269-77.

Ji YR, Kim HJ, Yu DH, Bae KB, Park SJ, Yi JK, Kim N, Park SJ, Oh KB, Hwang SS, Lee S, Kim SH, Kim MO, Lee JW*, Ryoo ZY

*Co-corresponding: jwlee@kribb.re.kr
Research Center of Integrative Cellulomics

To investigate the role of Roquin, a RING-type ubiquitin ligase family member, we used transgenic mice with enforced Roquin expression in T cells, with collagen-induced arthritis (CIA). Wild-type (WT) and Roquin transgenic (Tg) mice were immunized with bovine type II collagen (CII). Arthritis severity was evaluated by clinical score; histopathologic CIA severity; proinflammatory and anti-inflammatory cytokine levels; anti-CII antibody levels; and populations of Th1, Th2, germinal center B cells, and follicular helper T cells in CIA. T cell proliferation *in vitro* and cytokine levels were determined to assess the response to CII. Roquin Tg mice developed more severe CIA and joint destruction compared with WT mice. Production of TNF-α, IFN-γ, IL-6, and pathogenic anti-collagen CII-specific IgG and IgG2a antibodies was increased in Roquin Tg mice. In addition, *in vitro* T cell assays showed increased proliferation and proinflammatory cytokine production in response to CII as a result of enforced Roquin expression in T cells. Furthermore, the Th1/Th2 balance was altered by an increased Th1 and decreased Th2 population. These findings suggest that overexpression of Roquin exacerbates the development of CIA and that enforced expression of Roquin in T cells may promote autoimmune diseases such as CIA.

PMID:23066015

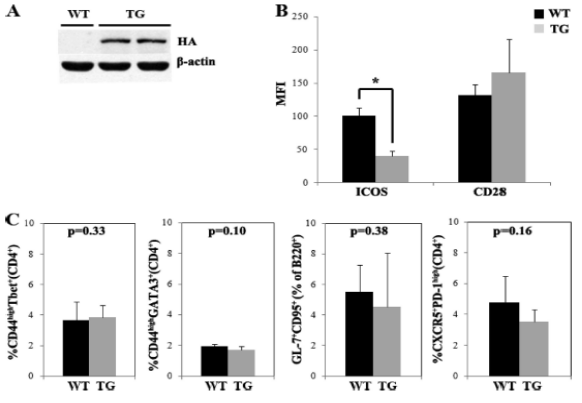

Keywords : Autoimmunity; Collagen induced arthritis (CIA); Rheumatoid arthritis; Roquin expression

Article 135

Regulation of dendritic arborization by BCR Rac1 GTPase-activating protein, a substrate of PTPRT

J Cell Sci. 125(19):4518-31.

Park AR, Oh D, Lim SH, Choi J, Moon J, Yu DY, Park SG, Heisterkamp N, Kim E, Myung PK, Lee JR*

*Corresponding: leejr@kribb.re.kr
BioMedical Proteomics Research Center

Dendritic arborization is important for neuronal development as well as the formation of neural circuits. Rac1 is a member of the Rho GTPase family that serve as regulators of neuronal development. Breakpoint cluster region protein (BCR) is a Rac1 GTPase-activating protein that is abundantly expressed in the central nervous system. Here, we show that BCR plays a key role in neuronal development. Dendritic arborization and actin polymerization were attenuated by overexpression of BCR in hippocampal neurons. Knockdown of BCR using specific shRNAs increased the dendritic arborization as well as actin polymerization. The number of dendrites in null mutant BCR$^{-/-}$ mice was considerably increased compared with that in wild-type mice. We found that the function of the BCR GTPase-activating domain could be modulated by protein tyrosine phosphatase receptor T (PTPRT), which is expressed principally in the brain. We demonstrate that tyrosine 177 of BCR was the main target of PTPRT and the BCR mutant mimicking dephosphorylation of tyrosine 177 alleviated the attenuation of dendritic arborization. Additionally the attenuated dendritic arborization found upon BCR overexpression was relieved upon co-expression of PTPRT. When PTPRT was knocked down by a specific shRNA, the dendritic arborization was significantly reduced. The activity of the BCR GTPase-activating domain was modulated by means of conversions between the intra- and inter-molecular interactions, which are finely regulated through the dephosphorylation of a specific tyrosine residue by PTPRT. We thus show conclusively that BCR is a novel substrate of PTPRT and that BCR is involved in the regulation of neuronal development via control of the BCR GTPase-activating domain function by PTPRT.
PMID: 22767509

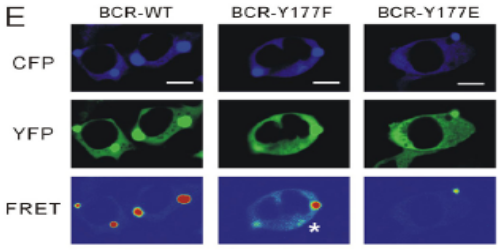

Keywords : Actin polymerization; BCR; Breakpoint cluster region; Dendritic arborization; Fyn; Protein tyrosine phosphatase receptor T; PTPRT

Article 136

Acetylation of malate dehydrogenase 1 promotes adipogenic differentiation via activating its enzymatic activity

J Lipid Res. 53(9):1864-76.

Kim EY, Kim WK, Kang HJ, Kim JH, Chung SJ, Seo YS, Park SG, Lee SC*, Bae KH*

*Co-corresponding: lesach@kribb.re.kr khbae@kribb.re.kr
Research Center of Integrative Cellulomics

Acetylation is one of the most crucial post-translational modifications that affect protein function. Protein lysine acetylation is catalyzed by acetyltransferases, and acetyl-CoA functions as the source of the acetyl group. Additionally, acetyl-CoA plays critical roles in maintaining the balance between carbohydrate metabolism and fatty acid synthesis. Here, we sought to determine whether lysine acetylation is an important process for adipocyte differentiation. Based on an analysis of the acetylome during adipogenesis, various proteins displaying significant quantitative changes were identified by LC-MS/MS. Of these identified proteins, we focused on malate dehydrogenase 1 (MDH1). The acetylation level of MDH1 was increased up to 6-fold at the late stage of adipogenesis. Moreover, overexpression of MDH1 in 3T3-L1 preadipocytes induced a significant increase in the number of cells undergoing adipogenesis. The introduction of mutations to putative lysine acetylation sites showed a significant loss of the ability of cells to undergo adipogenic differentiation. Furthermore, the acetylation of MDH1 dramatically enhanced its enzymatic activity and subsequently increased the intracellular levels of NADPH. These results clearly suggest that adipogenic differentiation may be regulated by the acetylation of MDH1 and that the acetylation of MDH1 is one of the cross-talk mechanisms between adipogenesis and the intracellular energy level.
PMID:22693256

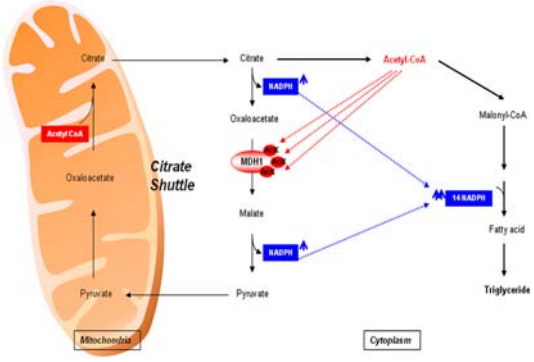

Keywords : Acetyl-CoA; Adipogenesis; Obesity; Protein acetylation

Article 137

Synthesis and structure-activity relationship of (*E*)-phenoxyacrylic amide derivatives as hypoxia-inducible factor (HIF) 1α inhibitors

J Med Chem. 55(23):10564-71.

Naik R, Won M*, Kim BK, Xia Y, Choi HK, Jin G, Jung Y, Kim HM, Lee K

*Co-first: misun@kribb.re.kr
BioMedical Genomics Research Center

A series of (*E*)-phenoxyacrylic amide derivatives were synthesized and evaluated as hypoxia inducible factor (HIF) 1α inhibitors. The present structure-activity relationship study on this series identified the morpholinoethyl containing ester 4p as a potent inhibitor of HIF-1α under hypoxic conditions (IC_{50}=0.12 μM in a cell-based HRE reporter assay) in HCT116 cells. The representative compound 4p suppressed hypoxia-induced HIF-1α accumulation and targeted gene expression in a dose-dependent manner. The effect of HIF-1α inhibition by 4p was further demonstrated by its inhibitory activity on *in vitro* tube formation and migration of cells, which may be valuable for development of novel therapeutics for cancer and tumor angiogenesis.

PMID:23153200

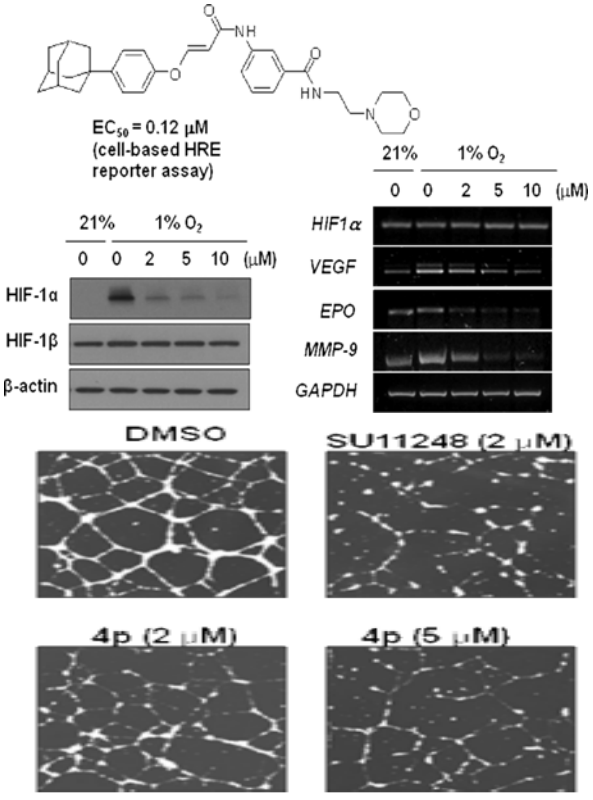

Keywords : Cancer; HIF-1α; Hypoxia-inducible factor; Novel therapeutics; Tumor angiogenesis

Article 138

Glyceraldehyde-3-phosphate, a glycolytic intermediate, prevents cells from apoptosis by lowering S-nitrosylation of glyceraldehyde-3-phosphate dehydrogenase

J Microbiol Biotechnol. 22(4):571-3.

Lee SY, Kim JH, Jung H, Chi SW, Chung SJ, Lee CK, Park BC, Bae KH*, Park SG*

*Co-corresponding: khbae@kribb.re.kr sgpark@kribb.re.kr
BioMedical Proteomics Research Center

Glyceraldehyde-3-phosphate (G-3-P), the substrate of glyceraldehyde-3-phosphate dehydrogenase (GAPDH), is a key intermediate in several metabolic pathways. Recently, we reported that G-3-P directly inhibits caspase-3 activity in a reversible noncompetitive mode, suggesting the intracellular G-3-P level as a cell fate decision factor. It has been known that apoptotic stimuli induce the generation of NO, and NO S-nitrosylates GAPDH at the catalytic cysteine residue, which confers GAPDH the ability to bind to Siah-1, an E3 ubiquitin ligase. The GAPDH-Siah-1 complex is translocated into the nucleus and subsequently triggers the apoptotic process. Here, we clearly showed that intracellular G-3-P protects GAPDH from S-nitrosylation at above a certain level, and consequently maintains the cell survival. In case G-3-P drops below a certain level as a result of exposure to specific stimuli, G-3-P cannot inhibit S-nitrosylation of GAPDH anymore, and consequently GAPDH translocates with Siah-1 into the nucleus. Based on these results, we suggest that G-3-P functions as a molecule switch between cell survival and apoptosis by regulating S-nitrosylation of GAPDH.

PMID: 22534308

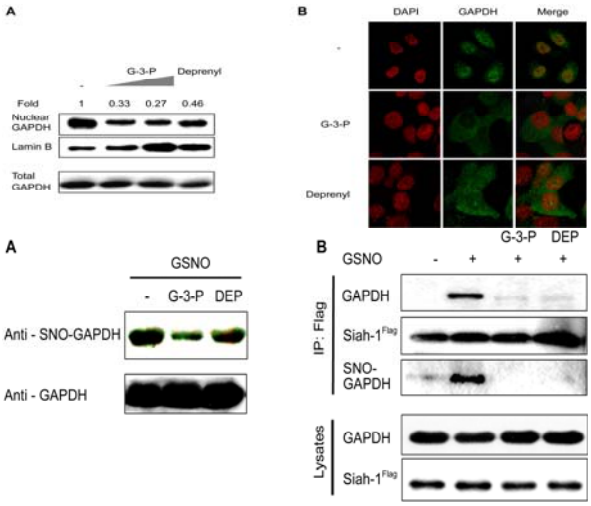

Keywords : Apoptosis; G-3-P function; GAPDH; Glyceraldehyde-3-phosphate; S-nitrosylation

Article 139

Protein tyrosine phosphatase profiling analysis of HIB-1B cells during brown adipogenesis

J Microbiol Biotechnol. 22(7):1029-33.

Choi HR, Kim WK, Kim EY, Jung H, Kim JH, Han BS, You KH, Lee SC*, Bae KH*

*Co-corresponding: lesach@kribb.re.kr khbae@kribb.re.kr
Research Center of Integrative Cellulomics

A number of evidence have been accumulated that the regulation of reversible tyrosine phosphorylation, which can be regulated by the combinatorial activity of protein tyrosine kinases (PTKs) and protein tyrosine phosphatases (PTPs), plays crucial roles in various biological processes including differentiation. There are a total of 107 PTP genes in the human genome, collectively referred to as the "PTPome." In this study, we performed PTP profiling analysis of the HIB-1B cell line, a brown preadipocyte cell line, during brown adipogenesis. Through RT-PCR and real-time PCR, several PTPs showing differential expression pattern during brown adipogenesis were identified. In the case of PTP-RE, it was shown to decrease significantly until 4 days after brown adipogenic differentiation, followed by a dramatic increase at 6 days. The overexpression of PTP-RE led to decreased brown adipogenic differentiation via reducing the tyrosine phosphorylation of the insulin receptor, indicating that PTP-RE functions as a negative regulator at the early stage of brown adipogenesis.

PMID: 22580324

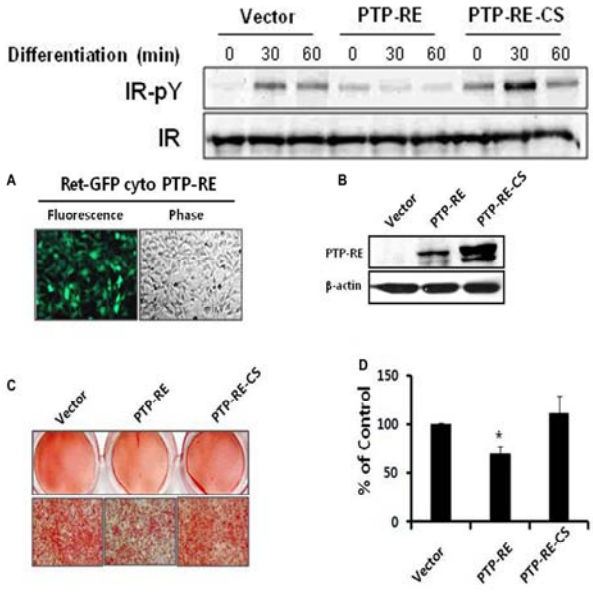

Keywords : Brown adipogenesis; HIB-1B cell line; Protein tyrosine phosphatase; PTPome; PTP-RE

Article 140

Structural analysis of α-L-arabinofuranosidase from *Thermotoga maritima* reveals characteristics for thermostability and substrate specificity

J Microbiol Biotechnol. 22(12):1724-30.

Dumbrepatil A, Park JM, Jung TY, Song HN, Jang MU, Han NS, Kim TJ, Woo EJ*

*Co-corresponding: ejwoo@kribb.re.kr
BioMedical Proteomics Research Center

An α-L-arabinofuranosidase (*Tm*AFase) from *Thermotoga maritima* MSB8 is a highly thermostable exo-acting hemicellulase that exhibits a relatively higher activity towards arabinan and arabinoxylan, compared with other glycoside hydrolase 51 family enzymes. In the present study, we carried out the enzymatic characterization and structural analysis of *Tm*AFase. Tight domain associations found in *Tm*AFase, such as an inter-domain disulfide bond (Cys306 and Cys476) in each monomer, a novel extended arm (amino acids 374-385) at the dimer interface, and total 12 salt bridges in the hexamer, may account for the thermostability of the enzyme. One of the xylan binding determinants (Trp96) was identified in the active site, and a region of amino acids (374-385) protrudes out forming an obvious wall at the substrate-binding groove to generate a cavity. The altered cavity shape with a strong negative electrostatic distribution is likely related to the unique substrate preference of *Tm*AFase towards branched polymeric substrates.

PMID:23221536

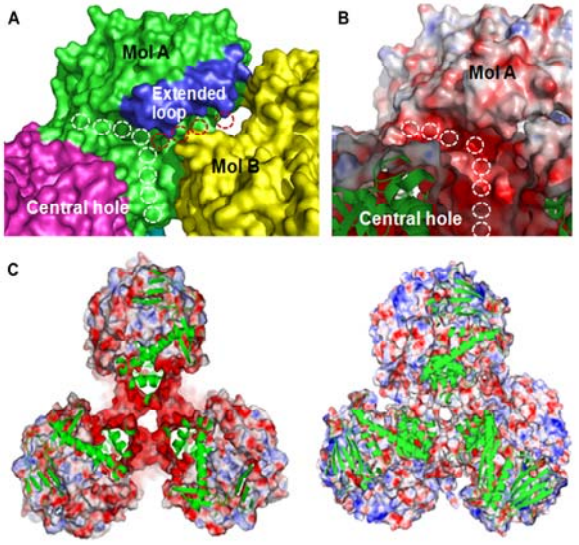

Keywords : α-L-arabinofuranosidase; Glycoside hydrolase; Structural analysis; *Thermotoga maritima*; X-ray crystallography

Article 141

Structure-based *de novo* design of Eya2 phosphatase inhibitors

J Mol Graph Model. 38:382-8.

Park H, Ryu SE, Kim SJ*

*Co-corresponding: ksj@kribb.re.kr
BioMedical Proteomics Research Center

Although Eyes absent protein tyrosine phosphatases proved to be involved in various human cancers by a series of persuasive experimental evidence, only a very few number of small-molecule inhibitors have been reported so far. We have been able to identify 29 novel inhibitors of Eyes absent homologue 2 (Eya2) by means of a structure-based *de novo* design with the two known inhibitor scaffolds that contain a proper chelating group for the active-site Mg^{2+} ion. Because these newly found inhibitors were screened for having desirable physicochemical properties as a drug candidate and exhibited a moderate inhibitory activity with IC_{50} values ranging from 6 to 50 μM, they deserve consideration for further investigation to develop new anticancer medicines. Structural features relevant to the stabilization of the identified inhibitors in the active site of Eya2 phosphatase are discussed in detail.
PMID:23085179

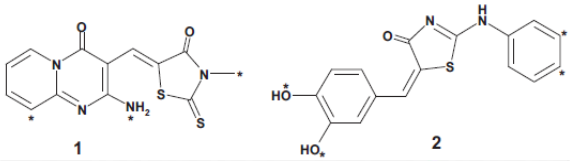

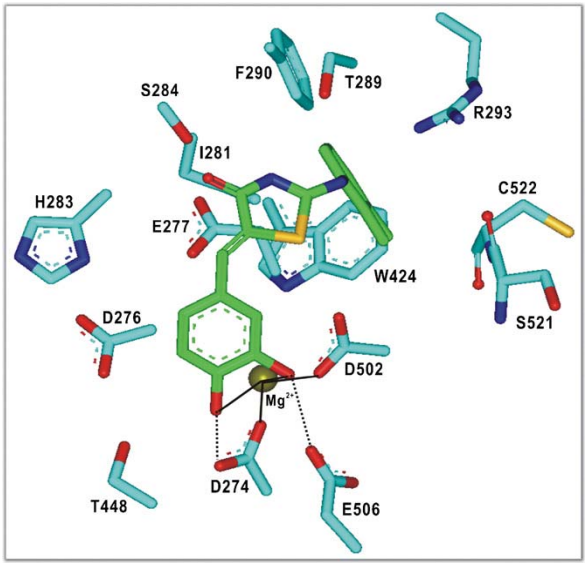

Keywords : Anticancer agents; Chelating group; *De novo* design; Eya2 phosphatase; Inhibitor

Article 142

Poly(arylene ether)s with low refractive indices: Poly(biphenylene oxide)s with trifluoromethyl pendant groups via a meta-activated nitro displacement Reaction

Macromolecules. 45(7):3023-31.

Kim SD, Ka D, Chung IS*, Kim SY

*Co-corresponding: cis123@kribb.re.kr
Research Center of Integrative Cellulomics

High-molecular-weight poly(biphenylene oxide)s (PBPO) were prepared from AB-type monomers, 4′(3′)-hydroxy-4-nitro-2,6-bis(trifluoromethyl) biphenyl, through a meta-activated nitro displacement reaction. The displacement of nitro leaving group activated by the two trifluoromethyl groups at the meta-position produced high-molecular-weight polymers, which implies that nucleophilic aromatic substitution reaction of the nitro leaving group proceeded very effectively with two activating groups at the meta-position. The obtained polymers have weight-average molecular weight of 20 800-143 300 g/mol and molecular weight distribution of 1.68-2.85. While two homopolymers of 4′- or 3′-hydroxy-4-nitro-2,6-bis(trifluoromethyl)biphenyl, p-PBPO and m-PBPO, showed a semicrystalline morphology, copolymers of the two monomers were amorphous and dissolved in a wide range of organic solvents. The PBPOs possessed a high glass transition temperature (T g) in the range of 169 to 208 °C depending on their structure and high thermal stability with 10% weight loss temperatures from 486 to 542 °C in nitrogen and from 465 to 516 °C in air. Moreover, PBPOs containing two trifluoromethyl groups showed low refractive indices in the range of 1.4979-1.5052 as well as low birefringence values of 0.0095-0.0148.

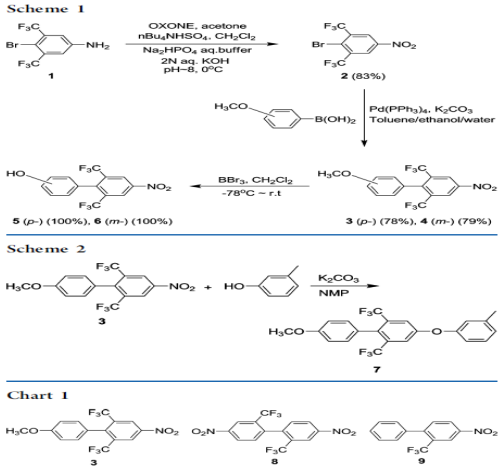

Keywords : Biphenylene; Displacement reactions; High-molecular weight polymers; High thermal stability; Leaving

Article 143

Humanization by guided selections

Methods Mol Biol. 907:247-57.

Kim SJ*, Hong HJ

*First: sjick@kribb.re.kr
Research Center of Integrative Cellulomics

Guided selection provides a powerful tool for humanization of the preexisting nonhuman antibodies as exemplified by HUMIRA, the world's first human antibody approved. This chapter describes the sequential guided selection procedure in which mouse VL and VH domains are replaced sequentially with human VL and VH, respectively to derive completely human antibody. The detailed protocols for construction of phage-displayed antibody library, panning, screening, and characterization, are included to achieve successful selection of human antibody with similar characteristics to original mouse antibody.

PMID: 22907356

KRIBB-Fab

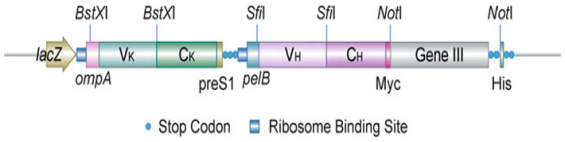

Keywords : Antibody library; Chain shuffling; Guided selection; Human antibody; Panning; Phage display

Article 144

Phosphoproteomic analysis of electroacupuncture analgesia in an inflammatory pain rat model

Mol Med Rep. 6(1):157-62.

Lee SH, Kim SY, Kim JH, Jung HY, Moon JH, Bae KH*, Choi BT

*Co-corresponding: khbae@kribb.re.kr
Research Center of Integrative Cellulomics

The phosphorylation changes of nociceptive signaling proteins in the spinal cord dorsal horn (SCDH) are important in creating exaggerated pain following peripheral inflammation. Electroacupuncture (EA) has been widely used to relieve acute and chronic inflammatory pain in human and experimental pain models. In the present study, we performed a phosphoproteomic analysis to investigate whether EA alters protein phosphorylation in SCDH to attenuate pain development. Inflammatory hyperalgesia was induced by intraplantar injection of complete Freund's adjuvant (CFA) into the rat hind paw. EA treatment at ST36 and SP6 acupoints alleviated thermal hyperalgesia of the CFA-induced inflammatory pain model rats. The SCDH proteins from the control, inflammatory pain model and EA treatment rats were separated by 2-dimensional gel electrophoresis and the alterations in phosphoproteins were detected by Pro-Q Diamond staining. Eight proteins were differentially phosphorylated following EA treatment in the inflammatory pain model. Aldolase C, nascent polypeptide-associated complex α, stress-induced phosphoprotein 1 and heat shock protein 90 were identified as phosphoproteins whose expression was increased, whereas GDP dissociation inhibitor 1, thiamine triphosphatase, phosphoglycerate kinase 1 and 14-3-3 γ were phosphoproteins whose expression was decreased. This is the first phosphoproteomic screening study to elucidate the working mechanisms of EA analgesia. The results suggest that the regulation of cellular pathways in which the identified proteins are involved may be associated with an EA analgesic mechanism.

PMID:22576741

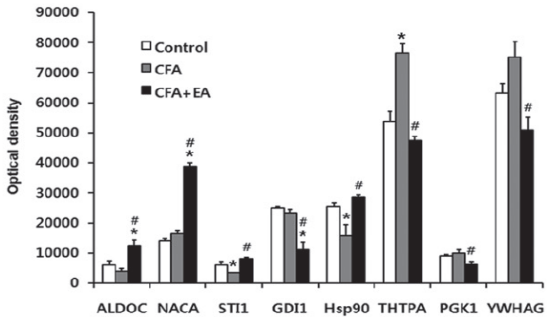

Keywords : Analgesia; Complete Freund's adjuvant; Electroacupuncture; Phosphoproteomics; Spinal cord

Article 145

Adenovirus-mediated E2-EPF UCP gene transfer prevents autoamputation in a mouse model of hindlimb ischemia

Mol Ther. 20(4):778-87.

Lim JH, Shin HJ, Park KS, Lee CH, Jung CR*, Im DS*

*Co-corresponding: crjung@kribb.re.kr imdongsu@kribb.re.kr
BioMedical Genomics Research Center

E2-EPF ubiquitin carrier protein (UCP) stabilizes hypoxia-inducible factor-1α (HIF-1α) inducing ischemic vascular responses. Here, we investigated the effect of UCP gene transfer on therapeutic angiogenesis. Adenovirus-encoded UCP (Ad-F-UCP) increased the expression of vascular endothelial growth factor (VEGF) and fibroblast growth factor-2 (FGF-2) in cells and mice. Conditioned media from UCP-overexpressing cells promoted proliferation, tubule formation, and invasion of human umbilical-vascular-endothelial cells (HUVECs), and vascularization in chorioallantoic membrane (CAM) assay. Ad-F-UCP increased the vessel density in the Martigel plug assay, and generated copious vessel-like structures in the explanted muscle. The UCP effect on angiogenesis was dependent on VEGF and FGF-2. In mouse hindlimb ischemia model (N = 30/group), autoamputation (limb loss) occurred in 87% and 68% of the mice with saline and Ad encoding β-galactosidase (Ad-LacZ), respectively, whereas only 23% of the mice injected with Ad-F-UCP showed autoamputation after 21 days of treatment. Ad-F-UCP increased protein levels of HIF-1α, platelet-endothelial cell adhesion molecule-1 (PECAM-1), smooth muscle cell actin (SMA) in the ischemic muscle, and augmented blood vessels doubly positive for PECAM-1 and SMA. Consequently, UCP gene transfer prevented muscle degeneration and autoamputation of ischemic limb. The results suggest that E2-EPF UCP may be a target for therapeutic angiogenesis.

PMID: 22294149

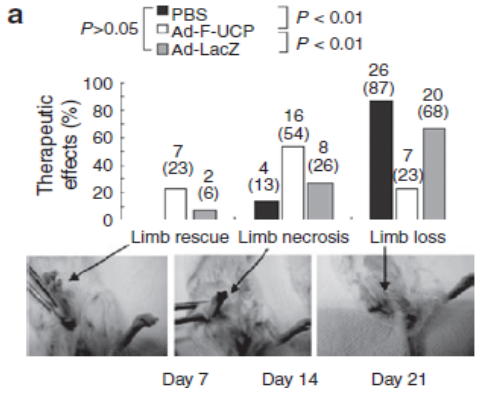

Keywords : E2-EPF ubiquitin carrier protein (UCP); Hindlimb ischemia; Hypoxia inducible factor-1a (HIF-1a); Therapeutic angiogenesis

Article 146

Structural characterization of an intrinsically unfolded mini-HBX protein from hepatitis B virus

Mol Cells. 34(2):165-9.

Lee SH, Cha EJ, Lim JE, Kwon SH, Kim DH, Cho H, Han KH*

*Corresponding: khhan600@kribb.re.kr
BioMedical Translational Research Center

The hepatitis B virus x protein (HBX) is expressed in HBV-infected liver cells and can interact with a wide range of cellular proteins. In order to understand such promiscuous behavior of HBX we expressed a truncated mini-HBX protein (named Tr-HBX) (residues 18-142) with 5 Cys → Ser mutations and characterized its structural features using circular dichroism (CD) spectropolarimetry, NMR spectroscopy as well as bioinformatics tools for predicting disorder in intrinsically unstructured proteins (IUPs). The secondary structural content of Tr-HBX from CD data suggests that Tr-HBX is only partially folded. The protein disorder prediction by IUPred reveals that the unstructured region encompasses its N-terminal ~30 residues of Tr-HBX. A two-dimensional ^{1}H-^{15}N HSQC NMR spectrum exhibits fewer number of resonances than expected, suggesting that Tr-HBX is a hybrid type IUP where its folded C-terminal half coexists with a disordered N-terminal region. Many IUPs are known to be capable of having promiscuous interactions with a multitude of target proteins. Therefore the intrinsically disordered nature of Tr-HBX revealed in this study provides a partial structural basis for the promiscuous structure-function behavior of HBX.

PMID: 22820921

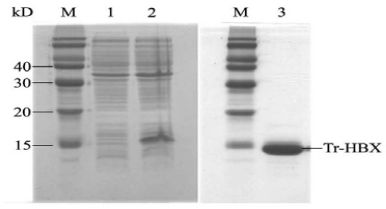

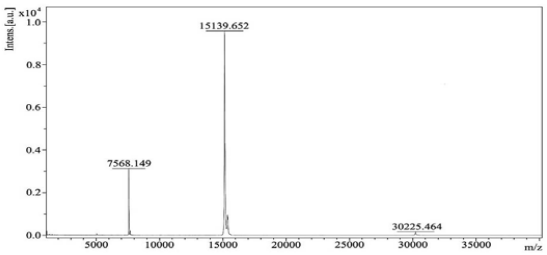

Keywords : Circular dichroism spectropolarimetry; Hepatitis B virus-X (HBX); Intrinsically unstructured/unfolded protein (IUP); Nuclear Magnetic Resonance (NMR) spectroscopy; Promiscuity; Truncated mini-HBX (Tr-HBX)

Article 147

TIP30 directly binds p53 tumor suppressor protein *in vitro*

Mol Cells. 34(5):495-500.

Lee SH, Ju SK, Lee TY, Huh SH, Han KH*

*Co-corresponding: khhan600@kribb.re.kr
BioMedical Translational Research Center

TIP30 (30 kDa HIV-1 TAT-interacting protein), also called HTATIP2 or CC3, is a tumor suppressor protein that acts as an angiogenesis inhibitor. TIP30 blocks nuclear import of the mRNA-binding protein HuR, and thereby promotes the cytoplasmic accumulation of HuR by binding to importin-β, which is known to facilitate the cytoplasm-tonuclear transport of HuR. Accumulation of HuR in the cytoplasm, in turn, enhances the expression of the transcription factor p53, a tumor suppressor that plays an essential role in preserving genome stability and inhibiting cancer growth. In addition to such a post-transcriptional mechanism via which TIP30 increases the p53 level, it has been proposed that TIP30 may regulate p53 protein at the protein level by directly binding to it. In order to investigate the possibility of direct interaction between p53 and TIP30, we have used on three functional regions in p53 and examined their interactions with TIP30 using GST pull-down assay and surface plasmon resonance technique. The results show that that TIP30 binds to the DNA-binding domain and the C-terminal domain of p53.

PMID: 23178973

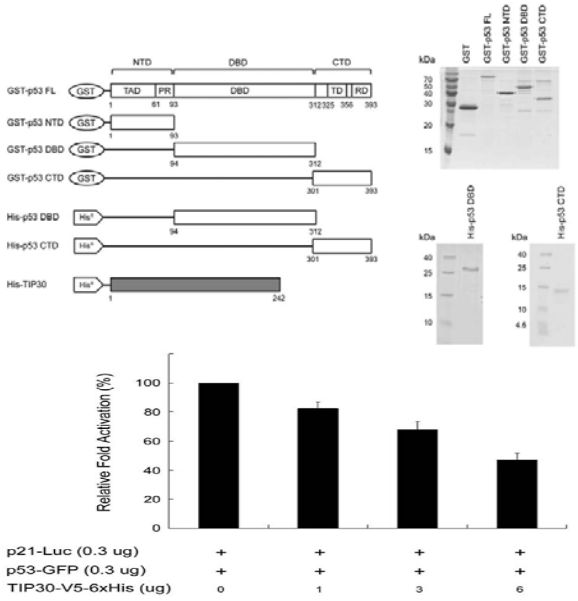

Keywords : GST pull-down assay; p53; Protein-protein interaction; Surface plasmon resonance; TIP30

Article 148

Quantitative analysis of cell-free DNA in the plasma of gastric cancer patients

Oncol Lett. 3(4):921-6.

Park JL, Kim HJ, Choi BY, Lee HC, Jang HR, Song KS, Noh SM, Kim SY, Han DS, Kim YS*

*Corresponding: yongsung@kribb.re.kr
BioMedical Genomics Research Center

In the present study, an accurate and reproducible method for quantifying cell-free DNA (cfDNA) in human blood was established and tested for its ability to predict gastric cancer in patients. Using 'Alu81-qPCR' to amplify 81-bp Alu DNA sequences, we first estimated the amount of cfDNA in the serum or plasma of 130 patients with gastric cancer to identify which source of cfDNA is more suitable for the biomarker screening of these patients. The results of Alu81-qPCR revealed that the amount of cfDNA in the plasma was low compared with that in the serum, but was found at similar levels among the samples, indicating that the plasma may be a more suitable source of cfDNA for biomarker screening. For the 54 patients with gastric cancer and the 59 age-matched healthy controls, the mean levels of plasma cfDNA were 2.4-fold higher in the patient group compared with the control group, indicating that plasma cfDNA levels may be useful for predicting patients with gastric cancer. The results of our study suggest that Alu81-qPCR is a more reliable method than other techniques, such as the PicoGreen assay, for quantifying cfDNA in human blood, demonstrating the potential to complement current diagnostic procedures for the management of gastric cancer patients.

PMID: 22741019

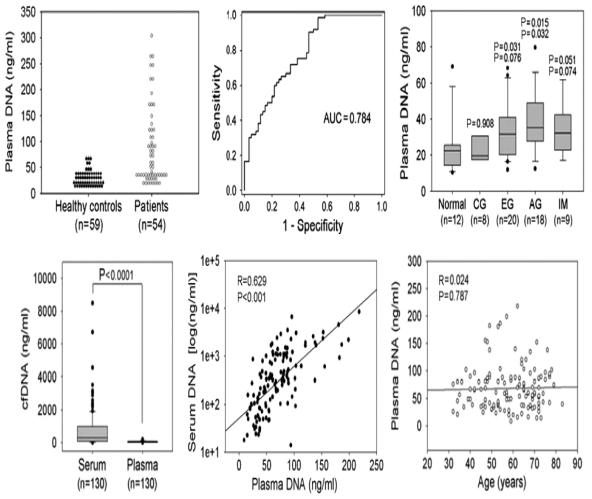

Keywords : Alu sequence; Cell-free DNA; Gastric cancer; Plasma; Serum

Article 149

Expression of endothelial cell-specific molecule-1 regulated by hypoxia inducible factor-1α in human colon carcinoma: impact of ESM-1 on prognosis and its correlation with clinicopathological features

Oncol Rep. 28(5):1701-8.

Kim JH, Park MY, Kim CN, Kim KH, Kang HB, Kim KD, Kim JW*

*Co-corresponding: yjkim@kribb.re.kr
BioMedical Genomics Research Center

Based on a previous finding that endothelial cell-specific molecule-1 (ESM-1) is a potential serum marker for colorectal cancer (CRC), the aim of this study was to clarify the clinicopathological significance of ESM-1 expression in CRC, and to explore the correlation between ESM-1 and HIF-1α in the tumorigenesis of CRC related to hypoxic conditions. ESM-1 mRNA expression was examined in CRC and corresponding normal mucosal tissues by reverse transcriptase-polymerase chain reaction (RT-PCR) and real-time RT-PCR. This experiment confirmed that ESM-1 levels were high in CRC. We screened the tissue samples of 143 CRC patients. By immunohistochemistry, we determined that the ESM-1 immunoreactivity was significantly correlated with the tumor size, depth of invasion, nodal status, distant metastasis and Dukes' stage, and was an independent prognostic factor for disease recurrence and worse survival outcome (P=0.001). The modulation of ESM-1 under hypoxia was investigated, and it was confirmed that ESM-1 expression was induced by HIF1-α and significantly attenuated by small interfering RNA (siRNA) targeting HIF-1α in CRC cells. These results showed that ESM-1 is significantly overexpressed, which is regulated by HIF-1α in CRC patients, and can be used as a potential biomarker and a therapeutic target for CRC.
PMID:22948784

Keywords : Biomarker; Colorectal cancer; ESM-1; HIF1-α; Therapeutic target

Article 150

Intrinsically disordered proteins

Physics Today. 65(8):64-5.

Tompa P, Han KH*

*Corresponding: khhan600@kribb.re.kr
BioMedical Translational Research Center

Researchers are discovering an everincreasing number of proteins that perform key cellular tasks without having the fixed, three-dimensional structure once thought mandatory for a protein to do its job. Proteins are the protagonists of life. The variety of proteins comes from the many possible permutations of those amino acids and the resulting ability of the protein chains to fold into three- dimensional structures of seemingly limitless diversity. Some IDPs derive their functionality directly from structural disorder and are described as having entropic chain functionality. Chains often appear as linkers in multidomain proteins and enable the IDP to flexibly search for binding partners. That flexibility influences the kinetics, thermodynamics, and specificity of the action of the protein. In the case of bacterial cellulase, the entropic chain functionality allows the enzyme to cleave its macroscopic cellulose substrate many times without having to release. Other IDPs operate through a process called molecular recognition, in which the active sites of the IDP weakly bind to a target molecule. The protein's disorder increases the interaction speed and allows the IDP to adapt to distinct partners. Its interaction with the enzyme protein phosphatase 1 results in a complex regulation as the enzyme–inhibitor complex transits between inhibited, de-inhibited, and activated states. The complex regulation is possible only because of the structural disorder in inhibitor 2, which enables various segments of the protein to independently bind or release. For almost 100 years, the structure–function paradigm served biologists well, and indeed, it is still the best paradigm for understanding enzymes. But nature is subtle, and also acts through IDPs. The varied, important, and fascinating functions of those proteins fully justifies the increasing study they are receiving.

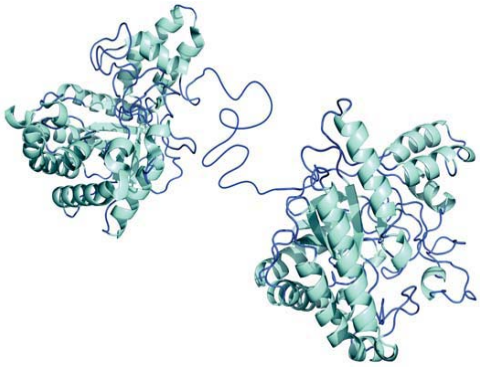

Keywords : Binding partners; Disordered proteins; IDPs; Independently bind

Article 151

Immunosensing using a metal clad leaky waveguide biosensor for clinical diagnosis

Sensor Actuator B. 173:288-94.

Im WJ, Kim BB, Byun JY, Kim HM, Kim MG , Shin YB*

*Co-corresponding: ybshin@kribb.re.kr
Research Center of Integrative Cellulomics

The optical detection technologies have been used in biosensors for the highly sensitive, real-time and label-free detection of biomolecules. In this report, a metal clad leaky waveguide (MCLW) was used as an immunosensing tools. We optimized the structure of the sensor chip for highly sensitive detection, followed by fabrication of the MCLW sensor chips and construction of a detection system for immunosensing. Titanium and SiO_2 films were deposited onto a BK7 substrate using an E-beam evaporator and the thickness of the films was 9 nm and 347 nm, respectively. The sensing response of the system to the bulk refractive index was calibrated using various concentrations of a glycerol solution. As a result, the MCLW sensor system was able to detect a change of $\sim 3.8 \times 10^{-6}$ RIU in the refractive index of the ambient solution. In addition, immunosensing was achieved using the MCLW sensor for an antigen-antibody reaction in real time. The biotin-labeled antibody of human interleukin 5 (hIL5) was immobilized on the sensor surface containing modified with streptavidin. The hIL5 in a bio-solution was quantitatively analyzed in real time using the MCLW sensor system.

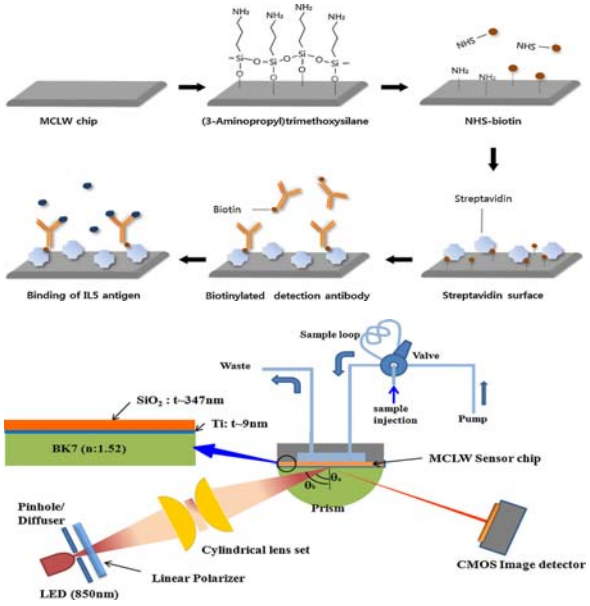

Keywords : Biosensor; Clinical diagnosis; Immunosensing; Metal clad; Optical waveguide; Sensor chips

Article 152

Comparative proteomic analysis of human somatic cells, induced pluripotent stem cells, and embryonic stem cells

Stem Cells Dev. 21(8):1272-86.

Kim SY, Kim MJ, Jung H, Kim WK, Kwon SO, Son MJ, Jang IS, Choi JS, Park SG, Park BC, Han YM, Lee SC, Cho YS*, Bae KH*

*Co-corresponding: june@kribb.re.kr khbae@kribb.re.kr
Research Center of Integrative Cellulomics

Induced pluripotent stem cells (iPSCs) are somatic cells that have been reprogrammed to a pluripotent state via introduction of defined transcription factors. iPSCs are a valuable resource for regenerative medicine, but whether iPSCs are identical to embryonic stem cells (ESCs) remains unclear. In this study, we performed comparative proteomic analyses of human somatic cells [human newborn foreskin fibroblasts (hFFs)], human iPSCs (hiPSCs) derived from hFFs, and H9 human ESCs (hESCs). We reprogrammed hFFs to a pluripotent state using 4 core transcription factors: Oct4 (O), Sox2 (S), Klf4 (K), and c-Myc (M). The proteome of hiPSCs induced by 4 core transcription factors was relatively similar to that of hESCs. However, several proteins, including dUTPase, GAPDH, and FUSE binding protein 3, were differentially expressed between hESCs and hiPSCs, implying that hiPSCs are not identical to hESCs at the proteomic level. The proteomes of iPSCs induced by introducing 3, 5, or 6 transcription factors were also analyzed. Our proteomic profiles provide valuable insight into the factors that contribute to the similarities and differences between hESCs and hiPSCs and the mechanisms of reprogramming.

PMID: 21787230

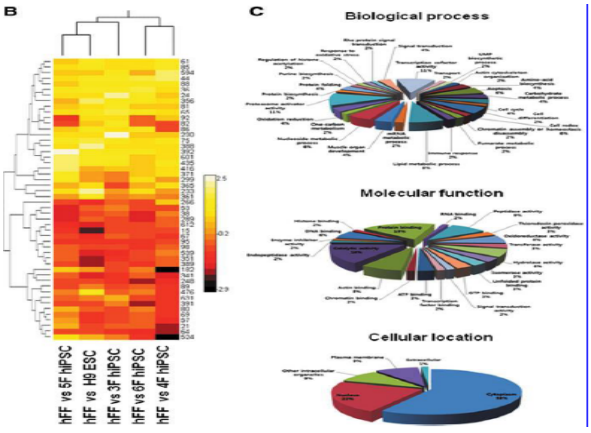

Keywords : c-myc; Comparative proteomic analyses; Differentiation; Fibroblasts; iPSCs; Translocation

Article 153

Repeated intravenous infusion of human apolipoprotein(a) kringle V is associated with reversible dose-dependent acute tubulointerstitial nephritis without affecting glomerular filtration function

Toxicol Lett. 212(3):298-306.

Lee HJ, Yu HK, Ahn JH, Park YK, Yoon Y, Kim JS*, Kim SJ

*Co-corresponding: jangskim@kribb.re.kr
Research Center of Integrative Cellulomics

Because anti-angiogenic agents have shown various toxicities in clinical applications, the determination of their toxicities and their reversibility is important in the design of clinical trials. This study was performed to investigate the potential toxicities of an angiogenesis inhibitor, apolipoprotein(a) (Apo(a)) kringle V (rhLK8) in rats. Rats administered an intravenous (IV) bolus injection of rhLK8 (200 mg/kg) for 7 days showed significant increases in serum blood urea nitrogen (BUN), creatinine and the BUN/creatinine ratio, which was compatible with acute tubulointerstitial nephritis (TIN) in pathological examination. Because anti-angiogenic therapies are usually based on long-term treatment strategies, rats were administered 200 mg/kg/day of rhLK8 by intravenous infusion for 28 days. Rats receiving 200 mg/kg of rhLK8 showed abnormal serological and histologic findings, but their levels returned to within normal ranges 2 weeks after the cessation of administration. The creatinine clearance rate (CCr) was not affected by rhLK8 treatment. Collectively, our data indicate that the intravenous infusion of rhLK8 at therapeutic doses may induce renal toxicities, such as acute TIN, but these toxicities are clinically tolerable and reversible with close monitoring and a recovery period.
PMID:22659101

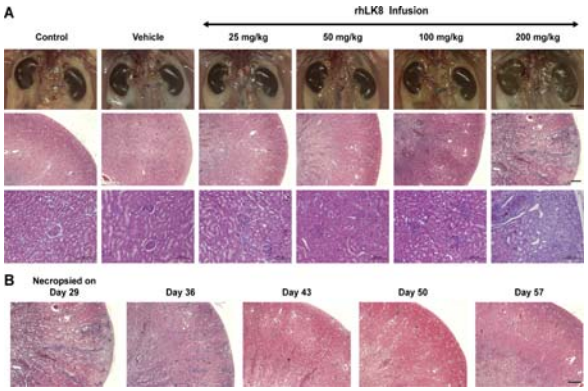

Keywords : Angiogenesis inhibitors; Apolipoprotein(a); Kringle; Tubulointerstitial nephritis

Article 154

Upregulation and secretion of kallikrein-related peptidase 6 (KLK6) in gastric cancer

Tumour Biol. 33(3):731-8.

Kim JJ, Kim JT, Yoon HR, Kang MA, Kim JH, Lee YH, Kim JW, Lee SJ, Song EY, Myung PK, Lee HG*

*Co-corresponding: hglee@kribb.re.kr
BioMedical Genomics Research Center

KLK6 encoding kallikrein-related peptidase 6, a trypsin-like serine protease, has been shown to be upregulated in several cancers, although the tumorigenic role of KLK6 has not been elucidated. In this study, *KLK6* was identified as a highly upregulated gene in gastric cancer; therefore, the possibility that KLK6 might be a suitable candidate tumor marker was examined. RT-PCR and immunohistochemical analysis showed overexpression of KLK6 in gastric cancer tissues compared to nontumor regions. Sera from gastric cancer patients had a 1.7-fold increase in KLK6 (373.1 μg/L, P = 0.048) compared to healthy individuals (214.2 μg/L), although there was no significant difference among patients with various tumor stages. Cellular invasiveness decreased by 45% in cells transfected with KLK6-specific small interfering RNA. Exogenous overexpression of KLK6 led to decreased activity of the E-cadherin promoter. This study shows that KLK6 is significantly upregulated and secreted in gastric cancer tissues and sera, suggesting that KLK6 might be used as a potential biomarker and therapeutic target for gastric cancer.
PMID: 22373580

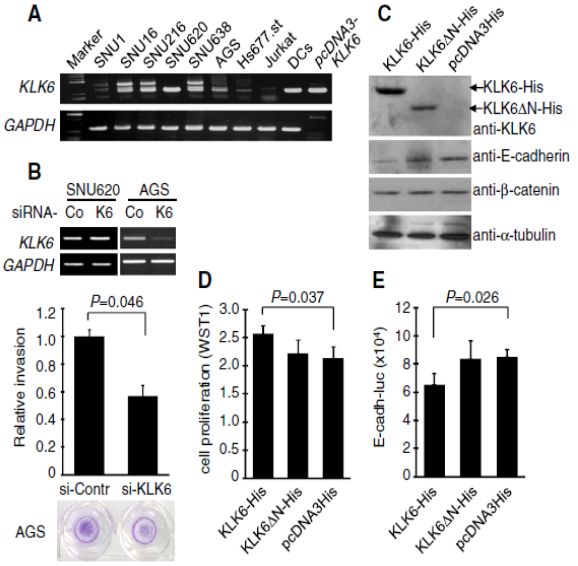

Keywords : Gastric cancer; Immunohistochemistry; Invasiveness; Kallikrein; KLK6


KRIBB
www.kribb.re.kr

2012
KRIBB Article Abstracts : First or corresponding articles indexed in SCIE, Scopus, and PubMed

Division of Biosystems Research

- Plant Systems Engineering Research Center
- Industrial Bio-materials Research Center
- Environmental Biotechnology Research Center

Korea Research Institute of Bioscience and Biotechnology

Article 155

Novel modular endo-β-1,4-xylanase with transglycosylation activity from *Cellulosimicrobium* sp. strain HY-13 that is homologous to inverting GH family 6 enzymes

Bioresour Technol. 107:25-32.

Kim DY, Ham SJ, Kim HJ, Kim J, Lee MH, Cho HY, Shin DH, Rhee YH, Son KH*, Park HY*

*Co-corresponding: sonkh@kribb.re.kr hypark@kribb.re.kr
Industrial Bio-materials Research Center

The gene (2304-bp) encoding a novel xylanolytic enzyme (XylK2) with a catalytic domain, which is 70% identical to that of *Cellulomonas flavigena* DSM 20109 GH6 β-1,4-cellobiohydrolase, was identified from an earthworm (*Eisenia fetida*)-symbiotic bacterium, *Cellulosimicrobium* sp. strain HY-13. The enzyme consisted of an N-terminal catalytic GH6-like domain, a fibronectin type 3 (Fn3) domain, and a C-terminal carbohydrate-binding module 2 (CBM 2). XylK2ΔFn3-CBM 2 displayed high transferase activity (788.3 IU mg^{-1}) toward p-nitrophenyl (PNP) cellobioside, but did not degrade xylobiose, glucose-based materials, or other PNP-sugar derivatives. Birchwood xylan was degraded by XylK2ΔFn3-CBM 2 to xylobiose (59.2%) and xylotriose (40.8%). The transglycosylation activity of the enzyme, which enabled the formation of xylobiose (33.6%) and xylotriose (66.4%) from the hydrolysis of xylotriose, indicates that it is not an inverting enzyme but a retaining enzyme. The endo-β-1,4-xylanase activity of XylK2Δ Fn3-CBM 2 increased significantly by approximately 2.0-fold in the presence of 50mM xylobiose.

PMID: 22230776

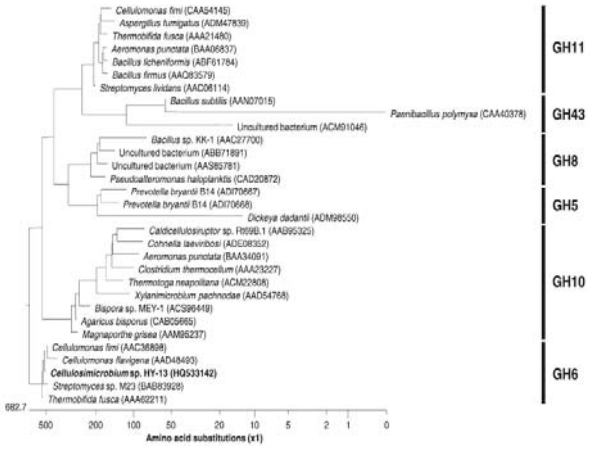

Keywords : *Cellulosimicrobium* sp. strain HY-13; *Eisenia fetida*; Endo-b-1,4-xylanase; Gut bacterium; Transglycosylation activity

Article 156

Effective screening of *Scenedesmus* sp. from environmental microalgae communities using optimal sonication conditions predicted by statistical parameters of fluorescence-activated cell sorting

Bioresour Technol. 114:478-83.

La HJ, Lee JY, Kim SG, Choi GG, Ahn CY, Oh HM*

*Corresponding: heemock@kribb.re.kr
Environmental Biotechnology Research Center

The effects of the sonication parameters, including the power and time, were investigated for the effective isolation of *Scenedesmus* sp. from environmental microalgae communities when using fluorescence-activated cell sorting (FACS). The selectivity, defined as the percentage of *Scenedesmus* sp. successfully isolated and grown in microplates, appeared as peaks in contour plots spanned by the sonication power and time. For fast screening of the optimal sonication conditions, correlations between the selectivity and the statistical parameters from the FACS analysis were investigated. A graphical comparison analysis of the contour plots showed a pattern similarity of over 82% between the coefficients of variation for the side scatter (SSC-CV) and the selectivity. This predictability of the optimal sonication conditions enabled a *Scenedesmus* sp. selectivity of ca. 2 times using only one-third of the sonication condition sets arbitrarily chosen around the peaks of the SSC-CV, thereby saving resources and time for subsequent processes.

PMID: 22459962

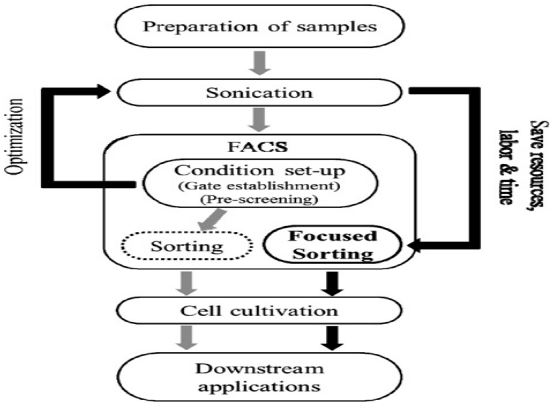

Keywords : Coefficient of variation; Environmental microalgae communities; FACS; *Scenedesmus* sp.; Sonication

Article 157

Non-ionic polysorbate surfactants: alternative inducers of medium-chain-length poly(3-hydroxyalkanoates) (MCL-PHAs) for production of extracellular MCL-PHA depolymerases

Bioresour Technol. 121:47-53.

Seo BS, Kim DY*, Ni YY, Son KH, Park HY, Rhee YH

*Co-first: kdy119@kribb.re.kr
Industrial Bio-materials Research Center

The potential of non-ionic polysorbate surfactants as alternative inducers of medium-chain-length poly(3-hydroxyalkanoates) (MCL-PHAs) for the production of diverse bacterial MCL-PHA depolymerases was evaluated. When grown with corn oil as the sole carbon substrate, *Pseudomonas alcaligenes* LB19 preferentially produced lipolytic enzymes, but its MCL-PHA depolymerase was not induced by the substrate. However, the results of activity staining and sodium dodecyl sulfate-polyacrylamide gel electrophoresis analysis clearly revealed that Tween 20 induced simultaneous production of lipolytic enzymes and the MCL-PHA depolymerase with the molecular mass (26.5 kDa) of *P. alcaligenes* LB19, which has been previously identified. Moreover, the co-production of two functionally distinct hydrolytic enzymes induced by Tween 20 was commonly observed in various Gram-positive and Gram-negative bacteria that were fed the substrate. Thus, it is expected that non-ionic polysorbate surfactants including Tween 20 can be widely exploited as promising universal substrates for the facile and efficient production of diverse MCL-PHA depolymerases.

PMID:22858467

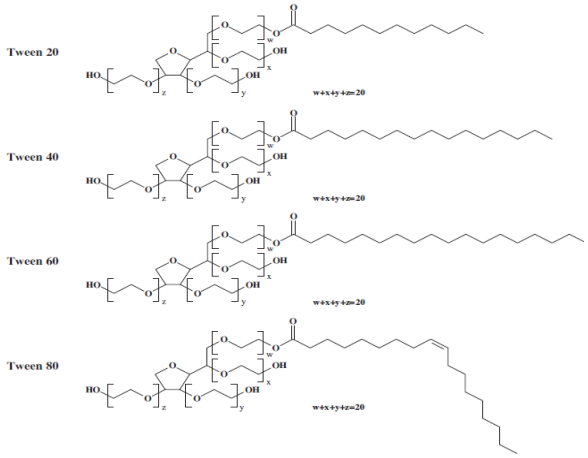

Keywords : MCL-PHA; Medium-chain-length poly depolymerase; Polysorbate surfactants; *Pseudomonas alcaligenes* LB19; Tween compounds

Article 158

A new Arctic *Chlorella* species for biodiesel production

Bioresour Technol. 125:340-3.

Ahn JW, Hwangbo K, Lee SY, Choi HG, Park YI, Liu JR, Jeong WJ*

*Corresponding: wonjoong@kribb.re.kr
Plant Systems Engineering Research Center

Microalgae are a potential resource for biodiesel production. A green alga, *Chlorella* sp., was isolated from Arctic sea ice, which was named ArM0029B. These algae displayed faster growth at a wide temperature range of 4-32°C compared to *Chlorella vulgaris*. ArM0029B also accumulated high levels of total fatty acids under nitrogen starvation conditions, reaching 39% of dry cell weight, with the proportion of oleic acid (18:1) and linoleic acid (18:2) reaching 54% of total fatty acids. Taken together, these results indicate that the newly identified *Chlorella* species, ArM0029B, is a promising candidate for biodiesel production.

PMID: 23069611

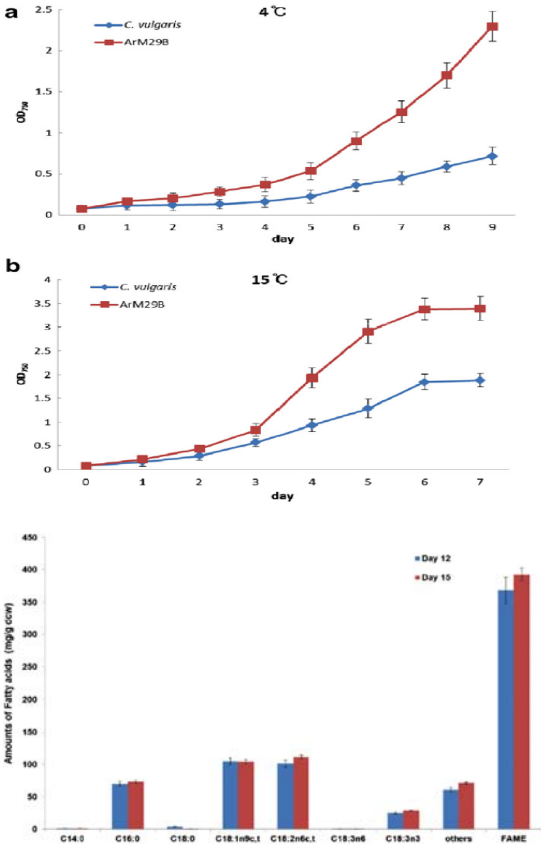

Keywords : Biodiesel; *Chlorella*; Fatty acid; Linoleic (18:2); Microalgae; Oleic acid (18:1)

Article 159

Toxoflavin lyase enzyme as a marker for selecting potato plant transformants

Biosci Biotechnol Biochem. 76(12):2354-6.

Kim MS, Kim H, Moon JS, Hwang I, Joung H, Jeon JH*

*Corresponding: jeonjh@kribb.re.kr
Plant Systems Engineering Research Center

This study established a new system for potato transformation using toxoflavin as selection agent and toxoflavin lyase (*tflA*) as selectable marker gene. Potato plants expressing *tflA* was successfully transformed on toxoflavin medium with 27% efficiency, similar to that for the hygromycin/hpt selection system. The transgenic potato expressing *tflA* also showed resistance to *Burkholderia glumea* infection.
PMID: 23221711

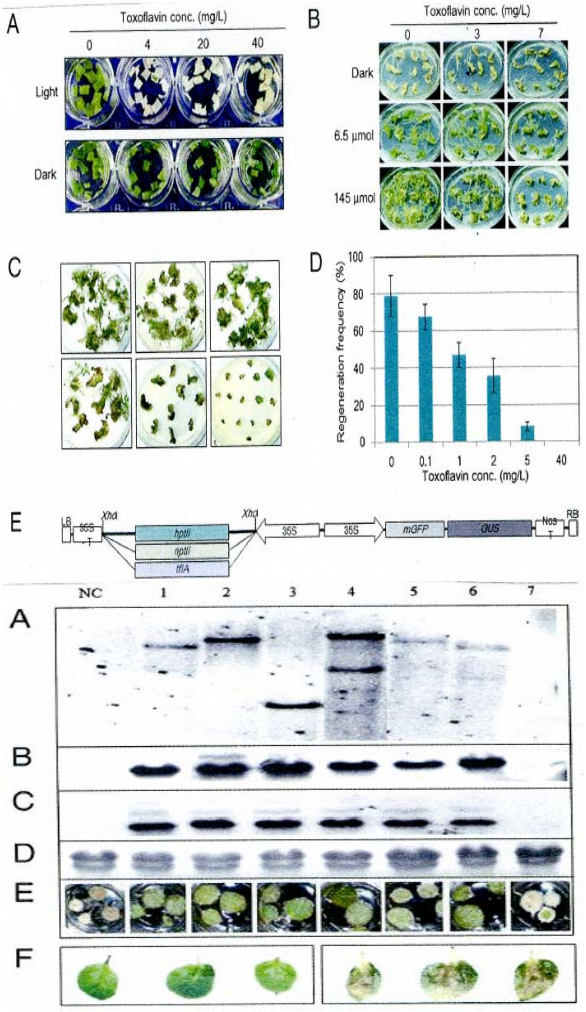

Keywords : Light-dependence; Selection marker system; Toxoflavin lyase (*tflA*); Transformation efficiency

Article 160

Small RNA and transcriptome deep sequencing proffers insight into floral gene regulation in *Rosa* cultivars

BMC Genomics. 13:657.

Kim J, Park JH, Lim CJ, Lim JY, Ryu JY, Lee BW, Choi JP, Kim WB, Lee HY, Choi Y, Kim D, Hur CG, Kim S, Noh YS, Shin C, Kwon SY*

*Co-corresponding: sykwon@kribb.re.kr
Plant Systems Engineering Research Center

BACKGROUND: Roses (*Rosa* sp.), which belong to the family Rosaceae, are the most economically important ornamental plants--making up 30% of the floriculture market. However, given high demand for roses, rose breeding programs are limited in molecular resources which can greatly enhance and speed breeding efforts. A better understanding of important genes that contribute to important floral development and desired phenotypes will lead to improved rose cultivars. For this study, we analyzed rose miRNAs and the rose flower transcriptome in order to generate a database to expound upon current knowledge regarding regulation of important floral characteristics. A rose genetic database will enable comprehensive analysis of gene expression and regulation via miRNA among different *Rosa* cultivars.

RESULTS: We produced more than 0.5 million reads from expressed sequences, totalling more than 110 million bp. From these, we generated 35,657, 31,434, 34,725, and 39,722 flower unigenes from *Rosa hybrid*: 'Vital', 'Maroussia', and 'Sympathy' and *Rosa rugosa* Thunb., respectively. The unigenes were assigned functional annotations, domains, metabolic pathways, Gene Ontology (GO) terms, Plant Ontology (PO) terms, and MIPS Functional Catalogue (FunCat) terms. Rose flower transcripts were compared with genes from whole genome sequences of Rosaceae members (apple, strawberry, and peach) and grape. We also produced approximately 40 million small RNA reads from flower tissue for *Rosa*, representing 267 unique miRNA tags. Among identified miRNAs, 25 of them were novel and 242 of them were conserved miRNAs. Statistical analyses of miRNA profiles revealed both shared and species-specific miRNAs, which presumably effect flower development and phenotypes.

CONCLUSIONS: In this study, we constructed a Rose miRNA and transcriptome database, and we analyzed the miRNAs and transcriptome generated from the flower tissues of four *Rosa* cultivars. The database provides a comprehensive genetic resource which can be used to better understand rose flower development and to identify candidate genes for important phenotypes.
PMID:23171001

Keywords : Floral gene regulation; Flower development; Plant micrornas; *Rosa* cultivars; Transcriptome database

Article 161

Translocation of phospholipase A2α to apoplasts is modulated by developmental stages and bacterial infection in *Arabidopsis*

Front Plant Sci. 3:126.

Jung J, Kumar K, Lee HY, Park YI, Cho HT, Ryu SB*

*Corresponding: sbryu@kribb.re.kr
Environmental Biotechnology Research Center

Phospholipase A_2 (PLA_2) hydrolyzes phospholipids at the *sn*-2 position to yield lysophospholipids and free fatty acids. Of the four paralogs expressed in *Arabidopsis*, the cellular functions of $PLA_2\alpha$ *in planta* are poorly understood. The present study shows that $PLA_2\alpha$ possesses unique characteristics in terms of spatiotemporal subcellular localization, as compared with the other paralogs that remain in the ER and/or Golgi apparatus during secretory processes. Only $PLA_2\alpha$ is secreted out to extracellular spaces, and its secretion to apoplasts is modulated according to the developmental stages of plant tissues. Observation of $PLA_2\alpha$ -RFP transgenic plants suggests that $PLA_2\alpha$ localizes mostly at the Golgi bodies in actively growing leaf tissues, but is gradually translocated to apoplasts as the leaves become mature. When *Pseudomonas syringae* pv. *tomato* DC3000 carrying the avirulent factor *avrRpm1* infects the apoplasts of host plants, $PLA_2\alpha$ rapidly translocates to the apoplasts where bacteria attempt to become established. *$PLA_2\alpha$ promoter*::*GUS* assays show that $PLA_2\alpha$ gene expression is controlled in a developmental stage- and tissue-specific manner. It would be interesting to investigate if $PLA_2\alpha$ functions in plant defense responses at apoplasts where secreted $PLA_2\alpha$ confronts with invading pathogens.

PMID: 22719742

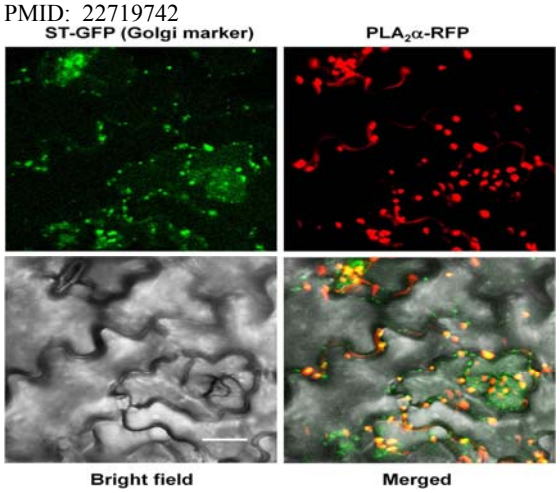

Keywords : Apoplast; Bacterial infection; Phospholipase A2; Subcellular localization; Ttranslocation

Article 162

RISA: a new web-tool for Rapid Identification of SSRs and Analysis of primers

Genes Genom. 34(6):583-90.

Kim J, Choi JP, Ahmad R, Oh Sk, Kwon SY, Hur CG*

*Co-corresponding: hurlee@kribb.re.kr
Plant Systems Engineering Research Center

The simple sequence repeats (SSRs) are short tandem arrayed sequence motifs consisting of 2-6 bp, which are not only involved in causing human fatal diseases but also have various applications in plant genetic studies. Thanks to the advancements made in sequencing technology, now we can easily generate genomic/transcriptomic sequences in a shorter period of time. Therefore, trend to identify SSR markers needs up gradation to handle these high-throughput data. Unfortunately, existing web programs for identifying SSR markers are useful but they are unable to process high-throughput data. To overcome this disadvantage, we have constructed a web-based tool, RISA (http://sol.kribb.re.kr/RISA/), with a goal of one-click service to identify SSR markers from high-throughput data (up to 200 Mbp). RISA controls automatic input and output pipeline by demon which combines the SSR classification and investigation by Robert Kofler (SciRoKo) to search SSRs and Primer3 to identify primers specific to SSRs simultaneously. In our test, 45,495 qualified primer sets specific to 47,070 SSRs were identified by RISA from whole *Arabidopsis lyrata* genome (about 207 Mbp) in 15 minutes. In results, it includes SSR statistics generated from user's queries and SSR markers information along with primers suitable for their amplification. To support handling of large amount of results, RISA provides various filtering options such as motif length, repeat units, total length and PCR product size. Therefore, we propose that RISA minimizes labour-intensive works or any other considerations which can be required during the development of SSR markers without having deep understanding of computer system and/or algorithms.

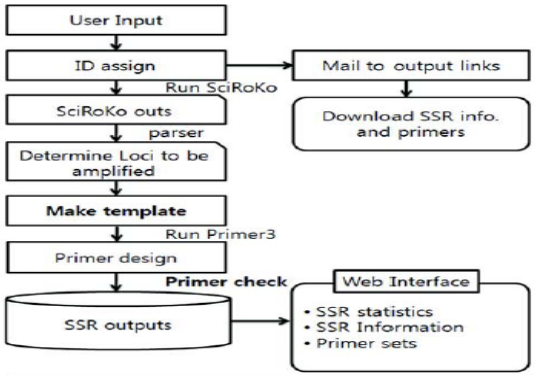

Keywords : High-throughput analysis; Molecular marker; Primer3; Sci-RoKo; Simple sequence repeat (SSR)

Article 163

Transient erythropoietin overexpression with cucumber mosaic virus suppressor 2b in *Nicotiana benthamiana*

Horticult Env Biotech. 53(5):434-40.

Moon KB, Jeon JH, Lee WS, Kim H*

*Corresponding: hyuns@kribb.re.kr
Plant Systems Engineering Research Center

Erythropoietin (EPO) is a glycoprotein hormone that regulates red blood cell formation in mammals. It also plays an important role in wound healing and the brain's response to neuronal injury. Recombinant EPO has been produced in various hosts including *Escherichia coli*, insect cells, and yeast. Plant systems are also useful for the production of recombinant proteins. In this study, we used *Nicotiana benthamiana* for the production of recombinant human EPO (rhEPO) using an *Agrobacterium*-mediated transient expression system. We evaluated the effect of repeated agroinfiltration and *Agrobacterium* density on the rhEPO production. In addition, the rhEPO expression vector was coinfiltrated with a vector expressing cucumber mosaic virus suppressor 2b (CMV2b), which suppresses posttranscriptional gene silencing. We found that rhEPO expression was increased approximately 5. 5-fold in *N. benthamiana* leaves coinfiltrated with CMV2b. In contrast, neither *Agrobacterium* density nor the number of infiltrations influenced rhEPO expression.

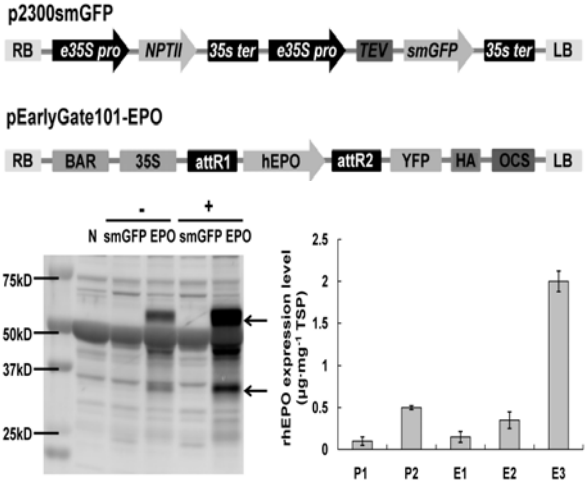

Keywords : *Agrobacterium*; Biopharmaceuticals; Posttranscriptional gene silencing; Recombinant proteins

Article 164

Laticifer tissue-specific activation of the *Hevea SRPP* promoter in *Taraxacum brevicorniculatum* and its regulation by light, tapping and cold stress

Indust Crop Prod. 40(1):219-24.

Tata SK, Choi JY, Jung JY, Lim KY, Shin JS, Ryu SB*

*Corresponding: sbryu@kribb.re.kr
Environmental Biotechnology Research Center

Hevea brasiliensis is an important plant species currently cultivated for the commercial production of natural rubber. As the demand for rubber continues to increase, it is important to identify alternative sources of natural rubber and to increase plant rubber content using molecular approaches. *Taraxacum kok-saghyz*, a Russian dandelion, produces natural rubber that is of high quality. In this study, the *SMALL RUBBER PARTICLE PROTEIN (SRPP)* promoter from *H. brasiliensis* was characterized to determine its suitability for the expression of latex-specific genes in *Taraxacum brevicorniculatum* which is another Russian dandelion species of *T. kok-saghyz* from the similar geographical areas. Studies using transgenic *Taraxacum* plants carrying the *SRPP* promoter::*β-glucuronidase (GUS)* sequence indicate that the *SRPP* promoter does induce gene expression primarily in laticiferous tissues. Additionally, the promoter was regulated by various external conditions including light, tapping, and cold. These findings suggest that the *SRPP* promoter will be a useful molecular tool for the manipulation of gene expression in the laticiferous tissues of *Taraxacum* plant species.

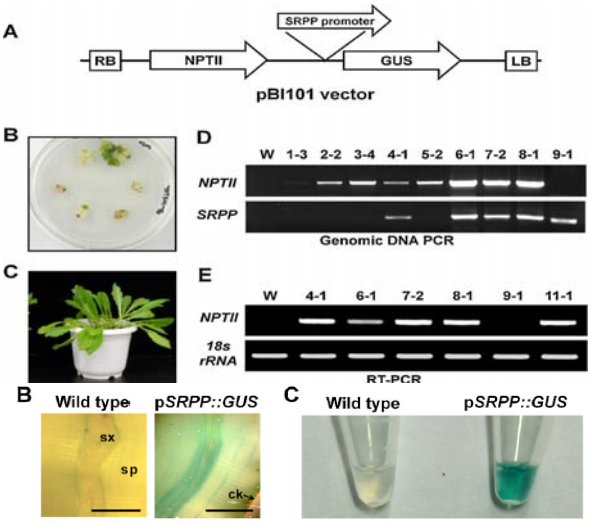

Keywords : Cold stress; Glucuronidase; *Hevea brasiliensis*; Latex; Natural rubber; SRPP promoter; *Taraxacum brevicorniculatum*; Taraxacum kok-saghyz

Article 165

Arenimonas daejeonensis sp. nov., isolated from compost

Int J Syst Evol Microbiol. 62(Pt 7):1674-8.

Jin L, Kim KK, An KG, Oh HM*, Lee ST

*Co-corresponding: heemock@kribb.re.kr
Environmental Biotechnology Research Center

A Gram-negative, aerobic, motile and rod-shaped bacterium, designated strain T7-07^T, was isolated from compost in Daejeon, Korea. Phylogenetic analysis based on 16S rRNA gene sequencing showed that strain T7-07^T had 99.0% gene sequence similarity with *Arenimonas malthae* KACC 14618^T and 94.7-95.9% with other recognized species of the genus *Arenimonas*. Cells formed creamy white to yellowish colonies on R2A agar and contained Q-8 as the predominant ubiquinone, $C_{15:0}$ iso, $C_{16:0}$ iso, $C_{17:1}$ iso ω9c and $C_{11:0}$ iso 3-OH as the major fatty acids, and diphosphatidylglycerol, phosphatidylethanolamine, phosphatidylglycerol, phosphatidylmethylethanolamine and an unknown aminolipid as the major polar lipids. The DNA G+C content of strain T7-07^T was 68.3 mol%. DNA-DNA reassociation experiments between T7-07^T and *Arenimonas malthae* KACC 14618^T resulted in a mean relatedness value of 22.2%. Combined genotypic and phenotypic data supported the conclusion that the strain T7-07^T represents a novel species, for which the name *Arenimonas daejeonensis* sp. nov. is proposed. The type strain is T7-07^T (=KCTC 12667^T=DSM 18060^T).

PMID: 21890720

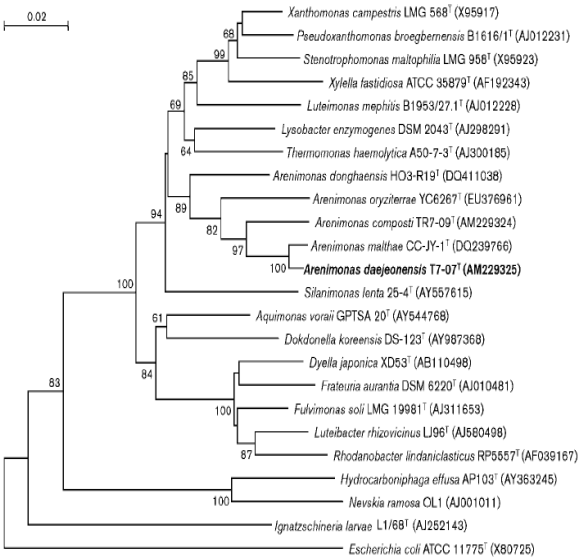

Keywords : *Arenimonas daejeonensis*; Compost; Phenotypic property; Phylogenetic analysis

Article 166

Variovorax defluvii sp. nov., isolated from sewage

Int J Syst Evol Microbiol. 62(Pt 8):1779-83.

Jin L, Kim KK, Ahn CY*, Oh HM*

*Co-corresponding: cyahn@kribb.re.kr heemock@kribb.re.kr
Environmental Biotechnology Research Center

A polyphasic taxonomic study was carried out on 2C1-b^T and 2C-21, two strains isolated from sewage flowing into River Geumho in Korea. Cells of the two strains were Gram-negative, non-spore-forming, motile and oval or rod-shaped. Comparative 16S rRNA gene sequence studies showed a clear affiliation of these two isolates with members of the *Betaproteobacteria*; they were most closely related to *Variovorax boronicumulans* KCTC 22010^T, *Variovorax dokdonensis* KCTC 12544^T, *Variovorax ginsengisoli* KCTC 12583^T, *Variovorax paradoxus* ATCC 17713^T and *Variovorax soli* KACC 11579^T showing 16S rRNA gene sequence similarities of 97.4-98.8% with these strains and shared 100% similarity with each other. The genomic DNA G+C contents of strains 2C1-b^T and 2C1-21 were 65.5 and 65.2 mol%, respectively. Phenotypic and chemotaxonomic data [Q-8 as the major ubiquinone; $C_{16:0}$, summed feature 4 ($C_{16:1}$ω7c and/or iso-$C_{15:0}$ 2-OH), $C_{17:0}$ cyclo and summed feature 7 ($C_{18:1}$ω7c and/or ω9t and/or ω12t) as major fatty acids] supported the affiliation of strains 2C1-b^T and 2C-21 to the genus *Variovorax*. Based on evidence derived from this polyphasic analysis, it is proposed that strains 2C1-b^T and 2C1-21 represent a novel species for which the name *Variovorax defluvii* sp. nov. is proposed; the type strain is 2C1-b^T (=KCTC 12768^T=JCM 17804^T).

PMID: 21948092

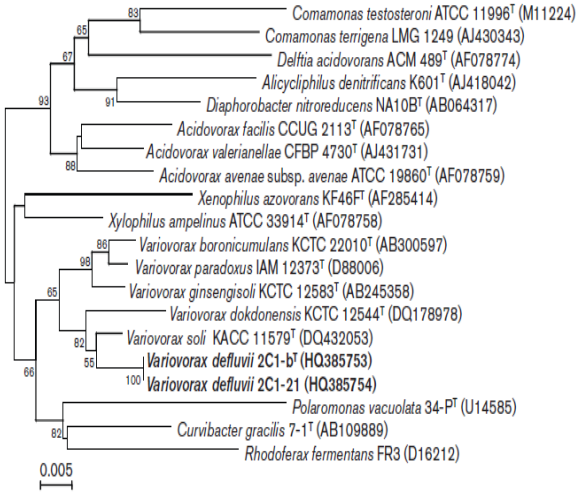

Keywords : Phenotypic property; Polyphasic analysis; Sewage flowing; *Variovorax defluvii*

Article 167

Kaistia defluvii sp. nov., isolated from river sediment

Int J Syst Evol Microbiol. 62(Pt 12):2878-82.

Jin L, Kim KK, Lee HG, Ahn CY*, Oh HM*

*Co-corresponding: cyahn@kribb.re.kr heemock@kribb.re.kr
Environmental Biotechnology Research Center

A Gram-stain-negative, aerobic, non-motile, rod- and coccus-shaped bacterium, designated strain B6-12^T, was isolated from sediment collected from the River Geumho in South Korea. In comparative 16S rRNA gene sequence analysis, the novel strain appeared to be affiliated with the class *Alphaproteobacteria* and to be most closely related to *Kaistia adipata* KCTC 12095^T, *Kaistia dalseonensis* DSM 18800^T, *Kaistia geumhonensis* DSM 18799^T, *Kaistia granuli* KCTC 12575^T, *Kaistia soli* KACC 12605^T and *Kaistia terrae* KACC 12910^T, with sequence similarities of 96.2-99.1%. The predominant ubiquinone in the isolate was Q-10, major fatty acids were $C_{18:0}$, $C_{18:1}\omega7c$ and $C_{19:0}\omega8c$ cyclo, and genomic DNA G+C content was 63.0 mol%. Based on the phylogenetic and chemotaxonomic evidence and the results of DNA-DNA hybridizations, strain B6-12^T represents a novel species in the genus Kaistia, for which the name *Kaistia defluvii* sp. nov. is proposed. The type strain is B6-12^T (= KCTC 23766^T = JCM 18034^T).

PMID: 22247212

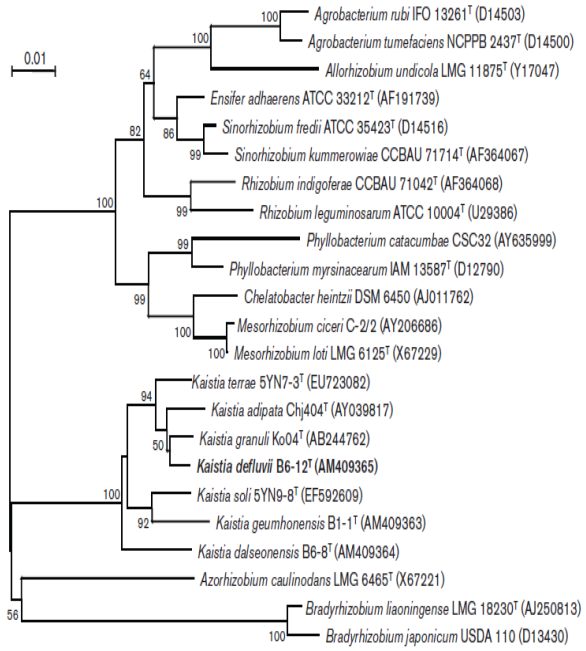

Keywords : Chemotaxonomic; *Kaistia defluvii*; Phenotypic property; Phylogenetic analysis; Sediment

Article 168

Development of an expression system using the heat shock protein 70 promoter in the red macroalga, *Porphyra tenera*

J Appl Phycol. 24(1):79-87.

Son SH, Ahn JW, Uji T, Choi DW, Park EJ, Hwang MS, Liu JR, Choi D, Mikami K, Jeong WJ*

*Corresponding: wonjoong@kribb.re.kr
Plant Systems Engineering Research Center

Porphyra is a commercially valuable source of food and drugs and an important model organism for algal research. However, genetic research on *Porphyra tenera* has been limited by a lack of a heterologous gene expression system. In this study, we isolated native promoter *PtHSP70* for the efficient expression of foreign genes in this organism. This promoter lies approximately 1 kb upstream of the heat shock protein 70 coding sequence and was isolated using adapter ligation-mediated genomic polymerase chain reaction. Promoter activity was evaluated using the synthetic GUS gene (PyGUS) with optimized codons for *Porphyra yezoensis*. Interestingly, the *PtHSP70* promoter allowed the efficient expression of PyGUS in *P. tenera* and *P. yezoensis*, whereas the *PyGAPDH* promoter from *P. yezoensis* was not fully functional in *P. tenera*. The PtHSP70 promoter may have a more conserved regulatory mechanism than the *PyGAPDH* promoter between these species, suggesting that *PtHSP70* could serve as a universal promoter for *Porphyra* species. We also established an efficient transient transformation system for *P. tenera* by evaluating transformation parameters including gold particle quantity, helium and vacuum pressure, developmental stages of leafy gametophytes, and target distance. Under optimal conditions of transient transformation, the frequency of GUS expression was determined by histochemical staining as 30-50 cells per bombardment. In addition, PyGUS expression was detected during the regeneration of monospores in *P. tenera*, indicating successful genetic transformation. Therefore, the new transient transformation system using the *PtHSP70* promoter can be used for foreign gene expression in *P. tenera*, which may advance the development of *P. tenera* as a model organism.

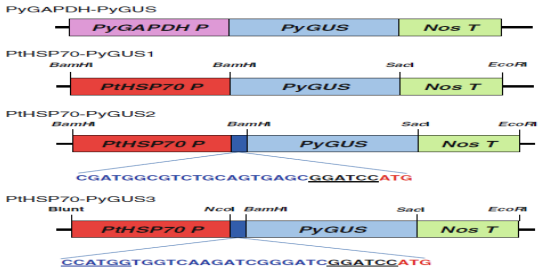

Keywords : Algae; Heat shock protein 70; *HSP70*; Particle bombardment; *Porphyra tenera*; *Porphyra yezoensis*; Transient gene expression

Article 169

Increasing γ-linolenic acid content in *Spirulina platensis* using fatty acid supplement and light-dark illumination

J Appl Phycol. 24(4):743-50

Kim EK, Choi GG, Kim HS, Ahn CY, Oh HM*

*Corresponding: heemock@kribb.re.kr
Environmental Biotechnology Research Center

Spirulina platensis, a filamentous cyanobacterium, produces γ-linolenic acid (GLA, 18:3), which is an important anti-inflammatory for pharmaceutical use. Thus, to increase the GLA content in *S. platensis*, this study investigated the combined effect of a light-dark (LD) two-stage culture and mixotrophic culture including a precursor of GLA. When compared with a photoautotrophic culture, the supplement of a GLA precursor, such as a long- or short-chain carbon source, enhanced the total fatty acid and GLA contents in the cells in the two-stage culture. The highest GLA content of 2% (w/w) and productivity of 27. 6 ± 4. 7 mg L^{-1} were obtained in *S. platensis* when using 0. 01 mM palmitic acid as a supplement in the two-stage culture. This study also suggests that a mixotrophic and LD two-stage culture may represent a method for increasing the total lipid production, which can then be converted to biofuels.

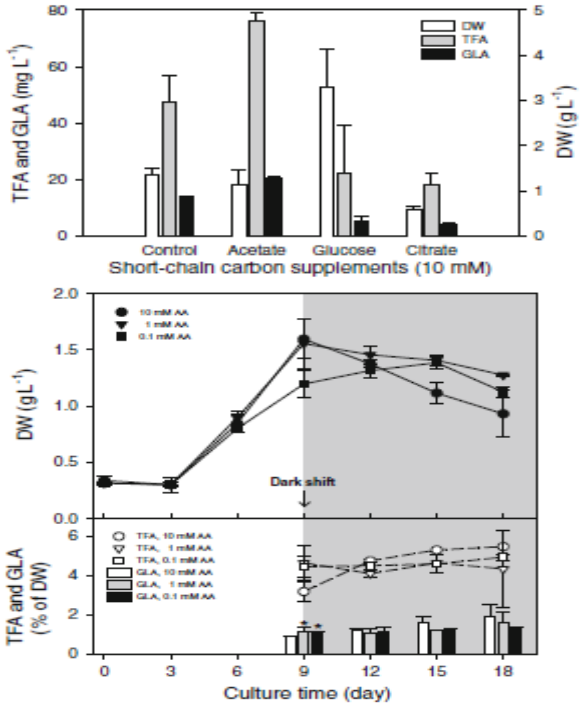

Keywords : Fatty acids; γ-Linolenic acid (GLA); Mixotroph; *Spirulina platensis*; Two-stage culture

Article 170

Genome sequence of the plant growth-promoting rhizobacterium *Bacillus* sp. strain JS

J Bacteriol. 194(14):3760-1.

Song JY, Kim HA, Kim JS, Kim SY, Jeong H, Kang SG, Kim BK, Kwon SK, Lee CH, Yu DS, Kim BS, Kim SH, Kwon SY*, Kim JF

*Co-corresponding: sykwon@kribb.re.kr
Plant Systems Engineering Research Center

Volatile and nonvolatile compounds emitted from the plant growth-promoting rhizobacterium *Bacillus* sp. strain JS enhance the growth of tobacco and lettuce. Here, we report the high-quality genome sequence of this bacterium. Its 4.1-Mb genome reveals a number of genes whose products are possibly involved in promotion of plant growth or antibiosis.
PMID:22740679

Keywords : Antibiosis; Genome sequence; Plant growth-promoting; Rhizobacterium *Bacillus*

Article 171

Draft genome sequence of the novel enteric bacterium *Galloisinimonas intestini* B14T KCTC 32180, isolated from the gut of a *Galloisiana* species (Notoptera: Grylloblattidae) fossil insect

J Bacteriol. 194(23):6648.

Park DS, Bae KS, Kim H, Shin KS, Choi SH, Kim DS, Kim BW, Oh HW*

*Corresponding: hwoh@kribb.re.kr
Industrial Bio-materials Research Center

We report the 3.74-Mb genome sequence of *Galloisinimonas intestini* $B14^T$, isolated from the gut of one of the world's rarest insect species, *Galloisiana* sp., collected at a Mosan cave, Moonkyung, Gyungsangbook-do, South Korea. Strain $B14^T$ is a novel genus candidate of the family *Enterobacteriaceae*.
PMID: 23144398

Keywords : Enteric bacterium; *Galloisinimonas intestini*; Genome sequence; Gut

Article 172

Monitoring of horizontal gene transfer from agricultural microorganisms to soil bacteria and analysis of microbial community in soils

J Microbiol Biotechnol. 22(4):563-6.

Kim SE, Moon JS, Choi WS, Lee SH, Kim SU*

*Corresponding: kimsu@kribb.re.kr
Industrial Bio-materials Research Center

To investigate the possibility of horizontal gene transfer between agricultural microorganisms and soil microorganisms in the environment, *Bacillus subtilis* KB producing iturin and the PGPR recombinant strain *Pseudomonas fluorescens* MX1 were used as model microorganisms. The soil samples of cucumber or tomato plants cultivated in pots and the greenhouse for a six month period were investigated by PCR, real-time PCR, Southern hybridization, and terminal restriction fragment length polymorphism (T-RFLP) fingerprinting. Our data from Southern blotting and TRFLP patterns suggest that the model bacteria do not give significant impacts on the other bacteria in the pots and greenhouse during cultivation.

PMID: 22534306

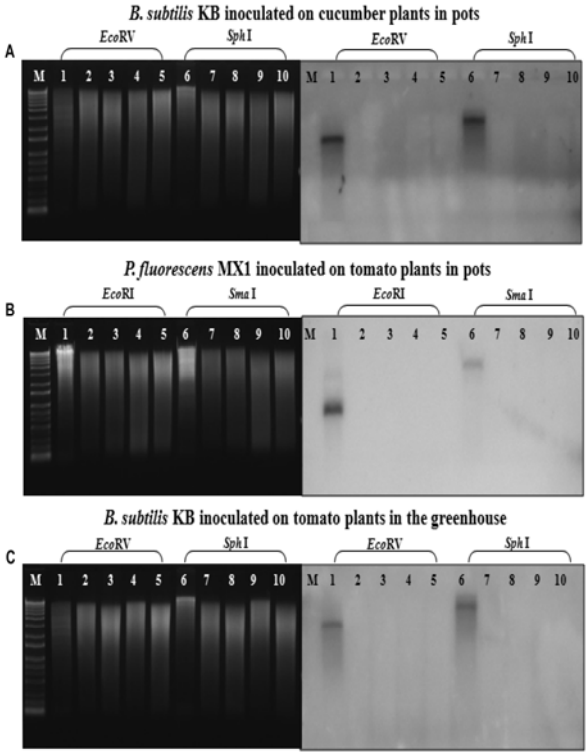

Keywords : Agricultural microorganism; Horizontal gene transfer; Microbial community; Soil bacteria; T-RFLP

Article 173

Molecular characterization of two ethylene response factor genes in sweetpotato that respond to stress and activate the expression of defense genes in tobacco leaves

J Plant Physiol. 169(11):1112-20.

Kim YH, Jeong JC, Park S, Lee HS, Kwak SS*

*Corresponding: sskwak@kribb.re.kr
Plant Systems Engineering Research Center

Two ethylene response factor (ERF) genes, *IbERF1* and *IbERF2*, were isolated from a library of expressed sequence tags (EST) prepared from suspension-cultured cells and dehydration-treated fibrous roots of sweetpotato (*Ipomoea batatas*). The deduced IbERFs contained a nuclear localization signal and the AP2/ERF DNA-binding domain. RT-PCR analysis revealed that *IbERF1* was expressed abundantly during the growth of suspension-cultured cells, whereas the expression levels of *IbERF2* transcripts were high in fibrous, thick pigmented roots. Two ERF genes also showed different responses to various types of abiotic stress and pathogen infection. Transient expression of the two ERF genes in tobacco (*Nicotiana tabacum*) leaves resulted in increased transcript levels of the pathogenesis-related 5 (PR5) gene, the early response to dehydration ten gene (ERD10), the CuZn superoxide dismutase gene (CuZnSOD) and the catalase gene (CAT). It is suggested that the two ERF genes play roles in the stress defense-signaling pathway as transcriptional regulators of the PR5, ERD10, CuZnSOD and CAT genes.

PMID: 22459326

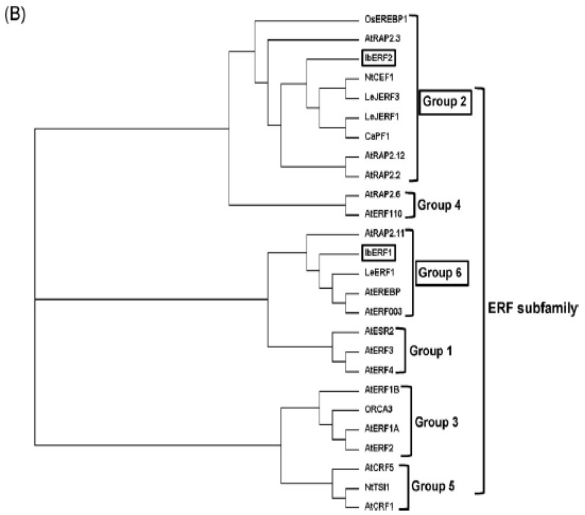

Keywords : Environmental stress; Ethylene response factor; Sweetpotato; Tobacco; Transient expression assay

Article 174

Municipal wastewater treatment and microbial diversity analysis of microalgal mini raceway open pond

Kor J Microbiol. 48(3):192-9.

Kang Z, Kim BH, Shin SY, Oh HM, Kim HS*

*Corresponding: hkim@kribb.re.kr
Environmental Biotechnology Research Center

Microalgal biotechnology has gained prominence because of the ability of microalgae to produce value-added products including biodiesel through photosynthesis. However, carbon and nutrient source is often a limiting factor for microalgal growth leading to higher input costs for sufficient biomass production. Use of municipal wastewater as a low cost alternative to grow microalgae as well as to treat the same has been demonstrated in this study using mini raceway open ponds. Municipal wastewater was collected after primary treatment and microalgae indigenous in the wastewater were encouraged to grow in open raceways under optimum conditions. The mean removal efficiencies of TN, TP, COD_{Mn}, NH_3-N after 6 days of retention time was 80.18%, 63.56%, 76.34%, and 96.74% respectively. The 18S rRNA gene analysis of the community revealed the presence of *Chlorella vulgaris* and *Scenedesmus obliquus* as the dominant microalgae. In addition, 16S rRNA gene analysis demonstrated that *Rhodobacter*, *Luteimonas*, *Porphyrobacter*, *Agrobacterium*, and *Thauera* were present along with the microalgae. From these results, it is concluded that microalgae could be used to effectively treat municipal wastewater without aerobic treatment, which incurs additional energy costs. In addition, municipal wastewater shall also serve as an excellent carbon and nitrogen source for microalgal growth. Moreover, the microalgal biomass shall be utilized for commercial purposes.

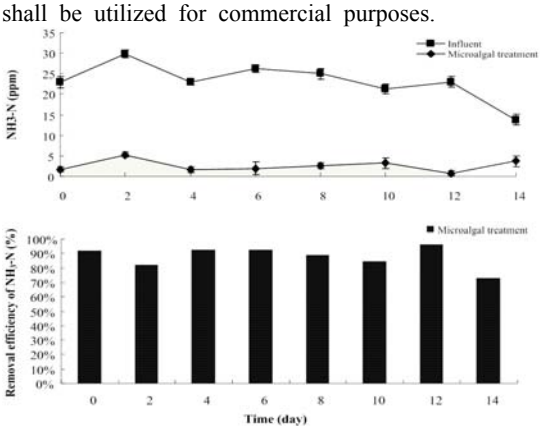

Keywords : Microalgae; Microbial diversity; Open culture system; Wastewater treatment

Article 175

Heat shock protein gene family of the *Porphyra seriata* and enhancement of heat stress tolerance by *PsHSP70* in *Chlamydomonas*

Mar Biotechnol. 14(3):332-42.

Park HS, Jeong WJ*, Kim E, Jung Y, Lim JM, Hwang MS, Park EJ, Ha DS, Choi DW

*Co-first: wonjoong@kribb.re.kr
Plant Systems Engineering Research Center

Heat shock proteins and molecular chaperones are key components contributing to survival in the abiotic stress response. *Porphyra seriata* grows on intertidal rocks exposed to dynamic environmental changes associated with the turning tides, including desiccation and heat stress. Analysis of the ESTs of *P. seriata* allows us to identify the nine *HSP* cDNAs, which are predicted to be *PsHSP90*, three *PsHSP70*, *PsHSP40* and *PsHSP20*, and three 5'-truncated *HSP* cDNAs. RT-PCR results show that most of the *PsHSP* transcripts were detected under normal cell growth conditions as well as heat stress, with the exception of two cDNAs. In particular, *PsHSP70b* and *PsHSP20* transcripts were upregulated by heat stress. When the putative mitochondrial *PsHSP70b* was introduced and overexpressed in *Chlamydomonas*, transformed *Chlamydomonas* evidenced higher rates of survival and growth than those of the wild type under heat stress conditions. Constitutive overexpression of the *PsHSP70b* gene increases the transcription of the *HSF1* as well as the *CrHSP20* and *CrHSP70* gene. These results indicate that *PsHSP70b* is involved in tolerance to heat stress and the effects on transcription of the *CrHSP20* and *CrHSP70* genes.
PMID:22068390

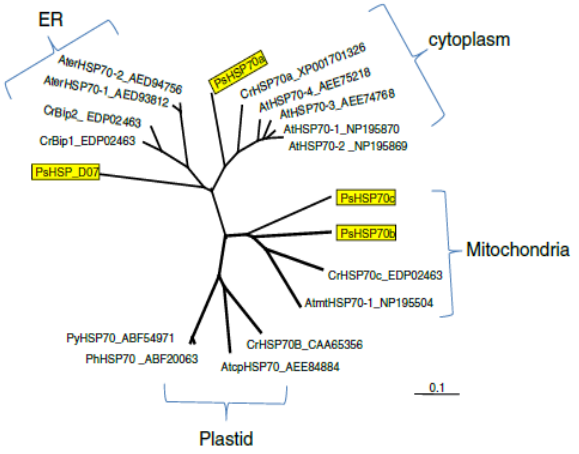

Keywords : *Chlamydomonas*; Heat tolerance; HSP; *Porphyra seriata*

Article 176

Three *Brassica rapa* metallothionein genes are differentially regulated under various stress conditions

Mol Biol Rep. 39(3):2059-67.

Ahn YO, Kim SH, Lee J, Kim H, Lee HS, Kwak SS*

*Corresponding: sskwak@kribb.re.kr
Plant Systems Engineering Research Center

The expression profiles of three *Brassica rapa* metallothionein genes (*BrMT 1-3*) were determined in 7-day-old seedlings exposed to various exogenous factors including plant hormones, heavy metals and abiotic stresses. *BrMT1*, *BrMT2*, and *BrMT3* were representatives of *MT* gene type 1, type 2, and type 3, respectively, according to their cysteine alignment. *BrMT2* showed a relatively higher basal expression level compared to *BrMT1* and *BrMT3* under normal conditions. The *BrMT1* transcript was markedly increased by various factors including ethephon, polyethylene glycol and hydrogen peroxide, with no down-regulation evident. On the contrary, *BrMT2* expression was down-regulated by abscisic acid, salicylic acid, and methyl jasmonate. Heavy metals did not increase *BrMT2* expression. *BrMT3* expression was only marginally and non-significantly up- and down-regulated by the stress conditions tested. Promoter regions of *BrMT1* and *BrMT2* display different cis-acting elements supporting the different responses of both genes against various stresses. The results demonstrate the differential regulation of *BrMT1-3* by various plant exogenous factors, and indicate the utility of the *BrMT1* promoter as a multiple stress inducible promoter.
PMID: 21643753

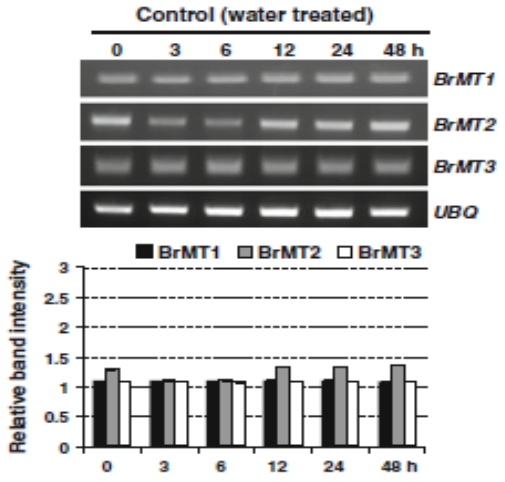

Keywords : *Brassica rapa*; Heavy metals; Metallothioneins; Phytoremediation; Promoter; ROS

Article 177

Prioritization of SNPs for genome-wide association studies using an interaction model of genetic variation, gene expression, and trait variation

Mol Cells. 33(4):351-61.

Paik H, Kim J, Lee S, Heo HS, Hur CG*, Lee D

*Co-corresponding: hurlee@kribb.re.kr
Plant Systems Engineering Research Center

The identification of true causal loci to unravel the statistical evidence of genotype-phenotype correlations and the biological relevance of selected single-nucleotide polymorphisms (SNPs) is a challenging issue in genome-wide association studies (GWAS). Here, we introduced a novel method for the prioritization of SNPs based on *p-values* from GWAS. The method uses functional evidence from populations, including phenotype-associated gene expressions. Based on the concept of genetic interactions, such as perturbation of gene expression by genetic variation, phenotype and gene expression related SNPs were prioritized by adjusting the *p-values* of SNPs. We applied our method to GWAS data related to drug-induced cytotoxicity. Then, we prioritized loci that potentially play a role in druginduced cytotoxicity. By generating an interaction model, our approach allowed us not only to identify causal loci, but also to find intermediate nodes that regulate the flow of information among causal loci, perturbed gene expression, and resulting phenotypic variation.
PMID:22460606

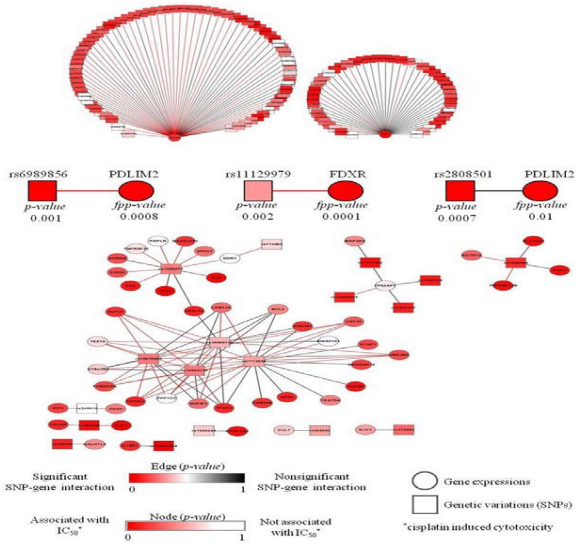

Keywords : Causal loci; Gene expression; Genetic variation; Interaction model; Trait variation

Article 178

A genome-wide comparison of NB-LRR type of resistance gene analogs (RGA) in the plant kingdom

Mol Cells. 33(4):385-92.

Kim J, Lim CJ, Lee BW, Choi JP, Oh SK, Ahmad R, Kwon SY, Ahn J, Hur CG*

*Corresponding: hurlee@kribb.re.kr
Plant Systems Engineering Research Center

Plants express resistance (*R*) genes to recognize invaders and prevent the spread of pathogens. To analyze nucleotide binding site, leucine-rich repeat (NB-LRR) genes, we constructed a fast pipeline to predict and classify the *R* gene analogs (RGAs) by applying in-house matrices. With predicted ~37,000 RGAs, we can directly compare RGA contents across entire plant lineages, from green algae to flowering plants. We focused on the highly divergent NBLRRs in land plants following the emergence of mosses. We identified entire loss of Toll/Interleukin-1 receptor, NBLRR (TNL) in Poaceae family of monocots and interestingly from *Mimulus guttatus* (a dicot), which leads to the possibility of species-specific TNL loss in other sequenced flowering plants. Using RGA maps, we have elucidated a positive correlation between the cluster sizes of NB-LRRs and their numbers. The cluster members were observed to consist of the same class of NB-LRRs or their variants, which were probably generated from a single locus for an *R* gene. Our website (http://sol.kribb.re.kr/PRGA/), called plant resistance gene analog (PRGA), provides useful information, such as RGA annotations, tools for predicting RGAs, and analyzing domain profiles. Therefore, PRGA provides new insights into *R*-gene evolution and is useful in applying RGA as markers in breeding and or systematic studies.

PMID: 22453776

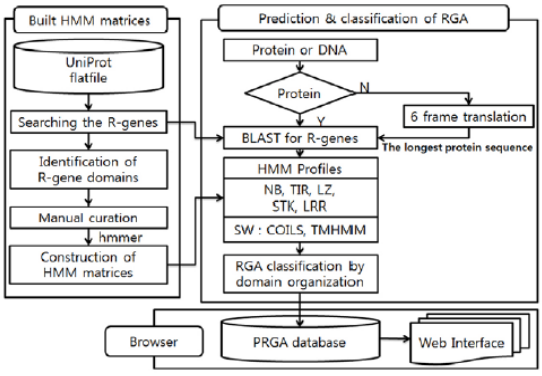

Keywords : NB-LRRs; Plant genome; PRGA; RGA maps; Resistance gene analogs (RGA)

Article 179

Screening of tissue-specific genes and promoters in tomato by comparing genome wide expression profiles of *Arabidopsis orthologues*

Mol Cells. 34(1):53-9.

Lim CJ, Lee HY, Kim WB, Lee BS, Kim J, Ahmad R, Kim HA, Yi SY, Hur CG, Kwon SY*

*Corresponding: sykwon@kribb.re.kr
Plant Systems Engineering Research Center

Constitutive overexpression of transgenes occasionally interferes with normal growth and developmental processes in plants. Thus, the development of tissue-specific promoters that drive transgene expression has become agriculturally important. To identify tomato tissue-specific promoters, tissue-specific genes were screened using a series of *in silico*-based and experimental procedures, including genome-wide orthologue searches of tomato and Arabidopsis databases, isolation of tissue-specific candidates using an Arabidopsis microarray database, and validation of tissue specificity by reverse transcription-polymerase chain reaction (RT-PCR) analysis and promoter assay. Using these procedures, we found 311 tissue-specific candidate genes and validated 10 tissue-specific genes by RT-PCR. Among these identified genes, histochemical analysis of five isolated *promoter::GUS* transgenic tomato and Arabidopsis plants revealed that their promoters have different but distinct tissue-specific activities in anther, fruit, and root, respectively. Therefore, it appears these *in silico*-based screening approaches in addition to the identification of new tissue-specific genes and promoters will be helpful for the further development of tailored crop development.

PMID: 22699756

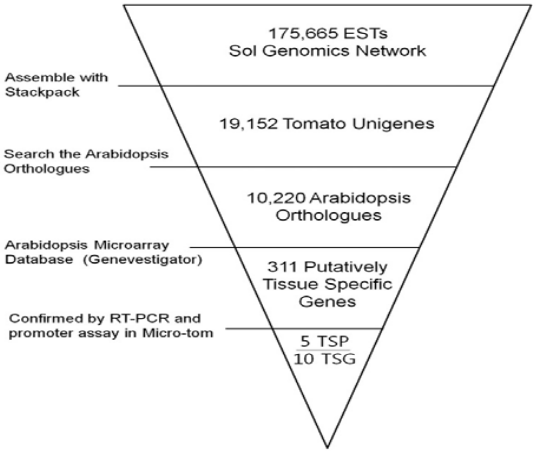

Keywords : Tailored crop development; Tissue-specific genes; Tissue-specific promoters; Tomato

Article 180

Down-regulation of β-carotene hydroxylase increases β-carotene and total carotenoids enhancing salt stress tolerance in transgenic cultured cells of sweetpotato

Phytochemistry. 74:69-78.

Kim SH, Ahn YO, Ahn MJ, Lee HS, Kwak SS*

*Corresponding: sskwak@kribb.re.kr
Plant Systems Engineering Research Center

Sweetpotato (*Ipomoea batatas* Lam.) is an important industrial crop and source of food that contains useful components, including antioxidants such as carotenoids. β-Carotene hydroxylase (*CHY-β*) is a key regulatory enzyme in the beta-beta-branch of carotenoid biosynthesis and it catalyzes hydroxylation into both β-carotene to β-cryptoxanthin and β-cryptoxanthin to zeaxanthin. To increase the β-carotene content of sweetpotato through the inhibition of further hydroxylation of β-carotene, the effects of silencing *CHY-β* in the carotenoid biosynthetic pathway were evaluated. A partial cDNA encoding *CHY-β* was cloned from the storage roots of orange-fleshed sweetpotato (cv. Shinhwangmi) to generate an RNA interference-*IbCHY-β* construct. This construct was introduced into cultured cells of white-fleshed sweetpotato (cv. Yulmi). Reverse transcription-polymerase chain reaction analysis confirmed the successful suppression of *IbCHY-β* gene expression in transgenic cultured cells. The expression level of phytoene synthase and lycopene β-cyclase increased, whereas the expression of other genes showed no detectable change. Down-regulation of *IbCHY-β* gene expression changed the composition and levels of carotenoids between non-transgenic (NT) and transgenic cells. In transgenic line #7, the total carotenoid content reached a maximum of 117 μg/g dry weight, of which β-carotene measured 34.43 μg/g dry weight. In addition, *IbCHY-β*-silenced calli showed elevated β-cryptoxanthin and zeaxanthin contents as well as high transcript level P450 gene. The 2,2-diphenyl-1-picrylhydrazyl radical scavenging activity (DPPH) in transgenic cells was more than twice that in NT cells. RNA-*IbCHY-β* calli increased abscisic acid (ABA) content, which was accompanied by enhanced tolerance to salt stress. In addition, the production of reactive oxygen species measured by 3,3'-diaminobenzidine (DAB) staining was significantly decreased in transgenic cultured cells under salt stress. Taken together, the present results indicate that down-regulation of *IbCHY-β* increased β-carotene contents and total carotenoids in transgenic plant cells and enhanced their antioxidant capacity.
PMID: 22154923

Keywords : β-Carotene hydroxylase; Carotenoid; Metabolic engineering; RNA interference; Sweetpotato

Article 181

Somatic embryogenesis in leaf tissue culture of Soapberry (*Sapindus mukorossi* Gaertn.)

Plant Biotechnol. 29(3):311-4.

Kim HT, Yang BH, Park YG, Liu JR*

*Corresponding: jrliu@kribb.re.kr
Plant Systems Engineering Research Center

Leaf explants formed embryogenic calluses at a frequency of 53.9% when cultured on B5 media supplemented with 0.1 mg l^{-1} 2,4-dichlorophenoxyacetic acid (2,4-D) and 0.01 mg l^{-1} 6-benzyladenine (BA) for 6 weeks. Upon transfer onto media with 5 mg l^{-1} abscisic acid, embryogenic calluses yielded somatic embryos at 73%. Somatic embryos developed into plantlets on media without plant growth regulators at 90%. Embryogenic calluses proliferated and maintained embryogenic capacity when subcultured on media with 0.1 mg l^{-1} 2,4-D and 0.01 mg l^{-1} BA at 4-week intervals. This culture system is an effective means for clonal propagation and genetic manipulation of soapberry because it ensures taproot development required for tree stability.

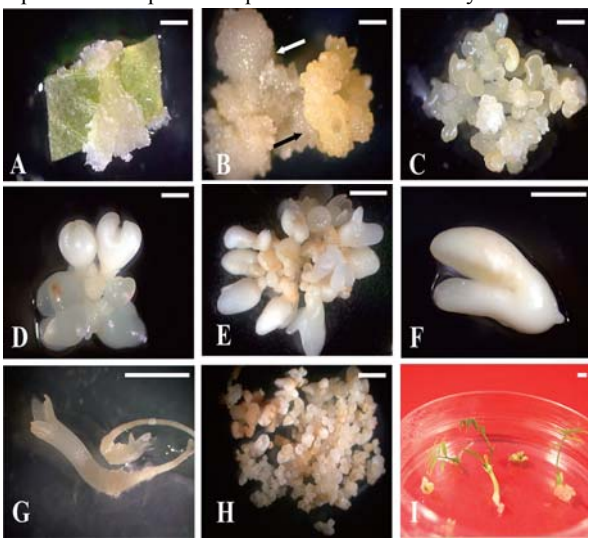

Keywords : Embryogenic callus; Plant regeneration; *Sapindus mukorossi*; Somatic embryo

Article 182

Stable expression of a fungal laccase protein using transplastomic tobacco

Plant Biotech Rep. 6(4):305-12.

Davarpanah SJ, Ahn JW, Ko SM, Jung SH, Park YI, Liu JR*, Jeong WJ*

*Co-corresponding: jrliu@kribb.re.kr wonjoong@kribb.re.kr
Plant Systems Engineering Research Center

Laccase catalyzes the oxidation of various phenolic compounds that can be used in a wide range of industrial applications such as waste detoxification and the textile industry. In the present study, we generated transplastomic tobacco plants to develop a reliable commercial source of laccase production. The stability of the laccase protein in the transgenic plants was increased by using the enhancer sequence from green fluorescent protein, resulting in three independent lines with high levels of laccase accumulation (up to 2 % of total protein); significant laccase activity, however, was not detected. Interestingly, the transplastomic lines showed slightly retarded vegetative growth, with a light green leaf color in comparison with the control, which may be attributable to copper deficiency induced by ligand chelation by abundantly produced laccase. These results suggest that the tobacco chloroplast is an efficient system for the mass production of laccase protein, but further studies are needed to obtain active enzyme.

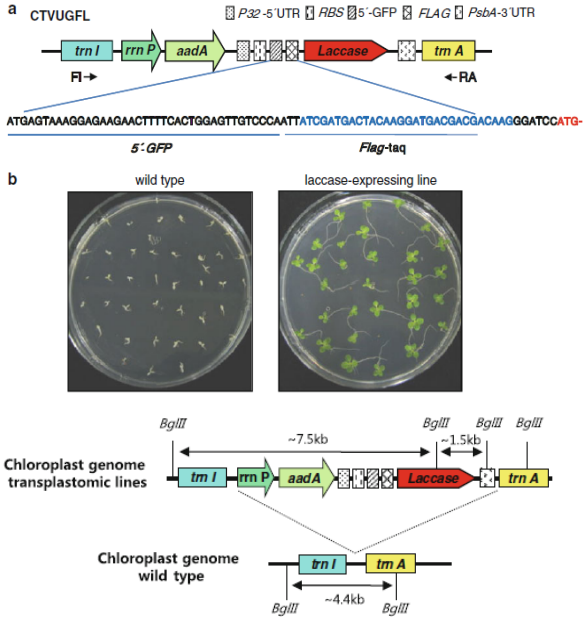

Keywords : Heterologous expression; Homoplasmy; Laccase; Nicotiana obtusifolia; Nicotiana tabacum; Transplastomic plant

Article 183

The rice thylakoid lumenal cyclophilin OsCYP20-2 confers enhanced environmental stress tolerance in tobacco and *Arabidopsis*

Plant Cell Rep. 31(2):417-26.

Kim SK, You YN, Park JC, Joung Y, Kim BG, Ahn JC, Cho HS*

*Co-corresponding: hscho@kribb.re.kr
Plant Systems Engineering Research Center

The role that the putative thylakoid lumenal cyclophilin (CYP) CYP20-2 locates in the thylakoid, and whether CYP20-2 is an essential gene, have not yet been elucidated. Here, we show that CYP20-2 is well conserved in several photosynthetic plants and that the transcript level of the rice *OsCYP20-2* gene is highly regulated under abiotic stress. We found that ectopic expression of rice OsCYP20-2 in both tobacco and *Arabidopsis* confers enhanced tolerance to osmotic stress and extremely high light. Based on these results, we suggest that although the exact biochemical function of OsCYP20-2 in the thylakoid lumen (TL) remains unclear, it may be involved in photosynthetic acclimation to help plants cope with environmental stress; the OsCYP20-2 gene may be a candidate for enhancing multiple abiotic stress tolerance.

PMID: 22041789

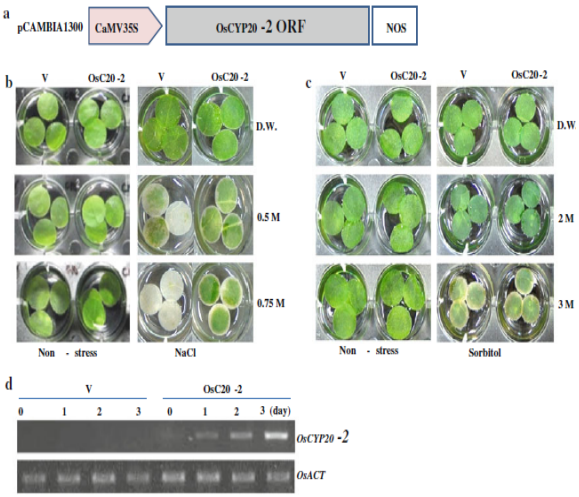

Keywords : Cyclophilin; CYP20-2; Salts/drought/high light stress; Stress tolerance

Article 184

Metabolic evaluation of cellular differentiation of tobacco leaf explants in response to plant growth regulators in tissue cultures using ^{1}H NMR spectroscopy and multivariate analysis

Plant Cell Tiss Org Cult. 108(2):303-13.

Kim SW, Kim JH, Ahn MS, Choung DH, Liu JR*

*Corresponding: jrliu@kribb.re.kr
Plant Systems Engineering Research Center

To investigate the metabolic changes that precede visible organogenesis in tissue culture, tobacco leaf explants were cultured on media supplemented with various plant growth regulators (PGRs) and analyzed with proton nuclear magnetic resonance (^{1}H NMR) spectroscopy. Principal component analysis (PCA) of ^{1}H NMR spectral data was unable to differentiate between leaf explants cultured with α -naphthaleneacetic acid and those cultured with 6-benzyladenine after 4 days of culture; however, a difference was evident after 8 days of culture. A hierarchical dendrogram from PCA analysis could be grouping leaf explants cultured with various auxins separately from those treated by various cytokinins. However, leaf explants cultured with thidiazuron (TDZ) were identified as an outlier group; TDZ appeared to produce pleiotropic metabolic effects that differed from those induced by other PGRs. These results show that dedifferentiation can be initiated by either auxins or cytokinins, which is reflected by similar metabolic changes produced by the two distinct PGRs during the initial incubation period. The subsequent redifferentiation differs according to the PGR treatment, which is reflected by differential metabolic changes, depending on the fate of cells in organogenesis. Glutamine and glutamate levels increased approximately twofold in cytokinin-treated leaf explants compared with auxin-treated explants; however, changes in the levels of sugar compounds did not differ between the two treatments, demonstrating auxin regulation of the carbon/nitrogen ratio in favor of rooting. Taken together, our results suggest that ^{1}H-NMR spectroscopy combined with multivariate analysis is a promising means for the metabolic evaluation of plant growth and differentiation.

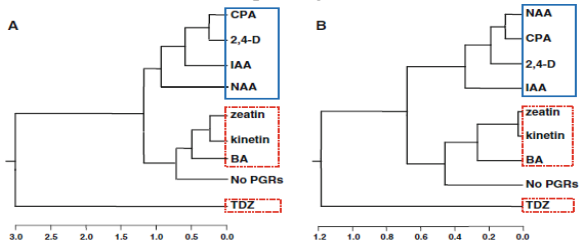

Keywords : ^{1}H NMR spectroscopy; Auxin regulation; Differentiation; Metabolite fingerprinting; Naphthaleneacetic acid; Principal component analysis; Thidiazuron; Tobacco leaf

Article 185

Comparative proteomic study between tuberous roots of light orange- and purple-fleshed sweetpotato cultivars

Plant Sci. 193:120-9.

Lee JJ, Park KW, Kwak YS, Ahn JY, Jung YH, Lee BH, Jeong JC, Lee HS, Kwak SS*

*Corresponding: sskwak@kribb.re.kr
Plant Systems Engineering Research Center

This study compares the differences in proteomes expressed in tuberous roots of a light orange-fleshed sweetpotato (*Ipomoea batatas* (L.) Lam. cultivar Yulmi) and a purple-fleshed sweetpotato cultivar (Shinjami). More than 370 protein spots were reproducibly detected by two-dimensional gel electrophoresis, in which 35 spots were up-regulated (Yulmi vs. Shinjami) or uniquely expressed (only Yulmi or Shinjami) in either of the two cultivars. Of these 35 protein spots, 23 were expressed in Yulmi and 12 were expressed in Shinjami. These protein spots were analyzed by matrix-assisted laser desorption/ionization-time of flight mass spectrometry and electrospray ionization tandem mass spectrometry. Fifteen proteins in Yulmi and eight proteins in Shinjami were identified from the up-regulated (Yulmi vs. Shinjami) or uniquely expressed (only Yulmi or Shinjami) proteins, respectively. In Yulmi, α-amylase and isomerase precursor-like protein were uniquely expressed or up-regulated and activities of α -amylase, monodehydroascorbate reductase, and dehydroascorbate reductase were higher than in Shinjami. In Shinjami, peroxidase precursor and aldo-keto reductase were uniquely expressed or up-regulated and peroxidase and aldo-keto reductase activities were higher than in Yulmi. PSG-RGH7 uniquely expressed only in Shinjami and the cultivar was evaluated more resistant than Yulmi against the root-knot nematode, *Meloidogyne incognita* (Kofold and White, 1919) Chitwood 1949 on the basis of shoot and root growth. Egg mass formation was 14.9-fold less in Shinjami than in Yulmi. These results provide important clues that can provide a foundation for sweetpotato proteomics and lead to the characterization of the physiological function of differentially expressed proteins.
PMID:22794925

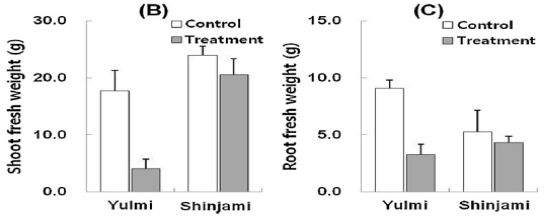

Keywords : Comparative proteomics; Light orange-fleshed cultivar; Purple-fleshed cultivar; Sweetpotato; Tuberous root

Article 186

Simple, rapid and cost-effective method for high quality nucleic acids extraction from different strains of *Botryococcus braunii*

PLoS One. 7(5):e37770.

Kim BH, Ramanan R, Cho DH, Choi GG, La HJ, Ahn CY, Oh HM, Kim HS*

*Corresponding: hkim@kribb.re.kr
Environmental Biotechnology Research Center

This study deals with an effective nucleic acids extraction method from various strains of *Botryococcus braunii* which possesses an extensive extracellular matrix. A method combining freeze/thaw and bead-beating with heterogeneous diameter of silica/zirconia beads was optimized to isolate DNA and RNA from microalgae, especially from *B. braunii*. Eukaryotic Microalgal Nucleic Acids Extraction (EMNE) method developed in this study showed at least 300 times higher DNA yield in all strains of *B. braunii* with high integrity and 50 times reduced working volume compared to commercially available DNA extraction kits. High quality RNA was also extracted using this method and more than two times the yield compared to existing methods. Real-time experiments confirmed the quality and quantity of the input DNA and RNA extracted using EMNE method. The method was also applied to other eukaryotic microalgae, such as diatoms, *Chlamydomonas* sp., *Chlorella* sp., and *Scenedesmus* sp. resulting in higher efficiencies. Cost-effectiveness analysis of DNA extraction by various methods revealed that EMNE method was superior to commercial kits and other reported methods by >15%. This method would immensely contribute to area of microalgal genomics.

PMID: 22662217

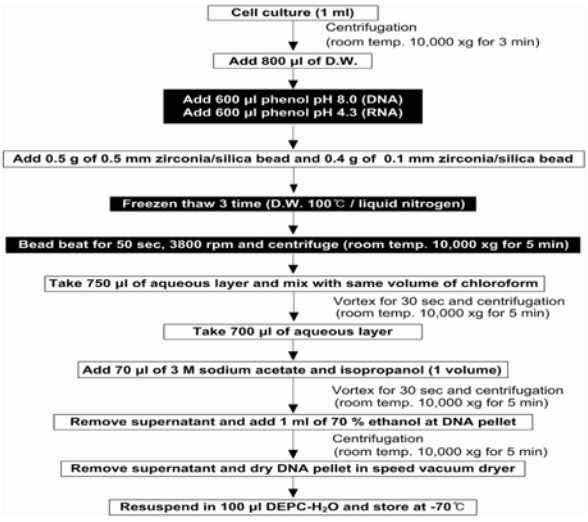

Keywords : *Botryococcus braunii*; EMNE method; Eukaryotic microalgae; Microalgal genomics

Article 187

Stable internal reference genes for the normalization of real-time PCR in different sweetpotato cultivars subjected to abiotic stress conditions

PLoS One. 7(12):e51502.

Park SC, Kim YH, Ji CY, Park S, Jeong JC, Lee HS, Kwak SS*

*Corresponding: sskwak@kribb.re.kr
Plant Systems Engineering Research Center

Reverse transcription quantitative real-time PCR (RT-qPCR) has become one of the most widely used methods for gene expression analysis, but its successful application depends on the stability of suitable reference genes used for data normalization. In plant studies, the choice and optimal number of reference genes must be experimentally determined for the specific conditions, plant species, and cultivars. In this study, ten candidate reference genes of sweetpotato (*Ipomoea batatas*) were isolated and the stability of their expression was analyzed using two algorithms, geNorm and NormFinder. The samples consisted of tissues from four sweetpotato cultivars subjected to four different environmental stress treatments, i.e., cold, drought, salt and oxidative stress. The results showed that, for sweetpotato, individual reference genes or combinations thereof should be selected for use in data normalization depending on the experimental conditions and the particular cultivar. In general, the genes *ARF, UBI, COX, GAP* and *RPL* were validated as the most suitable reference gene set for every cultivar across total tested samples. Interestingly, the genes *ACT* and *TUB*, although widely used, were not the most suitable reference genes in different sweetpotato sample sets. Taken together, these results provide guidelines for reference gene(s) selection under different experimental conditions. In addition, they serve as a foundation for the more accurate and widespread use of RT-qPCR in various sweetpotato cultivars.

PMID:23251557

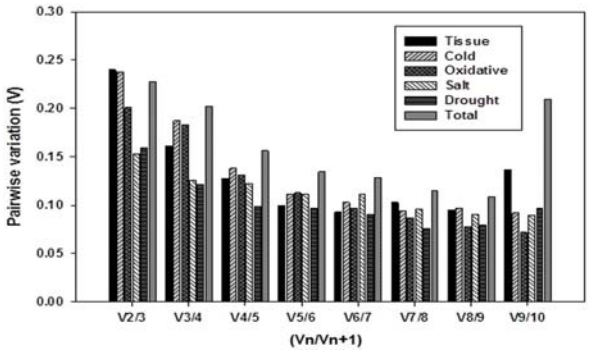

Keywords : Gene expression analysis; Reference gene; RT-qPCR; Sweetpotato cultivars

Article 188

Expression analysis of human β-secretase in transgenic tomato fruits

Protein Expr Purif. 82(1):125-31.

Kim HS, Youm JW, Moon KB, Ha JH, Kim YH, Joung H, Jeon JH*

*Corresponding: jeonjh@kribb.re.kr
Plant Systems Engineering Research Center

An emerging strategy in biomanufacturing involves using transgenic plants to express recombinant pharmaceutical and industrial proteins in large quantities. β-Site APP cleaving enzyme 1 (β-secretase 1, BACE1) is an enzyme involved in the abnormal production of Aβ42, the major component of senile plaques in Alzheimer's disease (AD). Thus, BACE1 represents a key target protein in the development of new potential drugs to treat Alzheimer's disease. We aimed to develop a tomato-derived recombinant BACE1 (rBACE1) protein to serve as a vaccine antigen that would promote an immune response. We utilized a plant expression cassette, pE8BACE, to optimize BACE1 expression in tomato fruits. Polyemerase chain reaction and Southern blot analyses verified integration of the BACE1 gene into the plant genome. Northern and Western blot analyses demonstrated successful mRNA and protein expression of rBACE1, respectively; the Sensizyme assay kit estimated the expression level of rBACE1 protein at 136 ± 7 ng mg^{-1} total soluble protein. The tomato-derived rBACE1 retains its activity for a long storage period at cool or room temperature, and is highly resistant to degradation in conditions such as low acidity. Tomato-derived rBACE1 was severely degraded by heat or boiling. The proteolytic activity of tomato-derived rBACE1, confirmed by fluorescence resonance transfer assay, was similar to that of a commercial sample of *Escherichia coli*-derived BACE1.

PMID: 22178732

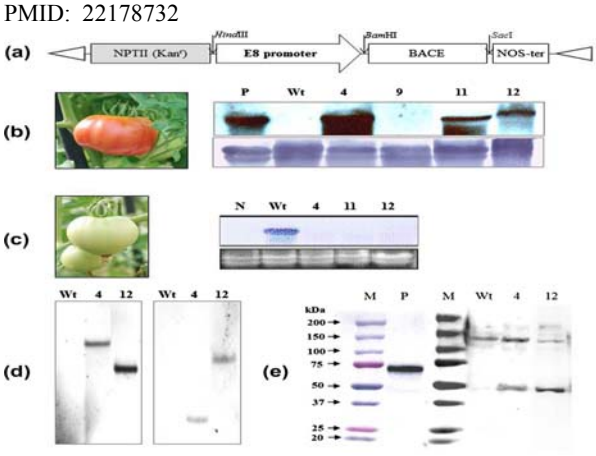

Keywords : Alzheimer's vaccine; β-Secretase; Lycopersicon esculentum; Recombinant protein; Transgenic plant

Article 189

Biological and molecular characterization of Soybean yellow common mosaic virus, a new species in the genus *Sobemovirus*

Virus Res. 163(1):363-7.

Nam M, Kim JS, Park SJ, Park CY, Lee JS, Choi HS, Kim JS, Kim HG, Lim S, Moon JS*, Lee SH

*Co-corresponding: jsmoon@kribb.re.kr
Plant Systems Engineering Research Center

A novel soybean-infecting sobemovirus termed Soybean yellow common mosaic virus (SYCMV) was characterized. The virus has a single, positive-strand RNA genome of 4152 nucleotides. The virus contains four putative open reading frames encoding P1 (78-566 nt), polyprotein ORF2a (524-2248 nt), polymerase domain ORF2b (1852-3417 nt), and CP (3227-4030 nt). The entire nucleotide sequence of SYCMV showed 31.2-71.3% nucleotide identity with the previously known eleven species of sobemovirus. In host range analysis of SYCMV, in which twenty one species and three different *Nicotiana tabacum* cultivars belonging to seven families were inoculated with the virus, SYCMV had a narrow host range, infecting only *Glycine max* and *G. soja*. Based on the obtained sequence, full-length clones of SYCMV were constructed. Symptoms produced by inoculation with clones were indistinguishable from those produced by inoculation with sap from symptomatic plants. Viral RNA accumulation of SYCMV was detected in the upper leaves by Northern blotting. This indicated that full-length clones of SYCMV were sufficient to produce disease symptoms. Genomic organization, the predicted amino acid sequence, and phylogenetic analyses with known sobemoviruses confirmed the assignment of SYCMV as a new member of the genus *Sobemovirus*.

PMID:21875629

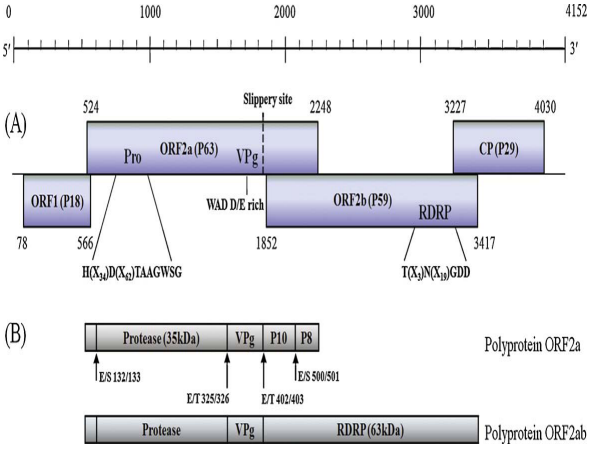

Keywords : Infectious clone; Plant virus; *Sobemovirus*; Soybean yellow common mosaic virus (SYCMV)

2012
KRIBB Article Abstracts : First or corresponding articles indexed in SCIE, Scopus, and PubMed

Division of Biological Infrastructure

- Microbial Resource Center
- Laboratory Animal Resource Center
- International Biological Material Research Center
- Human Derived Material Center
- Korea National Primate Research Center
- Bio-Evaluation Center
- Biotechnology Process Engineering Center
- LMO Research Safety Center

Korea Research Institute of Bioscience and Biotechnology

Article 190

Microneedles for drug and vaccine delivery

Adv Drug Deliv Rev. 64(14):1547-68.

Kim YC*, Park JH, Prausnitz MR

*Corresponding:
Biotechnology Process Engineering Center

Microneedles were first conceptualized for drug delivery many decades ago, but only became the subject of significant research starting in the mid-1990's when microfabrication technology enabled their manufacture as (i) solid microneedles for skin pretreatment to increase skin permeability, (ii) microneedles coated with drug that dissolves off in the skin, (iii) polymer microneedles that encapsulate drug and fully dissolve in the skin and (iv) hollow microneedles for drug infusion into the skin. As shown in more than 350 papers now published in the field, microneedles have been used to deliver a broad range of different low molecular weight drugs, biotherapeutics and vaccines, including published human studies with a number of small-molecule and protein drugs and vaccines. Influenza vaccination using a hollow microneedle is in widespread clinical use and a number of solid microneedle products are sold for cosmetic purposes. In addition to applications in the skin, microneedles have also been adapted for delivery of bioactives into the eye and into cells. Successful application of microneedles depends on device function that facilitates microneedle insertion and possible infusion into skin, skin recovery after microneedle removal, and drug stability during manufacturing, storage and delivery, and on patient outcomes, including lack of pain, skin irritation and skin infection, in addition to drug efficacy and safety. Building off a strong technology base and multiple demonstrations of successful drug delivery, microneedles are poised to advance further into clinical practice to enable better pharmaceutical therapies, vaccination and other applications.

PMID:22575858

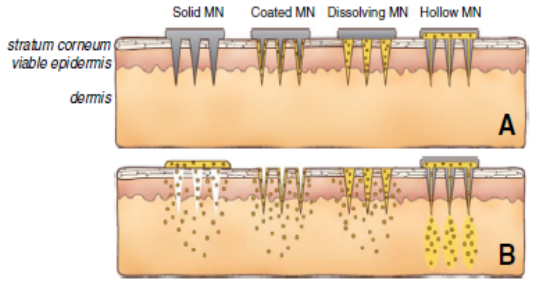

Keywords : Intracellular delivery; Microfabricated device; Microneedle; Ocular drug delivery; Skin vaccination; Transdermal drug delivery

Article 191

Dillenia tetrapetala (Dilleniaceae), a new species from HonBa Nature Reserve, Vietnam

Ann Bot Fennici. 49(5-6):369-76.

Choudhary RK, Bach TT, Van Nong L, Van Hai D, Quang BH, Lee YM, Park SH, Lee C, Lee J*

*Corresponding: joongku@kribb.re.kr
International Biological Material Research Center

A new species *Dillenia tetrapetala* Joongku Lee, T.B. Tran & R.K. Choudhary (Dilleniaceae) is described from HonBa Nature Reserve of the Khanh Hoa province of Vietnam. Detailed illustrations and taxonomic comments are provided along with a table listing the differential characters to the closely similar taxa. Phylogenetic analyses using nrITS region of ribosomal DNA and *psbA-trn*H intergenic spacer region of chloroplast DNA sequences were also performed and they supported the status of *D. tetrapetala* as a distinct species. The plant is considered endangered based on the IUCN red list criteria because of its restricted distribution.

Keywords : *Dillenia tetrapetala*; Dilleniaceae; Phylogenetic analyses; Taxonomic; Vietnam

Article 192

Characterization of a novel ginsenoside-hydrolyzing α-L-arabinofuranosidase, AbfA, from *Rhodanobacter ginsenosidimutans* Gsoil 3054T

Appl Microbiol Biotechnol. 94(3):673-82.

An DS, Cui CH, Sung BH, Yang HC, Kim SC, Lee ST, Im WT, Kim SG*

*Co-corresponding: sgkim@kribb.re.kr
Microbial Resource Center

The gene encoding an α-L-arabinofuranosidase that could biotransform ginsenoside Rc {3-O-[β-D-glucopyranosyl-(1-2)-β-D-glucopyranosyl]-20-O-[α-L-arabinofuranosyl-(1-6)-β-D-glucopyranosyl]-20(S)-protopanaxadiol} to ginsenoside Rd {3-O-[β-D-glucopyranosyl-(1-2)-β-D-glucopyranosyl]-20-O-β-D-glucopyranosyl-20(S)-protopanaxadiol} was cloned from a soil bacterium, *Rhodanobacter ginsenosidimutans* strain Gsoil 3054^T, and the recombinant enzyme was characterized. The enzyme (AbfA) hydrolyzed the arabinofuranosyl moiety from ginsenoside Rc and was classified as a family 51 glycoside hydrolase based on amino acid sequence analysis. Recombinant AbfA expressed in *Escherichia coli* hydrolyzed non-reducing arabinofuranoside moieties with apparent K_m values of 0.53 ± 0.07 and 0.30 ± 0.07 mM and V_{max} values of 27.1 ± 1.7 and 49.6 ± 4.1 μmol min^{-1} mg^{-1} of protein for *p*-nitrophenyl-α-L-arabinofuranoside and ginsenoside Rc, respectively. The enzyme exhibited preferential substrate specificity of the exo-type mode of action towards polyarabinosides or oligoarabinosides. AbfA demonstrated substrate-specific activity for the bioconversion of ginsenosides, as it hydrolyzed only arabinofuranoside moieties from ginsenoside Rc and its derivatives, and not other sugar groups. These results are the first report of a glycoside hydrolase family 51 α-L-arabinofuranosidase that can transform ginsenoside Rc to Rd.

PMID: 22159603

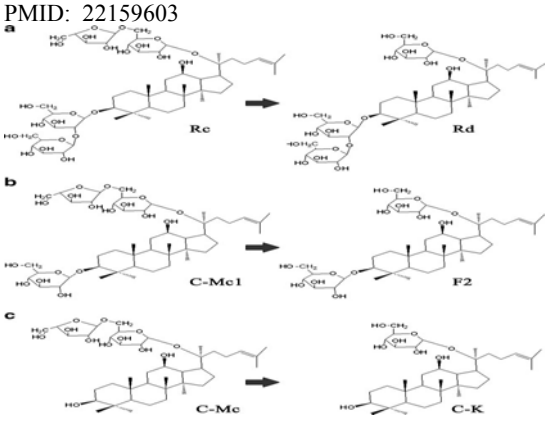

Keywords : Biotransformation; Compound Mc; Compound Mc1; Ginseng saponin; *Rhodanobacter ginsenosidimutans*; Transform ginsenoside

Article 193

Expression of hepatic and ovarian cytochrome P450 during estrous cycle in rats

Arch Toxicol. 86(1):75-85.

Lee SY, Oh SJ*, Yun KU, Kim HM, Kim BH, Lee K, Kim SK

*Co-first: diatree@kribb.re.kr
Bio-Evaluation Center

It is known that gender differences in drug metabolism are largely attributed to changes in sex and growth hormones. Serum concentrations of estradiol, progesterone, prolactin, follicle-stimulating hormone, and luteinizing hormone change markedly during the human menstrual cycle and the rat estrous cycle. However, little information is available regarding the effects of the human menstrual cycle or the rat estrous cycle on expression and activity of cytochrome P450 (CYP) isoforms. The present study was carried out to determine the expression and activity of CYP-dependent drug-metabolizing enzymes in the liver and ovary during the estrous cycle. The expression and activity of microsomal CYP isoforms (CYP1A1, CYP1A2, CYP1B1, CYP2B1, CYP2C11, CYP2C12, CYP2E1, CYP3A1, CYP3A2, and CYP4A), cytochrome b(5) and NADPH-dependent CYP reductase in the liver and ovary were measured in female rats in diestrus and proestrus. Our results indicated that hepatic and ovarian expression and activity of CYP isoforms, cytochrome b(5), and NADPH-dependent CYP reductase were not different between diestrus and proestrus, although serum estradiol concentration and uterus weight were markedly increased in the proestrus phase. These results suggest that the cytochrome P450-dependent system is not sensitive to changes in the estrous cycle, and further studies are warranted to determine the effects of the estrous cycle on *in vivo* metabolism of xenobiotics.

PMID:21717108

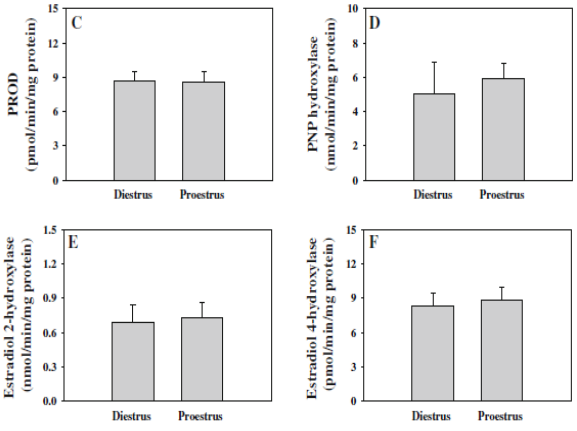

Keywords : Cytochrome P450; Drug-metabolizing enzyme; Estradiol; Estrous cycle; Liver; Ovary

Article 194

Bacterial genome mapper: A comparative bacterial genome mapping tool

Bioinformation. 8(11):532-4.

Lee KS, Kim RN, Yoon BH, Kim DS, Choi SH, Kim DW, Nam SH, Kim A, Kang A, Park KH, Jung JE, Chae SH, Park HS*

*Corresponding: hspark@kribb.re.kr
Human Derived Material Center

Recently, next generation sequencing (NGS) technologies have led to a revolutionary increase in sequencing speed and costefficacy. Consequently, a vast number of contigs from many recently sequenced bacterial genomes remain to be accurately mapped and annotated, requiring the development of more convenient bioinformatics programs. In this paper, we present a newly developed web-based bioinformatics program, Bacterial Genome Mapper, which is suitable for mapping and annotating contigs that have been assembled from bacterial genome sequence raw data. By constructing a multiple alignment map between target contig sequences and two reference bacterial genome sequences, this program also provides very useful comparative genomics analysis of draft bacterial genomes. AVAILABILITY: The database is available for free at http://mbgm.kribb.re.kr.

PMID: 22829725

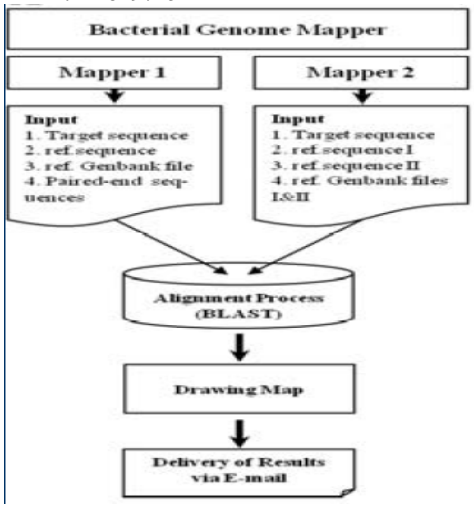

Keywords : Bacterial genome; Bioinformatics program; Contig mapping program; Contig sequence; Genomics analysis

Article 195

easySEARCH: A user-friendly bioinformatics program that enables BLAST searching with a massive number of query sequences

Bioinformation. 8(16):792-4.

Kim DW, Kim RN, Kim DS, Choi SH, Chae SH, Park HS*

*Corresponding: hspark@kribb.re.kr
Human Derived Material Center

Many biologists are familiar with BLAST (Basic Local Alignment Search Tool). A major difficulty with BLAST is searching a massive number of queries without depending on professional help with scripting languages. Hence, we describe the development of an interface for BLAST to perform sequence search for a set of query sequences at one instance. This software interface runs on all Windows-based personal computers (PCs) and can be widely used by biologists who are not familiar with professional informatics command languages and yet want to perform massive sequence analysis. easySEARCH is freely available as a standalone program. AVAILABILITY: http://210.219.44.213/easysearch_down.html.

PMID: 23055632

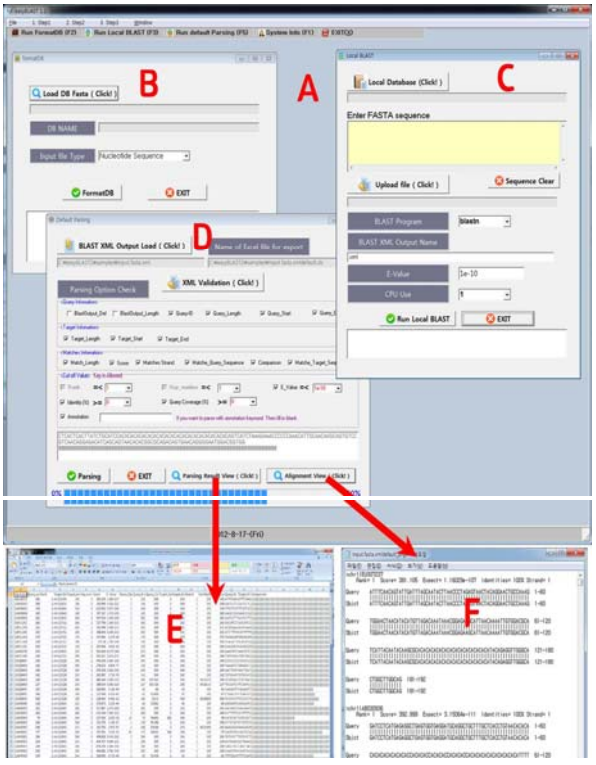

Keywords : Bioinformatics program; BLAST search; easySEARCH; Massive sequence analysis

Article 196

Two-year field study shows little evidence that PPO-transgenic rice affects the structure of soil microbial communities

Biol Fertil Soil. 48(4):453-61.

Chun YJ, Kim HJ, Park KW, Jeong SC, Lee B, Back K, Kim HM, Kim CG*

*Corresponding: cgkim@kribb.re.kr
Bio-Evaluation Center

There is global concern about the environmental consequences associated with transgenic crops. Their effects on the soil ecosystem are of special interest when assessing ecological safety and integrity. Although many efforts have been made to develop crops genetically modified to have resistance to protoporphyrin oxidase (PPO)-inhibiting herbicides, little is known about their influence on soil microbial communities. We conducted a 2-year field study and an analysis via terminal restriction fragment length polymorphism (T-RFLP) to assess the impacts of PPO-transgenic rice on bacterial and fungal communities. In the first year we sampled the rhizosphere and surrounding bulk soil, while in the second year we sampled rhizosphere soil only. No differences were observed in the diversity indices and community composition of microbial communities between transgenic rice and its parental non-transgenic counterpart (cultivar Dongjin). Instead, community variation was strongly dependent on growth stage and year. Therefore, we observed no adverse effects by these crops of modified rice on the microbial community composition in paddy soils.

Source	DF	Richness	Evenness	Shannon's	Simpson's
Bacteria					
Year	1	10.54**	53.90***	21.09***	24.46***
Stage (year)	6	6.40***	11.29***	8.67***	8.33***
Genotype	1	0.29	2.07	0.02	0.17
Genotype×year	1	0.29	2.00	0.37	0.24
Genotype×stage (year)	6	1.55	0.81	1.76	1.42
Fungi					
Year	1	0.74	34.59***	12.59***	25.39***
Stage (year)	6	5.54***	7.34***	7.20***	6.18***
Genotype	1	0.02	0.03	0.06	0.14
Genotype×year	1	0.84	0.13	0.20	0.00
Genotype×stage (year)	6	1.42	1.91	2.01	2.39

Keywords : Genetically modified organism; Growth rate; Protoporphyrin oxidase; Rice; Soil microbial community; T-RFLP; Transgenic crop

Article 197

Induction of autophagy promotes preattachment development of bovine embryos by reducing endoplasmic reticulum stress

Biol Reprod. 87(1):8, 1-11.

Song BS, Yoon SB, Kim JS, Sim BW, Kim YH, Cha JJ, Choi SA, Min HK, Lee Y, Huh JW, Lee SR, Kim SH, Koo DB, Choo YK, Kim HM, Kim SU*, Chang KT*

*Co-corresponding: sunuk@kribb.re.kr changkt@kribb.re.kr
Korea National Primate Research Center

The coupling of autophagy and endoplasmic reticulum (ER) stress has been implicated in a variety of biological processes; however, little is known regarding the involvement of the autophagy/ER stress pathway in early embryogenesis or the underlying mechanism(s). Here, we showed that the developmental competence of in vitro-produced (IVP) bovine embryos was highly dependent on the autophagy/ER stress balance. Although relative abundances of autophagy-associated gene transcripts, including *LC3, Atg5*, and *Atg7* transcripts, were high in oocytes and throughout the early stages of preattachment development, extensive autophagosome formation was only detected in fertilized embryos. Using an inducer and inhibitor of autophagy, we showed that transient elevation of autophagic activity during early preattachment development greatly increased the blastocyst development rate, trophectoderm cell numbers, and blastomere survival; these same parameters were reduced by both inhibition and prolonged induction of autophagy. Interestingly, the induction of autophagy reduced ER stress and associated damage, while the developmental defects in autophagy-inhibited embryos were significantly alleviated by ER stress inhibitor treatment, indicating that autophagy is a negative regulator of ER stress in early embryos. Collectively, these results suggest that early embryogenesis of IVP bovine embryos depends on an appropriate balance between autophagy and ER stress. These findings may increase our understanding of important early developmental events by providing compelling evidence concerning the tight association between autophagy and ER stress, and may contribute to the development of strategies for the production of IVP bovine blastocysts with high developmental competence.
PMID:22539678

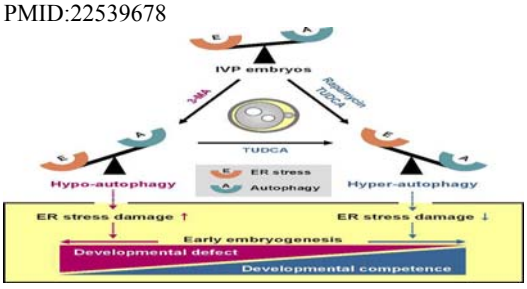

Keywords : Apoptosis; Autophagy; Early development; Embryo culture; Endoplasmic reticulum stress

Article 198

Differential in-gel electrophoresis (DIGE) analysis of CHO cells under hyperosmotic pressure: osmoprotective effect of glycine betaine addition

Biotechnol Bioeng. 109(6):1395-403.

Kim JY, Kim YG*, Lee GM

*Co-first: ygkim@kribb.re.kr
Biotechnology Process Engineering Center

The use of glycine betaine combined with hyperosmolality is known to be an efficient means for achieving high protein production in recombinant Chinese hamster ovary (rCHO) cells. In order to understand the intracellular events and identify the key factors in rCHO cells cultivated with glycine betaine under hyperosmotic conditions, two-dimensional differential in-gel electrophoresis (2D-DIGE) followed by mass spectrometric analysis was applied. Differentially expressed 19 protein spots were selected and 16 different kinds of proteins were successfully identified. The identified proteins were associated with cellular metabolism (PEPCK, GAPDH, and PK), cellular architecture (β-tubulin and β -actin), protein folding (GRP78 and OSP94), mRNA processing (Rbm34, ACF, and IPMK), and protein secretion (γ-COP). 2D-Western blot analysis of β-tubulin, GAPDH, Peroxidoxin-1, and GRP78 confirmed the proteomic findings. The proteins identified from this study, which are related to cell growth and antibody production, can be applied to cell engineering for maximizing the efficacy of the use of glycine betaine combined with hyperosmolality in rCHO cells.

PMID:22252946

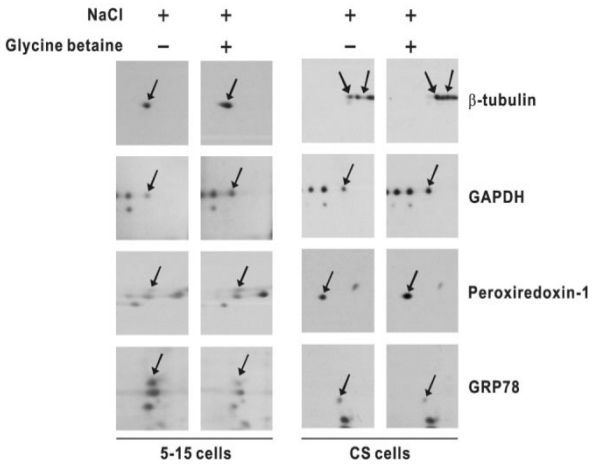

Keywords : DIGE; Glycine betaine; Hyperosmolality; Osmoprotective effect; Proteomics; rCHO cells

Article 199

New cell line development for antibody-producing Chinese hamster ovary cells using split green fluorescent protein

BMC Biotechnol. 12:24.

Kim YG, Park B, Ahn JO, Jung JK, Lee HW, Lee EG*

*Corresponding: eglee@kribb.re.kr
Biotechnology Process Engineering Center

BACKGROUND: The establishment of high producer is an important issue in Chinese hamster ovary (CHO) cell culture considering increased heterogeneity by the random integration of a transfected foreign gene and the altered position of the integrated gene. Fluorescence-activated cell sorting (FACS)-based cell line development is an efficient strategy for the selection of CHO cells in high therapeutic protein production.
RESULTS: An internal ribosome entry site (IRES) was introduced for using two green fluorescence protein (GFP) fragments as a reporter to both antibody chains, the heavy chain and the light chain. The cells co-transfected with two GFP fragments showed the emission of green fluorescence by the reconstitution of split GFP. The FACS-sorted pool with GFP expression had a higher specific antibody productivity (q_{Ab}) than that of the unsorted pool. The q_{Ab} was highly correlated with the fluorescence intensity with a high correlation coefficient, evidenced from the analysis of median GFP and q_{Ab} in individual selected clones.
CONCLUSIONS: This study proved that the fragment complementation for split GFP could be an efficient indication for antibody production on the basis of high correlation of q_{Ab} with reconstitution of GFP. Taken together, we developed an efficient FACS-based screening method for high antibody-producing CHO cells with the benefits of the split GFP system.

PMID: 22587529

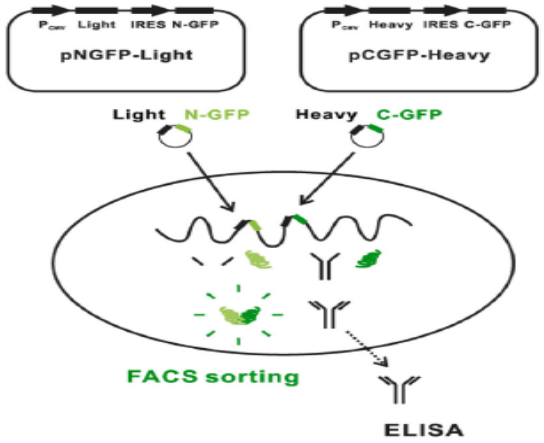

Keywords : Antibody production; Cell line development; CHO cells; FACS; Split GFP

Article 200

The evolutionary history of protein fold families and proteomes confirms that the archaeal ancestor is more ancient than the ancestors of other superkingdoms

BMC Evol Biol. 12:13.

Kim KM*, Caetano-Anollés G

*First: kmkim@kribb.re.kr
Microbial Resource Center

BACKGROUND: The entire evolutionary history of life can be studied using myriad sequences generated by genomic research. This includes the appearance of the first cells and of superkingdoms Archaea, Bacteria, and Eukarya. However, the use of molecular sequence information for deep phylogenetic analyses is limited by mutational saturation, differential evolutionary rates, lack of sequence site independence, and other biological and technical constraints. In contrast, protein structures are evolutionary modules that are highly conserved and diverse enough to enable deep historical exploration.
RESULTS: Here we build phylogenies that describe the evolution of proteins and proteomes. These phylogenetic trees are derived from a genomic census of protein domains defined at the fold family (FF) level of structural classification. Phylogenomic trees of FF structures were reconstructed from genomic abundance levels of 2,397 FFs in 420 proteomes of free-living organisms. These trees defined timelines of domain appearance, with time spanning from the origin of proteins to the present. Timelines are divided into five different evolutionary phases according to patterns of sharing of FFs among superkingdoms: (1) a primordial protein world, (2) reductive evolution and the rise of Archaea, (3) the rise of Bacteria from the common ancestor of Bacteria and Eukarya and early development of the three superkingdoms, (4) the rise of Eukarya and widespread organismal diversification, and (5) eukaryal diversification. The relative ancestry of the FFs shows that reductive evolution by domain loss is dominant in the first three phases and is responsible for both the diversification of life from a universal cellular ancestor and the appearance of superkingdoms. On the other hand, domain gains are predominant in the last two phases and are responsible for organismal diversification, especially in Bacteria and Eukarya.
CONCLUSIONS: The evolution of functions that are associated with corresponding FFs along the timeline reveals that primordial metabolic domains evolved earlier than informational domains involved in translation and transcription, supporting the metabolism-first hypothesis rather than the RNA world scenario. In addition, phylogenomic trees of proteomes reconstructed from FFs appearing in each of the five phases of the protein world show that trees reconstructed from ancient domain structures were consistently rooted in archaeal lineages, supporting the proposal that the archaeal ancestor is more ancient than the ancestors of other superkingdoms.
PMID:22284070

Keywords : Archaeal ancestor; Metabolic domains; Phylogenomic analysis; Protein fold families

Article 201

Large-scale transcriptome sequencing and gene analyses in the crab-eating macaque (*Macaca fascicularis*) for biomedical research

BMC Genomics. 13:163.

Huh JW, Kim YH, Park SJ, Kim DS, Lee SR, Kim KM, Jeong KJ, Kim JS, Song BS, Sim BW, Kim SU, Kim SH, Chang KT*

*Corresponding: changkt@kribb.re.kr
Korea National Primate Research Center

BACKGROUND: As a human replacement, the crab-eating macaque (*Macaca fascicularis*) is an invaluable non-human primate model for biomedical research, but the lack of genetic information on this primate has represented a significant obstacle for its broader use.
RESULTS: Here, we sequenced the transcriptome of 16 tissues originated from two individuals of crab-eating macaque (male and female), and identified genes to resolve the main obstacles for understanding the biological response of the crab-eating macaque. From 4 million reads with 1.4 billion base sequences, 31,786 isotigs containing genes similar to those of humans, 12,672 novel isotigs, and 348,160 singletons were identified using the GS FLX sequencing method. Approximately 86% of human genes were represented among the genes sequenced in this study. Additionally, 175 tissue-specific transcripts were identified, 81 of which were experimentally validated. In total, 4,314 alternative splicing (AS) events were identified and analyzed. Intriguingly, 10.4% of AS events were associated with transposable element (TE) insertions. Finally, investigation of TE exonization events and evolutionary analysis were conducted, revealing interesting phenomena of human-specific amplified trends in TE exonization events.
CONCLUSIONS: This report represents the first large-scale transcriptome sequencing and genetic analyses of *M. fascicularis* and could contribute to its utility for biomedical research and basic biology.
PMID:22554259

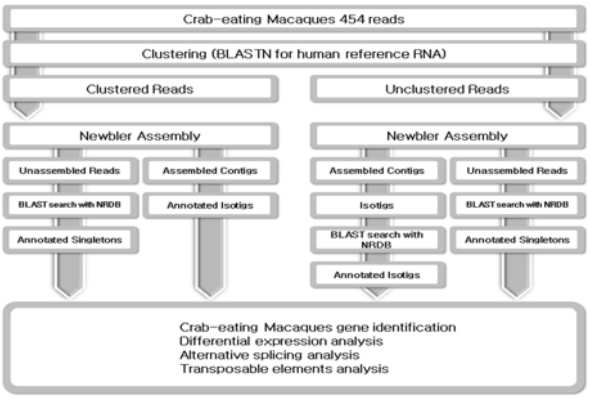

Keywords : Biomedical research; Crab-eating macaque; Genetic analyses; Transcriptome sequencing

Article 202

SpiroESTdb: a transcriptome database and online tool for sparganum expressed sequences tags

BMC Res Notes. 5:130.

Kim DW, Kim DW, Yoo WG, Nam SH, Lee MR, Yang HW, Park J, Lee K, Lee S, Cho SH, Lee WJ, Park HS*, Ju JW

*Co-corresponding: hspark@kribb.re.kr
Human Derived Material Center

BACKGROUND: Sparganum (plerocercoid of Spirometra erinacei) is a parasite that possesses the remarkable ability to survive by successfully modifying its physiology and morphology to suit various hosts and can be found in various tissues, even the nervous system. However, surprisingly little is known about the molecular function of genes that are expressed during the course of the parasite life cycle. To begin to decipher the molecular processes underlying gene function, we constructed a database of expressed sequence tags (ESTs) generated from sparganum.
FINDINGS: SpiroESTdb is a web-based information resource that is built upon the annotation and curation of 5,655 ESTs data. SpiroESTdb provides an integrated platform for expressed sequence data, expression dynamics, functional genes, genetic markers including single nucleotide polymorphisms and tandem repeats, gene ontology and KEGG pathway information. Moreover, SpiroESTdb supports easy access to gene pages, such as (i) curation and query forms, (ii) *in silico* expression profiling and (iii) BLAST search tools. Comprehensive descriptions of the sparganum content of all sequenced data are available, including summary reports. The contents of SpiroESTdb can be viewed and downloaded from the web (http://pathod.cdc.go.kr/spiroestdb).
CONCLUSIONS: This integrative web-based database of sequence data, functional annotations and expression profiling data will serve as a useful tool to help understand and expand the characterization of parasitic infections. It can also be used to identify potential industrial drug targets and vaccine candidate genes.
PMID:22397686

Keywords : Expressed sequence tags (ESTs); Database; Plerocercoid; *Spirometra erinacei*

Article 203

The dorsal striatum expressing adenylyl cyclase-5 controls behavioral sensitivity of the righting reflex to high-dose ethanol

Brain Res. 1489:27-36.

Kim KS*, Kim H, Park SK, Han PL

*First: kskim@kribb.re.kr
Laboratory Animal Resource Center

High-dose ethanol inflicts sedation and loss of righting reflex (LORR). Recently, it was reported that AC5 knockout ($AC5^{-/-}$) mice consumed more ethanol and showed reduced sensitivity to high-dose ethanol compared to wild-type mice. As an extension of the previous study, in the present study we examined the signaling mechanism regulating altered behavioral sensitivity of LORR in $AC5^{-/-}$ mice. $AC5^{-/-}$ mice had enhanced phosphorylation of the NR2B subunit of NMDA receptors in the dorsal striatum and a partial reduction of MK801 (NMDA receptor antagonist)/ethanol-induced LORR. $AC5^{-/-}$ mice showed increased levels of phospho-CaMKIIα, phospho-CREB, and BDNF in the dorsal striatum. $CaMKII\alpha5^{+/-}$ or $BDNF5^{+/-}$ mice displayed enhanced LORR, a behavioral phenotype opposite to that displayed by $AC5^{-/-}$ mice. Consistently with these results, stereotaxic infusion of KN62 (CaMKII inhibitor), siRNA-CaMKIIα, or siRNA-BDNF, within the dorsal striatum was sufficient to prolong LORR. These results suggest that neural mechanism is important for regulating behavioral sensitivity of LORR and that the signaling pathway(s) interplayed by AC5, CaMKIIα and BDNF within the dorsal striatum is important for regulating the duration of ethanol-induced LORR.
PMID: 23063718

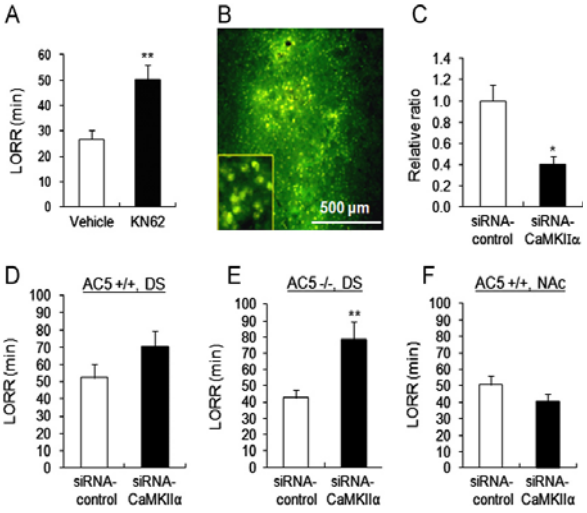

Keywords : Adenylylcyclasetype5; BDNF; Dorsal striatum; LORR; Signaling pathway

Article 204

Hepatic expression of cytochrome P450 in type 2 diabetic Goto-Kakizaki rats

Chem Biol Interact. 195(3):173-9.

Oh SJ*, Choi JM, Yun KU, Oh JM, Kwak HC, Oh JG, Lee KS, Kim BH, Heo TH, Kim SK

*First: diatree@kribb.re.kr
Bio-Evaluation Center

Although hepatic expression of cytochrome P450 (CYP) changes markedly in diabetes, the role of ketone bodies in the regulation of CYP in diabetes is controversial. The present study was performed to determine the expression and activity of CYP in non-obese type II diabetic Goto-Kakizaki (GK) rats with normal levels of ketone bodies. In the present study, basal serum glucose levels increased 1.95-fold in GK rats, but acetoacetate and β-hydroxybutyrate levels were not significantly different. Hepatic expression of CYP reductase and CYP3A2 was up-regulated in the GK rats, and consequently, activities of CYP reductase and midazolam 4-hydroxylase, mainly catalyzed by CYP3A2, increased. In contrast, hepatic expression of CYP1A2 and CYP3A1 was down-regulated and the activities of 7-ethoxyresorufin-*O*-deethylase and 7-methoxyresorufin-*O*-demethylase, mainly catalyzed by CYP1A, also decreased in GK rats. Hepatic levels of microsomal protein and total CYP and hepatic expression of cytochrome b_5, CYP1B1, CYP2B1 and CYP2C11 were not significantly different between the GK rats and normal Wistar rats. Moreover, the expression and activity of CYP2E1, reported to be up-regulated in diabetes with hyperketonemia, were not significantly different between GK rats and control rats, suggesting that elevation of ketone bodies plays a critical role in the up-regulation of hepatic CYP2E1 in diabetic rats. Our results showed that the expression of hepatic CYP is regulated in an isoform-specific manner. The present results also show that the GK rat is a useful animal model for the pathophysiological study of non-obese type II diabetes with normal ketone body levels.
PMID:22244987

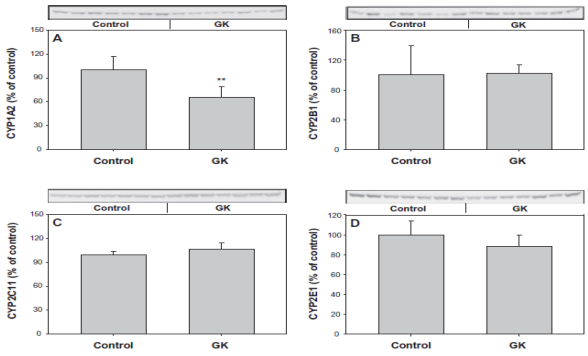

Keywords : Cytochrome P450; Diabetes; GK rat; Hepatic metabolism; Ketone body

Article 205

Intron Retention and TE Exonization Events in *ZRANB2*

Comp Funct Genomics. 2012:170208.

Park SJ, Huh JW, Kim YH, Kim HS, Chang KT*

*Corresponding: changkt@kribb.re.kr
Korea National Primate Research Center

The Zinc finger, RAN-binding domain-containing protein 2 (*ZRANB2*), contains arginine/serine-rich (RS) domains that mediate its function in the regulation of alternative splicing. The *ZRANB2* gene contains 2 LINE elements (L3b, Plat_L3) between the 9th and 10th exons. We identified the exonization event of a LINE element (Plat_L3). Using genomic PCR, RT-PCR amplification, and sequencing of primate DNA and RNA samples, we analyzed the evolutionary features of *ZRANB2* transcripts. The results indicated that 2 of the LINE elements were integrated in human and all of the tested primate samples (hominoids: 3 species; Old World monkey: 8 species; New World monkey: 6 species; prosimian: 1 species). Human, rhesus monkey, crab-eating monkey, African-green monkey, and marmoset harbor the exon derived from LINE element (Plat_L3). RT-PCR amplification revealed the long transcripts and their differential expression patterns. Intriguingly, these long transcripts were abundantly expressed in Old World monkey lineages (rhesus, crab-eating, and African-green monkeys) and were expressed via intron retention (IR). Thus, the *ZRANB2* gene produces 3 transcript variants in which the Cterminus varies by transposable elements (TEs) exonization and IR mechanisms. Therefore, *ZRANB2* is valuable for investigating the evolutionary mechanisms of TE exonization and IR during primate evolution.
PMID:22778693

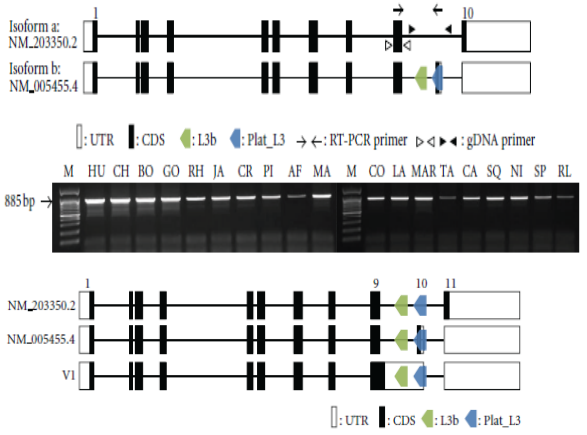

Keywords : Evolutionary mechanisms; Expression pattern; Transcript variants; Zinc finger

Article 206

Metformin inhibits growth hormone-mediated hepatic *PDK4* gene expression through induction of orphan nuclear receptor small heterodimer partner

Diabetes. 61(10):2484-94.

Kim YD, Kim YH, Tadi S, Yu JH, Yim YH, Jeoung NH, Shong M, Hennighausen L, Harris RA, Lee IK, Lee CH*, Choi HS

*Co-corresponding: chullee@kribb.re.kr
Laboratory Animal Resource Center

Growth hormone (GH) is a counter-regulatory hormone that plays an important role in preventing hypoglycemia during fasting. Because inhibition of the pyruvate dehydrogenase complex (PDC) by pyruvate dehydrogenase kinase 4 (PDK4) conserves substrates for gluconeogenesis, we tested whether GH increases PDK4 expression in liver by a signaling pathway sensitive to inhibition by metformin. The effects of GH and metformin were determined in the liver of wild-type, small heterodimer partner (SHP)-, PDK4-, and signal transducer and activator of transcription 5 (STAT5)-null mice. Administration of GH *in vivo* increased PDK4 expression via a pathway dependent on STAT5 phosphorylation. Metformin inhibited the induction of PDK4 expression by GH via a pathway dependent on AMP-activated protein kinase (AMPK) and SHP induction. The increase in PDK4 expression and PDC phosphorylation by GH was reduced in STAT5-null mice. Metformin decreased GH-mediated induction of PDK4 expression and metabolites in wild-type but not in SHP-null mice. In primary hepatocytes, dominant-negative mutant-AMPK and SHP knockdown prevented the inhibitory effect of metformin on GH-stimulated PDK4 expression. SHP directly inhibited STAT5 association on the *PDK4* gene promoter. Metformin inhibits GH-induced PDK4 expression and metabolites via an AMPK-SHP-dependent pathway. The metformin-AMPK-SHP network may provide a novel therapeutic approach for the treatment of hepatic metabolic disorders induced by the GH-mediated pathway.

PMID:22698918

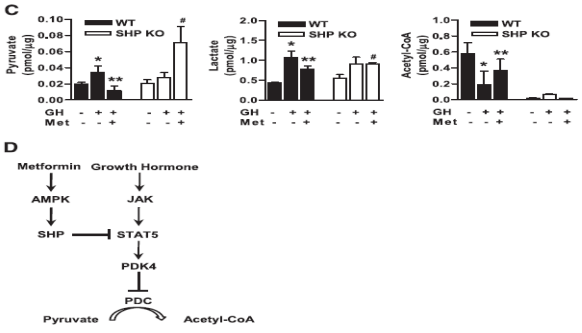

Keywords : GH-mediated pathway; Growth hormone; Hepatic metabolic disorders; PDK4 expression

Article 207

Metformin ameliorates IL-6-induced hepatic insulin resistance via induction of orphan nuclear receptor small heterodimer partner (SHP) in mouse models

Diabetologia. 55(5):1482-94.

Kim YD, Kim YH, Cho YM, Kim DK, Ahn SW, Lee JM, Chanda D, Shong M, Lee CH*, Choi HS

*Co-corresponding: chullee@kribb.re.kr
Laboratory Animal Resource Center

AIMS/HYPOTHESIS: IL-6 is a proinflammatory cytokine associated with the pathogenesis of hepatic diseases. Metformin is an anti-diabetic drug used for the treatment of type 2 diabetes, and orphan nuclear receptor small heterodimer partner (SHP, also known as NR0B2), a transcriptional co-repressor, plays an important role in maintaining metabolic homeostasis. Here, we demonstrate that metformin-mediated activation of AMP-activated protein kinase (AMPK) increases SHP protein production and regulates IL-6-induced hepatic insulin resistance.
METHODS: We investigated metformin-mediated SHP production improved insulin resistance through the regulation of an IL-6-dependent pathway (involving signal transducer and activator of transcription 3 [STAT3] and suppressor of cytokine signalling 3 [SOCS3]) in both Shp knockdown and Shp null mice.
RESULTS: IL-6-induced STAT3 transactivation and SOCS3 production were significantly repressed by metformin, adenoviral constitutively active AMPK (Ad-CA-AMPK), and adenoviral SHP (Ad-SHP), but not in Shp knockdown, or with the adenoviral dominant negative form of AMPK (Ad-DN-AMPK). Chromatin immunoprecipitation (ChIP), co-immunoprecipitation (Co-IP) and protein localisation studies showed that SHP inhibits DNA binding of STAT3 on the Socs3 gene promoter via interaction and colocalisation within the nucleus. Upregulation of inflammatory genes and downregulation of hepatic insulin signalling by acute IL-6 treatment were observed in wild-type mice but not in Shp null mice. Finally, chronic IL-6 exposure caused hepatic insulin resistance, leading to impaired insulin tolerance and elevated gluconeogenesis, and these phenomena were aggravated in Shp null mice.
CONCLUSIONS/INTERPRETATION: Our results demonstrate that SHP upregulation by metformin may prevent hepatic disorders by regulating the IL-6-dependent pathway, and that this pathway can help to ameliorate the pathogenesis of cytokine-mediated metabolic dysfunction.

PMID:22349108

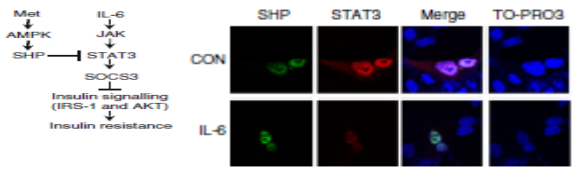

Keywords : AMP-activated protein kinase; Insulin resistance; Insulin sensitivity; Interleukin-6; Metformin; Nr0b2; Shp; Small heterodimer partne

Article 208

Genome analysis of the domestic dog (Korean Jindo) by massively parallel sequencing

DNA Res. 19(3):275-87.

Kim RN, Kim DS, Choi SH, Yoon BH, Kang A, Nam SH, Kim DW, Kim JJ, Ha JH, Toyoda A, Fujiyama A, Kim A, Kim MY, Park KH, Lee KS, Park HS*

*Corresponding: hspark@kribb.re.kr
Human Derived Material Center

Although pioneering sequencing projects have shed light on the boxer and poodle genomes, a number of challenges need to be met before the sequencing and annotation of the dog genome can be considered complete. Here, we present the DNA sequence of the Jindo dog genome, sequenced to 45-fold average coverage using Illumina massively parallel sequencing technology. A comparison of the sequence to the reference boxer genome led to the identification of 4 675 437 single nucleotide polymorphisms (SNPs, including 3 346 058 novel SNPs), 71 642 indels and 8131 structural variations. Of these, 339 non-synonymous SNPs and 3 indels are located within coding sequences (CDS). In particular, 3 non-synonymous SNPs and a 26-bp deletion occur in the *TCOF1* locus, implying that the difference observed in cranial facial morphology between Jindo and boxer dogs might be influenced by those variations. Through the annotation of the Jindo olfactory receptor gene family, we found 2 unique olfactory receptor genes and 236 olfactory receptor genes harbouring non-synonymous homozygous SNPs that are likely to affect smelling capability. In addition, we determined the DNA sequence of the Jindo dog mitochondrial genome and identified Jindo dog-specific mtDNA genotypes. This Jindo genome data upgrade our understanding of dog genomic architecture and will be a very valuable resource for investigating not only dog genetics and genomics but also human and dog disease genetics and comparative genomics.

PMID: 22474061

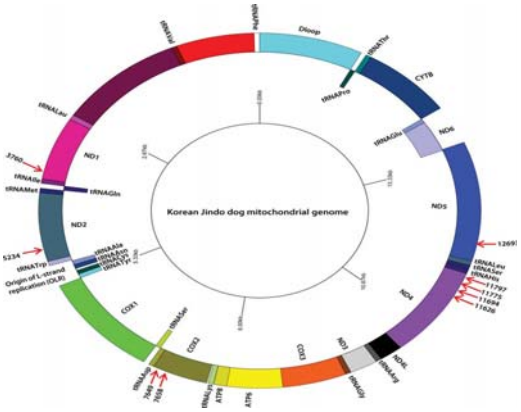

Keywords : DNA sequence; Genome sequencing; Jindo dog; Massively parallel sequencing

Article 209

Repeated short-term (2h×14d) emotional stress induces lasting depression-like behavior in mice

Exp Neurobiol. 21(1):16-22.

Kim KS*, Kwon HJ, Baek IS, Han PL

*First: kskim@kribb.re.kr
Laboratory Animal Resource Center

Chronic behavioral stress is a risk factor for depression. To understand chronic stress effects and the mechanism underlying stress-induced emotional changes, various animals model have been developed. We recently reported that mice treated with restraints for 2 h daily for 14 consecutive days (2h-14d or 2h×14d) show lasting depression-like behavior. Restraint provokes emotional stress in the body, but the nature of stress induced by restraints is presumably more complex than emotional stress. So a question remains unsolved whether a similar procedure with "emotional" stress is sufficient to cause depression-like behavior. To address this, we examined whether "emotional" constraints in mice treated for 2h×14d by enforcing them to individually stand on a small stepping platform placed in a water bucket with a quarter full of water, and the stress evoked by this procedure was termed "water-bucket stress". The water-bucket stress activated the hypothalamus-pituitary-adrenal gland (HPA) system in a manner similar to restraint as evidenced by elevation of serum glucocorticoids. After the 2h×14d water-bucket stress, mice showed behavioral changes that were attributed to depression-like behavior, which was stably detected >3 weeks after last water-bucket stress endorsement. Administration of the anti-depressant, imipramine, for 20 days from time after the last emotional constraint completely reversed the stress-induced depression-like behavior. These results suggest that emotional stress evokes for 2h×14d in mice stably induces depression-like behavior in mice, as does the 2h×14d restraint.

PMID: 22438675

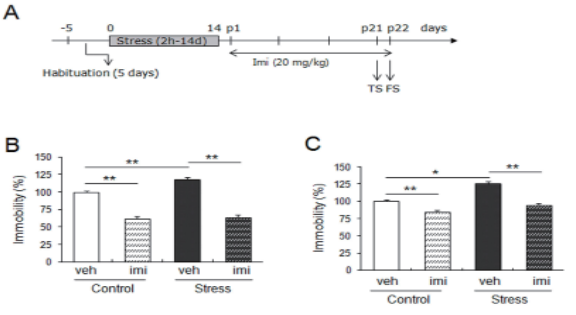

Keywords : Anxiety; Behavior; Chronic behavioral stress; Depression; Emotional stress; Mice

Article 210

Evaluation of hepatotoxicity and oxidative stress in rats treated with *tert*-butyl hydroperoxide

Food Chem Toxicol. 50(5):1215-21.

Oh JM, Jung YS, Jeon BS, Yoon BI, Lee KS, Kim BH, Oh SJ*, Kim SK

*Co-corresponding: diatree@kribb.re.kr
Bio-Evaluation Center

Although *tert*-butyl hydroperoxide (*t*-BHP) is commonly used to induce oxidative stress, little is known about the time- or dose-dependence of its oxidative effects. In this study, we examined hepatotoxicity and oxidative stress in male rats at various times (0-24 h) after *t*-BHP (0, 0.2, 0.5, 1 or 3 mmol/kg, ip) treatment. Serum hepatotoxicity parameters were increased from 2 h following 1 mmol/kg *t*-BHP and reached their maximum values at 8 h. Plasma malondialdehyde levels were maximally elevated by 62% at 0.5 h and returned to control levels by 4 h. Hepatic glutathione levels were decreased between 0.5 and 2 h, and hepatic glutathione disulfide levels were increased at 2h. Interestingly, hepatic glutathione levels were increased at 24 h, which may be attributed to up-regulation of glutathione synthesis through induction of gamma-glutamylcysteine ligase expression. The elevation of hepatotoxic parameters and plasma MDA was observed from 0.5 to 1 mmol/kg *t*-BHP, respectively, in a dose-dependent manner. Considering that the maximal dose resulted in 20% lethality, 1 mmol/kg of *t*-BHP may be suitable for evaluating antioxidant activity of tested compounds. Our results provide essential information to characterize the *t*-BHP-induced oxidative stress and hepatotoxicity.

PMID:22326806

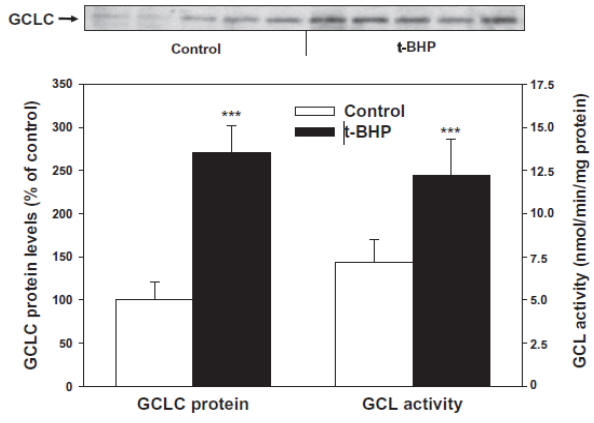

Keywords : Antioxidant activity; GSH; Hepatotoxicity; Oxidative stress; t-BHP

Article 211

Prevention of salt-induced renal injury by activation of NAD(P)H:quinone oxidoreductase 1, associated with NADPH oxidase

Free Radic Biol Med. 52(5):880-8.

Kim YH, Hwang JH, Noh JR, Gang GT, Tadi S, Yim YH, Jeoung NH, Kwak TH, Lee SH, Kweon GR, Kim JM, Shong M, Lee IK, Lee CH*

*Corresponding: chullee@kribb.re.kr
Laboratory Animal Resource Center

NADPH oxidase (NOX) is a predominant source of reactive oxygen species (ROS), and the activity of NOX, which uses NADPH as a common rate-limiting substrate, is upregulated by prolonged dietary salt intake. β-Lapachone (βL), a well-known substrate of NAD(P)H:quinone oxidoreductase 1 (NQO1), decreases the cellular NAD(P)H/NAD(P)$^+$ ratio via activation of NQO1. In this study, we evaluated whether NQO1 activation by βL modulates salt-induced renal injury associated with NOX-derived ROS regulation in an animal model. Dahl salt-sensitive (DS) rats fed a high-salt (HS) diet were used to investigate the renoprotective effect of NQO1 activation. βL treatment significantly lowered the cellular NAD(P)H:NAD(P)$^+$ ratio and dramatically reduced NOX activity in the kidneys of HS diet-fed DS rats. In accordance with this, total ROS production and expression of oxidative adducts also decreased in the βL-treated group. Furthermore, HS diet-induced proteinuria and glomerular damage were markedly suppressed, and inflammation, fibrosis, and apoptotic cell death were significantly diminished by βL treatment. This study is the first to demonstrate that activation of NQO1 has a renoprotective effect that is mediated by NOX activity via modulation of the cellular NAD(P)H:NAD(P)$^+$ ratio. These results provide strong evidence that NQO1 might be a new therapeutic target for the prevention of salt-induced renal injury.

PMID: 22227174

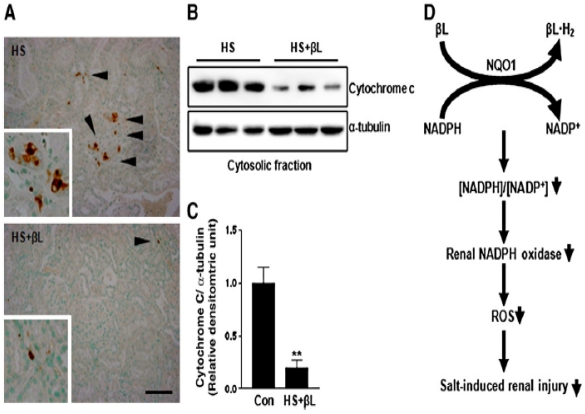

Keywords : β-Lapachone; Free radicals; High-salt; NADPH oxidase; NQO1; Reactive oxygen species

Article 212

Novel mechanism of conjoined gene formation in the human genome

Funct Integr Genomics. 12(1):45-61.

Kim RN, Kim A, Choi SH, Kim DS, Nam SH, Kim DW, Kim DW, Kang A, Kim MY, Park KH, Yoon BH, Lee KS, Park HS*

*Corresponding: hspark@kribb.re.kr
Human Derived Material Center

Recently, conjoined genes (CGs) have emerged as important genetic factors necessary for understanding the human genome. However, their formation mechanism and precise structures have remained mysterious. Based on a detailed structural analysis of 57 human CG transcript variants (CGTVs, discovered in this study) and all (833) known CGs in the human genome, we discovered that the poly(A) signal site from the upstream parent gene region is completely removed via the skipping or truncation of the final exon; consequently, CG transcription is terminated at the poly(A) signal site of the downstream parent gene. This result led us to propose a novel mechanism of CG formation: the complete removal of the poly(A) signal site from the upstream parent gene is a prerequisite for the CG transcriptional machinery to continue transcribing uninterrupted into the intergenic region and downstream parent gene. The removal of the poly(A) signal sequence from the upstream gene region appears to be caused by a deletion or truncation mutation in the human genome rather than post-transcriptional trans-splicing events. With respect to the characteristics of CG sequence structures, we found that intergenic regions are hot spots for novel exon creation during CGTV formation and that exons farther from the intergenic regions are more highly conserved in the CGTVs. Interestingly, many novel exons newly created within the intergenic and intragenic regions originated from transposable element sequences. Additionally, the CGTVs showed tumor tissue-biased expression. In conclusion, our study provides novel insights into the CG formation mechanism and expands the present concepts of the genetic structural landscape, gene regulation, and gene formation mechanisms in the human genome.
PMID: 22231539

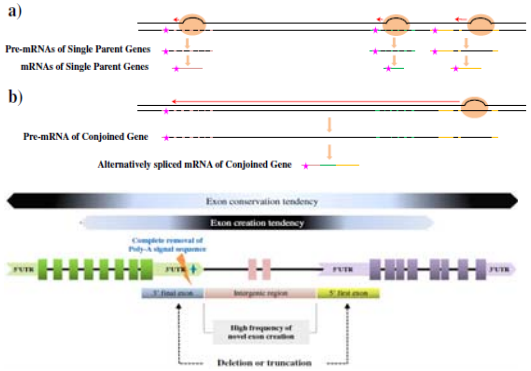

Keywords : CGTVs; Conjoined genes; Formation mechanism; Human genome; Precise structures

Article 213

UbC gene allele frequency in Korean population and novel *UbC* mosaic repeat unit formation

Genes Genom. 34(4):415-22.

Kim RN, Kang A, Choi SH, Kim DS, Kim DW, Nam SH, Kim A, Park KH, Yoon BH, Lee KS, Park HS*

*Corresponding: hspark@kribb.re.kr
Human Derived Material Center

The genomic structural organization of human *UbC* CDS repeat units could be representative of concerted evolution. The structure of the *UbC* gene and its repeat unit number frequency at scales of different human ethnic populations remain to be sufficiently determined. In this study, we performed comparative analysis of *UbC* CDS regions in genomes from 140 Korean individuals. We found that the *UbC* gene allele types 9, 8 and 7 are present in the Korean population in proportions of 97.1%, 0.4% and 2.5%, respectively. Interestingly, we discovered that the allele types 7 and 8 harbor the novel *UbC* gene mosaic repeat units 3^5 (combined between sequence parts derived from standard repeat units 3 and 5) and 8^9 (combined between sequence parts derived from standard repeat units 8 and 9) within their sequence structures, respectively. Our analysis showed that the novel mosaic repeat unit 3^5 lacks the highly human-specific amino acid S38, implying a functional consequence. These results suggest that the genomic organization of *UbC* repeat units is still undergoing dynamic structural changes due to concerted evolution through unequal crossing-over. Our results could represent valuable data for future investigations related to treating genetic diseases caused by *UbC* gene mutations and variations.

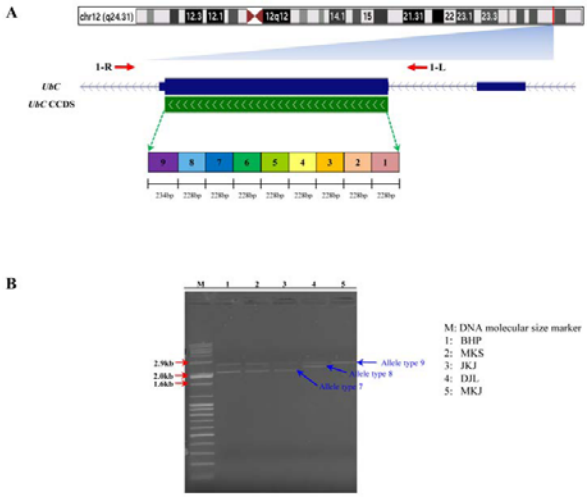

Keywords : Genomic DNA; Korean population; Novel *UbC* mosaic repeat unit; *UbC* gene allele frequency

Article 214

CACG: a database for comparative analysis of conjoined genes

Genomics. 100(1):14-7.

Kim DS, Kim DW, Kim MY, Nam SH, Choi SH, Kim RN, Kang A, Kim A, Park HS*

*Corresponding: hspark@kribb.re.kr
Human Derived Material Center

A conjoined gene is defined as one formed at the time of transcription by combining at least part of one exon from each of two or more distinct genes that lie on the same chromosome, in the same or opposite orientation, which translate independently into different proteins. We comparatively studied the extent of conjoined genes in thirteen genomes by analyzing the public databases of expressed sequence tags and mRNA sequences using a set of computational tools designed to identify conjoined genes on the same DNA strand or opposite DNA strands of the same genomic locus. The CACG database, available at http://cgc.kribb.re.kr/map/, includes a number of conjoined genes (7131-human, 2-chimpanzee, 5-orangutan, 57-chicken, 4-rhesus monkey, 651-cow, 27-dog, 2512-mouse, 263-rat, 1482-zebrafish, 5-horse, 29-sheep, and 8-medaka) and is very effective and easy to use to analyze the evolutionary process of conjoined genes when comparing different species.
PMID: 22584068

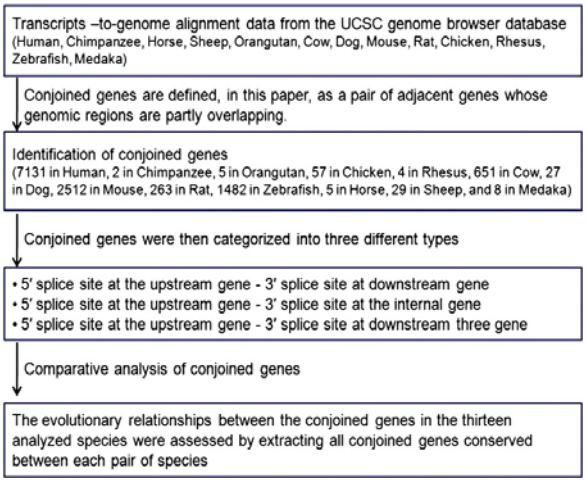

Keywords : Bioinformatics; CACG database; Comparative analysis; Conjoined gene; mRNA sequences; Sequence tags

Article 215

Vitamin D_3 upregulated protein 1 deficiency promotes *N*-methyl-*N*-nitrosourea and *Helicobacter pylori*-induced gastric carcinogenesis in mice

Gut. 61(1):53-63.

Kwon HJ, Won YS, Nam KT, Yoon YD, Jee H, Yoon WK, Nam KH, Kang JS, Han SU, Choi IP, Kim DY, Kim HC*

*Corresponding: hckim@kribb.re.kr
Laboratory Animal Resource Center

OBJECTIVE: Vitamin D_3 upregulated protein 1 (VDUP1) is a potent tumour suppressor whose expression is dramatically reduced in various types of human cancers, including gastric cancer. However, the precise mechanisms underlying tumour development remain unclear. In the present study, the authors examined the effect of VDUP1 on *Helicobacter pylori*-induced gastric carcinogenesis in mice.
DESIGN: Gastric cancer was generated in VDUP1 knockout (KO) and wild-type mice using a combination of *N*-methyl-*N*-nitrosourea treatment and *H pylori* infection. Fifty weeks after treatment, gastric tissues from both types of mice were examined by histopathology, immunohistochemistry and immunoblotting. *In vitro* tests on the human gastric cancer cell line, AGS, were also performed to identify the underlying mechanisms of cancer development.
RESULTS: The overall incidence of gastric cancer was significantly higher in VDUP1 KO mice than in wild-type mice. Similarly, VDUP1 KO mice showed more severe chronic gastritis, glandular atrophy, foveolar hyperplasia, metaplasia and dysplasia. Although no differences in the apoptotic index were apparent, lack of VDUP1 increased the rate of gastric epithelial cell proliferation in non-cancerous stomachs, with corresponding increases in tumour necrosis factor alpha (TNFα) level, nuclear transcription factor kappa B (NF-κB) activation and cyclooxygenase-2 (COX-2) expression. An *in vitro* study showed that *H pylori*-associated cell proliferation and induction of TNFα, NF-κB and COX-2 were inhibited in cells transfected with VDUP1. In addition, overexpression of VDUP1 in AGS cells suppressed TNFα-induced NF-κB activation and COX-2 expression.
CONCLUSION: Our data show that VDUP1 negatively regulates *H pylori*-associated gastric carcinogenesis, in part by disrupting cell growth and inhibiting the induction of TNFα, NF-κB and COX-2. These findings provide important insights into the role of VDUP1 in *H pylori*-associated tumourigenesis.
PMID:21917648

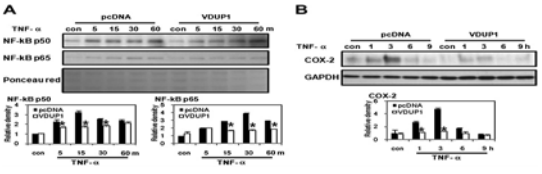

Keywords : Gastric carcinogenesis; Tumourigenesis; VDUP1

Article 216

Artemisinin inhibits lipopolysaccharide-induced interferon-β production in RAW 264.7 cells: implications on signal transducer and activator of transcription-1 signaling and nitric oxide production

Int Immunopharmacol. 14(4):580-4.

Park KH, Yoon YD, Han SB, Oh SJ, Yun J, Lee CW, Lee K, Park SK, Kim HM, Kang JS*

*Corresponding: kanjon@kribb.re.kr
Bio-Evaluation Center

Artemisinin is a well-known anti-malarial drug and has been shown to inhibit nitric oxide (NO) production. In this study, we investigated the effect of artemisinin on lipopolysaccharide (LPS)-induced production of IFN-β and characterized the potential relationship between artemisinin-mediated inhibition of IFN-β and NO production. Artemisinin suppressed IFN-β production and mRNA expression in a dose-dependent manner in LPS-stimulated RAW 264.7 cells. LPS-induced phosphorylation of signal transducer and activator of transcription-1 (STAT-1) was also inhibited by artemisinin treatment in RAW 264.7 cells. In addition, artemisinin suppressed LPS-induced production of NO in RAW 264.7 cells. Further study demonstrated that artemisinin-mediated inhibition of NO production and STAT-1 phosphorylation was reversed by addition of exogenous IFN-β. Moreover, artemisinin does not affect IFN-β-induced STAT-1 phosphorylation in RAW 264.7 cells. Collectively, these results suggest that the inhibition of IFN-β production by artemisinin and concomitant attenuation of STAT-1 activation might be involved in artemisinin-mediated inhibition of NO production in macrophages.

PMID:23041519

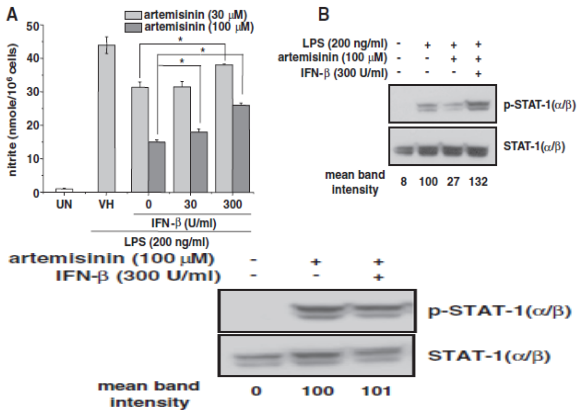

Keywords : Artemisinin; IFN-β; Nitric oxide; STAT-1

Article 217

Expression, immobilization and enzymatic properties of glutamate decarboxylase fused to a cellulose-binding domain

Int J Mol Sci. 13(1):358-68.

Park H, Ahn J, Lee J, Lee H, Kim C, Jung JK, Lee H, Lee EG*

*Corresponding: eglee@kribb.re.kr
Biotechnology Process Engineering Center

Escherichia coli-derived glutamate decarboxylase (GAD), an enzyme that catalyzes the conversion of glutamic acid to gamma-aminobutyric acid (GABA), was fused to the cellulose-binding domain (CBD) and a linker of *Trichoderma harzianum* endoglucanase II. To prevent proteolysis of the fusion protein, the native linker was replaced with a S_3N_{10} peptide known to be completely resistant to *E. coli* endopeptidase. The CBD-GAD expressed in *E. coli* was successfully immobilized on Avicel, a crystalline cellulose, with binding capacity of 33 ± 2 $nmol_{CBD\text{-}GAD}/g_{Avicel}$ and the immobilized enzymes retained 60% of their initial activities after 10 uses. The results of this report provide a feasible alternative to produce GABA using immobilized GAD through fusion to CBD.

PMID: 22312257

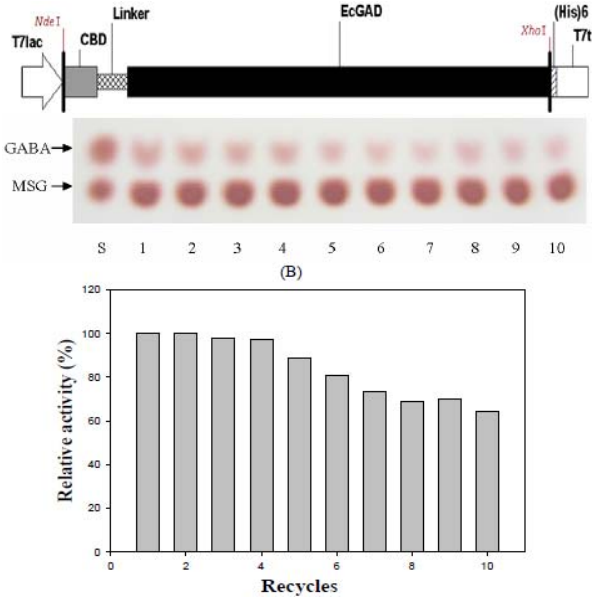

Keywords : Cellulose-binding domain; Fusion protein; GAD; Immobilization

Article 218

Mucilaginibacter angelicae sp. nov., isolated from the rhizosphere of *Angelica polymorpha* Maxim

Int J Syst Evol Microbiol. 62(Pt 1):55-60.

Kim BC, Poo H, Lee KH, Kim MN, Kwon OY, Shin KS*

*Corresponding: ksshin@kribb.re.kr
Microbial Resource Center

A Gram-negative-staining, non-motile rod, designated GG-w14^T, was isolated from the rhizosphere of *Angelica polymorpha* Maxim. Phylogenetic analysis of 16S rRNA gene sequences revealed that the isolate belonged to the genus *Mucilaginibacter* and exhibited 93.9-97.4% 16S rRNA gene sequence similarity with recognized members of the genus *Mucilaginibacter* (closest relative *Mucilaginibacter gossypii* Gh-67^T). DNA-DNA relatedness between strain GG-w14^T and *M. gossypii* KCTC 22380^T was <41%. Strain GG-w14^T grew at 4-35 °C, at pH 5.0-8.0 and with 0-1% (w/v) NaCl. The isolate hydrolysed casein, CM-cellulose and starch and contained menaquinone 7 as the major menaquinone. The major cellular fatty acids were summed feature 3 ($C_{16:1}\omega7c$ and/or iso-$C_{15:0}$ 2-OH; 39.9%), iso-$C_{15:0}$ (24.2%) and iso-$C_{17:0}$ 3-OH (12.4%). The DNA G+C content was 42.5 mol%. These data suggest that strain GG-w14^T should be considered as a representative of a novel species of the genus *Mucilaginibacter*, for which the name *Mucilaginibacter angelicae* sp. nov. is proposed. The type strain is GG-w14^T (=KCTC 23250^T=NCAIM B 02415^T).
PMID: 21317281

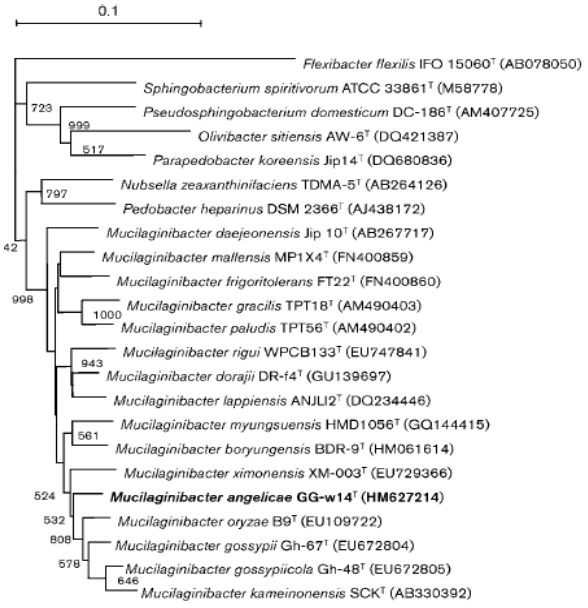

Keywords : *Mucilaginibacter angelicae*; Phylogenetic analysis; Rhizosphere

Article 219

Herbiconiux moechotypicola sp. nov., a xylanolytic bacterium isolated from the gut of hairy long-horned toad beetles, *Moechotypa diphysis* (Pascoe)

Int J Syst Evol Microbiol. 62(Pt 1):90-5.

Kim BC, Park DS, Kim H, Oh HW, Lee KH, Shin KS, Bae KS*

*Corresponding: ksbae@kribb.re.kr
Microbial Resource Center

A novel Gram-positive, non-motile, rod-shaped bacterium, designated strain RB-62^T, was isolated during a study of culturable bacteria from the gut of *Moechotypa diphysis* (Pascoe) and its taxonomic position was investigated. Strain RB-62^T grew at 15-30 °C and pH 5.0-8.5. The isoprenoid quinones were menaquinones MK-11 (77.1%), MK-10 (11.7%) and MK-12 (11.2%). The major cellular fatty acids were anteiso-$C_{15:0}$ (34.6%), anteiso-$C_{17:0}$ (29.8%), iso-$C_{16:0}$ (17.0%) and cyclohexyl-$C_{17:0}$ (11.4%). The diagnostic diamino acid of the cell-wall peptidoglycan was 2,4-diaminobutyric acid. The G+C content of the genomic DNA of strain RB-62^T was 70.3 mol%. Phylogenetic analysis based on 16S rRNA gene sequences showed that strain RB-62^T was affiliated with the genus *Herbiconiux* cluster within the family *Microbacteriaceae*, and was related most closely to *Herbiconiux ginsengi* wged11^T (98.08% similarity). The level of DNA-DNA relatedness between strain RB-62^T and *H. ginsengi* wged11^T was 43.2% (reciprocal 66.7%). Phenotypic and phylogenetic characteristics clearly distinguished strain RB-62^T from recognized species of the genus *Herbiconiux*. Based on data from the present polyphasic study, strain RB-62^T is considered to represent a novel species of the genus *Herbiconiux*, for which the name *Herbiconiux moechotypicola* sp. nov. is proposed. The type strain is RB-62^T (=KCTC 19653^T=JCM 16117^T).
PMID: 21335498

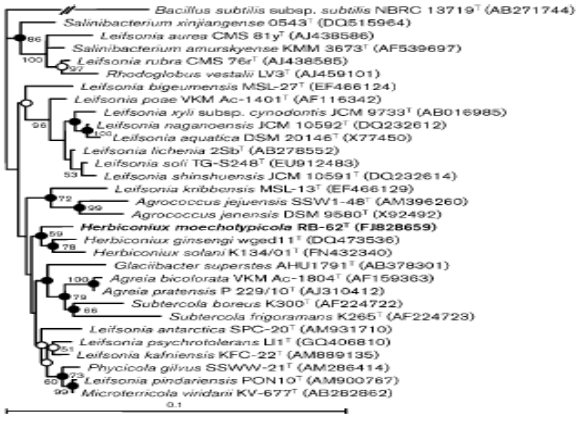

Keywords : Culturable bacteria; *Herbiconiux moechotypicola*; Phenotypic property; Phylogenetic analysis

Article 220

Patulibacter ginsengiterrae sp. nov., isolated from soil of a ginseng field, and an emended description of the genus *Patulibacter*

Int J Syst Evol Microbiol. 62(Pt 3):563-8.

Kim KK, Lee KC, Lee JS*

*Corresponding: jslee@kribb.re.kr
Microbial Resource Center

A novel actinobacterial strain, designated P4-5^T, was isolated from soil of a ginseng field located in Geumsan County, Republic of Korea. Cells of strain P4-5^T were Gram-stain-positive, oxidase- and catalase-positive, motile, short rods and the strain produced creamy white colonies on trypticase soy agar. The isolate contained demethylmenaquinone 7 (DMK-7) as the predominant isoprenoid quinone, $C_{18:1}\omega9c$ and anteiso-$C_{15:0}$ as major fatty acids, diphosphatidylglycerol, phosphatidylglycerol and several unknown lipids in the polar lipid profile, galactose, glucose, mannose, arabinose, xylose (trace) and rhamnose as cell-wall sugars, and *meso*-diaminopimelic acid as the diagnostic diamino acid in the cell-wall peptidoglycan. The DNA G+C content of strain P4-5^T was 74.6 mol%. Phylogenetic analysis based on 16S rRNA gene sequencing showed that strain P4-5^T was related most closely to *Patulibacter minatonensis* KV-614^T and *Patulibacter americanus* CP177-2^T (98.4 and 98.2% similarity, respectively) and that it formed a separate lineage in the genus *Patulibacter*. Combined phenotypic and DNA-DNA hybridization data supported the conclusion that strain P4-5^T represents a novel species of the genus *Patulibacter*, for which the name *Patulibacter ginsengiterrae* sp. nov. is proposed. The type strain is P4-5^T (=KCTC 19427^T =CECT 7603^T). An emended description of the genus *Patulibacter* is also provided.

PMID: 21515709

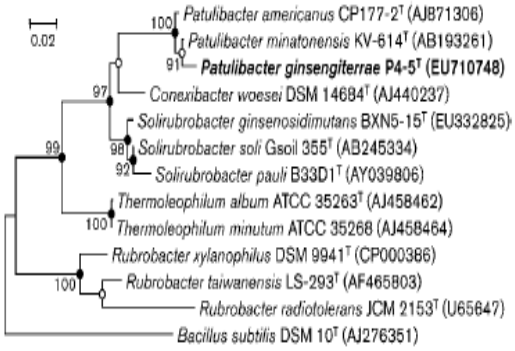

Keywords : *Patulibacter ginsengiterrae*; Phenotypic property; Phylogenetic analysis; Soil

Article 221

Simiduia areninigrae sp. nov., an agarolytic bacterium isolated from sea sand

Int J Syst Evol Microbiol. 62(Pt 4):906-11.

Kim BC, Poo H, Lee KH, Kim MN, Park DS, Oh HW, Lee JM, Shin KS*

*Corresponding: ksshin@kribb.re.kr
Microbial Resource Center

During a study intended to screen for agar-degrading bacteria, strain M2-5^T was isolated from black sand off the shore of Jeju Island, Republic of Korea. Strain M2-5^T exhibited agarase activity; the β-agarase gene of the isolate had 62 % amino acid sequence identity to the β-agarase gene of *Microbulbifer thermotolerans* JAMB A94^T. The isolate was closely related to members of the genus *Simiduia* but was clearly discernible from reported *Simiduia* species, based on a polyphasic analysis. Cells of strain M2-5^T were Gram-negative, catalase- and oxidase-positive, motile rods. The DNA G+C content was 53.3 mol%. The predominant isoprenoid quinone was Q-8. The major cellular fatty acids were $C_{17:1}\omega8c$ (25.9%), summed feature 3 (iso-$C_{15:0}$ 2-OH and/or $C_{16:1}\omega7c$; 17.2%) and $C_{17:0}$ (15.0%). Phylogenetic analysis using 16S rRNA gene sequences showed that strain M2-5^T had 96.6% gene sequence similarity to *Simiduia agarivorans* SA1^T, the most closely related type strain of the genus *Simiduia*. These results suggest that strain M2-5^T represents a novel species in the genus *Simiduia*, for which the name *Simiduia areninigrae* sp. nov. is proposed; the type strain is M2-5^T (=KCTC 23293^T=NCAIM B 02424^T).

PMID: 21669928

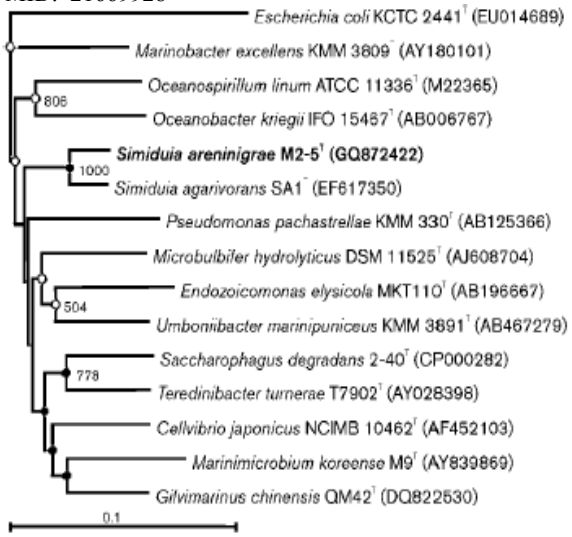

Keywords : Black sand; Phenotypic property; Phylogenetic analysis; *Simiduia areninigrae*

Article 222

Gracilibacillus bigeumensis sp. nov., a moderately halophilic bacterium from solar saltern soil

Int J Syst Evol Microbiol. 62(Pt 8):1857-63.

Kim P, Lee JC, Park DJ, Shin KS, Kim JY, Kim CJ*

*Corresponding: changjin@kribb.re.kr
Microbial Resource Center

A Gram-staining-positive, moderately halophilic bacterium, designated strain BH097^T, was isolated from solar saltern soil of Bigeum Island in south-west Korea. Cells were motile rods, producing spherical endospores at a terminal position in swollen sporangia. Strain BH097^T was strictly aerobic, grew at pH 5.5-9.5 (optimum, pH 8.0), at 10-52 °C (optimum, 37 °C) and at salinities of 1-22% (w/v) NaCl (optimum, 7% NaCl). On the basis of 16S rRNA gene sequence analysis, strain BH097^T was shown to belong to the genus *Gracilibacillus* within the phylum Firmicutes, and showed closest sequence similarity to *Gracilibacillus saliphilus* DSM 19802^T (95.8%), *Gracilibacillus thailandensis* TP2-8^T (95.6%), *Gracilibacillus boraciitolerans* DSM 17256^T (95.5%), '*Gracilibacillus quinghaiensis*' DSM 17858 (95.4%) and *Gracilibacillus halophilus* DSM 17856^T (95.2%). The DNA G+C content of this novel isolate was 37.9 mol%. The major cellular fatty acids of strain BH097^T were anteiso-$C_{15:0}$, iso-$C_{15:0}$ and $C_{16:0}$, and its polar lipid pattern consisted of diphosphatidylglycerol, phosphatidylglycerol two unknown phospholipids and a glycolipid. The isoprenoid quinone was MK-7, and the peptidoglycan type was A1γ, with *meso*-diaminopimelic acid as the diagnostic diamino acid. On the basis of polyphasic evidence from this study, strain BH097^T represents a novel species of the genus *Gracilibacillus* for which the name *Gracilibacillus bigeumensis* sp. nov. is proposed. The type strain is BH097^T (=KCTC 13130^T=DSM 19028^T).

PMID:21984665

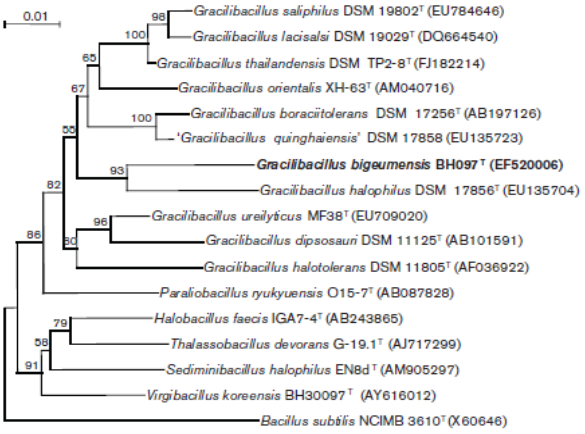

Keywords : *Gracilibacillus bigeumensis*; Phenotypic property; Polyphasic evidence; Solar saltern soil

Article 223

Cohnella cellulosilytica sp. nov., isolated from buffalo faeces

Int J Syst Evol Microbiol. 62(Pt 8):1921-5.

Khianngam S, Tanasupawat S, Akaracharanya A, Kim KK, Lee KC, Lee JS*

*Co-corresponding: jslee@kribb.re.kr
Microbial Resource Center

A cellulose-degrading bacterium, strain FCN3-3^T, was isolated from buffalo faeces collected in Nakhonnayok province, Thailand. The strain was characterized based on its phenotypic and genotypic characteristics. Strain FCN3-3^T was a Gram-positive, aerobic, spore-forming, rod-shaped bacterium. It contained *meso*-diaminopimelic acid in cell-wall peptidoglycan. The major menaquinone was MK-7. Anteiso-$C_{15:0}$ (52.5%), iso-$C_{16:0}$ (18.9%) and $C_{16:0}$ (9.1%) were the predominant cellular fatty acids, and diphosphatidylglycerol, phosphatidylglycerol, phosphatidylethanolamine and lysyl-phosphatidylglycerol were the major phospholipids. The DNA G+C content was 58.0 mol%. Phylogenetic analysis using 16S rRNA gene sequences showed that strain FCN3-3^T was affiliated to the genus *Cohnella* and was closely related to *Cohnella phaseoli* GSPC1^T, *Cohnella luojiensis* HY-22R^T and *Cohnella hongkongensis* HKU3^T, with 97.2, 96.8 and 96.3% sequence similarity, respectively. Strain FCN3-3^T could be clearly distinguished from all known species of the genus *Cohnella* by its physiological and biochemical characteristics as well as its phylogenetic position and level of DNA-DNA relatedness. Therefore, the strain represents a novel species of the genus *Cohnella*, for which the name *Cohnella cellulosilytica* sp. nov. is proposed; the type strain is FCN3-3^T (=KCTC 13645^T=TISTR 1996^T=PCU 323^T).

PMID:22003039

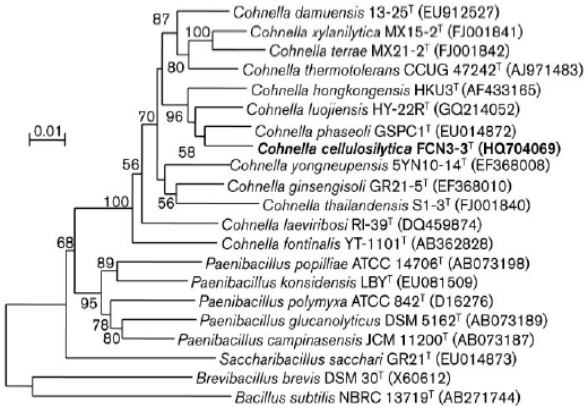

Keywords : Buffalo faeces; *Cohnella cellulosilytica*; Phenotypic property; Phylogenetic analysis

Article 224

Description of *Lysinibacillus sinduriensis* sp. nov., and transfer of *Bacillus massiliensis* and *Bacillus odysseyi* to the genus *Lysinibacillus* as *Lysinibacillus massiliensis* comb. nov. and *Lysinibacillus odysseyi* comb. nov. with emended description of the genus *Lysinibacillus*

Int J Syst Evol Microbiol. 62(Pt 10):2347-55.

Jung MY, Kim JS, Paek WK, Styrak I, Park IS, Sin Y, Paek J, Park KA, Kim H, Kim HL, Chang YH*

*Corresponding: yhchang@kribb.re.kr
Microbial Resource Center

A Gram-positive, rod-shaped, endospore-forming bacterium, designated strain BLB-1^T, was isolated from samples of tidal flat sediment from the Yellow Sea. 16S rRNA gene sequence analysis demonstrated that the isolate belonged to the *Bacillus* rRNA group 2 and was closely related to *Bacillus massiliensis* CIP 108446^T (97.4%), *Bacillus odysseyi* ATCC PTA-4993^T (96.7%), *Lysinibacillus fusiformis* DSM 2898^T (96.2%) and *Lysinibacillus boronitolerans* DSM 17140^T (95.9%). Sequence similarities with related species in other genera, including *Caryophanon, Sporosarcina and Solibacillus*, were <96.1%. Chemotaxonomic data supported the affiliation of strain BLB-1^T with the genus *Lysinibacillus*. The major menaquinone was MK-7, the cell-wall sugars were glucose and xylose, the cell-wall peptidoglycan type was A4α (L-Lys-D-Asp), the major polar lipids were diphosphatidylglycerol, phosphatidylglycerol, phosphatidyl-ethanolamine and several unknown phospholipids, and the major fatty acids were anteiso-$C_{15:0}$ (35.6%), iso-$C_{15:0}$ (25.6%) and anteiso-$C_{17:0}$ (16.5%). The most closely related species, *Bacillus massiliensis* and *Bacillus odysseyi*, were also assigned to this genus based on phylogenetic analysis and phenotypic data. The results of DNA-DNA hybridizations and phenotypic tests supported the differentiation of all three taxa from species of the genus *Lysinibacillus* with validly published names. Thus, strain BLB-1^T (=KCTC 13296^T =JCM 15800^T) represents a novel species, for which the name *Lysinibacillus sinduriensis* sp. nov. is proposed. It is also proposed that *Bacillus massiliensis* CIP 108446^T (=4400831^T=CCUG49529^T =KCTC 13178^T) and *Bacillus odysseyi* NBRC 100172^T (=34hs-1^T =ATCC PTA-4993^T =NRRL B-30641^T =DSM 18869^T =CIP 108263^T =KCTC 3961^T) be transferred to the genus *Lysinibacillus* as *Lysinibacillus massiliensis* comb. nov. and *Lysinibacillus odysseyi* comb. nov., respectively.
PMID: 22140163

Keywords : *Lysinibacillus massiliensis*; *Lysinibacillus odysseyi; Lysinibacillus sinduriensis*; Phenotypic property; Phylogenetic analysis; Tidal flat sediment

Article 225

Gryllotalpicola gen. nov., with descriptions of *Gryllotalpicola koreensis* sp. nov., *Gryllotalpicola daejeonensis* sp. nov. and *Gryllotalpicola kribbensis* sp. nov. from the gut of the African mole cricket, *Gryllotalpa africana*, and reclassification of *Curtobacterium ginsengisoli* as *Gryllotalpicola ginsengisoli* comb. nov.

Int J Syst Evol Microbiol. 62(Pt 10):2363-70.

Kim H, Park DS, Oh HW, Lee KH, Chung DH, Park HY, Park HM, Bae KS*

*Co-corresponding: ksbae@kribb.re.kr
Microbial Resource Center

Strains RU-16^T, RU-28, RU-04^T and PU-02^T were isolated from the gut of the African mole cricket, *Gryllotalpa africana*. Phylogenetic analyses based on 16S rRNA gene sequences revealed that the strains belonged to the family *Microbacteriaceae*. All four strains were most closely related to *Curtobacterium ginsengisoli* DCY26^T (below 97% 16S rRNA gene sequence similarity). These isolates were Gram-stain-positive, motile (by gliding), rod-shaped and exhibited ivory-coloured colonies. Their chemotaxonomic properties included MK-11 as the major respiratory quinone, ornithine as the cell-wall diamino acid, acetyl as the acyl type of the peptidoglycan, cyclohexyl-$C_{17:0}$ as the major fatty acid and phosphatidylglycerol and diphosphatidylglycerol as the major polar lipids. On the basis of phenotypic, chemotaxonomic and phylogenetic analyses, we propose a new genus in the family *Microbacteriaceae*, *Gryllotalpicola* gen. nov., with three novel species, *Gryllotalpicola daejeonensis* sp. nov. (type strain RU-04^T =KCTC 13809^T =JCM 17590^T), *Gryllotalpicola koreensis* sp. nov. (type strain RU-16^T =KCTC 13810^T =JCM 17591^T) and *Gryllotalpicola kribbensis* sp. nov. (type strain PU-02^T =KCTC 13808^T =JCM 17593^T). *Gryllotalpicola koreensis* is the type species of the genus. Additionally, we propose that *Curtobacterium ginsengisoli* should be reclassified in the genus as *Gryllotalpicola ginsengisoli* comb. nov. (type strain DCY26^T =KCTC 13163^T =JCM 14773^T).
PMID: 22140167

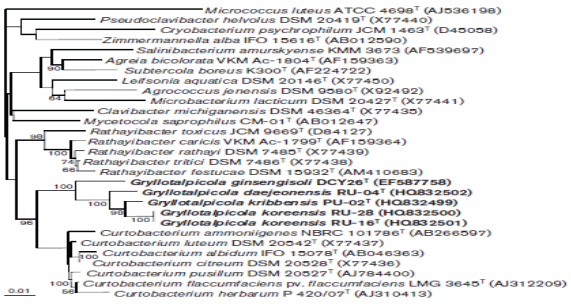

Keywords : *Gryllotalpicola daejeonensis*; *Gryllotalpicola koreensis*; *Gryllotalpicola kribbensis*; Gut; Phenotypic property; Phylogenetic analysis

Article 226

Genome sequence of *Lactobacillus fructivorans* KCTC 3543

J Bacteriol. 194(8):2111-2.

Nam SH, Choi SH, Kang A, Lee KS, Kim DW, Kim RN, Kim DS, Park HS*

*Corresponding: hspark@kribb.re.kr
Human Derived Material Center

Lactobacillus fructivorans is important in the generation of particular flavors and in other ripening processes associated with fermented food. Here, we present the draft genome sequence of the type strain *Lactobacillus fructivorans* KCTC 3543 (1,373,326 bp, with a G+C content of 38.9%), which consists of 5 scaffolds. The genome sequence was obtained by using a whole-genome shotgun strategy with Roche 454 GS (FLX Titanium) pyrosequencing, and all of the reads were assembled using Newbler Assembler 2.3.
PMID: 22461550

Keywords : Genome sequence; *Lactobacillus fructivorans*

Article 227

Genome sequence of *Peptoniphilus rhinitidis* 1-13T, an anaerobic coccus strain isolated from clinical specimens

J Bacteriol. 194(9):2405-6.

Kim DS, Jung MY, Kang A, Cho J, Sin Y, Paek J, Kim DW, Kim RN, Nam SH, Kim A, Park HS, Choi SH*, Chang YH*

*Co-corresponding: shchoi@kribb.re.kr yhchang@kribb.re.kr
Microbial Resource Center

A new *Peptoniphilus* species has been isolated from samples from a patient who was scheduled for endoscopic sinus surgery for chronic rhinosinusitis. The isolate, *Peptoniphilus rhinitidis* 1-13^T (KCTC 5985^T), can use peptone as a sole carbon source and produce butyrate as a metabolic end product. This is the first report of the draft genome sequence of a novel species in the genus *Peptoniphilus* within the group of Gram-positive anaerobic cocci.
PMID: 22493209

Keywords : Anaerobic coccus; Genome sequence; *Peptoniphilus rhinitidis*

Article 228

Genome sequence of *Myroides injenensis* M09-0166^T, isolated from clinical specimens

J Bacteriol. 194(10):2748-9.

Kim DS, Paek J, Shin JH, Kim DW, Jung MY, Kim RN, Sin Y, Kook JK, Nam SH, Kim A, Kang A, Park HS, Choi SH*, Chang YH*

*Co-corresponding: shchoi@kribb.re.kr yhchang@kribb.re.kr
Microbial Resource Center

A new *Myroides* species has been isolated from the urine of a patient with fever in spite of multiple antibiotic treatments who had undergone a radical hysterectomy for cervical cancer and percutaneous nephrostomies for hydronephrosis in the past. The isolate, *Myroides injenensis* M09-0166^T (KCTC 23367^T), showed a high level of resistance to multiple antibiotic agents. Here we provide the first report of the draft genome sequence of a novel species in the genus *Myroides* within the nonfermenting Gram-negative group.
PMID: 22535932

Keywords : Antibiotic agents; Genome sequence; *Myroides injenensis*

Article 229

Genome sequence of the anaerobic bacterium *Clostridium arbusti* SL206^T

J Bacteriol. 194(10):2758.

Kim DS, Jung MY, Sin Y, Kim DW, Paek J, Kim RN, Park IS, Kook JK, Nam SH, Kim A, Kang A, Park HS, Choi SH*, Chang YH*

*Co-corresponding: shchoi@kribb.re.kr yhchang@kribb.re.kr
Microbial Resource Center

A new *Clostridium* species has been isolated from pear orchard soil in Daejeon, Republic of Korea. The isolate, *Clostridium arbusti* SL206^T (KCTC 5449^T), showed a nitrogenase activity as well as an organic acid production. Here we first report the draft genome sequence of a novel species in the genus *Clostridium* within the largest Gram-positive group.
PMID: 22535938

Keywords : Anaerobic bacterium; *Clostridium arbusti*; Genome sequence

Article 230

Genome sequence of the probiotic bacterium *Sporolactobacillus vineae* SL153T

J Bacteriol. 194(11):3015-6.

Kim DS, Sin Y, Kim DW, Paek J, Kim RN, Jung MY, Park IS, Kim A, Kang A, Park HS, Choi SH*, Chang YH*

*Co-corresponding: shchoi@kribb.re.kr yhchang@kribb.re.kr
Microbial Resource Center

The novel *Sporolactobacillus vineae* SL153^T strain has excellent intestinal adherence and growth inhibitory effect on pathogenic microorganisms, including *Vibrio* genus microorganisms, and therefore can be effectively used for the prevention and treatment of disease caused by pathogenic microorganisms. Here, we first report the draft genome sequence of a novel species in the genus *Sporolactobacillus*.
PMID: 22582374

Keywords : Genome sequence; Pathogenic microorganisms; Probiotic bacterium; *Sporolactobacillus vineae*

Article 231

Draft genome sequence of the human pathogen *Halomonas stevensii* S18214T

J Bacteriol. 194(18):5143.

Kim KK, Lee KC, Jeong H, Stevens DA, Lee JS*

*Corresponding: jslee@kribb.re.kr
Microbial Resource Center

Halomonas stevensii is a Gram-negative, moderately halophilic bacterium causing environmental contamination and infections in a dialysis center. Here we present the 3.7-Mb draft genome sequence of the type strain (S18214^T) of *H. stevensii*, which will give insight into the pathogenic potential of *H. stevensii*.
PMID: 22933767

Keywords : Genome sequence; Halophilic bacterium; *Halomonas stevensii*

Article 232

Draft genome sequence of *Virgibacillus halodenitrificans* 1806

J Bacteriol. 194(22):6332.

Lee SJ, Lee YJ, Jeong H, Lee SJ, Lee HS, Pan JG, Kim BC*, Lee DW

*Co-corresponding: bckim@kribb.re.kr
Microbial Resource Center

Virgibacillus halodenitrificans 1806 is an endospore-forming halophilic bacterium isolated from salterns in Korea. Here, we report the draft genome sequence of *V. halodenitrificans* 1806, which may reveal the molecular basis of osmoadaptation and insights into carbon and anaerobic metabolism in moderate halophiles.
PMID: 23105070

Keywords : Genome sequence; Halophilic bacterium; *Virgibacillus halodenitrificans*

Article 233

Genome sequence of *Oscillibacter ruminantium* strain GH1, isolated from rumen of Korean native cattle

J Bacteriol. 194(22):6362.

Lee GH, Kumar S, Lee JH, Chang DH, Kim DS, Choi SH, Rhee MS, Lee DW, Yoon MH, Kim BC*

*Corresponding: bckim@kribb.re.kr
Microbial Resource Center

Oscillibacter ruminantium strain GH1 was isolated from the rumen of Korean native cattle (HanWoo; *Bos taurus coreanae*). Here, we present the 3.07-Mb draft genome of this strain, which could reveal the presence of certain fiber-specific glycoside hydrolases and butyric acid-producing genes.
PMID:23105088

Keywords : Fiber-specific glycoside hydrolases; Genome sequence; HanWoo; Korean native cattle; *Oscillibacter ruminantium*

Article 234

Draft genome sequence of the extremely halophilic archaeon *Halogranum salarium* B-1T

J Bacteriol. 194(23):6659.

Kim KK, Lee KC, Lee JS*

*Corresponding: jslee@kribb.re.kr
Microbial Resource Center

Halogranum salarium is an extremely halophilic archaeon isolated from evaporitic salt crystals and belongs to the family *Halobacteriaceae*. Here, we present the 4.5-Mb draft genome sequence of the type strain (B-1^T) of *H. salarium*. This is the first report of the draft genome sequence of a haloarchaeon in the genus *Halogranum*.
PMID: 23144405

Keywords : Evaporitic salt crystals; Genome sequence; *Halogranum salarium*; Halophilic archaeon

Article 235

Activation of cannabinoid receptor type 1 (*Cb1r*) disrupts hepatic insulin receptor signaling via cyclic AMP-response element-binding protein H (*Crebh*)-mediated induction of *Lipin1* gene

J Biol Chem. 287(45):38041-9.

Chanda D, Kim YH, Kim DK, Lee MW, Lee SY, Park TS, Koo SH, Lee CH*, Choi HS

*Co-corresponding: chullee@kribb.re.kr
Laboratory Animal Resource Center

Activation of hepatic cannabinoid 1 receptor (*Cb1r*) signaling has been implicated in the development of phenotypes associated with fatty liver, hypertriglyceridemia, and insulin resistance. In the current study, we have elucidated the critical role of endoplasmic reticulum-bound transcription factor cyclic AMP-response element-binding protein H (*Crebh*) in mediating activated *Cb1r* signaling in inducing phosphatidic acid phosphatase *Lipin1* gene expression and subsequently deregulating hepatic insulin receptor signaling. *Cb1r* agonist (2-arachidonoylglycerol (2-AG)) treatment induced *Lipin1* gene expression in a *Crebh*-dependent manner via recruiting CREBH to the endogenous *Lipin1* gene promoter. Adenoviral overexpression of *Crebh* or 2-AG treatment in mice induced *Lipin1* gene expression to increase the hepatic diacylglycerol (DAG) level and phosphorylation of protein kinase Cε (PKC ε). This in turn inhibited hepatic insulin receptor signaling. Knockdown of *Crebh* or *Cb1r* antagonism attenuated 2-AG-mediated induction of *Lipin1* gene expression and decreased DAG production in mouse liver and subsequently restored insulin receptor signaling. Similarly, knockdown of *Lipin1* attenuated the 2-AG-induced increase in the DAG level and PKCε phosphorylation. Finally, shRNA-mediated knockdown of *Crebh* partially but significantly blunted *Lipin1* expression and the DAG level in *db/db* mice. These results demonstrate a novel mechanism by which *Cb1r* signaling induces *Lipin1* gene expression and increases DAG production by activating *Crebh*, thereby deregulating insulin receptor signaling pathway and lipid homeostasis.
PMID:22989885

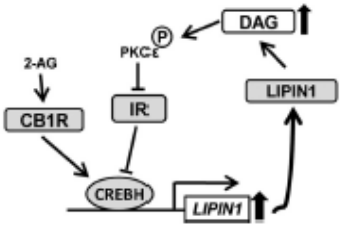

Keywords : DAG production; Hepatic cannabinoid 1 receptor (*Cb1r*); Hepatic insulin receptor signaling

Article 236

Analysis of indel variations in the human disease-associated genes *CDKN2AIP, WDR66, USP20* and *OR7C2* in a Korean population

J Genet. 91(1):e1-e11.

Kim RN, Kim A, Kim DW, Choi SH, Kim DS, Nam SH, Kang A, Kim MY, Park KH, Yoon BH, Lee KS, Park HS*

*Corresponding: hspark@kribb.re.kr
Human Derived Material Center

The human genes *CDKN2AIP, WDR66, USP20* and *OR7C2* have emerged as important genetic factors that could be biologically associated with cancer, haematological diseases and olfactory dysfunction. In this study, we performed PCR amplifications and sequencing of the loci of these four genes using genomic DNA from 100 Korean individuals. We identified the allele and genotype frequencies of indels in the human genetic disease-associated genes *CDKN2AIP, WDR66, USP20* and *OR7C2* at the scale of a Korean population for the first time and predicted the functional consequences of these variations. Another important finding of this study was the high frequency of the 3-bp deletion in the USP20 gene in Korean individuals (allele frequency, 0.99; homozygous genotype frequency, 0.98). The allele and genotype frequencies of the indels described here and the related predicted functional consequences elucidated in this study present new opportunities for future studies on genetic diseases that are likely to be more prevalent in Korean populations than in other ethnic groups and for the search for drug targets for the treatment of these diseases. Our results could help to identify therapeutic targets for treating possible genetic diseases in individuals possessing homozygous genotypes for these indels in future studies.
PMID: 22552337

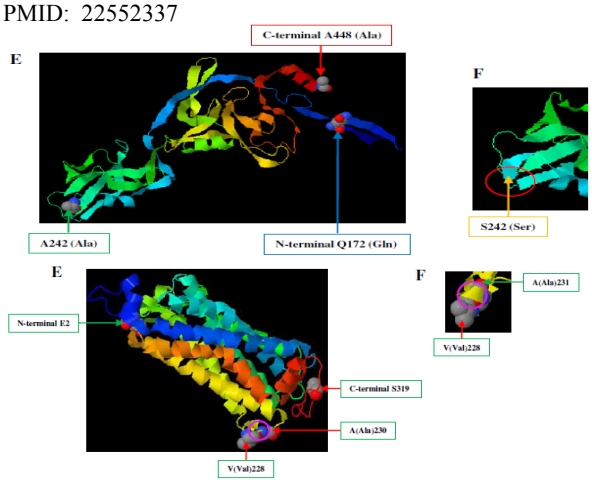

Keywords : Genetic diseases; Indel variations; Korean population; Therapeutic targets; Tumor-suppressor

Article 237

Tissue-specific expression of human calcineurin-binding protein 1 in mouse synovial tissue can suppress inflammatory arthritis

J Interferon Cytokine Res. 32(1):6-11.

Yu DH, Yi JK, Park SJ, Kim MO, Kim HJ, Yuh HS, Bae KB, Ji YR, Lee HS, Lee SG, Choo YS, Kim JY, Yoon du H, Hyun BH*, Ryoo ZY

*Co-corresponding:
Laboratory Animal Resource Center

Calcineurin (CN) is a calcium- and calmodulin-dependent serine/threonine phosphatase. In immune cells, CN controls the activity of a wide range of transcription factors, including nuclear factor of activated T, nuclear factor-kappa B, c-fos, and Elk-1. CN plays an important role in synoviocyte activation and arthritis progression *in vivo* and this function is tightly linked to dysregulated intracellular Ca^{2+} store and Ca^{2+} response triggered by proinflammatory cytokines. In the present study, transgenic mice expressing human calcineurin-binding protein 1 (hCabin1) were generated, driven by type II collagen promoter, and the efficiency of these mice was investigated by experimental arthritis. These transgenic mice successfully expressed hCabin1 in joint tissue as well as other organs such as liver, heart, and brain. The overexpression of hCabin1 reduced the disease severity during collagen-induced arthritis. In fibroblast-like synoviocytes (FLSs) from hCabin1 transgenic mice, the productions of these cytokines, including interleukin (IL)-2, IL-4, and IFN-γ, were decreased and matrix metalloproteinases were also depressed in transgenic mice FLS. In addition, these effects were only found in the joint tissue, which is a major inflammation site. These findings will provide a better knowledge of the pathogenic mechanisms of rheumatoid arthritis and a potential animal model of the chronic inflammatory conditions, including atherosclerosis and transplantation.
PMID:22175542

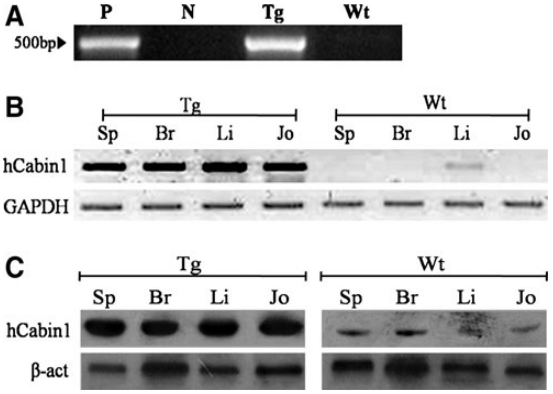

Keywords : Calcineurin (CN); Inflammatory arthritis; Synoviocyte activation; Transcription factors

Article 238

Phycicoccus ochangensis sp. nov., isolated from soil of a potato cultivation field

J Microbiol. 50(2):349-53.

Kim H, Oh HW, Park DS, Lee KH, Kim SU, Park HM, Bae KS*

*Corresponding: ksbae@kribb.re.kr
Microbial Resource Center

Two novel, Gram-positive, motile, coccal bacteria, strains L1b-b9^T and B5a-b5, were isolated from a potato cultivation field in Ochang, Korea. These isolates grew at 10-45°C, pH 5.0-10.0, and in the presence of 8% (w/v) NaCl. The diagnostic diamino acid in the cell-wall peptidoglycan was *meso*-diaminopimelic acid. The major menaquinone was MK-8(H_4) and the main cellular fatty acids were iso-$C_{15:0}$, iso-$C_{14:0}$, and anteiso-$C_{15:0}$. Polar lipids in strain L1b-b9^T consisted of diphosphatidylglycerol, phosphatidylglycerol, phosphatidylinositol, and an unknown glyco-amino lipid. The G+C content of genomic DNA was 73.6 mol%. A phylogenetic analysis based on 16S rRNA gene sequences showed that strains L1b-b9^T and B5a-b5 shared 99.36% similarity and formed a robust clade with the type species of the genus *Phycicoccus*. Strain L1b-b9^T is related most closely to *Phycicoccus cremeus* V2M29^T (97.52% 16S rRNA gene sequence similarity). On the basis of phylogenetic characteristics, the name *Phycicoccus ochangensis* sp. nov. is proposed for strain LIb-b9^T (=KCTC 19695^T [corrected] =JCM 17595^T).

PMID: 22538666

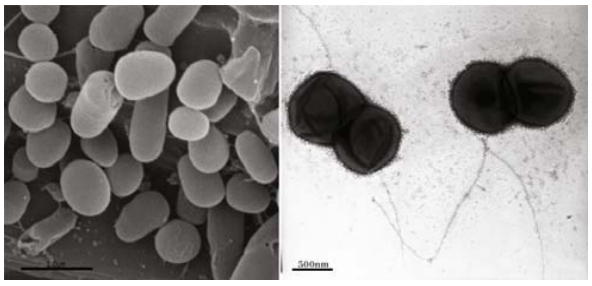

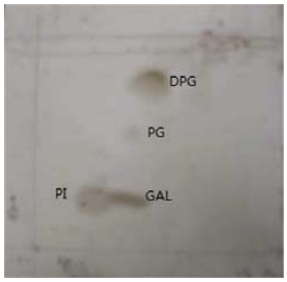

Keywords : *Intrasporangiaceae*; *Phycicoccus ochangensis*; Potato field; Soil

Article 239

PyroTrimmer: a software with GUI for pre-processing 454 amplicon sequences

J Microbiol. 50(5):766-9.

Oh J, Kim BK, Cho WS, Hong SG, Kim KM*

*Corresponding: kmkim@kribb.re.kr
Microbial Resource Center

The ultimate goal of metagenome research projects is to understand the ecological roles and physiological functions of the microbial communities in a given natural environment. The 454 pyrosequencing platform produces the longest reads among the most widely used next generation sequencing platforms. Since the relatively longer reads of the 454 platform provide more information for identification of microbial sequences, this platform is dedicated to microbial community and population studies. In order to accurately perform the downstream analysis of the 454 multiplex datasets, it is necessary to remove artificially designed sequences located at either ends of individual reads and to correct low-quality sequences. We have developed a program called PyroTrimmer that removes the barcodes, linkers, and primers, trims sequence regions with low quality scores, and filters out low-quality sequence reads. Although these functions have previously been implemented in other programs as well, PyroTrimmer has novelty in terms of the following features: i) more sensitive primer detection using Levenstein distance and global pairwise alignment, ii) the first stand-alone software with a graphic user interface, and iii) various options for trimming and filtering out the low-quality sequence reads. PyroTrimmer, written in JAVA, is compatible with multiple operating systems and can be downloaded free at http://pyrotrimmer.kobic.re.kr.

PMID: 23124743

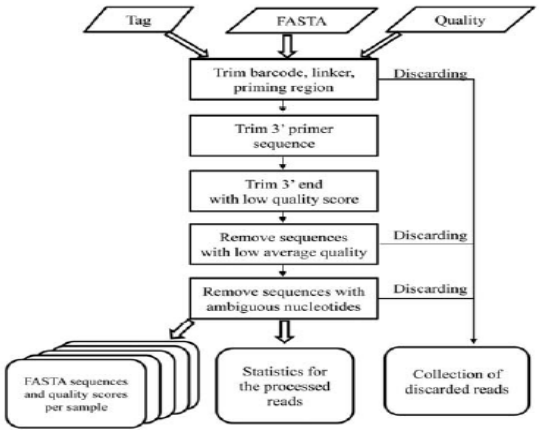

Keywords : 454 pyrosequencing platform; Pre-processing; PyroTrimmer; Software; Trimming

Article 240

Soluble expression of OmpA from *Haemophilus parasuis* in *Escherichia coli* and its protective effects in the mouse model of infection

J Microbiol Biotechnol. 22(9):1307-9.

Ahn J, Hong M, Yoo S, Lee E, Won H, Yoon I, Jung JK, Lee H*

*Corresponding: hwlee@kribb.re.kr
Biotechnology Process Engineering Center

Haemophilus parasuis causes contagious porcine Glässer's disease leading to severe losses in the swine industry. In this study, we established an efficient *Escherichia coli* based system for the expression of *H. parasuis* major outer-membrane protein (MOMP) that has been known as a good vaccine candidate against Glässer's disease. Use of an *E. coli*-derived pelB leader sequence made it possible to produce recombinant MOMP (rMOMP) as the soluble forms without an additional refolding process. Using two different animal models, it was evaluated that the rMOMP was capable of inducing a significant immune response and providing protection against *H. parasuis* infection.
PMID: 22814508

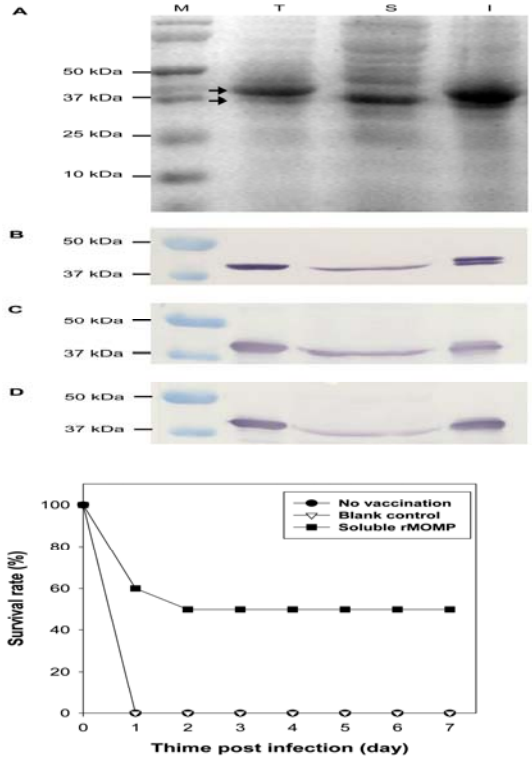

Keywords : Antigen; *Escherichia coli*; *Haemophilus parasuis*; OmpA; pelB leader sequence; Soluble expression

Article 241

Beneficial effects of endogenous and exogenous melatonin on neural reconstruction and functional recovery in an animal model of spinal cord injury

J Pineal Res. 52(1):107-19.

Park S, Lee SK, Park K, Lee Y, Hong Y, Lee S, Jeon JC, Kim JH, Lee SR, Chang KT*, Hong Y

*Co-corresponding: changkt@kribb.re.kr
Korea National Primate Research Center

The purpose of this study was to investigate the beneficial effects of endogenous and exogenous melatonin on functional recovery in an animal model of spinal cord injury (SCI). Eight-week-old male Sprague-Dawley (SD, 250-260 g) rats were used for contusion SCI surgery. All experimental groups were maintained under one of the following conditions: 12/12-hr light/dark (L/D) or 24:0-hr constant light (LL). Melatonin (10 mg/kg) was injected subcutaneously for 4 wk, twice daily (07:00, 19:00). Locomotor recovery, inducible nitric oxide synthase (iNOS), glial fibrillary acidic protein gene expression, and muscle atrophy-related genes, including muscle atrophy F-box (MAFbx) and muscle-specific ring-finger protein 1 (MuRF1) gene expression were evaluated. Furthermore, autophagic signaling such as Beclin-1 and LC3 protein expression was examined in the spinal cord and in skeletal muscle. The melatonin treatment resulted in increased hind-limb motor function and decreased iNOS mRNA expression in the L/D condition compared with the LL condition ($P < 0.05$), indicating that endogenous melatonin had neuroprotective effects. Furthermore, the MAFbx, MuRF1 mRNA level, and converted LC3 II protein expression were decreased in the melatonin-treated SCI groups under the LL ($P < 0.05$), possibly in response to the exogenous melatonin treatment. Therefore, it seems that both endogenous and exogenous melatonin contribute to neural recovery and to the prevention of skeletal muscle atrophy, promoting functional recovery after SCI. Finally, this study supports the benefit of endogenous melatonin and use of exogenous melatonin as a therapeutic intervention for SCI.
PMID:21854445

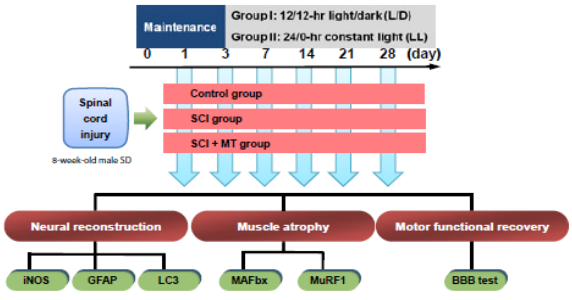

Keywords : Atrogenes; Autophagy; Functional recovery; Glial fibrillary acidic protein; Inducible nitric oxide synthase; Melatonin; Spinal cord injury

Article 242

Interactions among LOX metabolites regulate temperature-mediated flower bud formation in morning glory (*Pharbitis nil*)

J Plant Physiol. 169(18):1815-20.

Nam KH*, Yoshihara T

*Corresponding: namkh@kribb.re.kr
Bio-Evaluation Center

We examined the relationship between temperature (15-35°C) and flower induction as it is influenced by linolenic acid (LA) cascade products, lipoxygenase (LOX; EC 1.13.11.12), allene oxide synthase (AOS; EC 4.2.1.92), and allene oxide cyclase (AOC; EC 5.3.99.6) generated in morning glory (*Pharbitis nil* Choisy). The maximum amount of LOX protein was detected when plants were grown at 30°C, whereas endogenous AOS and AOC proteins were markedly accumulated at 15°C. Although both test levels of 9(S)- and 13(S)-hydroperoxy linolenic acid (HPOT) showed similar temperature dependencies, reflecting the profile of LOX, the relative amount of 13(S)-HPOT was much higher than that of 9(S)-HPOT, regardless of temperature regime. This implied a faster reaction pathway to 9,10-α-ketol octadecadienoic acid (KODA) in the LA cascade. In the 13(S)-HPOT pathway, the highest level of endogenous jasmonic acid (JA) was observed at 15°C. Our results suggest that at a high temperature (30°C), 9(S)-HPOT may be readily metabolized into KODA to promote flower bud formation. By contrast, at a low temperature, high levels of AOS and AOC result in an accumulation of JA that inhibits this developmental process. Accordingly, depending on the growing temperature, flower bud formation in *P. nil* is possibly regulated by the interactions among LOX metabolites, with KODA serving as a promoter and JA as an inhibitor.

PMID:22902207

Keywords : 9,10-Ketol-octadecadienoic acid; Hydroperoxy linolenic acid; Jasmonic acid; Lipoxygenase; Theobroxide

Article 243

Bilateral ovarian cysts originating from rete ovarii in an African green monkey (*Cercopithecus aethiops*)

J Vet Med Sci. 74(9):1229-32.

Kim SW, Lee YH, Lee SR, Kim KM, Lee YJ, Jung KJ, Chang KS, Kim D, Son HY, Reu DS, Chang KT*

*Corresponding: changkt@kribb.re.kr
Korea National Primate Research Center

Ovarian cyst is common incidental finding in humans and many animals and includes follicular cysts, cystic rete ovarii and mesonephric duct cysts. Ovarian cyst is often associated with reproductive disorders in humans and animals. We found accidentally bilateral cystic masses in ovaries in an African green monkey. Grossly, the left and right ovarian cystic masses were single unilocular cystic structures measuring 0.6 and 1.8 cm in diameter, respectively. Histologically, both cysts were thin-walled structures that arose from the center of the ovary and displaced ovarian tissue peripherally. The cysts were lined by a single layer of nonciliated low cuboidal epithelium. Immunohistochemically, epithelial cells in the cysts were positive for cytokeratin, and the stromal cells were positive for smooth muscle actin but negative for vimentin. These results suggest that these ovarian cysts in an African green monkey are cystic rete ovarii. To our knowledge, this is the first report of cystic rete ovarii in African green monkeys and may be of value in relation to research of the pathogenesis and treatment of ovarian cyst.

PMID:22673701

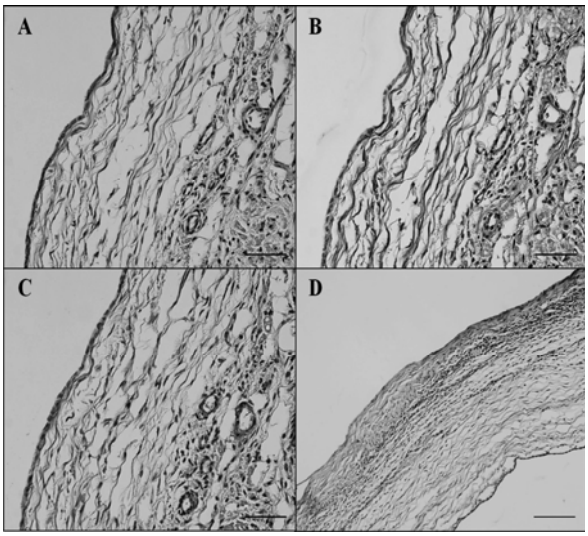

Keywords : African green monkey; Cystic rete ovarii; Ovarian cyst; Pathogenesis

Article 244

Beneficial effects of melatonin on stroke-induced muscle atrophy in focal cerebral ischemic rats

Lab Anim Res. 28(1):47-54.

Lee S, Shin J, Hong Y, Lee M, Kim K, Lee SR, Chang KT*, Hong Y

*Co-corresponding: changkt@kribb.re.kr
Korea National Primate Research Center

Muscle atrophy is the result of two opposing conditions that can be found in pathological or diseased muscles: an imbalance in protein synthesis and degradation mechanisms. Thus, we investigated whether exogenous melatonin could regulate muscle components in stroke-induced muscle atrophy in rats. Comparing muscle phenotypes, we found that long-term melatonin administration could influence muscle mass. Muscle atrophy-related genes, including muscle atrophy F-box (MAFbx) and muscle ring finger 1 (MuRF1) were significantly down-regulated in melatonin-administered rats in the gastrocnemius. However, only MAFbx at the mRNA level was attenuated in the soleus of melatonin-administered rats. Insulin-like growth factor-1 receptor (IGF-1R) was significantly over-expressed in melatonin-administered rats in both the gastrocnemius and soleus muscles. Comparing myosin heavy chain (MHC) components, in the gastrocnemius, expression of both slow- and fast-type isoforms were significantly enhanced in melatonin-administered rats. These results suggest that long-term exogenous melatonin-administration may have a prophylactic effect on muscle atrophy through the MuRF1/MAFbx signaling pathway, as well as a potential therapeutic effect on muscle atrophy through the IGF-1-mediated hypertrophic signaling pathway in a stroke animal model.

PMID:22474474

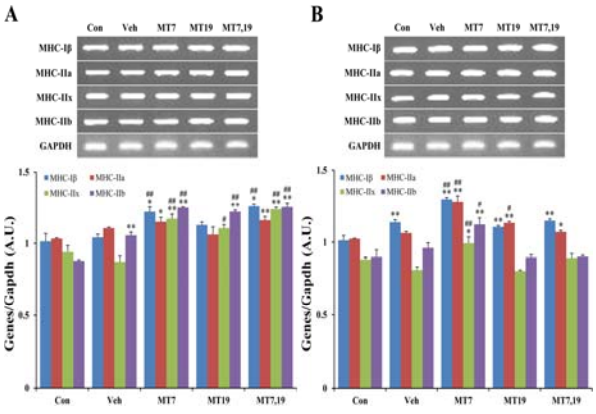

Keywords : Focal cerebral ischemia; Exogenous melatonin; Muscle atrophy; Prophylactic effect

Article 245

Acute gastrointestinal dilation in laboratory rhesus monkeys in the Korea National Primate Research Center

Lab Anim Res. 28(3):217-21.

Kim KM, Lee SR, Chang KS, Lee YH, Kim SW, Jung KJ, Lee Y, Kim D, Chang KT*

*Corresponding: changkt@kribb.re.kr
Korea National Primate Research Center

Acute gastrointestinal dilation is a medical condition in which the stomach and intestine become overstretched by excessive gas content. In laboratory monkeys, cases of bloating involving gastrointestinal dilation are rarely seen, and the cause thereof is not clearly defined. Two rhesus monkeys in the Korea National Primate Research Center were found to suffer from acute gastrointestinal dilation. One of the monkeys showed severe gastric bloating after recovering from general anesthesia with isoflurane, where after it died suddenly. During necropsy, severe congestion of the lung was observed. The other monkey showed gastrointestinal dilation and died after treatment. During necropsy, severe dilation of the large intestine was observed. Severe congestion was detected in small and large intestines. Histopathologically, erythrocytes were found to fill the alveoli and alveolar capillaries of the lung. In stomach, epithelial cells were found to be sloughed from the mucosal layer, and erythrocytes were found to fill the blood vessels of the submucosal and mucosal layers. In small and large intestines, epithelial cells were also found to be sloughed from the mucosal layer, and inflammatory cells were found to have infiltrated in the submucosa (only large intestine) and mucosa. Microbiologically, *Enterococcus faecalis* and the pathogenic *Staphylococcus haemolyticus*, which do not form gas in the gastrointestinal tract, were detected in the gastrointestinal contents of both monkeys. These results suggest that the cause of the acute gastrointestinal dilation in these monkeys was not infection by gas-forming bacteria, but rather multiple factors such as diet, anesthesia, and excessive water consumption.

PMID: 23091523

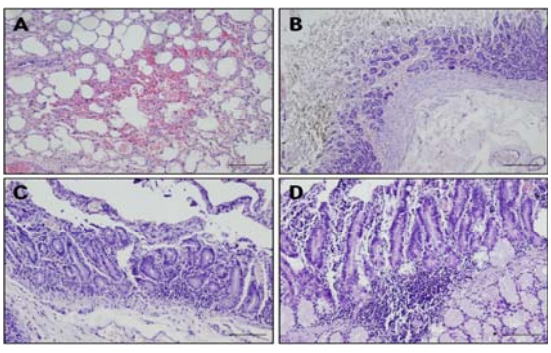

Keywords : Acute gastrointestinal dilation; Laboratory monkey; Non-bacterial multiple causes

Article 246

Human leukocytes regulate ganglioside expression in cultured micro-pig aortic endothelial cells

Lab Anim Res. 28(4):255-63.

Cho JH, Kim JS, Lim MU, Min HK, Kwak DH, Ryu JS, Lee JT, Kim SU, Kim CH, Kim CH, Koo DB, Chang KT*, Choo YK

*Co-corresponding: changkt@kribb.re.kr
Korea National Primate Research Center

Gangliosides are ubiquitous components of the membranes of mammalian cells that are thought to play important roles in various cell functions such as cell-cell interaction, cell adhesion, cell differentiation, growth control, and signaling. However, the role that gangliosides play in the immune rejection response after xenotransplantation is not yet clearly understood. In this study, the regulatory effects of human leukocytes on ganglioside expression in primary cultured micro-pig aortic endothelial cells (PAECs) were investigated. To determine the impact of human leukocytes on the expression of gangliosides in PAECs, we performed high-performance thin layer chromatography (HPTLC) in PAECs incubated with FBS, FBS containing human leukocytes, human serum containing human leukocytes, and FBS containing TNF-α. Both HPTLC and immunohistochemistry analyses revealed that PAECs incubated with FBS predominantly express the gangliosides GM3, GM1, and GD3. However, the expression of GM1 significantly decreased in PAECs incubated for 5 h with TNF-α (10 ng/mL), 10% human serum containing human leukocytes, and 10% FBS containing human leukocytes. Taken together, these results suggest that human leukocytes induced changes in the expression profile of ganglioside GM1 similar to those seen upon treatment of PAECs with TNF-α. This finding may be relevant for designing future therapeutic strategies intended to prolong xenograft survival.
PMID:23326286

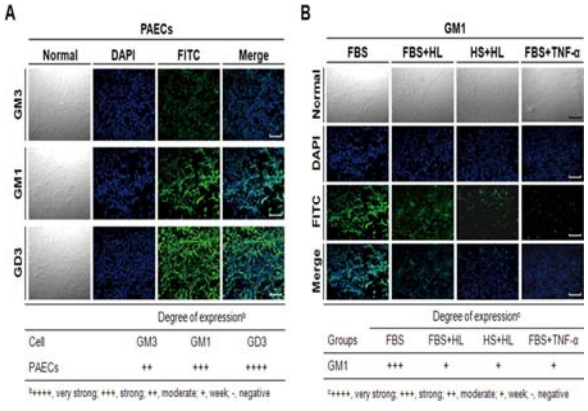

Keywords : Ganglioside GM1; Human leukocyte; Human serum; Micro-pig aortic endothelial cells; Tumor necrosis factor-α

Article 247

Melatonin combined with exercise cannot alleviate cerebral injury in a rat model of focal cerebral ischemia/reperfusion injury

Neural Regen Res. 7(13):993-9.

Lee S, Shin J, Lee M, Hong Y, Lee SK, Lee Y, Lkhagvasuren T, Kim DW, Yang YA, Chang KT*, Hong Y

*Co-corresponding: changkt@kribb.re.kr
Korea National Primate Research Center

Previous studies have demonstrated that melatonin combined with exercise can alleviate secondary damage after spinal cord injury in rats. Therefore, it is hypothesized that melatonin combined with exercise can also alleviate ischemic brain damage. In this study, adult rats were subjected to right middle cerebral artery occlusion after receiving 10 mg/kg melatonin or vehicle subcutaneously twice daily for 14 days. Forced exercise using an animal treadmill was performed at 20 m/min for 30 minutes per day for 6 days prior to middle cerebral artery occlusion. After middle cerebral artery occlusion, each rat received melatonin combined with exercise, melatonin or exercise alone equally for 7 days until sacrifice. Interestingly, rats receiving melatonin combined with exercise exhibited more severe neurological deficits than those receiving melatonin or exercise alone. Hypoxia-inducible factor 1α mRNA in the brain tissue was upregulated in rats receiving melatonin combined with exercise. Similarly, microtubule associated protein-2 mRNA expression was significantly upregulated in rats receiving melatonin alone. Chondroitin sulfate proteoglycan 4 (NG2) mRNA expression was significantly decreased in rats receiving melatonin combined with exercise as well as in rats receiving exercise alone. Furthermore, neural cell loss in the primary motor cortex was significantly reduced in rats receiving melatonin or exercise alone, but the change was not observed in rats receiving melatonin combined with exercise. These findings suggest that excessive intervention with melatonin, exercise or their combination may lead to negative effects on ischemia/reperfusion-induced brain damage.

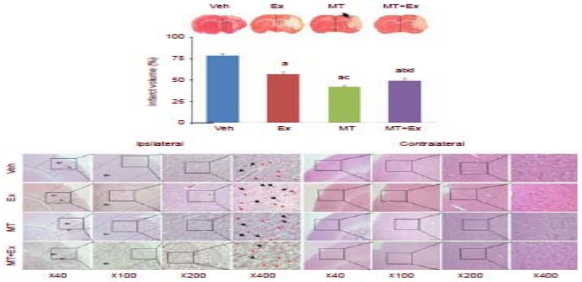

Keywords : Brain tissue loss; Chondroitin sulfate proteoglycan 4; Focal cerebral ischemia/reperfusion; Hypoxia-inducible factor 1 alpha; Melatonin; Microtubule associated protein-2; Neural regeneration; NG2

Article 248

Gene expression profiling of KBH-A42, a novel histone deacetylase inhibitor, in human leukemia and bladder cancer cell lines

Oncol Lett. 3(1):113-8.

Kang MR, Kang JS*, Yang JW, Kim BG, Kim JA, Jo YN, Lee K, Lee CW, Lee KH, Yun J, Kim HM, Han G, Kang JS, Park SK

*Co-first: kanjon@kribb.re.kr
Bio-Evaluation Center

The aim of this study was to investigate the anti-tumor activity of KBH-A42, a novel synthetic histone deacetylase (HDAC) inhibitor. KBH-A42 was shown to significantly suppress the proliferation of all 14 human cancer cell lines tested. Among these cell lines, the human leukemia cell line K562 was the most sensitive, whereas the UM-UC-3 bladder cancer cells were the least sensitive. Additionally, in a human tumor xenograft model using Balb/c nude mice, KBH-A42 was shown to significantly inhibit the growth of K562 tumors, although it only slightly inhibited the growth of UM-UC-3 tumors. The results of flow cytometry analysis and caspase 3/7 activation assays showed that the growth inhibition of K562 cells by KBH-A42 was mediated, at least in part, by the induction of apoptosis, but its growth inhibitory effects on UM-UC-3 cells were not mediated by apoptotic induction. In an effort to gain insight into the mechanism by which KBH-A42 inhibits the growth of cancer cells, a microarray analysis was conducted. Four genes were selected from the genes that were down-regulated or up-regulated by KBH-A42 and confirmed via reverse transcription-polymerase chain reaction as follows: Harakiri (*HRK*), tumor necrosis factor receptor superfamily, member 10b (*TNFRSF10B*), PYD and CARD domain containing protein gene (*PYCARD*) and tumor necrosis factor receptor superfamily, member 8 (*TNFRSF8*). Collectively, the *in vitro* and *in vivo* results suggested that KBH-A42 exhibits anti-cancer activity, but various types of cells may be regulated differentially by KBH-A42.
PMID:22740865

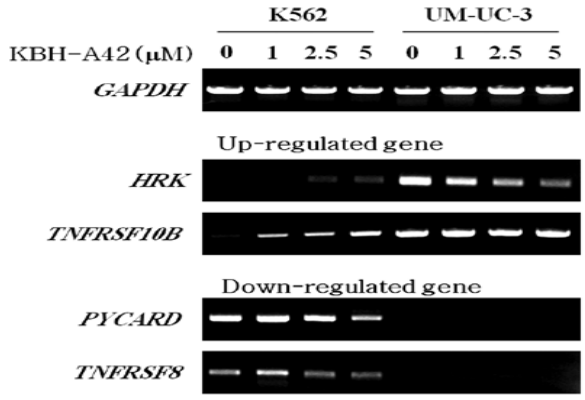

Keywords : Apoptosis; Cell cycle arrest; Histone deacetylase inhibitor; Microarray

Article 249

Widdrol induces apoptosis via activation of AMP-activated protein kinase in colon cancer cells

Oncol Rep. 27(5):1407-12.

Kang MR, Park SK, Lee CW, Cho IJ, Jo YN, Yang JW, Kim JA, Yun J, Lee KH, Kwon HJ, Kim BW, Lee K, Kang JS*, Kim HM

*Co-corresponding: kanjon@kribb.re.kr
Bio-Evaluation Center

Widdrol, a natural sesquiterpene present in *Juniperus* sp., has been shown to exert anticancer and antifungal effects. Emerging evidence has suggested that AMP-activated protein kinase (AMPK), which functions as a cellular energy sensor, is a potential therapeutic target for human cancers. In this study, we found that AMPK mediates the anticancer effects of widdrol through induction of apoptosis in HT-29 colon cancer cells. We showed that widdrol induced the phosphorylation of AMPK in a dose- and time-dependent manner. The selective AMPK inhibitor compound C abrogated the inhibitory effect of widdrol on HT-29 cell growth. In addition, we demonstrated that widdrol induced apoptosis and this was associated with the activation of caspases, including caspase-3/7 and caspase-9, in HT-29 cells. We also demonstrated that transfection of HT-29 cells with AMPK siRNAs significantly suppressed the widdrol-mediated apoptosis and the activation of caspases. However, cell cycle arrest induced by widdrol was not affected by transfection of HT-29 cells with AMPK siRNAs. Furthermore, widdrol inhibited HT-29 tumor growth in a human tumor xenograft model. Taken together, our results suggest that the anticancer effect of widdrol may be mediated, at least in part, by induction of apoptosis via AMPK activation.
PMID:22266984

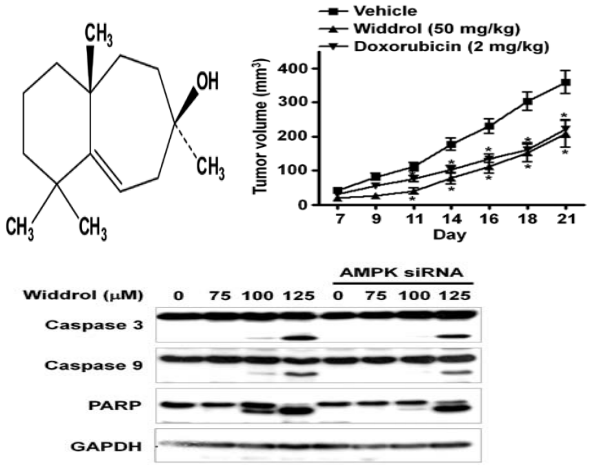

Keywords : AMP-activated protein kinase; Apoptosis; Colon cancer; Widdrol

Article 250

Ln is a key regulator of leaflet shape and number of seeds per pod in soybean

Plant Cell. 24(12):4807-18.

Jeong N, Suh SJ, Kim MH, Lee S, Moon JK, Kim HS, Jeong SC*

*Corresponding: scjeong@kribb.re.kr
Bio-Evaluation Center

Narrow leaflet soybean (*Glycine max*) varieties tend to have more seeds per pod than broad leaflet varieties. Narrow leaflet in soybean is conferred by a single recessive gene, ln. Here, we show that the transition from broad (*Ln*) to narrow leaflet (*ln*) is associated with an amino acid substitution in the EAR motif encoded by a gene (designated Gm-*JAGGED1*) homologous to *Arabidopsis JAGGED* (*JAG*) that regulates lateral organ development and the variant exerts a pleiotropic effect on fruit patterning. The genomic region that regulates both the traits was mapped to a 12.6-kb region containing only one gene, Gm-*JAG1*. Introducing the Gm-*JAG1* allele into a loss-of-function *Arabidopsis jagged* mutant partially restored the wild-type *JAG* phenotypes, including leaf shape, flower opening, and fruit shape, but the Gm-*jag1* (*ln*) and EAR-deleted Gm-*JAG1* alleles in the jagged mutant did not result in an apparent phenotypic change. These observations indicate that despite some degree of functional change of Gm-*JAG1* due to the divergence from *Arabidopsis JAG*, Gm-*JAG1* complemented the functions of JAG in *Arabidopsis thaliana*. However, the Gm-*JAG1* homoeolog, Gm-*JAG2*, appears to be sub- or neofunctionalized, as revealed by the differential expression of the two genes in multiple plant tissues, a complementation test, and an allelic analysis at both loci.

PMID:23243125

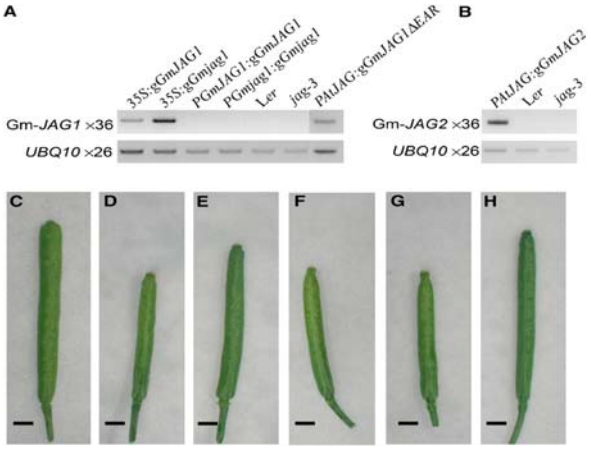

Keywords : Arabidopsis thaliana; Flower development; Genetic linkage; Lateral organs; Leaflet shape; Phantastica; Seed

Article 251

Effect of mitochondrial and ER-targeted Bcl-2 overexpression on apoptosis in recombinant Chinese hamster ovary cells treated with sodium butyrate

Process Biochem. 47(12):2518-22.

Kim YG, Park B, Lee S, Ahn JO, Jung JK, Lee HW, Lee GM, Lee EG*

*Corresponding: eglee@kribb.re.kr
Biotechnology Process Engineering Center

Overexpression of Bcl-2, a typical anti-apoptotic protein, is one of the most effective means to maintain mitochondria integrity in recombinant CHO (rCHO) cell culture treated with sodium butyrate (NaBu). NaBu is known as a typical specific productivity-enhancing factor and also a well-known apoptosis inducer. Bcl-2 is distributed to and functions in multiple intracellular organelles such as the nucleus, mitochondria, and endoplasmic reticulum (ER). To evaluate the effect of organelle-specific overexpression of Bcl-2 on NaBu-induced apoptosis in rCHO cells, Bcl-2 expression was restricted to the mitochondria or to the ER either by employing a mitochondrial insertion sequence of ActA or by insertion of an ER-specific sequence of cytochrome b5 to their respective sequences. The rCHO cell lines overexpressing wild-type Bcl-2 (WT-Bcl-2), mitochondrial Bcl-2 (MT-Bcl-2), and ER-targeted Bcl-2 (ER-Bcl-2) were established. Overexpression of WT-Bcl-2, MT-Bcl-2, and ER-Bcl-2 could increase cell viability and decrease LDH release under NaBu-treated conditions. Additionally, overexpression of WT-Bcl-2, MT-Bcl-2, and ER-Bcl-2 could suppress NaBu-induced apoptosis, as demonstrated by a DNA fragmentation assay. A mitochondrial membrane potential assay revealed that ER-Bcl-2 overexpression can maintain the mitochondrial membrane integrity without being affected by MT-Bcl-2 overexpression, indicating that the role of ER should be considered in alleviating NaBu-induced apoptosis by a genetic modulation strategy. Taken together, it was found that restricted Bcl-2 overexpression at the ER can inhibit the NaBu-induced apoptosis by maintaining mitochondria integrity in rCHO cells.

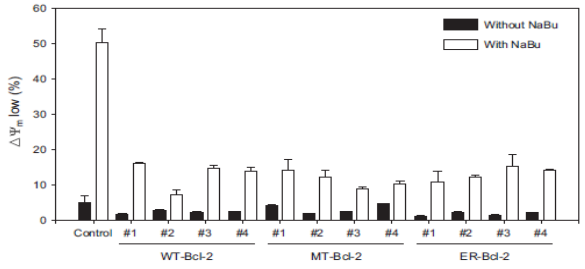

Keywords : Anti-apoptotic protein; Apoptosis; Cell viability; Cytochrome b5; DNA fragmentation; ER-targeted Bcl-2; Intracellular organelle; Mitochondrial Bcl-2; rCHO cells; Sodium butyrate

Article 252

Tauroursodeoxycholic acid enhances the pre-implantation embryo development by reducing apoptosis in pigs

Reprod Domest Anim. 47(5):791-8.

Kim JS*, Song BS, Lee KS, Kim DH, Kim SU, Choo YK, Chang KT, Koo DB

*Co-first: vjman@kribb.re.kr
Korea National Primate Research Center

Apoptosis is an important determinant of the normal development of pre-implantation embryos *in vitro*. Recently, endoplasmic reticulum (ER) stress-mediated apoptosis has been extensively investigated in a wide variety of diseases. Efficient functioning of the ER is essential for most cellular activities and survival. Tauroursodeoxycholic acid (TUDCA), an endogenous bile acid, has been reported to attenuate ER stress-mediated cell death by interrupting the classic pathways of apoptosis. Therefore, in this study, the anti-apoptotic effect of TUDCA on ER stress-induced apoptosis was examined in pre-implantation pig embryos. Also, tunicamycin was used to investigate the effects of ER stress on pig embryo development. After *in vitro* maturation and fertilization, presumptive pig embryos were cultured in NCSU-23 medium supplemented with TUDCA or TM for 6 days at 39 °C, 5% CO_2 in air. All data were analysed using one-way anova and Duncan's multiple range test in the statistical analysis system (SAS). In addition, we also determined the optimal TM and TUDCA concentrations. Samples were treated with TM at concentrations of 0, 1, 2 or 5 μm and with TUDCA at concentrations of 0, 100, 200 or 300 μm. When TM was used during *in vitro* culture, only 8.2% (8/97) of the embryos developed to the blastocyst stage when the treatment concentration was 1 μm compared with 27.4% (28/102) of the embryos in the control group ($p < 0.05$). In contrast, the frequency of blastocyst formation and the number of cells were higher when treated with 200 μm TUDCA compared with the control group (32.8% and 39.5 vs 22.2% and 35.6, $p < 0.05$). Moreover, the developmental rate to the blastocyst stage embryo in the group treated with TM and TUDCA was not significantly different from that of the control group (17.8%, 26/142 vs 24.9%, 36/145). Furthermore, the blastocyst cell number was enhanced (31.9 vs 36.9) and apoptosis reduced (TUNEL-positive nuclei number, 6.0 vs 3.2) by TUDCA treatment in pig embryos. In the real-time quantitative RT-PCR analysis, the expression of anti-apoptotic Bcl-XL gene was shown to be increased in the blastocyst stage because of TUDCA treatment, whereas expression of pro-apoptotic Bax was decreased. In addition, we also found that TUDCA decreased the rate of TM-induced apoptosis in the pre-implantation stage. Taken together, our results indicate that TUDCA improves the developmental competence of pig embryos by modulating ER stress-induced apoptosis during the pre-implantation stage.
PMID:22151574

Keywords : Embryo development; ER stress-induced apoptosis; Reducing apoptosis; TUDCA

Article 253

Protein domain structure uncovers the origin of aerobic metabolism and the rise of planetary oxygen

Structure. 20(1):67-76.

Kim KM*, Qin T, Jiang YY, Chen LL, Xiong M, Caetano-Anollés D, Zhang HY, Caetano-Anollés G

*Co-first: kmkim@kribb.re.kr
Microbial Resource Center

The origin and evolution of modern biochemistry remain a mystery despite advances in evolutionary bioinformatics. Here, we use a structural census in nearly 1,000 genomes and a molecular clock of folds to define a timeline of appearance of protein families linked to single-domain enzymes. The timeline sorts out enzymatic recruitment, validates patterns in metabolic history, and reveals that the most ancient reaction of aerobic metabolism involved the synthesis of pyridoxal 5'-phosphate or pyridoxal and appeared 2.9 Gyr ago. The oxygen source for this primordial reaction was probably Mn catalase, which appeared at the same time and could have generated oxygen as a side product of hydrogen peroxide detoxification. Finally, evolutionary analysis of transferred groups and metabolite fragments revealed that oxidized sulfur did not participate in metabolism until the rise of oxygen. The evolutionary patterns we uncover in molecules and chemistries provide strong support for the coevolution of biochemistry and geochemistry.
PMID:22244756

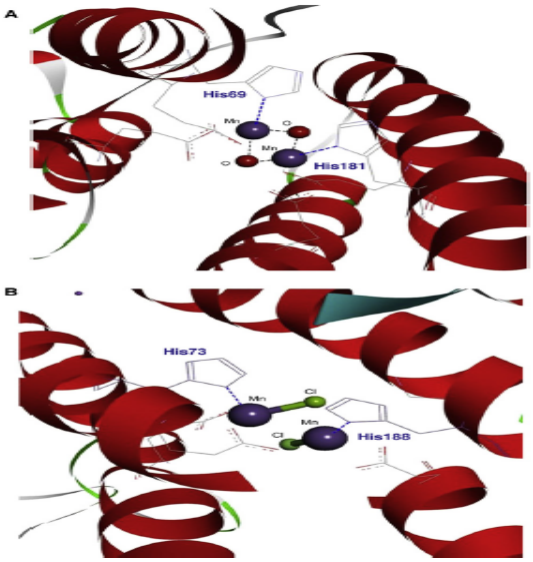

Keywords : Aerobic metabolism; Hydrogen peroxide detoxification; Oxidized sulfur; Planetary oxygen; Structural census

Article 254

Nakamurella panacisegetis sp. nov. and proposal for reclassification of *Humicoccus flavidus* Yoon *et al.*, 2007 and *Saxeibacter lacteus* Lee *et al.*, 2008 as *Nakamurella flavida* comb. nov. and *Nakamurella lactea* comb. nov.

Syst Appl Microbiol. 35(5):291-6.

Kim KK, Lee KC, Lee JS*

*Corresponding: jslee@kribb.re.kr
Microbial Resource Center

A novel actinobacterial strain, designated P4-7^T, was isolated from soil of a ginseng field located in Geumsan County, Korea. Cells of the strain were aerobic, Gram-stain-positive, non-motile, short rods. The isolate contained MK-8(H_4) as the predominant menaquinone, iso-$C_{16:0}$, anteiso-$C_{15:0}$ and anteiso-$C_{17:0}$ as the major fatty acids, diphosphatidylglycerol, phosphatidylethanolamine and phosphatidylinositol as the major polar lipids, glucose, mannose, xylose, ribose and rhamnose as whole-cell sugars, and *meso*-diaminopimelic acid as the diagnostic diamino acid in the cell-wall peptidoglycan. Phylogenetic analysis based on 16S rRNA gene sequences showed that strain P4-7^T belongs to the family *Nakamurellaceae* and is most closely related to *Nakamurella multipartita, Humicoccus flavidus* and *Saxeibacter lacteus* (96.3, 97.0 and 96.4% similarity to the respective type strains). Based on comparative analyses of the 16S rRNA and *rpoB* gene sequences and chemotaxonomic data, it is proposed that *H. flavidus* and *S. lacteus* be transferred to the genus *Nakamurella*. Combined genotypic and phenotypic data also suggested that strain P4-7^T be placed in a novel species of the genus *Nakamurella*, for which the name *Nakamurella panacisegetis* sp. nov. is proposed; the type strain is P4-7^T (=KCTC 19426^T=CECT 7604^T).

PMID: 22703716

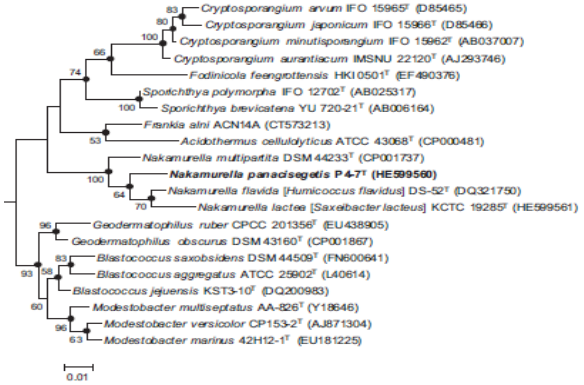

Keywords : *Nakamurella panacisegetis*; Phylogenetic analysis; Reclassification; *rpoB* gene; Soil

Article 255

Dendrobium multilineatum Kerr (Orchidaceae): A new distributional record for Vietnam

Taiwania. 57(2):225-8.

Choudhary RK, Bach TT, Huyen DD, Van Nong L, Van Hai D, Quang BH, Kumar P, Park SH, Lee C, Lee YM, Lee J*

*Corresponding: joongku@kribb.re.kr
International Biological Material Research Center

Dendrobium multilineatum Kerr, is being reported as an addition to the orchid flora of Vietnam. Line drawing and color illustration of the taxon has been provided in support of taxonomic treatment and to facilitate easy identification of the species.

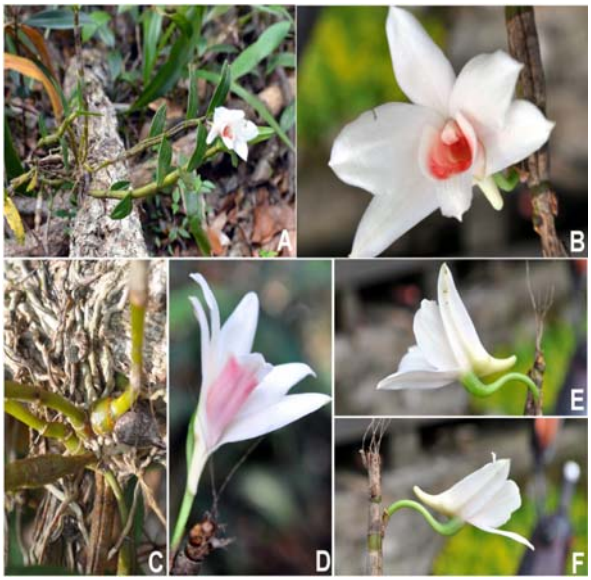

Keywords : *Dendrobium multilineatum*; New record; Orchidaceae; Taxonomic treatment; Vietnam

Article 256

Methanolic extract isolated from root of *Lycoris aurea* inhibits cancer cell growth and endothelial cell tube formation *in vitro*

Toxicol Res. 28(1):33-8.

Kang MR, Lee CW, Yun J, Oh SJ, Park SK, Lee K, Kim HM, Han SB, Kim HC, Kang JS*

*Corresponding: kanjon@kribb.re.kr
Bio-Evaluation Center

In this study, we investigated the effect of methanolic extract isolated from the root of *Lycoris aurea* (LA) on the growth of cancer cells and the tube formation activity of endothelial cells. Various cancer cells were treated with LA at doses of 0.3, 1, 3, 10 or 30 μg/ml and LA significantly suppressed the growth of several cancer cell lines, including ACHN, HCT-15, K-562, MCF-7, PC-3 and SK-OV-3, in a dose-dependent manner. We also found that LA induced cell cycle arrest at G2/M phase in ACHN renal cell adenocarcinoma cells. Further study demonstrated that LA concentration-dependently inhibited the tube formation, which is a widely used *in vitro* model of reorganization stage of angiogenesis, in human umbilical vein endothelial cells. Collectively, these results show that LA inhibits the growth of cancer cells and tube formation of endothelial cells and the growth-inhibitory effect of LA might be mediated, at least in part, by blocking cell cycle progression.

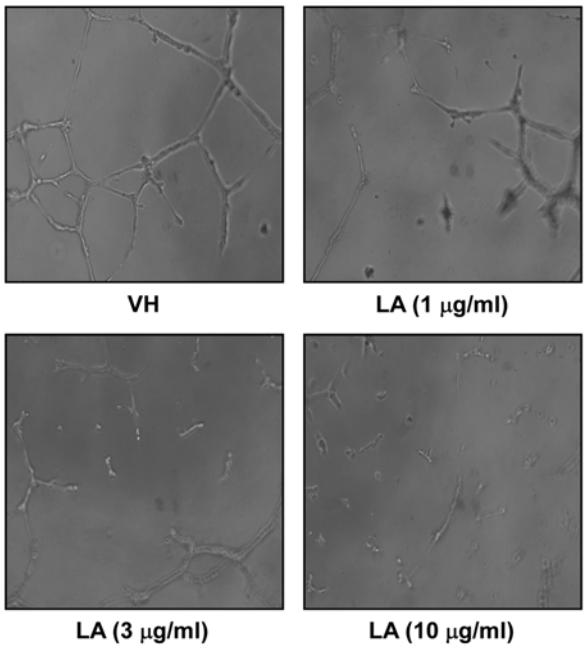

Keywords : Cancer; Cell cycle; Growth; *Lycoris aurea*; Tube formation

Article 257

Susceptibility to gold nanoparticle-induced hepatotoxicity is enhanced in a mouse model of nonalcoholic steatohepatitis

Toxicology. 294(1):27-35.

Hwang JH, Kim SJ, Kim YH, Noh JR, Gang GT, Chung BH, Song NW, Lee CH*

*Co-corresponding: chullee@kribb.re.kr
Laboratory Animal Resource Center

Although the safety of gold nanoparticle (AuNP) use is of growing concern, most toxicity studies of AuNPs had focused on their chemical characteristics, including their physical dimensions, surface chemistry, and shape. The present study examined the susceptibility of rodents with healthy or damaged livers to AuNP-induced hepatotoxicity. To induce a model of liver injury, mice were fed a methionine- and choline-deficient (MCD) diet for 4 weeks. Sizes and biodistribution of 15-nm PEGylated AuNPs were analyzed by transmission electron microscopy. Levels of alanine aminotransferase (ALT) and aspartate aminotransferase (AST) were estimated with an automatic chemical analyzer, and liver sections were subjected to pathological examination. Activities of antioxidant enzymes were determined by biochemical assay. Lateral tail vein injection of MCD diet-fed mice with 5 mg kg^{-1} AuNPs significantly elevated the serum ALT and AST levels compared to MCD diet-fed mice injected with mPEG (methylpolyethylene glycol). Similarly, severe hepatic cell damage, acute inflammation, and increased apoptosis and reactive oxygen species (ROS) production were observed in the livers of AuNP-injected mice on the MCD diet; these liver injuries were attenuated in mice fed a normal chow diet. The results suggest that AuNPs display toxicity in a stressed liver environment by stimulating the inflammatory response and accelerating stress-induced apoptosis. These conclusions may point to the importance of considering health conditions, including liver damage, in medical applications of AuNPs.
PMID: 22330258

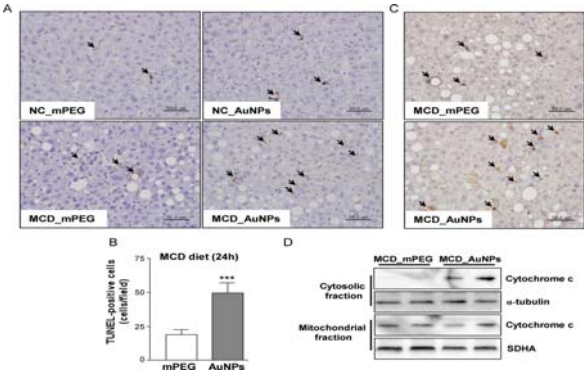

Keywords : Gold nanoparticles; Hepatotoxicity; Liver; Methionine-choline deficient; Nonalcoholic steatohepatitis


KRIBB
www.kribb.re.kr

2012
KRIBB Article Abstracts : First or corresponding articles indexed in SCIE, Scopus, and PubMed

Division of KRIBB Strategic Projects

- Korea Biosafety Clearing House
- Biotech Policy Research Center
- Viral Infectious Disease Research Center
- KRIBB-KAIST BINT Convergence Cooperation Center

Korea Research Institute of Bioscience and Biotechnology

Article 258

Delivery of IL-12p40 ameliorates DSS-induced colitis by suppressing IL-17A expression and inflammation in the intestinal mucosa

Clin Immunol. 144(3):190-9.

Kim DJ*, Kim KS, Song MY, Seo SH, Kim SJ, Yang BG, Jang MH, Sung YC

*Corresponding: golddj@kribb.re.kr
Viral Infectious Disease Research Center

IL-12p40 homodimer is a natural antagonist of IL-12 and IL-23, which are potent pro-inflammatory cytokines required for Th1 and Th17 immune responses, respectively. It has been reported that Th17 response is involved in inflammatory bowel disease (IBD), a chronic disorder of the digestive system with steadily increasing incidence. Here, we investigated the effects of IL-12p40 delivered via recombinant adenovirus (rAd/IL-12p40) or mesenchymal stem cells (MSC/IL-12p40) in a dextran sulfate sodium salt (DSS)-induced colitis model. Injection of rAd/IL-12p40 or MSC/IL-12p40 efficiently attenuated colitis symptoms and tissue damage, leading to an increased survival rate. Moreover, IL-12p40 delivery suppressed IL-17A, but enhanced IFN-γ production from mesenteric lymph node cells, supporting the preferential suppression of IL-23 by IL-12p40 homodimer *in vitro* and the suppression of Th17 responses *in vivo*. Our results demonstrate that IL-12p40 delivery ameliorates DSS-induced colitis by suppressing IL-17A production and inflammation in the intestinal mucosa, providing an effective new therapeutic strategy for IBDs.

PMID: 22836084

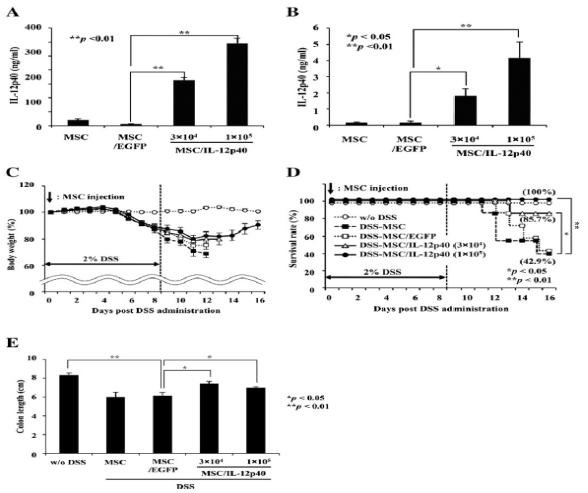

Keywords : DSS-induced colitis; Inflammatory bowel disease (IBD); IL-12p40; IL-17A

Article 259

A novel reassortant canine H3N1 influenza virus between pandemic H1N1 and canine H3N2 influenza viruses in Korea

J Gen Virol. 93(Pt 3):551-4.

Song D*, Moon HJ, An DJ, Jeoung HY, Kim H, Yeom MJ, Hong M, Nam JH, Park SJ, Park BK, Oh JS, Song M, Webster RG, Kim JK, Kang BK

*First: sds1@kribb.re.kr
Viral Infectious Disease Research Center

During recent canine influenza surveillance in South Korea, a novel H3N1 canine influenza virus (CIV) that is a putative reassortant between pandemic H1N1 2009 and H3N2 CIVs was isolated. Genetic analysis of eight genes of the influenza virus revealed that the novel H3N1 isolate presented high similarities (99.1-99.9%) to pandemic influenza H1N1, except for in the haemagglutinin (HA) gene. The HA gene nucleotide sequence of the novel CIV H3N1 was similar (99.6%) to that of CIV H3N2 isolated in Korea and China. Dogs infected with the novel H3N1 CIV did not show any notable symptoms, in contrast to dogs infected with H3N2 CIV. Despite no visible clinical signs of disease, nasal shedding of virus was detected and the infected dogs presented mild histopathological changes.

PMID: 22131311

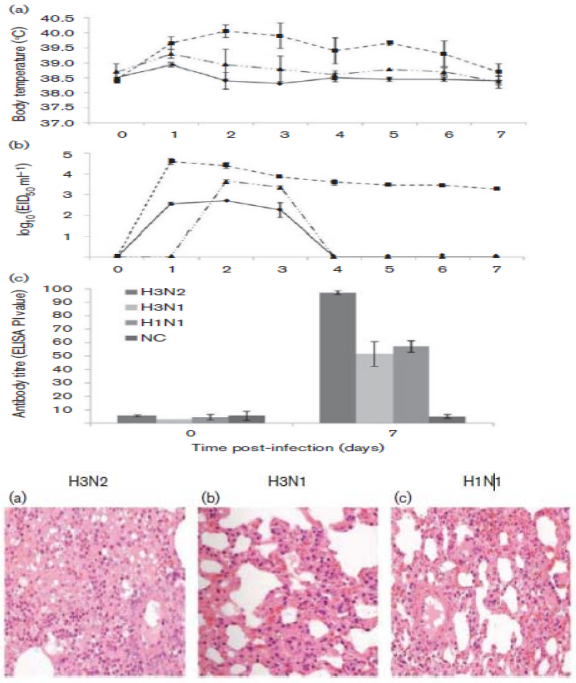

Keywords : Dogs; H1N1 2009; H3N1 canine influenza virus (CIV); H3N2 CIVs; Histopathological changes

Article 260

Complete genome sequence of an avian-origin H3N2 canine influenza virus isolated from dogs in South Korea

J Virol. 86(17):9548-9.

Park SJ, Moon HJ, Kang BK, Hong M, Na W, Kim JK, Poo H, Park BK, Song DS*

*Co-corresponding: sds1@kribb.re.kr
Viral Infectious Disease Research Center

An avian-origin Korean H3N2 canine influenza virus (CIV) strain, designated A/canine/Korea/01/2007 (H3N2), was isolated from nasal swabs of pet dogs exhibiting severe respiratory syndrome in 2007. In the present study, we report the first complete genome sequence containing 3' and 5' noncoding regions (NCRs) of H3N2 CIV, which will provide important insights into the molecular basis of pathogenesis, transmission, and evolution of CIV.
PMID: 22879618

Keywords : Genome sequence; H3N2 canine influenza virus (CIV); Pathogenesis; Pet dogs

Article 261

Complete genome analysis of porcine enterovirus B isolated in Korea

J Virol. 86(18):10250.

Moon HJ, Song D*, Seon BH, Kim HK, Park SJ, An DJ, Kim JM, Kang BK, Park BK

*Co-first: sds1@kribb.re.kr
Viral Infectious Disease Research Center

The complete genome sequence of porcine enterovirus B (PEV-B) from a Korean isolate was analyzed. The genome size was 7,393 bp. Previously, full genome sequences of PEV-B had been reported from the United Kingdom, Hungary, and China. The Korean PEV-B isolate presented polyprotein gene nucleotide sequence similarities of 77.9, 73.7, 78.9, and 80.3%, respectively, to PEV-B UKG/410/73, LP54, PEV15, and Chinese strains (Ch-ah-f1).
PMID:22923807

Keywords : Genome sequence; Polyprotein gene nucleotide sequence; Porcine enterovirus B (PEV-B)

Article 262

Porcine epidemic diarrhoea virus: a comprehensive review of molecular epidemiology, diagnosis, and vaccines

Virus Genes. 44(2):167-75.

Song D*, Park B

*First: sds1@kribb.re.kr
Viral Infectious Disease Research Center

The porcine epidemic diarrhoea virus (PEDV), a member of the Coronaviridae family, causes acute diarrhoea and dehydration in pigs. Although it was first identified in Europe, it has become increasingly problematic in many Asian countries, including Korea, China, Japan, the Philippines, and Thailand. The economic impacts of the PEDV are substantial, given that it results in significant morbidity and mortality in neonatal piglets and is associated with increased costs related to vaccination and disinfection. Recently, progress has been made in understanding the molecular epidemiology of PEDV, thereby leading to the development of new vaccines. In the current review, we first describe the molecular and genetic characteristics of the PEDV. Then we discuss its molecular epidemiology and diagnosis, what vaccines are available, and how PEDV can be treated.
PMID: 22270324

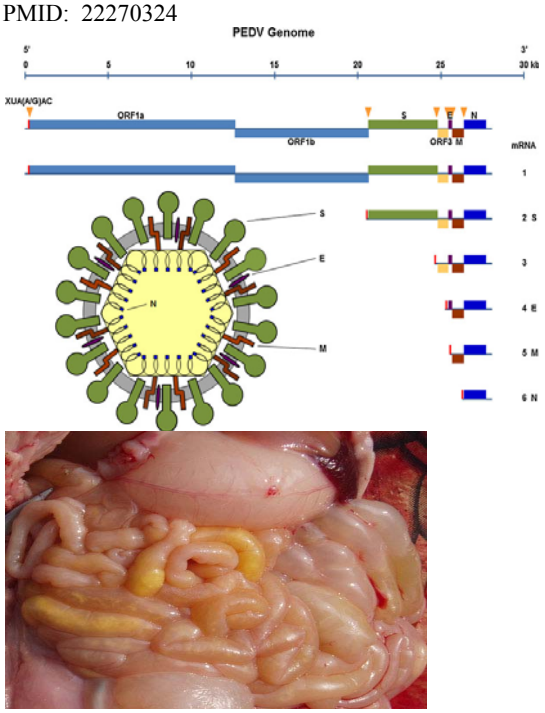

Keywords : Diagnosis; Molecular epidemiology; Porcine epidemic diarrhoea virus; Review; Vaccine


KRIBB
www.kribb.re.kr

Korean Bioinformation Center

Korean Bioinformation Center

Article 263

GoBean: a Java GUI application for visual exploration of GO term enrichments

BMB Rep. 45(2):120-5.

Lee S*, Cha JY, Kim H, Yu U

*First:
Korean Bioinformation Center

We have developed a biologist-friendly, Java GUI application (GoBean) for GO term enrichment analysis. It was designed to be a comprehensive and flexible GUI tool for GO term enrichment analysis, combining the merits of other programs and incorporating extensive graphic exploration of enrichment results. An intuitive user interface with multiple panels allows for extensive visual scrutiny of analysis results. The program includes many essential and useful features, such as enrichment analysis algorithms, multiple test correction methods, and versatile filtering of enriched GO terms for more focused analyses. A unique graphic interface reflecting the GO tree structure was devised to facilitate comparisons of multiple GO analysis results, which can provide valuable insights for biological interpretation. Additional features to enhance user convenience include built in ID conversion, evidence code-based gene-GO association filtering, set operations of gene lists and enriched GO terms, and user -provided data files. It is available at http://neon.gachon.ac.kr/GoBean/.
PMID:22360891

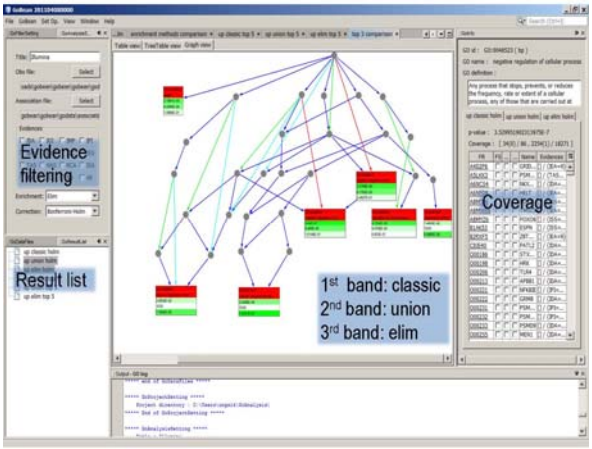

Keywords : Bioinformatics; Gene list analysis; Gene ontology; GoBean; Java GUI application

Article 264

Comparison and evaluation of pathway-level aggregation methods of gene expression data

BMC Genomics. 13(Suppl 7):S26.

Hwang S*

*Corresponding: swhwang@kribb.re.kr
Korean Bioinformation Center

BACKGROUND: Microarray experiments produce expression measurements in genomic scale. While a common practice for the pathway-level analysis has been functional enrichment analysis such as over-representation analysis and gene set enrichment analysis, an alternative approach has also been explored. In this approach, gene expression data are first aggregated at pathway level to transform the original data into a compact representation. Thereafter the pathway expression data can be used for differential expression and classification analyses in pathway space, leveraging existing algorithms usually applied to gene expression data. It remains unclear how they compare with one another, since the evaluations were done to a limited extent.
RESULTS: The compared methods include five existing methods--mean of all member genes (*Mean all*), mean of condition-responsive genes (*Mean CORGs*), analysis of sample set enrichment scores (ASSESS), principal component analysis (PCA), and partial least squares (PLS)--and a variant of an existing method (*Mean top 50%*, averaging top half of member genes). Comprehensive and stringent benchmarking was performed by collecting seven pairs of related but independent datasets encompassing various phenotypes. Aggregation was done in the space of KEGG pathways. Performance of the methods was assessed by classification accuracy validated both internally and externally, and by examining the correlative extent of pathway signatures between the dataset pairs. The assessment revealed that (i) the best accuracy and correlation were obtained from ASSESS and *Mean top 50%*, (ii) *Mean all* showed the lowest accuracy, and (iii) *Mean CORGs* and PLS gave rise to the largest extent of discordance in the pathway signature correlation.
CONCLUSIONS: The two best performing method (ASSESS and *Mean top 50%*) are suggested to be preferred. The benchmarking analysis also suggests that there is both room and necessity for developing a novel method for pathway-level aggregation.
PMID: 23282027

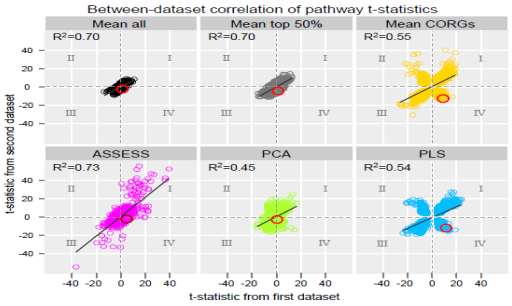

Keywords : Compared methods; Gene expression data; Pathway-level aggregation; Pathway signatures

Article 265

A hybrid modeling strategy using Nuclear Overhauser Effect data with contact information

Chem Phys Lett. 554:190-4.

Kim TR, Ji S, Lee S, Chu IS, Shin S, Lee J*

*Corresponding: jinhyuk@kribb.re.kr
Korean Bioinformation Center

A hybrid modeling strategy using readily assigned Nuclear Overhauser Effect (NOE) data and main chain N-O contact information from homology template proteins is suggested. They are designed to be complementary. The strategy yields structures with reasonable root-mean square distance (RMSD) and NOE violation. When compared to homology-modeled structures, the hybrid-modeled structures are better in terms of RMSD, RMS NOE violation, and protein-like scores, although the number of used restraints is smaller than the homology modeling. The structure itself can be used as a theoretically modeled structure and also as a starting point for further NOE data assignment in structure determination.

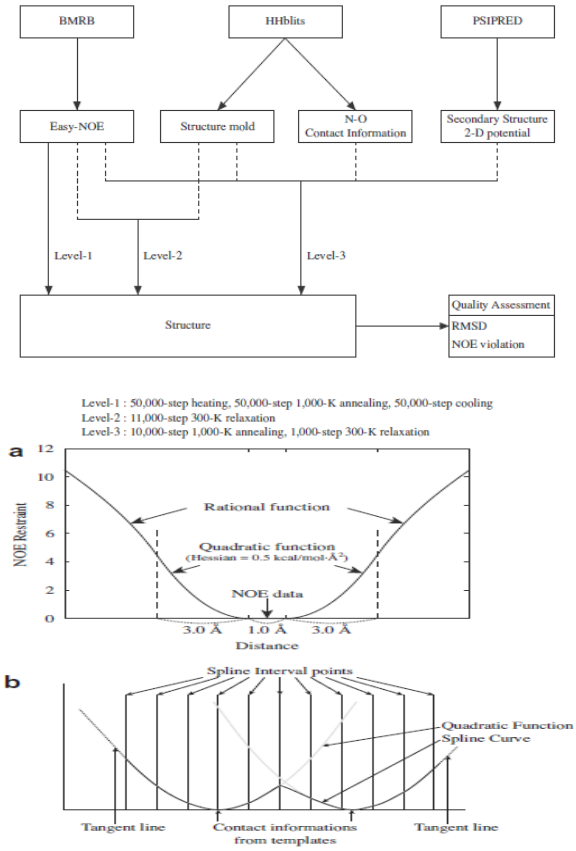

Keywords : Homology modeling; Hybrid modeling; Main chains; Nuclear overhauser effects; Root Mean Square; Structure determination

Article 266

Computational prediction of protein-protein interactions of human tyrosinase

Enzyme Res. 2012:192867.

Wang SF, Oh S, Si YX, Wang ZJ, Han HY, Lee J*, Qian GY

*Co-corresponding: jinhyuk@kribb.re.kr
Korean Bioinformation Center

The various studies on tyrosinase have recently gained the attention of researchers due to their potential application values and the biological functions. In this study, we predicted the 3D structure of human tyrosinase and simulated the protein-protein interactions between tyrosinase and three binding partners, four and half LIM domains 2 (FHL2), cytochrome b-245 alpha polypeptide (CYBA), and RNA-binding motif protein 9 (RBM9). Our interaction simulations showed significant binding energy scores of -595.3 kcal/mol for FHL2, -859.1 kcal/mol for CYBA, and -821.3 kcal/mol for RBM9. We also investigated the residues of each protein facing toward the predicted site of interaction with tyrosinase. Our computational predictions will be useful for elucidating the protein-protein interactions of tyrosinase and studying its binding mechanisms.
PMID:22577521

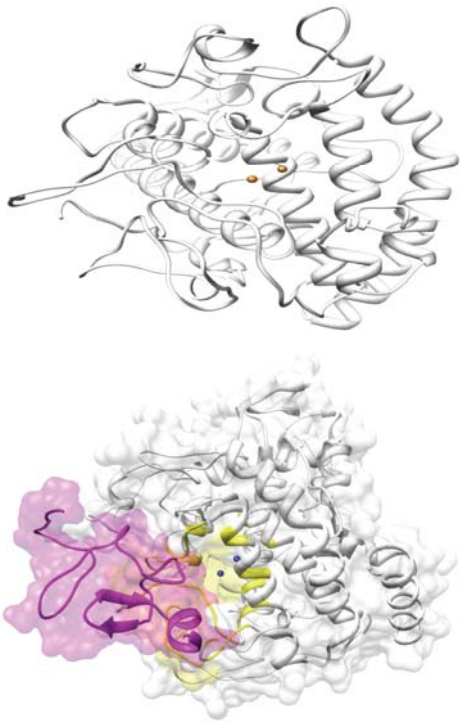

Keywords : Binding mechanisms; Computational prediction; Human tyrosinase; Protein-protein interaction

Article 267

The Effect of D-(-)-arabinose on Tyrosinase: An Integrated Study Using Computational Simulation and Inhibition Kinetics

Enzyme Res. 2012:731427.

Liu HJ, Ji S, Fan YQ, Yan L, Yang JM, Zhou HM, Lee J*, Wang YL

*Co-corresponding: jinhyuk@kribb.re.kr
Korean Bioinformation Center

Tyrosinase is a ubiquitous enzyme with diverse physiologic roles related to pigment production. Tyrosinase inhibition has been well studied for cosmetic, medicinal, and agricultural purposes. We simulated the docking of tyrosinase and D-(-)-arabinose and found a binding energy of -4.5 kcal/mol for theup-formof D-(-)-arabinose and -4.4 kcal/mol for thedown-form of D-(-)-arabinose. The results of molecular dynamics simulation suggested that D-(-)-arabinose interacts mostly with HIS85, HIS259, and HIS263, which are believed to be in the active site. Our kinetic study showed that D-(-)-arabinose is a reversible, mixed-type inhibitor of tyrosinase (α-value = 6.11 ± 0.98, K_i = 0.21 ± 0.19 M). Measurements of intrinsic fluorescence showed that D-(-)-arabinose induced obvious tertiary changes to tyrosinase (binding constant K = 1.58 ± 0.02 M^{-1}, binding number *n* = 1.49 ± 0.06). This strategy of predicting tyrosinase inhibition based on specific interactions of aldehyde and hydroxyl groups with the enzyme may prove useful for screening potential tyrosinase inhibitors.
PMID:23365724

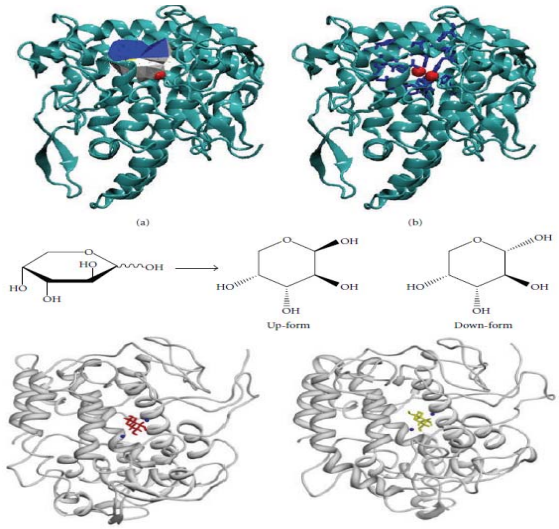

Keywords : Arabinose; Intrinsic fluorescence; Molecular dynamics simulation; Protein-ligand interaction; Tyrosinase inhibitors

Article 268

Genome sequence of the thermotolerant yeast *Kluyveromyces marxianus* var. *marxianus* KCTC 17555

Eukaryot Cell. 11(12):1584-5.

Jeong H*, Lee DH, Kim SH, Kim HJ, Lee K, Song JY, Kim BK, Sung BH, Park JC, Sohn JH, Koo HM, Kim JF

*Corresponding: hyjeong@kribb.re.kr
Korean Bioinformation Center

Kluyveromyces marxianus is a thermotolerant yeast that has been explored for potential use in biotechnological applications, such as production of biofuels, single-cell proteins, enzymes, and other heterologous proteins. Here, we present the high-quality draft of the 10.9-Mb genome of *K. marxianus* var. *marxianus* KCTC 17555 (= CBS 6556 = ATCC 26548).
PMID: 23193140

Keywords : Genome sequence; *Kluyveromyces marxianus*; Thermotolerant yeast

Article 269

Discovery of *ALK-PTPN3* gene fusion from human non-small cell lung carcinoma cell line using next generation RNA sequencing

Genes Chromosom Cancer. 51(6):590-7.

Jung Y, Kim P, Jung Y, Keum J, Kim SN, Choi YS, Do IG, Lee J, Choi SJ, Kim S, Lee JE, Kim J, Lee S*, Kim J

*Corresponding:
Korean Bioinformation Center

An increasing number of chromosomal aberrations is being identified in solid tumors providing novel biomarkers for various types of cancer and new insights into the mechanisms of carcinogenesis. We applied next generation sequencing technique to analyze the transcriptome of the non-small cell lung carcinoma (NSCLC) cell line H2228 and discovered a fusion transcript composed of multiple exons of *ALK* (anaplastic lymphoma receptor tyrosine kinase) and *PTPN3* (protein tyrosine phosphatase, nonreceptor Type 3). Detailed analysis of the genomic structure revealed that a portion of genomic region encompassing Exons 10 and 11 of *ALK* has been translocated into the intronic region between Exons 2 and 3 of *PTPN3*. The key net result appears to be the null mutation of one allele of *PTPN3*, a gene with tumor suppressor activity. Consistently, ectopic expression of *PTPN3* in NSCLC cell lines led to inhibition of colony formation. Our study confirms the utility of next generation sequencing as a tool for the discovery of somatic mutations and has led to the identification of a novel mutation in NSCLC that may be of diagnostic, prognostic, and therapeutic importance.
PMID:22334442

Keywords : Chromosomal aberrations; Genomic structure; Next generation sequencing; Novel mutation; Non-small cell lung carcinoma (NSCLC)

Article 270

Sixty-five gene-based risk score classifier predicts overall survival in hepatocellular carcinoma

Hepatology. 55(5):1443-52.

Kim SM, Leem SH, Chu IS*, Park YY, Kim SC, Kim SB, Park ES, Lim JY, Heo J, Kim YJ, Kim DG, Kaseb A, Park YN, Wang XW, Thorgeirsson SS, Lee JS

*Co-first: chu@kribb.re.kr
Korean Bioinformation Center

Clinical application of the prognostic gene expression signature has been delayed due to the large number of genes and complexity of prediction algorithms. In the current study we aimed to develop an easy-to-use risk score with a limited number of genes that can robustly predict prognosis of patients with hepatocellular carcinoma (HCC). The risk score was developed using Cox coefficient values of 65 genes in the training set (n = 139) and its robustness was validated in test sets (n = 292). The risk score was a highly significant predictor of overall survival (OS) in the first test cohort ($P = 5.6 \times 10^{-5}$, n = 100) and the second test cohort ($P = 5.0 \times 10^{-5}$, n = 192). In multivariate analysis, the risk score was a significant risk factor among clinical variables examined together (hazard ratio [HR], 1.36; 95% confidence interval [CI], 1.13-1.64; $P = 0.001$ for OS).
CONCLUSION: The risk score classifier we have developed can identify two clinically distinct HCC subtypes at early and late stages of the disease in a simple and highly reproducible manner across multiple datasets.
PMID:22105560

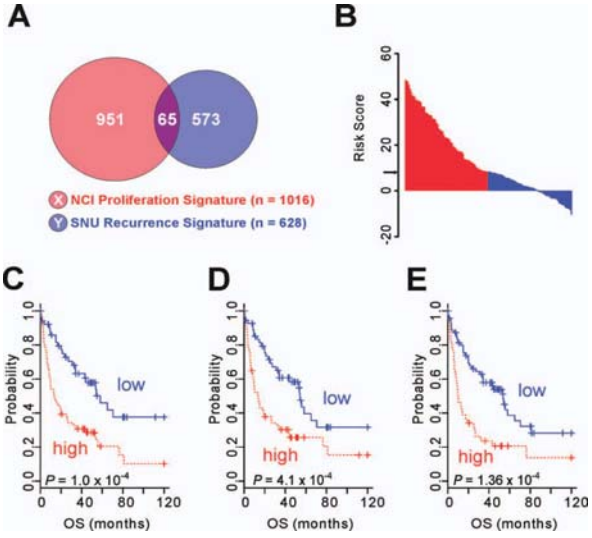

Keywords : Hepatocellular carcinoma (HCC); Multivariate analysis; Overall survival (OS); Prognostic gene expression signature; Risk score

Article 271

Draft genome sequence of *Paenibacillus peoriae* strain KCTC 3763T

J Bacteriol. 194(5):1237-8.

Jeong H*, Choi SK, Park SY, Kim SH, Park SH

*Corresponding: hyjeong@kribb.re.kr
Korean Bioinformation Center

Paenibacillus peoriae is a potentially plant-beneficial soil bacterium and is a close relative to *Paenibacillus polymyxa*, the type species of the genus *Paenibacillus*. Herein, we present the 5.77-Mb draft genome sequence of the *P. peoriae* type strain with the aim of providing insight into the genomic basis of plant growth-promoting *Paenibacillus* species.
PMID: 22328743

Keywords : Genome sequence; *Paenibacillus peoriae*; Plant growth-promoting; Soil bacterium

Article 272

Genome sequence of the hemolytic-uremic syndrome-causing strain *Escherichia coli* NCCP15647

J Bacteriol. 194(14):3747-8.

Jeong H*, Zhao F, Igori D, Oh KH, Kim SY, Kang SG, Kim BK, Kwon SK, Lee CH, Song JY, Yu DS, Park MS, Cho SH, Kim JF

*Co-first: hyjeong@kribb.re.kr
Korean Bioinformation Center

Enterohemorrhagic *Escherichia coli* (EHEC) causes a disease involving diarrhea, hemorrhagic colitis, and hemolytic-uremic syndrome (HUS). Here we present the draft genome sequence of NCCP15647, an EHEC isolate from an HUS patient. Its genome exhibits features of EHEC, such as genes for verotoxins, a type III secretion system, and prophages.
PMID:22740672

Keywords : Enterohemorrhagic *Escherichia coli* (EHEC); Genome sequence; Hemolytic-uremic syndrome (HUS)

Article 273

Complete genome sequence of the probiotic bacterium *Bifidobacterium bifidum* strain BGN4

J Bacteriol. 194(17):4757-8.

Yu DS*, Jeong H*, Lee DH, Kwon SK, Song JY, Kim BK, Park MS, Ji GE, Oh TK, Kim JF

*Co-first: axxa76@kribb.re.kr hyjeong@kribb.re.kr
Super-Bacteria Research Center

Bifidobacterium bifidum, a common endosymbiotic inhabitant of the human gut, is considered a prominent probiotic microorganism that may promote health. We completely decrypted the 2.2-Mb genome sequence of *B. bifidum* BGN4, a strain that had been isolated from the fecal sample of a healthy breast-fed infant, and annotated 1,835 coding sequences.
PMID: 22887663

Keywords : *Bifidobacterium bifidum*; Endosymbiotic inhabitant; Genome sequence; Probiotic bacterium

Article 274

Draft genome sequence of *Bacillus endophyticus* 2102

J Bacteriol. 194(20):5705-6.

Lee YJ, Lee SJ, Kim SH, Lee SJ, Kim BC, Lee HS, Jeong H*, Lee DW

*Co-corresponding: hyjeong@kribb.re.kr
Korean Bioinformation Center

Bacillus endophyticus 2102 is an endospore-forming, plant growth-promoting rhizobacterium isolated from a hypersaline pond in South Korea. Here we present the draft sequence of *B. endophyticus* 2102, which is of interest because of its potential use in the industrial production of algaecides and bioplastics and for the treatment of industrial textile effluents.
PMID: 23012284

Keywords : Algaecides; *Bacillus endophyticus*; Bioplastics; Genome sequence; Plant growth-promoting; Textile effluents

Article 275

Draft genome sequence of *Staphylococcus vitulinus* F1028, a strain isolated from a block of fermented soybean

J Bacteriol. 194(21):5961-2.

Nam YD, Chung WH*, Seo MJ, Lim SI.

*Co-first: whchung@kribb.re.kr
Super-Bacteria Research Center

Staphylococcus vitulinus is a coagulase-negative staphylococcus in the family *Staphylococcaceae*. This report describes the draft genome sequence of *S. vitulinus* F1028, which was isolated from a traditional Korean soybean food (meju). This 2.56-Mbp genome sequence is the first *S. vitulinus* genome of a strain isolated from a fermented soybean product.
PMID:23045483

Keywords : Genome sequence; Meju; Soybean; *Staphylococcus vitulinus*

Article 276

An integrated study of tyrosinase inhibition by rutin: progress using a computational simulation

J Biomol Struct Dyn. 29(5):999-1012.

Si YX, Yin SJ, Oh S, Wang ZJ, Ye S, Yan L, Yang JM, Park YD, Lee J*, Qian GY

*Co-corresponding: jinhyuk@kribb.re.kr
Korean Bioinformation Center

Tyrosinase inhibition studies have recently gained the attention of researchers due to their potential application values. We simulated docking (binding energies for AutoDock Vina: -9.1 kcal/mol) and performed a molecular dynamics simulation to verify docking results between tyrosinase and rutin. The docking results suggest that rutin mostly interacts with histidine residues located in the active site. A 10 ns molecular dynamics simulation showed that one copper ion at the tyrosinase active site was responsible for the interaction with rutin. Kinetic analyses showed that rutin-mediated inactivation followed a first-order reaction and mono- and biphasic rate constants occurred with rutin. The inhibition was a typical competitive type with K_i = 1.10±0.25 mM. Measurements of intrinsic and ANS-binding fluorescences showed that rutin showed a relatively strong binding affinity for tyrosinase and one possible binding site that could be a copper was detected accompanying with a hydrophobic exposure of tyrosinase. Cell viability testing with rutin in HaCaT keratinocytes showed that no toxic effects were produced. Taken together, rutin has the potential to be a potent anti-pigment agent. The strategy of predicting tyrosinase inhibition based on hydroxyl group number and computational simulation may prove useful for the screening of potential tyrosinase inhibitors.
PMID:22292957

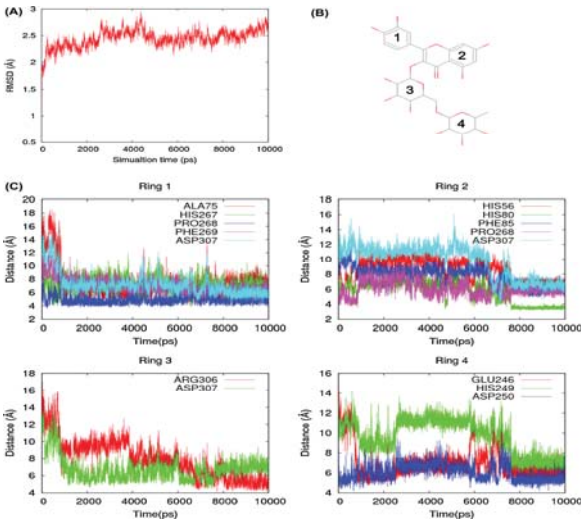

Keywords : Docking simulation; Hydroxyl group; Inhibition kinetics; Rutin; Tyrosinase

Article 277

The effect of fucoidan on tyrosinase: computational molecular dynamics integrating inhibition kinetics

J Biomol Struct Dyn. 2012;30(4):460-73.

Wang ZJ, Si YX, Oh S, Yang JM, Yin SJ, Park YD, Lee J*, Qian GY

*Co-corresponding: jinhyuk@kribb.re.kr
Korean Bioinformation Center

Fucoidan is a complex sulfated polysaccharide extracted from brown seaweed and has a wide variety of biological activities. In this study, we investigated the inhibitory effect of fucoidan on tyrosinase via a combination of inhibition kinetics and computational simulations. Fucoidan reversibly inhibited tyrosinase in a mixed-type manner. Time-interval kinetics showed that the inhibition was processed as first order with biphasic processes. For further insight, we simulated dockings with various sizes of molecular models (monomer to decamer) of fucoidan and showed that the best binding energy change results were obtained from the pentamer (-1.89 kcal/mol) and the hexamer (-1.97 kcal/mol) models of AutoDock Vina. The molecular dynamics simulation confirmed the binding mechanisms between tyrosinase and fucoidan and suggested that fucoidan mostly interacts with several residues including copper ions located in the active site. Our study suggests that fucoidan might be a potential natural antipigment agent.

PMID:22694253

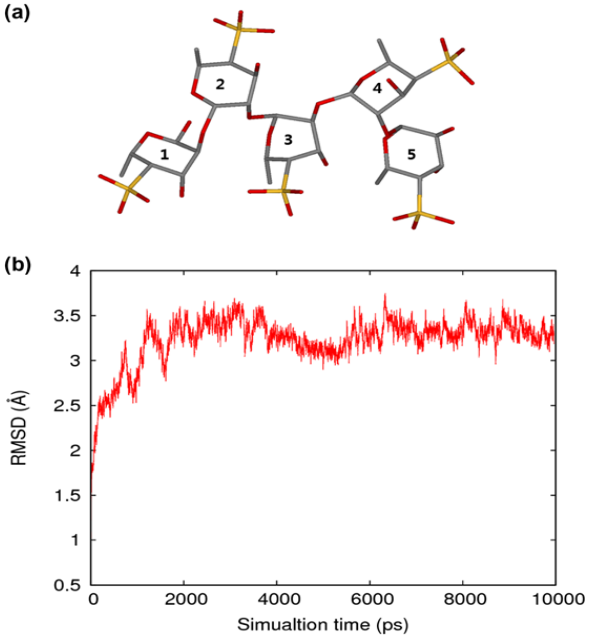

Keywords : Docking simulation; Fucoidan; Inhibition kinetics; Molecular dynamics simulation; Tyrosinase

Article 278

A simplified homology-model builder toward highly protein-like structures: an inspection of restraining potentials

J Comput Chem. 33(24):1927-35.

Kim TR, Oh S, Yang JS, Lee S, Shin S, Lee J*

*Co-corresponding: jinhyuk@kribb.re.kr
Korean Bioinformation Center

A homology model builder using simple restraining potentials based on spline-interpolated quadratic functions is developed and interfaced with CHARMM package. The continuity and stability of the potential function were validated, and the parameters were optimized using the CASP7 targets. The performance of the model builder was benchmarked to the Modeller program using the template-based modeling targets in CASP9. The benchmark results show that, while our builder yields the structures with slightly lower packing, backbone, and template modeling scores, our models show much better protein-like scores in terms of normalized discrete optimized protein energy, dipolar distance-scaled finite-ideal gas reference, Molprobity clash, Ramachandran appearance *Z*-score, and rotamer *Z*-score. As our model builder is interfaced with CHARMM, it is advantageous to directly use other CHARMM functionality and energy functions to refine the model structures or to use the models for other computational studies using CHARMM.

PMID:22648914

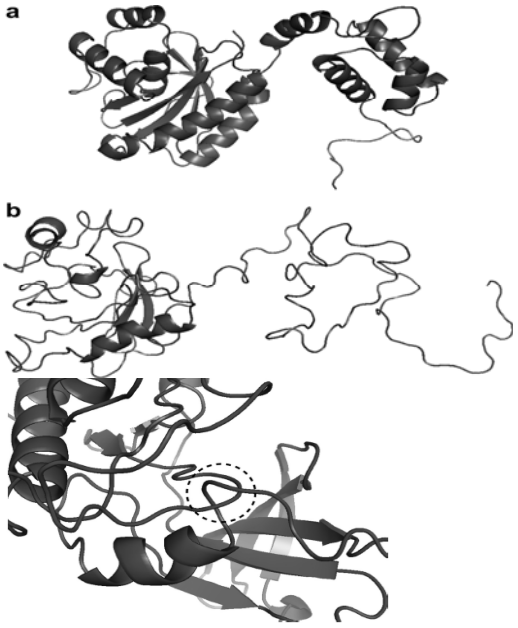

Keywords : CHARMM functionality; Homology modeling; Protein-like scores; PQR-SA

Article 279

Changes in membrane fatty acid composition through proton-induced *fabF* mutation enhancing 1-butanol tolerance in *E. coli*

J Kor Phys Soc. 61(2):227-33.

Jeong H*, Kim SH, Han SS, Kim MH, Lee KC

*Corresponding: hyjeong@kribb.re.kr
Korean Bioinformation Center

While a rational approach based on genomic data has become the preferred method for microbial strain development, radiation-induced random mutagenesis is still a robust method for organisms such as plants whose genome or target gene information is unavailable. We previously reported on a combined approach that consists of proton irradiation and a long-term experimental evolution to enhance 1-butanol tolerance of the *E. coli* C strain so that it can be used as a basal strain for the production of 1-butanol, a potential biofuel along with ethanol. Genome sequencing of one randomly chosen clone (PKH5000) from the endpoint population revealed eleven mutations occurring in the coding regions, and we found that a mutation (F74C) in *fabF* gene encoding β-ketoacyl-ACP synthases II is associated with a twofold increase in the major unsaturated fatty acid, *cis*-vaccenic acid. The increase of *cis*-vaccenic acid by wild-type FabF, which is more active at low temperatures or in the presence of organic compounds, is considered to be a protective mechanism against cold stress. A structural analysis of the FabF protein suggests that the F74C mutation may affect the enzyme activity through a change in flexibility around the catalytic site. The expression of a plasmid that harbors mutant *fabF* gene in the *fabF* knockout strain enhanced growth in a medium containing butanol with a concomitant elevation of the *cis*-vaccenic acid level. Among the eight available Keio knockout strains for genes that have amino acid substitution in the PKH5000 strain, the *fabF* mutant showed the slowest growth in the presence of 0. 7% butanol. We propose that *fabF*, as probably the gene most responsible for butanol tolerance in wild-type form, contributes further when converted into a F74C missense mutation, which is beneficial as it increases the level of *cis*-vaccenic acid.

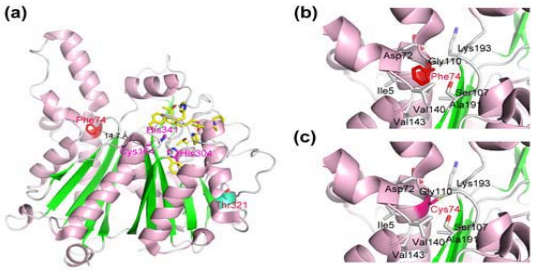

Keywords : 1-butanol; *cis*-vaccenic acid; *Escherichia coli*; *fabF*; Mutation; Proton beam; Tolerance

Article 280

Algorithm for predicting functionally equivalent proteins from BLAST and HMMER searches

J Microbiol Biotechnol. 22(8):1054-8.

Yu DS*, Lee DH, Kim SK, Lee CH, Song JY, Kong EB, Kim JF

*First: axxa76@kribb.re.kr
Korean Bioinformation Center

In order to predict biologically significant attributes such as function from protein sequences, searching against large databases for homologous proteins is a common practice. In particular, BLAST and HMMER are widely used in a variety of biological fields. However, sequencehomologous proteins determined by BLAST and proteins having the same domains predicted by HMMER are not always functionally equivalent, even though their sequences are aligning with high similarity. Thus, accurate assignment of functionally equivalent proteins from aligned sequences remains a challenge in bioinformatics. We have developed the FEP-BH algorithm to predict functionally equivalent proteins from protein-protein pairs identified by BLAST and from protein-domain pairs predicted by HMMER. When examined against domain classes of the Pfam-A seed database, FEP-BH showed 71.53% accuracy, whereas BLAST and HMMER were 57.72% and 36.62%, respectively. We expect that the FEP-BH algorithm will be effective in predicting functionally equivalent proteins from BLAST and HMMER outputs and will also suit biologists who want to search out functionally equivalent proteins from among sequence-homologous proteins.

PMID: 22713980

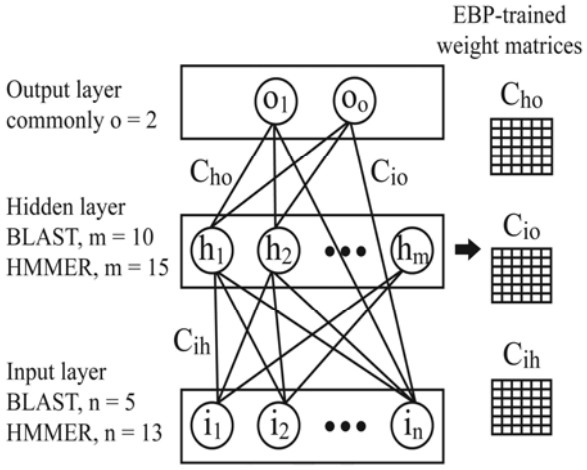

Keywords : Artificial neural network; Bioinformatics; Error backpropagation algorithm; Functionally equivalent protein; Sequence-based method

Article 281

Genome-wide identification of palmitate-regulated immediate early genes and target genes in pancreatic beta-cells reveals a central role of NF-κB

Mol Biol Rep. 39(6):6781-9.

Choi HJ, Hwang S*, Lee SH, Lee YR, Shin J, Park KS, Cho YM

*Co-first: swhwang@kribb.re.kr
Korean Bioinformation Center

Free fatty acid-induced pancreatic β-cell dysfunction plays a key role in the pathogenesis of type 2 diabetes. We conducted gene expression microarray analysis to comprehensively investigate the transcription machinery of palmitate-regulated genes in pancreatic β-cells *in vitro*. In particular, mouse pancreatic βTC3 cells were treated with palmitate in the presence or absence of cycloheximide (CHX), which blocks protein synthesis and thereby allows us to distinguish immediate early genes (IEGs) from their target genes. The microarray experiments identified 34 palmitate-regulated IEGs and 74 palmitate-regulated target genes. *In silico* promoter analysis revealed that transcription factor binding sites for NF-κB were over-represented, regulating approximately one-third of the palmitate-regulated target genes. In cells treated with CHX, *nfkb1* showed an up-regulation by palmitate, suggesting that NF-κB could be an IEG. Functional enrichment analysis of 27 palmitate-regulated genes with NF-κB binding sites showed an over-representation of genes involved in immune response, inflammatory response, defense response, taxis, regulation of cell proliferation, and regulation of cell death pathways. Electrophoretic mobility shift assay showed that palmitate stimulates NF-κB activity both in the presence and absence of CHX. In conclusion, by identifying IEGs and target genes, the present study depicted a comprehensive view of transcription machinery underlying palmitate-induced inflammation and cell proliferation/death in pancreatic β-cells and our data demonstrated the central role of NF-κB.

PMID:22302392

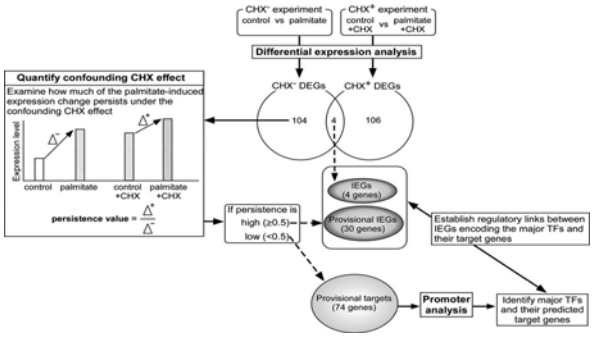

Keywords : Fatty acids; Immediate-early gene; Insulin-secreting cells; NF-κB; Nonesterified Genes; Oligonucleotide array sequence analysis; Palmitates

Article 282

STAP Refinement of the NMR database: a database of 2405 refined solution NMR structures

Nucleic Acids Res. 40(D):D525-30.

Yang JS, Kim JH, Oh S, Han G, Lee S, Lee J*

*Corresponding: jinhyuk@kribb.re.kr
Korean Bioinformation Center

According to several studies, some nuclear magnetic resonance (NMR) structures are of lower quality, less reliable and less suitable for structural analysis than high-resolution X-ray crystallographic structures. We present a public database of 2405 refined NMR solution structures [statistical torsion angle potentials (STAP) refinement of the NMR database, http://psb.kobic.re.kr/STAP/refinement] from the Protein Data Bank (PDB). A simulated annealing protocol was employed to obtain refined structures with target potentials, including the newly developed STAP. The refined database was extensively analysed using various quality indicators from several assessment programs to determine the nuclear Overhauser effect (NOE) completeness, Ramachandran appearance, χ_1-χ_2 rotamer normality, various parameters for protein stability and other indicators. Most quality indicators are improved in our protocol mainly due to the inclusion of the newly developed knowledge-based potentials. This database can be used by the NMR structure community for further development of research and validation tools, structure-related studies and modelling in many fields of research.

PMID: 22102572

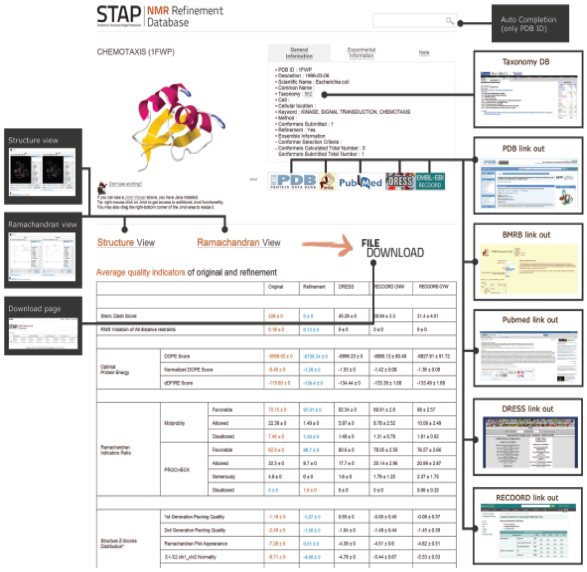

Keywords : Database; NMR; Nuclear Overhauser effect (NOE); Simulated annealing protocol; STAP

Article 283

hiPathDB: a human-integrated pathway database with facile visualization

Nucleic Acids Res. 40(D):D797-802.

Yu N, Seo J, Rho K, Jang Y, Park J, Kim WK, Lee S*

*Corresponding:
Korean Bioinformation Center

One of the biggest challenges in the study of biological regulatory networks is the systematic organization and integration of complex interactions taking place within various biological pathways. Currently, the information of the biological pathways is dispersed in multiple databases in various formats. hiPathDB is an integrated pathway database that combines the curated human pathway data of NCI-Nature PID, Reactome, BioCarta and KEGG. In total, it includes 1661 pathways consisting of 8976 distinct physical entities. hiPathDB provides two different types of integration. The pathway-level integration, conceptually a simple collection of individual pathways, was achieved by devising an elaborate model that takes distinct features of four databases into account and subsequently reformatting all pathways in accordance with our model. The entity-level integration creates a single unified pathway that encompasses all pathways by merging common components. Even though the detailed molecular-level information such as complex formation or post-translational modifications tends to be lost, such integration makes it possible to investigate signaling network over the entire pathways and allows identification of pathway cross-talks. Another strong merit of hiPathDB is the built-in pathway visualization module that supports explorative studies of complex networks in an interactive fashion. The layout algorithm is optimized for virtually automatic visualization of the pathways. hiPathDB is available at http://hiPathDB.kobic.re.kr.

PMID: 22123737

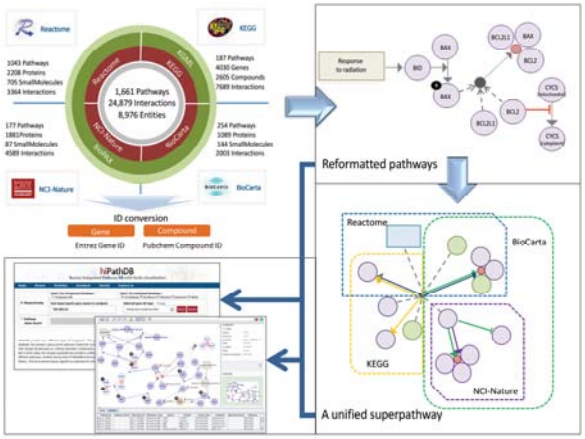

Keywords : Entity-level integration; hiPathDB; Integrated pathway database; Pathway-level integration; Signaling network

Article 284

Towards alpha-glucosidase folding induced by trifluoroethanol: Kinetics and computational prediction

Process Biochem. 47(12):2284-90.

Zeng YF, Lü ZR, Yan L, Oh S, Yang JM, Lee J*, Ye ZM

*Co-corresponding: jinhyuk@kribb.re.kr
Korean Bioinformation Center

Alpha-glucosidase (EC 3.2.1.20) is an enzyme, which is related with diabetes mellitus type 2 clinically, and is also generally used to convert starch to fermentable sugars in the industry. Therefore, study on this enzyme structures and functions is important. In this study, we investigated structural changes in the alpha-glucosidase during trifluoroethanol (TFE)-induced unfolding. The activity of alpha-glucosidase was significantly inactivated by TFE in a dose-dependent manner. The inactivation was composed of two-phases. TFE inhibited alpha-glucosidase in a parabolic mixed-type reaction (K_i = 0.72 ± 0.08 M). TFE directly induced the unfolding and hydrophobic exposure of alpha-glucosidase. We also simulated the docking between alpha-glucosidase and TFE, as well as molecular dynamics. The computational simulations suggested that several residues, such as ASP68, TYR71, VAL108, HIS111, PHE177, ASP214, THR215, GLU276, HIS348, ASP349, and ARG439, interact with TFE. The molecular dynamics simulation confirmed the binding mechanisms, between the alpha-glucosidase and TFE, and suggested that TFE inhibits the glucose binding site. Our study provides insights into the alpha-glucosidase folding behaviors, and cosolvent binding under a 3D structural simulation.

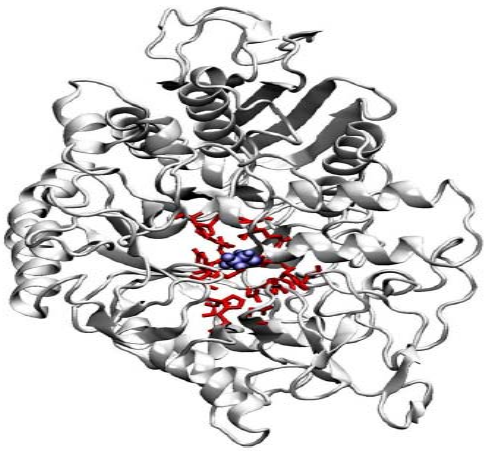

Keywords : α-Glucosidase; Computational simulation; Diabetes mellitus; Docking simulation; Molecular dynamics; Trifluoroethanol; Unfolding

Article 285

Inhibitory effect of Zn^{2+} on α-glucosidase: Inhibition kinetics and molecular dynamics simulation

Process Biochem. 47(12):2510-7.

Zeng YF, Lee J*, Si YX, Yan L, Kim TR, Qian GY, Lü ZR, Ye ZM, Yin SJ

*Co-first: jinhyuk@kribb.re.kr
Korean Bioinformation Center

α-Glucosidase (EC 3.2.1.20) is a critical enzyme with clinical relevance to type 2 diabetes mellitus. Therefore, research on this enzyme's inhibition is important. In the present study, we investigated Zn^{2+}-induced inhibition and the structural changes of α-glucosidase. α-Glucosidase activity was significantly inhibited by Zn^{2+} in a dose-dependent manner. The inhibition followed a multi-phase kinetic process with a first-order reaction. Zn^{2+} inhibited α-glucosidase in a parabolic mixed-type reaction (K_i = 0.102 ± 0.001 mM) and directly induced the unfolding of α-glucosidase, resulting in a slight hydrophobic exposure. We also performed 10 ns molecular dynamics simulations on α-glucosidase and Zn^{2+}. The simulations suggest that ten Zn^{2+} ions possibly interact with 57 α-glucosidase residues. The molecular dynamics simulations also confirmed the binding mechanism of Zn^{2+} to α-glucosidase and suggest that the Zn^{2+} binding sites are not located in the glucose binding pocket of α -glucosidase. Our study provides insights into the mechanism of Zn^{2+}-induced unfolding of α-glucosidase and inhibition of ligand binding and suggests that Zn^{2+} could act as a potent inhibitor of α-glucosidase for the treatment of type 2 diabetes mellitus.

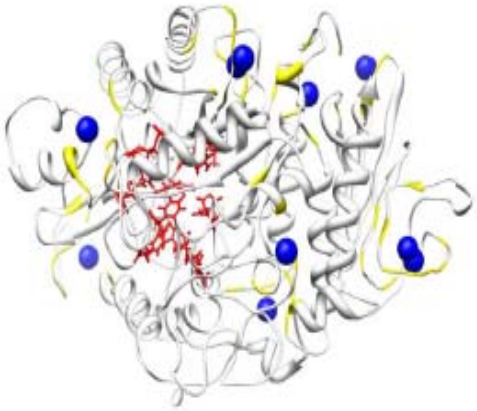

Keywords : α-Glucosidase; Inhibition kinetics; Ligand binding; Molecular dynamics simulations; Potent inhibitor; Type 2 diabetes mellitus; Unfolding; Zn2+

2012
KRIBB Article Abstracts : First or corresponding articles indexed in SCIE, Scopus, and PubMed

Ochang Branch Institute

- Natural Medicine Research Center
- Chemical Biology Research Center
- Targeted Medicine Research Center
- World Class Institute Center

Korea Research Institute of Bioscience and Biotechnology

Article 286

Enzymatic glycosylation of nonbenzoquinone geldanamycin analogs via *Bacillus* UDP-glycosyltransferase

Appl Environ Microbiol. 78(21):7680-6.

Wu CZ, Jang JH, Woo M, Ahn JS, Kim JS*, Hong YS*

*Co-corresponding: joongsu@kribb.re.kr hongsoo@kribb.re.kr
Chemical Biology Research Center

Geldanamycin (GM) is a naturally occurring anticancer agent isolated from several strains of *Streptomyces hygroscopicus*. However, its potential clinical utility is compromised by its severe toxicity and poor water solubility. For this reason, considerable efforts are under way to make new derivatives that have both good clinical efficacy and high water solubility. On the other hand, glycosylation is often a step that improves the water solubility and/or biological activity in many natural products of biosynthesis. Here, we report the facile production of glucose-conjugated nonbenzoquinone GM analogs using the *Bacillus* UDP-glycosyltransferase BL-C. Five aglycon substrates containing nonbenzoquinone aromatic rings were chosen to validate the *in vitro* glycosylation reaction. Putative glucoside compounds were determined through the presence of a product peak(s) and were also verified using LC/MS analyses. Further, the chemical structures of new glucoside compounds 6 and 7 were elucidated using spectroscopy data. These glucoside compounds showed a dramatic improvement in water solubility compared with that of the original aglycon, nonbenzoquinone GM.

PMID: 22923401

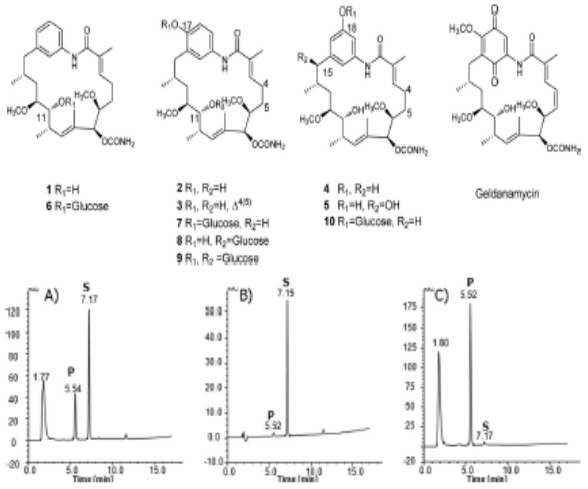

Keywords : Geldanamycin (GM); Glucose-conjugated nonbenzoquinone; Glycosylation; Putative glucoside compounds

Article 287

The effect of isolancifolide on the apoptosis in HL-60 cells through caspase-8-dependent and -independent pathways

Arch Pharm Res. 35(1):137-43.

Choi JJ, Kwon OK, Oh SR, Lee HK, Ahn KS*

*Corresponding: ksahn@kribb.re.kr
Natural Medicine Research Center

Isolancifolide is a compound extracted and isolated from *Actinodaphne lancifolia*, which is a traditional oriental medicine. To determine whether isolancifolide has therapeutic potential as an anticancer molecule, we assessed its apoptotic effects on HL-60 cells, a human leukemia cell line. Apoptotic activities were investigated using DNA fragmentation assay, immunoblotting, and flow cytometry. We found that the inhibitory concentration 50% of isolancifolide was approximately 20 M. The time- and dose-dependent effects of isolancifolide on apoptosis were determined by DNA fragmentation and propidium iodide staining, and the involvement of caspases and the Bcl-2 family in isolancifolide-induced apoptosis was assessed by Western blotting. During exposure to isolancifolide, the pro-forms or full length of caspases-8, -3, and Bid were decreased, as assessed by Western blotting, while the levels of cleaved forms of caspases-8, -3, and PARP were increased. We observed that the release of cytochrome c and Smac/DIABLO from the mitochondria to the cytosol was accompanied by the loss of mitochondrial membrane potential. The caspase specific inhibitors, z-IETD-fmk and z-LEHD-fmk, blocked the accumulation of sub-G1 cells and the release of cytochrome c, but not that of Smac/DIABLO. These results indicate that isolancifolide induces apoptosis of HL-60 cells through both death receptor and mitochondria pathways, in caspase-8-dependent and -independent manners, suggesting that isolancifolide may be useful in anticancer strategies.

PMID:22297752

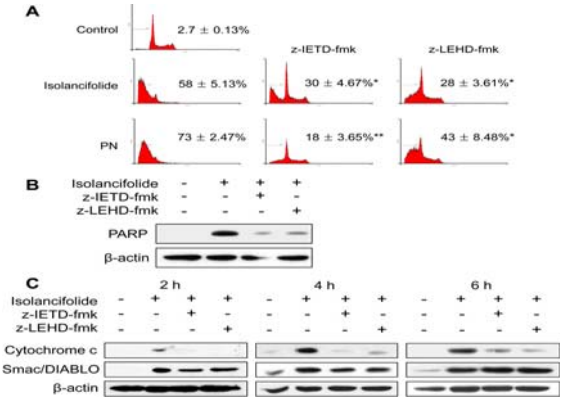

Keywords : Anticancer drug; Apoptosis pathways; Caspase-8; HL-60; Isolancifolide

Article 288

A novel therapeutic target, GPR43; where it stands in drug discovery

Arch Pharm Res. 35(9):1505-9.

Kim S*, Kim YM, Kwak YS

*First: sunhong@kribb.re.kr
Targeted Medicine Research Center

With growing interest in human microbiome for its implication in metabolic disorders, inflammatory diseases, immune disorders and so forth, understanding the biology at the interface of the gut flora and the host becomes very important for identifying novel therapeutic avenues. GPR43 has been deorphanized and the metabolites of microbiome, such as short-chain fatty acids, serve as its natural ligands. There are numerous reports that GPR43 might be a crucial link to the novel therapies for the unmet medical needs and many drug discovery organizations are making their moves in response.
PMID:23054706

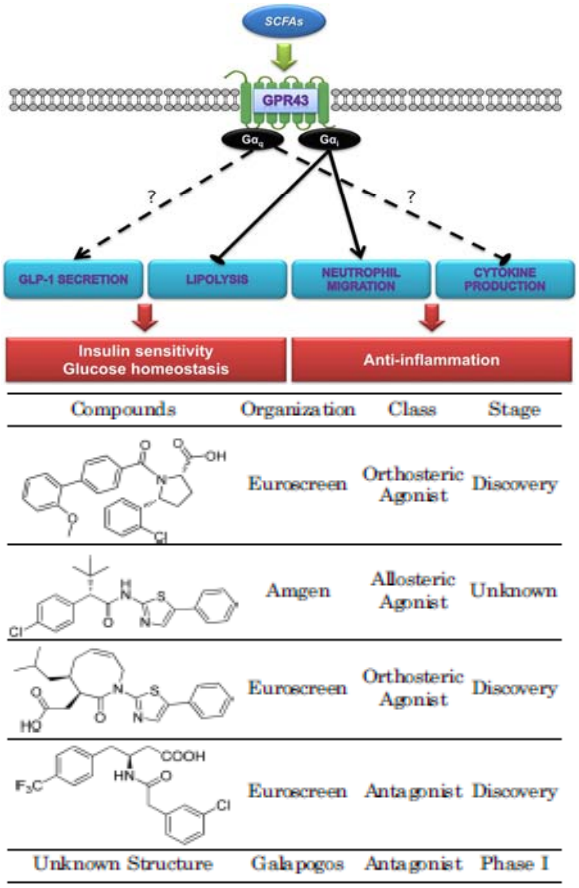

Keywords : Drug discovery; GPR43; Gut flora; Novel therapy; Therapeutic avenues

Article 289

Ingenane-type diterpenes with a modulatory effect on IFN-γ production from the roots of *Euphorbia kansui*

Arch Pharm Res. 35(9):1553-8.

Khiev P, Kim JW, Sung SJ, Song HH, Choung DH, Chin YW, Lee HK, Oh SR*

*Corresponding: seiryang@kribb.re.kr
Natural Medicine Research Center

A new ingenane-type diterpene, (3*S*,5*R*)5-*O*-(2,3-dimethylbutanoyl)-13-*O*-dodecanoyl-20-*O*-deoxyingenol (1), and six known compounds,3-*O*-(2,3-dimethylbutanoyl)-13-*O*-dodecanoyl-20-*O*-deoxyingenol (2), 20-*O*-decanoylingenol (3), 20-*O*-acetylingenol-3-*O*-(2'*E*,4'*Z*) decadienoate (4), kansuiphorin A (5), 3-*O*-(2,3-dimethylbutanoyl)-13-*O*-dodecanoylingenol (6), and kansuinin F (7) were isolated and evaluated for their effect on IFN-γ production in NK92 cells. Interestingly, subjection to compounds 4 and 6 (10 nM) displayed the most significant response in IFN-γ production, comparable to that produced by the same dose of phorbol 12-myistate 13-acetate (PMA). High doses of compounds 3 (100 nM), 1 (1. 25 μM) and 5 (5.0 μM) have also been shown to activate the IFN-γ production.
PMID: 23054711

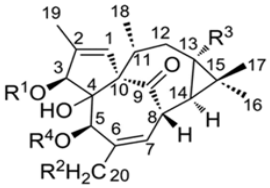

1 R^1 = H, R^2 = H, R^3 = OCO-$(CH_2)_{10}$-CH_3, R^4 =CO-CH(CH_3)-CH$(CH_3)_2$
2 R^1 = CO-CH(CH_3)-CH$(CH_3)_2$, R^2 = H, R^3 = OCO-$(CH_2)_{10}$-CH_3, R^4 =H
3 R^1 = H, R^2 =OCO-$(CH_2)_8$-CH_3, R^3 = H, R^4 =H
4 R^1= CO(CH=CH)-$(CH_2)_4$-CH_3, R^2 = OAc, R^3 = H, R^4 =H
5 R^1 = CO-CH(CH_3)-CH$(CH_3)_2$, R^2 = OCO-$(CH_2)_{14}$-CH_3, R^3 = OCO-$(CH_2)_{10}$-CH_3, R^4 =H
6 R^1 =CO-CH(CH_3)-CH$(CH_3)_2$, R^2= OH,R^3 = OCO-$(CH_2)_{10}$-CH_3, R^4 =H

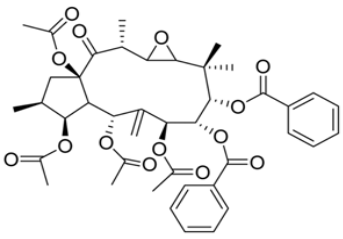

7

Keywords : *Euphorbia kansui*; Euphorbiaceae; IFN-γ; Ingenane-type diterpenes

Article 290

2,3,22,23-tetrahydroxyl-2,6,10,15,19,23-hexamethyl-6,10,14,18-tetracosatetraene, an acyclic triterpenoid isolated from the seeds of *Alpinia katsumadai*, Inhibits acyl-CoA : cholesterol acyltransferase activity

Biol Pharm Bull. 35(11):2092-6.

Choi SY, Lee MH, Choi JH, Kim YK*

*Corresponding: kimyk@kribb.re.kr
Natural Medicine Research Center

In order to isolate a cholesterol-lowering compound from *Alpinia katsumadai*, an inhibitor for acyl-CoA : cholesterol acyltransferase (ACAT), an enzyme responsible for the cholesterol ester formation in liver, was purified, its chemical structure was determined, and *in vivo* and *in vitro* inhibition activities were performed. In a high fat diet mouse model, we discovered that the ethanol extract of *Alpinia katsumadai* reduced plasma cholesterol, triglyceride, and low density lipoprotein (LDL) levels. An acyclic triterpenoid showing ACAT inhibitory activity was isolated from the extract of seeds of *A. katsumadai*. By NMR spectroscopic analysis of its ^{1}H-NMR, ^{13}C-NMR, ^{1}H-^{1}H correlation spectroscopy, heteronuclear multiple bond connectivity (HMBC), hetero multiquantum coherence (HMQC) and nuclear Overhauser effect, chemical structure of 2,3,22,23-tetrahydroxyl-2,6,10,15,19,23-hexamethyl-6,10,14,18-tetracosatetraene (1), were elucidated. The acyclic triterpenoid was found to be responsible for the ACAT inhibition activities of rat liver microsomes with IC_{50} values of 47.9 μM. It also decreased cholesteryl ester formation with IC_{50} values of 26 μM in human hepatocyte HepG2 cell. The experimental study revealed that the ethanol extract of *A. katsumadai* has a hypolipemic effect in high fat diet mice, and the isolated acyclic triterpenoid has ACAT inhibition activity, showing a potential novel therapeutic approach for the treatment of hyperlipidemia and atherosclerosis.

PMID:23123480

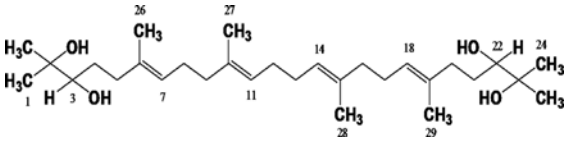

Keywords : Acyl CoA : cholesterol acyltransferase; *Alpinia katsumadai*; Atherosclerosis; Inhibitor; Triterpenoid

Article 291

Protuboxepin A, a marine fungal metabolite, inducing metaphase arrest and chromosomal misalignment in tumor cells

Bioorg Med Chem. 20(12):3799-806.

Asami Y, Jang JH, Soung NK, He L, Moon DO, Kim JW, Oh H, Muroi M, Osada H, Kim BY*, Ahn JS*

*Co-corresponding: bykim@kribb.re.kr jsahn@kribb.re.kr
Chemical Biology Research Center

Previously we reported the identification of a new oxepin-containing diketopiperazine-type marine fungal metabolite, named protuboxepin A which showed antiproliferative activity in several cancer cell lines. In this study we elucidated the mechanism by which protuboxepin A induces cancer cell growth inhibition. Here we report that protuboxepin A induced round-up morphology, M phase arrest, and an increase in the subG$_1$ population in tumor cells in a dose dependent manner. Our investigations revealed that protuboxepin A directly binds to α,β-tubulin and stabilizes tubulin polymerization thus disrupting microtubule dynamics. This disruption leads to chromosome misalignment and metaphase arrest which induces apoptosis in cancer. Overall, we identified protuboxepin A as a microtubule-stabilizing agent which has a distinctly different chemical structure from previously reported microtubule inhibitors. These results indicate that protuboxepin A has a potential of being a new and effective anti-cancer drug.

PMID: 22595423

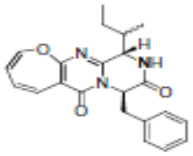

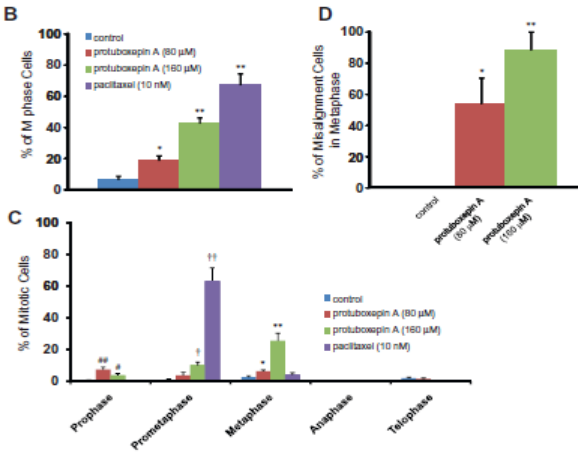

Keywords : Chromosomal misalignment; Marine fungal metabolite; Metaphase arrest; Protuboxepin A; Tubulin

Article 292

Tigliane diterpene esters with IFN γ-inducing activity from the leaves of *Aleurites fordii*

Bioorg Med Chem Lett. 22(6):2318-20.

Pei YH, Kim JW, Kang HB, Lee HK, Kim CS, Song HH, Chin YW, Oh SR*

*Corresponding: seiryang@kribb.re.kr
Natural Medicine Research Center

Bioactivity-guided fractionation on the leaves of *Aleurites fordii* led to the isolation of a new tigliane diterpene ester, 12-*O*-hexadecanoyl-7-oxo-5-ene-16-hydroxyphorbol-13-acetate (1) along with four known compounds, 12-*O*-hexadecanoyl-7-oxo-5-ene-phorbol-13-acetate (2), 12-*O*-hexadecanoyl-phorbol-13-acetate (3), 12-*O*-hexadecanoyl-16-hydroxyphorbol-13-acetate (4), and 12-*O*-hexadecanoyl-4-deoxy-4α-16-hydroxyphorbol-13-acetate (5). The structures of these compounds were determined by interpretation of NMR (1D and 2D) spectroscopic data and MS data. All the isolates were evaluated for their effects on the induction of IFN-γ in NK92 cells. Compounds 3 and 4 exhibited the most potent responses in IFN-γ induction, comparable to the positive control, phorbol 12-myristate 13-acetate (PMA).

PMID:22361132

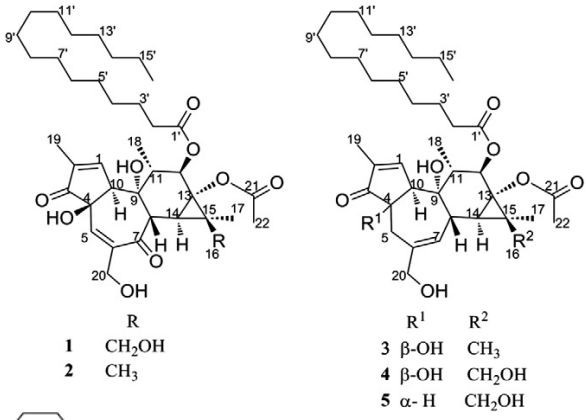

	R
1	CH_2OH
2	CH_3

	R^1	R^2
3	β-OH	CH_3
4	β-OH	CH_2OH
5	α- H	CH_2OH

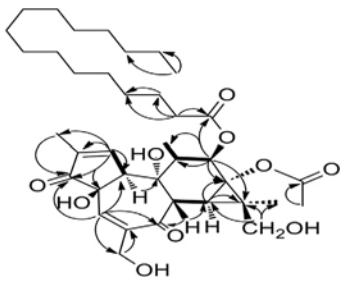

Keywords : *Aleurites fordii*; Euphorbiaceae; IFN-c production; Phorbol; Tigliane diterpene

Article 293

Discovery of a novel series of benzimidazole derivatives as diacylglycerol acyltransferase inhibitors

Bioorg Med Chem Lett. 22(24):7456-60.

Lee K, Goo JI, Jung HY, Kim M, Boovanahalli SK, Park HR, Kim MO, Kim DH, Lee HS*, Choi Y

*Co-corresponding: leehs@kribb.re.kr
Targeted Medicine Research Center

A novel series of benzimidazole derivatives was prepared and evaluated for their diacylglycerol acyltransferase (DGAT) inhibitory activity using microsome from rat liver. Among the newly synthesized compounds, furfurylamine containing benzimidazole carboxamide 10j showed the most potent DGAT inhibitory effect (IC_{50}=4.4 μM) and inhibited triglyceride formation in HepG2 cells. Furthermore, compound 10j reduced body weight gain of Institute of Cancer Research mice on a high-fat diet and decreased levels of total triglyceride, total cholesterol, and LDL-cholesterol in the blood accompanied with a significant increase in HDL-cholesterol level.

PMID:23141914

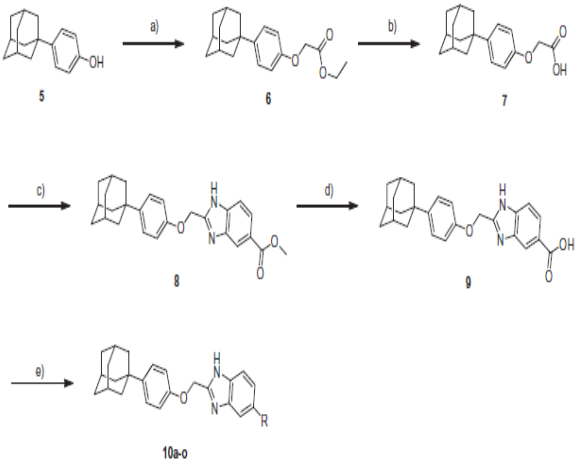

Keywords : Benzimidazole; DGAT inhibitors; Obesity; Triglycerides; Type II diabetes

Article 294

Violaceols function as actin inhibitors inducing cell shape elongation in fibroblast cells

Biosci Biotechnol Biochem. 76(8):1431-7.

Asami Y, Jang JH, Oh H, Sohn JH, Kim JW, Moon DO, Kwon O, Kawatani M, Osada H, Kim BY*, Ahn JS*

*Co-corresponding: bykim@kribb.re.kr jsahn@kribb.re.kr
Chemical Biology Research Center

Violaceol-I and -II were isolated from a fractionated library of marine-derived fungal metabolites. These compounds increased the calcium ion concentration inside the cell and caused F-actin aggregation in rat fibroblast 3Y1 cells within 3 h resulting in cell shape elongation. Calcium chelator BAPTA-AM (1,2-*bis*(2-aminophenoxy)ethane-*N,N,N′,N′*-tetraacetic acid tetrakis (acetoxymethyl ester) inhibited violaceol-I and -II induced F-actin aggregation in 3Y1 cells, and hence violaceol-I and -II act in a calcium dependent manner. Violaceol-I and -II inhibited G-actin polymerization *in vitro* in a dose-dependent manner and strongly associated with G-actin, at dissociation equilibrium constants of 1.44 $\times 10^{-8}$ M and 2.52 $\times$ 10^{-9} M respectively. Here we report the identification of a novel function of violaceol-I and -II as actin inhibitors. Violaceol-I and -II induced cell shape elongation through F-actin aggregation in 3Y1 fibroblasts. These compounds may give researchers new insights into the role of actin in tumorigenesis and lead to the development of additional anti-tumor drugs.

PMID: 22878183

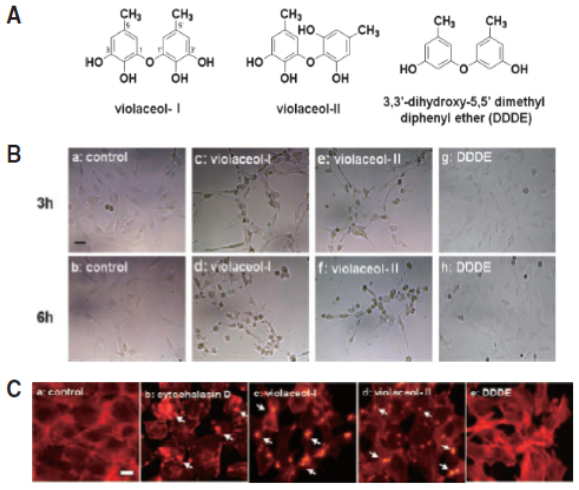

Keywords : Actin; Anti-tumor drugs; Calcium ion; Cell shape; Elongation; Fractionated library; Violaceols

Article 295

Selective gene delivery to cancer cells secreting matrix metalloproteinases using a gelatin/polyethylenimine/DNA complex

Biotechnol Bioproc Eng. 17(1):160-7.

Ge J, Min SH, Kim DM, Lee DC, Park KC, Yeom YI*

*Co-corresponding: yeomyi@kribb.re.kr
Ochang Branch Institute

We developed a gene delivery strategy targeting metastatic tumors by exploiting the specific matrix metalloproteinases (MMPs) secreting properties of metastatic tumor cells. A ternary polyplex has been formed by coating polyethylenimine/DNA (PD) complex with an excessive amount of negatively charged gelatin B (GPDB). We show that GPD-B's gene delivery activity could be targeted to cancer cells *via* the MMP-mediated proteolytic process, while GPD-A, made from positively charged gelatin A, was not successful in exhibiting such activity. The 1, 10-Phenanthroline, an MMP2 inhibitor, abrogated the MMPdependent transfection activity of GPD-B. GPD-B carried much less positive surface charges than PD, and thus exhibited significantly reduced interactions with erythrocytes. However, MMP2 elevated the positiveness in GPDB's surface charge and, thus, its interaction with erythrocytes. These results suggest that the anionic gelatin coating may confer improved stabilities on GPD-B in the surrounding medium, while MMP2-mediated disintegration of the gelatin coat enhances the gene delivery to metastatic cancer cells *via* increasing the likelihood of local chargemediated interactions between the polyplex and cancer cell membrane.

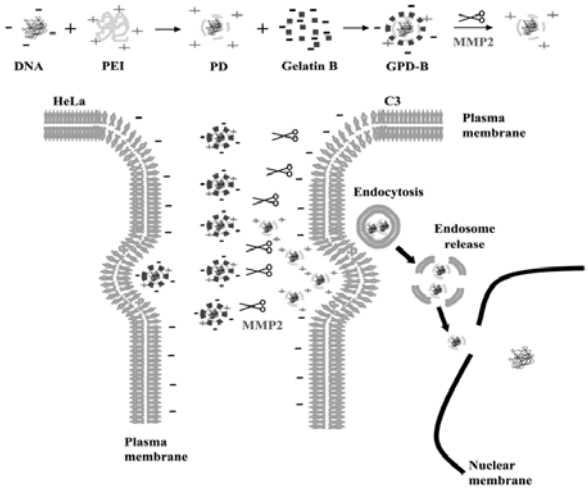

Keywords : Gelatin; Metastatic tumor; MMP; Polyethylenimine (PEI); Targeting

Article 296

Ginsenoside Rh2 inhibits osteoclastogenesis through down-regulation of NF-κB, NFATc1 and c-Fos

Bone. 50(6):1207-13.

He L, Lee J, Jang JH, Lee SH, Nan MH, Oh BC, Lee SG, Kim HH, Soung NK, Ahn JS*, Kim BY*

*Co-corresponding: jsahn@kribb.re.kr bykim@kribb.re.kr
World Class Institute Center

Ginsenoside Rh2 is one of the most active components of red ginseng, controlling cancer and other metabolic diseases including osteoclast differentiation. However, the molecular mechanism underlying the inhibition of osteoclast differentiation by ginsenoside Rh2 remains poorly understood. In the present study, it was found that ginsenoside Rh2 suppressed osteoclast differentiation from bone marrow macrophages (BMMs) treated with receptor activator of nuclear factor κB ligand (RANKL) without any cytotoxicity. Ginsenoside Rh2 significantly reduced RANKL-induced expression of transcription factors, c-Fos and nuclear factor of activated T-cells (NFATc1), as well as osteoclast markers, TRAP and OSCAR. In defining the signaling pathways, ginsenoside Rh2 was shown to moderately inhibit NF-κB activation and ERK phosphorylation in response to RANKL stimulation in BMM cells without any effect on p38 and c-Jun N-terminal kinase (JNK). Finally, ginsenoside Rh2 blocked osteoporosis *in vivo* as confirmed by restored bone mineral density (BMD) and other markers associated osteoclast differentiation. Hence, it is suggested that ginsenoside Rh2 could suppress RANKL-induced osteoclast differentiation *in vitro* and *in vivo* through the regulation of c-Fos and NFATc1 expressions, not excluding the involvement of NF-κB and ERK. Ginsenoside Rh2 is also suggested to be developed as a therapeutic drug for prevention and treatment of osteoporosis.

PMID:22484180

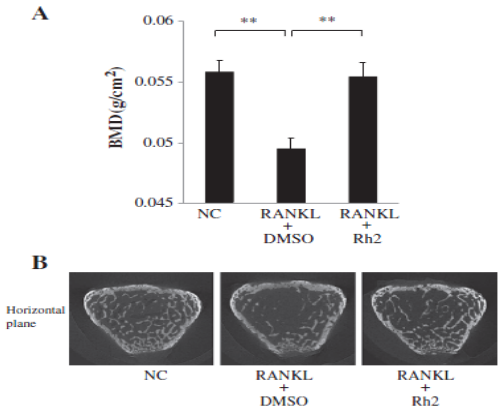

Keywords : Ginsenoside Rh2; NFATc1; NF-κB; Osteoclast; Osteoporosis

Article 297

Aloe-emodin suppresses prostate cancer by targeting the mTOR complex 2

Carcinogenesis. 33(7):1406-11.

Liu K, Park C, Li S, Lee KW, Liu H, He L, Soung NK, Ahn JS, Bode AM, Dong Z, Kim BY*, Dong Z

*Co-corresponding: bykim@kribb.re.kr
World Class Institute Center

Phosphatidylinositol 3-kinase (PI3-K) amplification and phosphatase and tensin homolog (PTEN) deletion-caused Akt activation contribute to the development of prostate cancer. Mammalian target of rapamycin complex 2 (mTORC2) is a kinase complex comprised of mTOR, Rictor, mSin1, mLST8/GβL and PRR5 and functions in the phosphorylation of Akt at Ser473. Herein, we report that mTORC2 plays an important role in PC3 androgen refractory prostate cell proliferation and anchorage-independent growth. Aloe-emodin, a natural compound found in aloe, inhibited both proliferation and anchorage-independent growth of PC3 cells. Protein content analysis suggested that activation of the downstream substrates of mTORC2, Akt and PKCα, was inhibited by aloe-emodin treatment. Pull-down assay and *in vitro* kinase assay results indicated that aloe-emodin could bind with mTORC2 in cells and inhibit its kinase activity. Aloe-emodin also exhibited tumor suppression effects *in vivo* in an athymic nude mouse model. Collectively, our data suggest that mTORC2 plays an important role in prostate cancer development and aloe-emodin suppresses prostate cancer progression by targeting mTORC2.

PMID:22532249

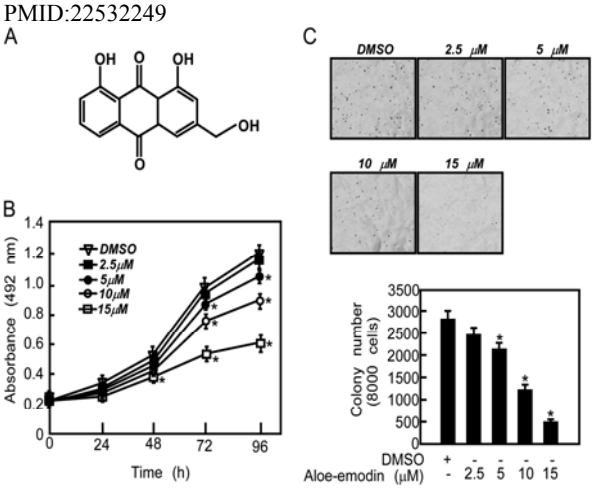

Keywords : Aloe-emodin; Phosphatase and tensin homolog (PTEN); Phosphatidylinositol 3-kinase (PI3-K); Prostate cancer development

Article 298

Patulin induces colorectal cancer cells apoptosis through EGR-1 dependent ATF3 up-regulation

Cell Signal. 24(4):943-50.

Kwon O, Soung NK, Thimmegowda NR, Jeong SJ, Jang JH, Moon DO, Chung JK, Lee KS, Kwon YT, Erikson RL, Ahn JS*, Kim BY*

*Co-corresponding: jsahn@kribb.re.kr bykim@kribb.re.kr
World Class Institute Center

Patulin is a fungal mycotoxin of *Aspergilus* and *Penicillium* that is commonly found in rotting fruits and exerts its potential toxic effect mainly by reactive oxygen species (ROS) generation. However, the effect of patulin on cancer cells as well as its intracellular mechanism has been controversial and not clearly defined yet. In this study, patulin was found to induce G1/S accumulation and cell growth arrest accompanied by caspase-3 activation, PARP cleavage and ATF3 expression in human colon cancer cell line HCT116. Ser/Thr phosphorylation of a transcription factor, EGR-1, was increased while its expression did not change upon patulin treatment to the cells. Knockdown of ATF3 and EGR-1 using their respective siRNAs showed EGR-1 dependent ATF3 expression. Moreover, treatment of the cells with antioxidants N-acetylcysteine (NAC) and glutathione (GSH) revealed that patulin induced ATF3 expression and apoptosis were dependent on ROS generation. ATF3 expression was also increased by patulin in other colorectal cancer cell types, Caco2 and SW620. Collectively, our data present a new anti-cancer molecular mechanism of patulin, suggesting EGR-1 and ATF3 as critical targets for the development of anti-cancer chemotherapeutics. In this regard, patulin could be a candidate for the treatment of colorectal cancers.

PMID: 22230687

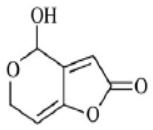

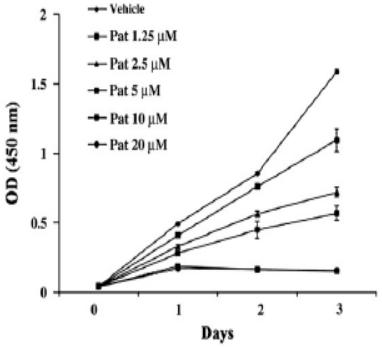

Keywords : Anti-cancer molecular; Antioxidants N-acetylcysteine; ATF3; Colorectal cancers; EGR-1; Patulin; ROS

Article 299

Cytotoxic terpenes from the stems of *Dipterocarpus obtusifolius* collected in Cambodia

Chem Pharm Bull. 60(8):955-61.

Khiev P, Kwon OK, Song HH, Oh SR, Ahn KS, Lee HK*, Chin YW

*Co-corresponding: hykylee@kribb.re.kr
Targeted Medicine Research Center

From the stems of *Dipterocarpus obtusifolius*, five new triterpenes, 3-oxo-20-hydroxy-30α-methyl,17(29)α-epoxy-28-norlupane (1), 3-oxo-20-hydroxy-30β-methyl-17(29)α-epoxy-28-norlupane (2), 3,20-dioxo-28,29-norlupan-17α-ol (3), 27-demethyl-20(S)-dammar-23-ene-20-ol-3,25-dione (4), and 3-*epi*-cecropic acid (5) together with 13 known compounds including diterpene, sesquiterpenes and triterpenes were isolated and characterized. All isolates were tested for their cytotoxicities against a small panel of human cancer cell lines. Of the tested compounds, compounds 4-11 were found to be cytotoxic against one or more human cancer cell lines.

PMID:22863697

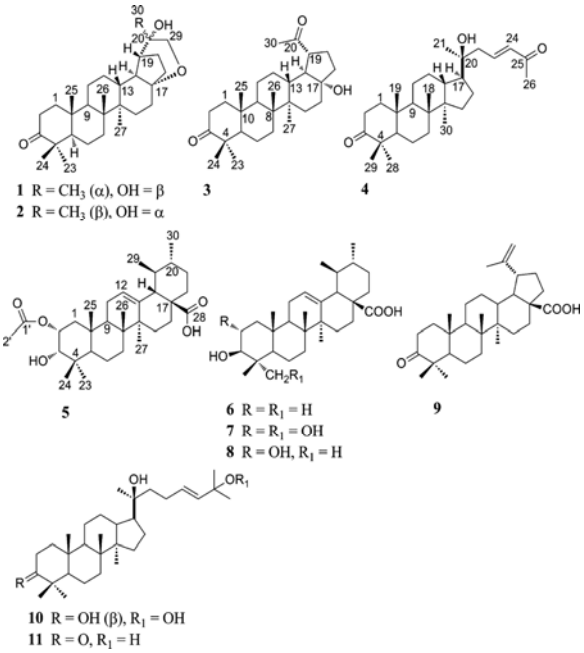

Keywords : Cancer cell; Cytotoxicity; Dipterocarpaceae; *Dipterocarpus obtusifolius*; Terpene

Article 300

Zuonin B inhibits lipopolysaccharide-induced inflammation via downregulation of the ERK1/2 and JNK pathways in RAW264.7 macrophages

Evid Based Compl Alternat Med. 2012:728196.

Lee MY, Yuk JE, Kwon OK, Oh SR, Lee HK, Ahn KS*

*Corresponding: ksahn@kribb.re.kr
Natural Medicine Research Center

We investigated whether Zuonin B exerts immunological effects on RAW264.7 cells. Zuonin B, isolated from flower buds of *Daphne genkwa*, suppressed the levels of nitric oxide and prostaglandin E_2, as well as proinflammatory cytokines, such as tumor necrosis factor-α and interleukin-(IL-) 6, in lipopolysaccharide-stimulated macrophages. Moreover, the compound inhibited cyclooxygenase-2 and inducible nitric oxide synthase expression. Zuonin B attenuated NF-kappaB (NF-κB) activation via suppressing proteolysis of inhibitor kappa B-alpha (IκB-α) and p65 nuclear translocation as well as phosphorylation of extracellular signal-regulated kinase 1/2 and c-Jun N-terminal kinase. Additionally, IL-4 and IL-13 production in ConA-induced splenocytes was inhibited by Zuonin B. In conclusion, the anti-inflammatory effects of Zuonin B are attributable to the suppression of proinflammatory cytokines and mediators via blockage of NF-κB and AP-1 activation. Based on these findings, we propose that Zuonin B is potentially an effective functional chemical candidate for the prevention of inflammatory diseases.

PMID:22454678

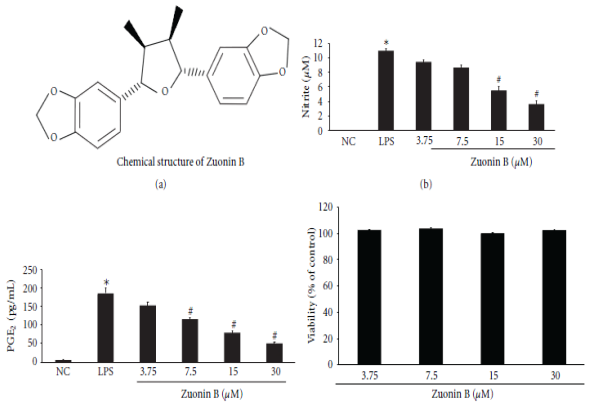

Keywords : Anti-inflammatory effects; Inflammatory diseases; Lipopolysaccharide-stimulated macrophages; Proinflammatory cytokines; Zuonin B

Article 301

Mangosteen xanthones mitigate ovalbumin-induced airway inflammation in a mouse model of asthma

Food Chem Toxicol. 50(11):4042-50.

Jang HY, Kwon OK, Oh SR, Lee HK, Ahn KS*, Chin YW

*Co-corresponding: ksahn@kribb.re.kr
Natural Medicine Research Center

α- and γ-Mangostin, which are the major xanthones purified from a Mangosteen, *Garcinia mangostana* Linn., exhibit a wide range of anticancer, antioxidant, and anti-inflammatory activities. Here, we assessed their therapeutic effects in a mouse model of ovalbumin (OVA)-induced allergic asthma. Animals were treated with α- and γ-mangostins orally for 3 days at doses of 10 and 30 mg/kg daily, 1h before the OVA challenge. Administration of α- and γ-mangostins significantly reduced the major pathophysiological features of allergic asthma, including inflammatory cell recruitment into the airway, airway hyperresponsiveness (AHR), and increased levels of Th2 cytokines. In addition, α- and γ -mangostins attenuated the increases in phosphoinositide 3-kinase (PI3K) activity, phosphorylation of Akt, and NF-κB in nuclear protein extracts after OVA challenge. In conclusion, α- and γ-mangostin may have therapeutic potential for the treatment of allergic asthma.

PMID:22943973

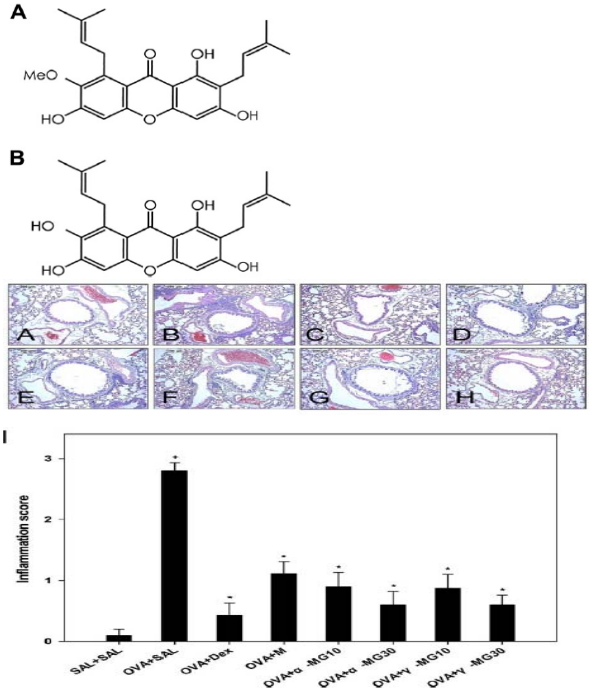

Keywords : Allergic asthma; α-Mangostin; γ-Mangostin; *Garcinia mangostana*; Therapeutic effects

Article 302

Evaluation of the total oxidant scavenging capacity of saponins isolated from *Platycodon grandiflorum*

Food Chem. 132(1):333-7.

Ryu CS, Kim CH, Lee SY, Lee KS, Choung KJ, Song GY, Kim BH, Ryu SY, Lee HS*, Kim SK

*Co-corresponding: leehs@kribb.re.kr
Targeted Medicine Research Center

The antioxidant activity of saponins isolated from *Platycodon grandiflorum* (PG; Balloon flower) was determined using the total oxidant-scavenging capacity (TOSC) assay. Platycodigenin, polygalacic acid, platycodin D, platycoside E and deapioplatycoside E were isolated and their structures were characterised based on their physical and spectral properties and by comparison of these results with similar data in the literature. Platycodin D showed the greatest TOSC value against peroxyl radicals, followed (in decreasing order) by polygalacic acid, platycodigenin, deapioplatycosides E and platycoside E. Although the TOSC value of the saponins against peroxyl radicals was less than that of glutathione (GSH) and Trolox used as positive controls. However, TOSC value of platycodigenin, deapioplatycoside E, platycodin D or platycoside E against peroxynitrite was 2.35-, 1.27-, 1.02- or 0.75-fold of GSH, respectively, while polygalacic acid exhibited no scavenging capacity of peroxynitrites. These results suggest importance of the presence of hydroxyl group at carbon 24 in platycodigenin in peroxynitrite scavenging. As the number of attached sugar residues in the saponin glycosides is increased, the scavenging capacity of peroxyl radical, but not peroxynitrite was significantly decreased. These results showed that PG saponins have potent antioxidant activities, which is different according to the structure of aglycones and the number of attached sugar residues.

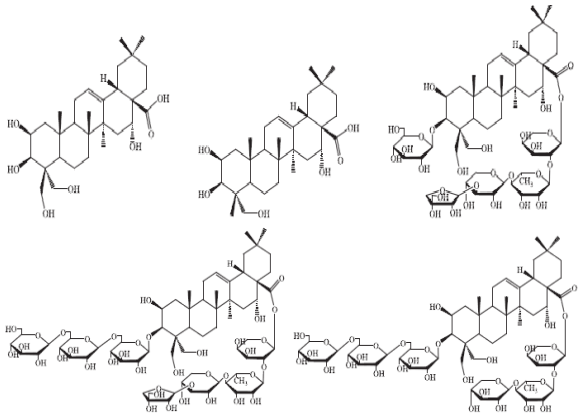

Keywords : Antioxidant activities; Oxidant-scavenging capacity; Oxidative stress; *Platycodon grandiflorum*; Saponin; Structure-activity relationship

Article 303

Abietane diterpenoids of *Rosmarinus officinalis* and their diacylglycerol acyltransferase-inhibitory activity

Food Chem. 132(4):1775-80.

Cui L, Kim MO, Seo JH, Kim IS, Kim NY, Lee SH, Park J, Kim J, Lee HS*

*Corresponding: leehs@kribb.re.kr
Targeted Medicine Research Center

Inhibition of acyl CoA:diacylglycerol acyltransferase (DGAT) has been proposed as one of the drug targets for treating obesity and type 2 diabetes. Bioassay-guided fractionation of the MeOH-soluble extract of *Rosmarinus officinalis* yielded two new diacylglycerol acyltransferase (DGAT) inhibitory-abietane diterpenoids, 7β -hydroxy-20-deoxo-rosmaquinone (1) and 7β -methoxy-20-deoxo-rosmanol (2), along with six known components, carnosol (3), 7α-methoxyrosmanol (4), 7β -methoxyrosmanol (5), 12-methoxy-canosic acid (6), rosmanol (7), and rosmadial (8). Compounds 1-8 inhibited DGAT1 activity, with the IC_{50} values ranging from 39.5 ± 0.6 to 144.2 ± 3.1 μM. In particular, carnosol (3), which is one of the major compounds of MeOH-soluble extract of *R. officinalis* exhibits inhibition of *de novo* intracellular triacylglycerol synthesis in human hepatocyte HepG2 cells.

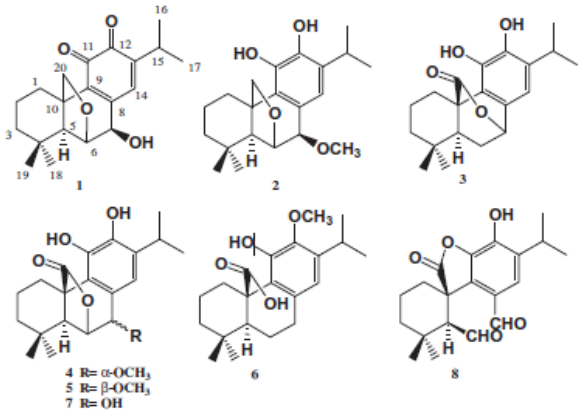

Keywords : Abietane diterpenoid; Carnosol; Diacylglycerol acyltransferase; *Rosmarinus officinalis*; Triacylglycerol synthesis

Article 304

A leaf methanolic extract of *Wercklea insignis* attenuates the lipopolysaccharide-induced inflammatory response by blocking the NF-κB signaling pathway in RAW 264.7 macrophages

Inflammation. 35(1):321-31.

Park JW, Kwon OK, Jang HY, Jeong H, Oh SR, Lee HK, Han SB, Ahn KS*

*Corresponding: ksahn@kribb.re.kr
Natural Medicine Research Center

The biological activity of *Wercklea insignis* (WI) in inflammation and the underlying mechanisms of action of extracts of this plant are largely unknown. In the present study, we investigated the effects of a WI methanolic extract on lipopolysaccharide-stimulated inflammation in the mouse macrophage cell line, RAW 264.7. A WI methanolic extract significantly inhibited NO, PGE_2, IL-6, IL-1β, and TNF-α production in LPS-stimulated RAW 264.7 cells. Expression of iNOS, COX-2, IL-6, IL-1β, and TNF-α were suppressed by the extract at both the mRNA and protein levels in lipopolysaccharide (LPS)-stimulated cells. Additionally, the attenuation of inflammatory responses in RAW 264.7 cells by the WI extract was closely associated with suppression of phosphorylation of mitogen-activated protein kinase (MAPK) molecules, including ERK, JNK1/2, and p38 MAPK and translocation of the nuclear factor (NF)-κB p65 subunit into the nucleus. The effect of WI extract was investigated against carrageenan-induced paw edema in female (20-25 g). Our results collectively indicate that the WI extract inhibits LPS-induced inflammatory responses by blocking the NF-κB signaling pathway in macrophages, supporting use of the extract as a therapeutic anti-inflammatory treatment.
PMID:21465277

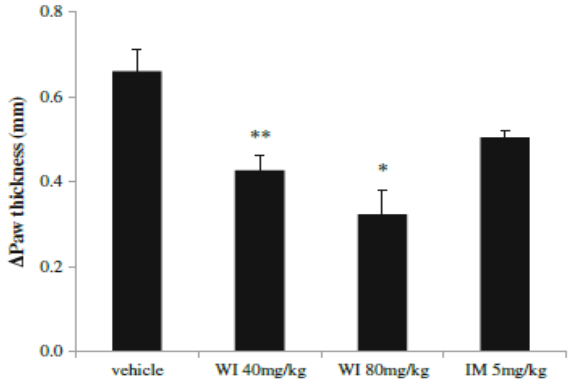

Keywords : Anti-inflammatory; Inflammation; MAPK; NF-κB; Nitric oxide; Signaling pathway; *Wercklea insignis*

Article 305

Ethanol extract of *Elaeocarpus petiolatus* inhibits lipopolysaccharide-induced inflammation in macrophage cells

Inflammation. 35(2):535-44.

Kwon OK, Ahn KS, Park JW, Jang HY, Joung H, Lee HK, Oh SR*

*Corresponding: seiryang@kribb.re.kr
Natural Medicine Research Center

Elaeocarpus petiolatus is known to exert active oxygen scavenging, anti-aging, and whitening actions. However, the biological effects of *E. petiolatus* on inflammation and the underlying mechanisms are yet to be established. In the present study, we investigated the anti-inflammatory effects of the ethanol extract from *E. petiolatus* (EPE) bark in murine Raw264.7 macrophages stimulated with lipopolysaccharide (LPS). EPE inhibited the production of PGE_2, TNF-α, and IL-1β in a dose-dependent manner in Raw264.7 cells stimulated with LPS. The decrease in PGE_2 production was correlated with reduced COX-2 expression. Furthermore, EPE suppressed the phosphorylation of extracellular signal-related kinases (ERK), c-Jun N-terminal kinase (JNK), and p38 as well as translocation of the NF-κB p65 subunit from the cytosol to nucleus. Our results suggest that EPE exerts anti-inflammatory activity through inhibition of inflammatory mediators, such as PGE_2, TNF-α, and IL-1β, and downregulation of COX-2 via suppression of NF-κB translocation and phosphorylation of ERK, JNK, and p38 in LPS-stimulated Raw264.7 cells.
PMID:21603972

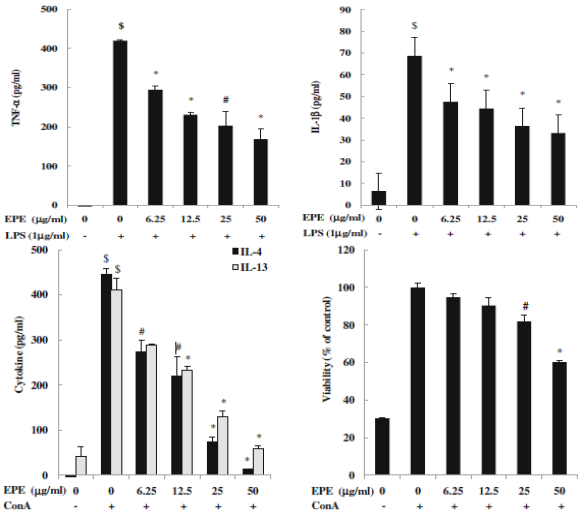

Keywords : Anti-inflammatory; COX-2; *Elaeocarpus petiolatus*; Inflammation; MAPK; NF-κB

Article 306

Tiarellic acid attenuates airway hyperresponsiveness and inflammation in a murine model of allergic asthma

Int Immunopharmacol. 12(1):117-24.

Lee MY, Ahn KS, Lim HS, Yuk JE, Kwon OK, Lee KY, Lee HK, Oh SR*

*Corresponding: seiryang@kribb.re.kr
Natural Medicine Research Center

Asthma is a persistent inflammatory disease characterized by airway obstruction and hyperresponsiveness in association with airway inflammation. In the current research, we studied the anti-inflammatory and anti-asthmatic effects of tiarellic acid (TA) isolated from *Tiarella polyphylla*, based on asthmatic parameters, such as immunoglobulin E (IgE) level, cytokine release, eosinophilia, airway hyperresponsiveness (AHR), reactive oxygen species (ROS) and mucus hypersecretion, in an ovalbumin (OVA)-sensitized/challenged mouse model. TA significantly inhibited increases in IgE, levels of ROS and T helper cytokines, such as interleukin (IL)-4, IL-5, TNF-α, and IL-13, in bronchoalveolar lavage fluid (BALF), and effectively suppressed airway hyperresponsiveness, eosinophilia, and mucus hypersecretion in the asthmatic mouse model. In addition, we found that administration of TA attenuated ovalbumin-induced increases in NF-κB activity in lungs. The efficacy of TA was comparable to that of montelukast, a currently available anti-asthmatic drug. Our results support the utility of TA as a herbal medicine for asthma treatment and may have application in the development of anti-inflammatory and anti-asthmatic drugs.
PMID:22085848

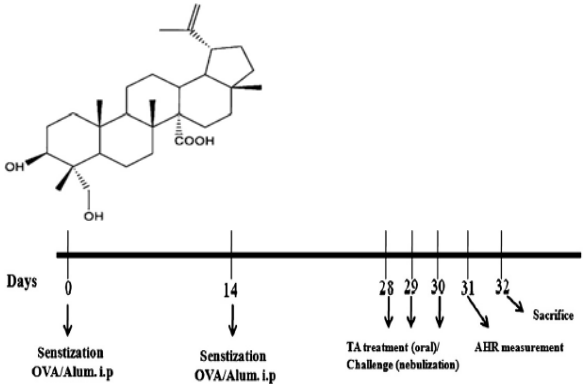

Keywords : Anti-asthmatic drugs; Anti-inflammatory drugs; Asthma; Cytokine; Reactive oxygen species; Tiarellic acid

Article 307

Skullcapflavone II inhibits ovalbumin-induced airway inflammation in a mouse model of asthma

Int Immunopharmacol. 12(4):666-74.

Jang HY, Ahn KS, Park MJ, Kwon OK, Lee HK, Oh SR*

*Corresponding: seiryang@kribb.re.kr
Natural Medicine Research Center

Skullcapflavone II is a flavonoid derived from *Scutellaria baicalensis*, a widely used herbal medicine in anti-inflammatory and anticancer therapy in Korea. Skullcapflavone II antagonized the bradykinin receptor more potently than any of the other flavonoids derived from this plant. Here, we were investigated its therapeutic effects in a mouse model of ovalbumin (OVA)-induced allergic asthma. Administration of skullcapflavone II significantly reduced airway hyperresponsiveness (AHR), airway eosinophilia, Th2 cytokine production, and increased transforming growth factor-β1 (TGF-β1) levels in bronchoalveolarlavage (BAL) fluids and lungs from OVA-sensitized and -challenged mice. Skullcapflavone II administration also significantly suppressed subepithelial collagen deposition and goblet cell hyperplasia, elevated Smad7 expression and suppressed pSmad2/3 levels. Collectively, these findings indicate that skullcapflavone II, a potential bradykinin antagonist, reduced the major pathophysiological features of allergic asthma, at least in part by acting on TGF-β1/Smad signaling pathways. Thus, skullcapflavone II may have therapeutic potential for the treatment of allergic asthma.
PMID:22314230

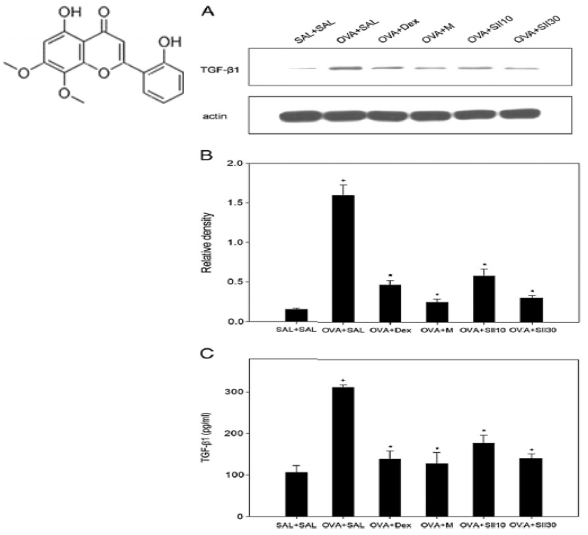

Keywords : Allergic asthma; Anti-inflammatory; Bradykinin antagonist; *Scutellaria baicalensis* Georgi; Skullcapflavone II; Therapeutic effects

Article 308

Benzomalvin E, an indoleamine 2,3-dioxygenase inhibitor isolated from *Penicillium* sp. FN070315

J Antibiot. 65(4):215-7.

Jang JP, Jang JH, Soung NK, Kim HM, Jeong SJ, Asami Y, Shin KS, Kim MR, Oh H, Kim BY*, Ahn JS*

*Co-corresponding: bykim@kribb.re.kr jsahn@kribb.re.kr
Chemical Biology Research Center

Indoleamine 2,3-dioxygenase (IDO) is an extrahepatic heme-containing dioxygenase. This is the initial and rate-limiting step in the catabolism of the essential amino acid Trp to N-formylkynurenine along the kynurenine pathway. T-cell lymphocytes are extremely sensitive to Trp shortage. Degradation of Trp by the placenta inhibits T-cell proliferation and prevents immunological rejection of tumor or fetus. In the course of our screening of the extracts of fungus for IDO inhibitors, we found activity in the culture broth of the soil fungus FN070315. Bioassay-guided fractionation of the extract led us to isolate a new benzodiazepine alkaloid. In this paper, we describe the fermentation, isolation, structure determination and biological activity of benzomalvins. Compounds 1, 2 and 3 were evaluated for inhibitory activity against IDO. Benzomalvin E (1) showed that the activity of IDO in a dosedependent manner, and its IC_{50} values were determined as 21.4±1.2 mM. A known IDO inhibitor, menadione (IC_{50} =3.7±0.5 μM), was employed as a positive control in the assay. On the other hand, compounds 2 and 3 showed weakly inhibitory activity against IDO with IC_{50} values of 126 and 130 μM, respectively. Benzomalvin derivatives have been reported to function as inhibitor against neuropeptide substance-P at the guinea pig, rat and human neurokinin-1 receptor. Several IDO inhibitors have been reported to date. 1-Methyltrytophan is the most frequently used inhibitor with a weak K_i of 34 μM and is in clinical development. The IDO inhibitory activity of the benzomalvin derivatives are now being reported for the first time in this study. Further investigation and optimization of benzomalvins might enable the preparation of new IDO inhibitors potentially useful in the treatment of cancer.

PMID:22318334

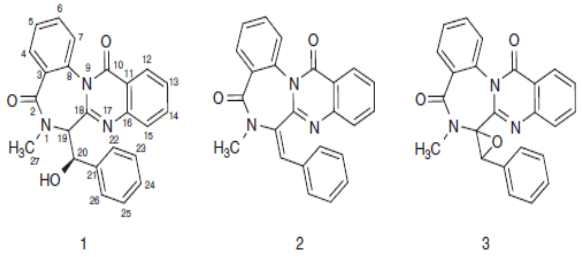

1 2 3

Keywords : Benzodiazepine alkaloid; Benzomalvin; IDO inhibitory activity; Indoleamine 2,3-dioxygenase; *Penicillium* sp.

Article 309

Characterization of arginylation branch of N-end rule pathway in G-protein-mediated proliferation and signaling of cardiomyocytes

J Biol Chem. 287(28):24043-52.

Lee MJ, Kim DE, Zakrzewska A, Yoo YD, Kim SH, Kim ST, Seo JW, Lee YS, Dorn GW 2nd, Oh U, Kim BY*, Kwon YT

*Co-corresponding: bykim@kribb.re.kr
World Class Institute Center

The N-end rule pathway is a proteolytic system in which destabilizing N-terminal amino acids of short lived proteins are recognized by recognition components (N-recognins) as an essential element of degrons, called N-degrons. In eukaryotes, the major way to generate N-degrons is through arginylation by ATE1 arginyl-tRNA-protein transferases, which transfer Arg from aminoacyl-tRNA to N-terminal Asp and Glu (and Cys as well in mammals). We have shown previously that ATE1-deficient mice die during embryogenesis with defects in cardiac and vascular development. Here, we characterized the arginylation-dependent N-end rule pathway in cardiomyocytes. Our results suggest that the cardiac and vascular defects in ATE1-deficient embryos are independent from each other and cell-autonomous. ATE1-deficient myocardium and cardiomyocytes therein, but not non-cardiomyocytes, showed reduced DNA synthesis and mitotic activity ~24 h before the onset of cardiac and vascular defects at embryonic day 12.5 associated with the impairment in the phospholipase C/PKC-MEK1-ERK axis of $G\alpha_q$-mediated cardiac signaling pathways. Cardiac overexpression of $G\alpha_q$ rescued ATE1-deficient embryos from thin myocardium and ventricular septal defect but not from vascular defects, genetically dissecting vascular defects from cardiac defects. The misregulation in cardiovascular signaling can be attributed in part to the failure in hypoxia-sensitive degradation of RGS4, a GTPase-activating protein for $G\alpha_q$. This study is the first to characterize the N-end rule pathway in cardiomyocytes and reveals the role of its arginylation branch in $G\alpha_q$-mediated signaling of cardiomyocytes in part through N-degron-based, oxygen-sensitive proteolysis of G-protein regulators.

PMID:22577142

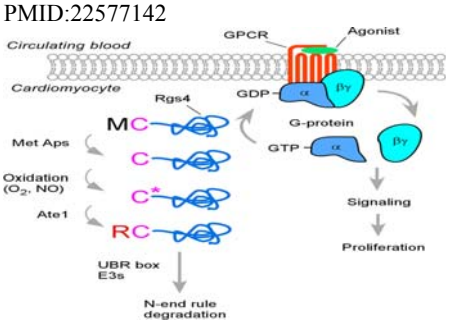

Keywords : Arginylation branch; Cardiomyocytes; G-protein regulators; N-end rule pathway; N-recognins

Article 310

Inhibitory effect of melanogenesis by 5-pentyl-2-furaldehyde isolated from *Clitocybe* sp.

J Microbiol Biotechnol. 22(6):814-7.

Kim YH, Choo SJ, Ryoo IJ, Kim BY, Ahn JS, Yoo ID*

*Corresponding: idyoo@kribb.re.kr
Chemical Biology Research Center

In the continued search for melanogenesis inhibitors from microbial metabolites, we found that the culture broth of *Clitocybe* sp. MKACC 53267 inhibited melanogenesis in B16F10 melanoma cells. The active component was purified by solvent extraction, silica gel chromatography, Sephadex LH-20 column chromatography, and finally by preparative HPLC. Its structure was determined as 5-pentyl-2-furaldehyde on the basis of the UV, NMR, and MS spectroscopic analysis. The 5-pentyl-2-furaldehyde potently inhibited melanogenesis in B16F10 cells with an IC_{50} value of 8.4 μg/ml, without cytotoxicity.
PMID: 22573159

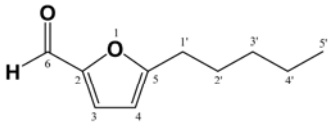

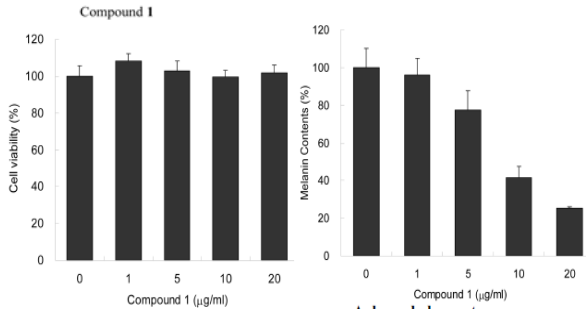

Keywords : 5-pentyl-2-furaldehyde; B16F10 melanoma; *Clitocybe* sp.; Inhibitory effect; Melanogenesis

Article 311

New geldanamycin analogs from *Streptomyces hygroscopicus*

J Microbiol Biotechnol. 22(11):1478-81.

Wu CZ, Jang JH, Ahn JS, Hong YS*

*Corresponding: hongsoo@kribb.re.kr
Chemical Biology Research Center

Geldanamycin (GM) and its analogs are important anticancer agents that inhibit heat shock protein (Hsp) 90, which is a major chaperone protein in cancer cells. Accordingly, based on interest in obtaining novel natural GM derivatives, the potential of *Streptomyces hygroscopicus* JCM4427, a GM producer, was explored for novel natural GM derivative(s), resulting in the discovery of new GM analogs as a biosynthetic shunt product and intermediates from its fermentation broth. In this study, the fermentation, isolation, structure determination, and biological activity of the compounds, two new tetracyclic thiazinogeldanamycin (1) and 19-hydroxy-4,5-dihydrogeldanamycin (3), together with the three known 4,5-dihydrothiazinogeldanamycin (2), reblastatin (4), and 17-demethoxy-reblastatin (5), are described.
PMID: 23124337

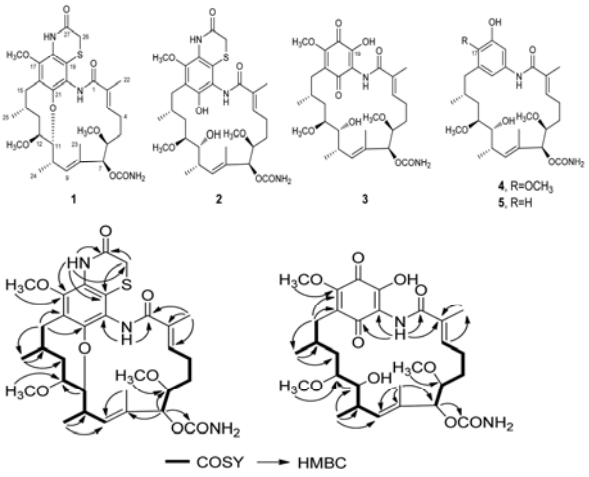

Keywords : Anticancer agents; Biosynthetic shunt product; Geldanamycin; Natural products

Article 312

Acute myeloid leukemia targeting by myxoma virus *in vivo* depends on cell binding but not permissiveness to infection *in vitro*

Leuk Res. 36(5):619-24.

Madlambayan GJ, Bartee E, Kim M*, Rahman MM, Meacham A, Scott EW, McFadden G, Cogle CR

*Co-first:
World Class Institute Center

Some oncolytic viruses, such as myxoma virus (MYXV), can selectively target malignant hematopoietic cells, while sparing normal hematopoietic cells. This capacity for discrimination creates an opportunity to use oncolytic viruses as *ex vivo* purging agents of autologous hematopoietic cell grafts in patients with hematologic malignancies. However, the mechanisms by which oncolytic viruses select malignant hematopoietic cells are poorly understood. In this study, we investigated how MYXV specifically targets human AML cells. MYXV prevented chloroma formation and bone marrow engraftment of two human AML cell lines, KG-1 and THP-1. The reduction in human leukemia engraftment after *ex vivo* MYXV treatment was dose-dependent and required a minimum MOI of 3. Both AML cell lines demonstrated MYXV binding to leukemia cell membranes following co-incubation: however, evidence of productive MYXV infection was observed only in THP-1 cells. This observation, that KG-1 can be targeted *in vivo* even in the absence of *in vitro* permissive viral infection, contrasts with the current understanding of oncolytic virotherapy, which assumes that virus infection and productive replication is a requirement. Preventing MYXV binding to AML cells with heparin abrogated the purging capacity of MYXV, indicating that binding of infectious virus particles is a necessary step for effective viral oncolysis. Our results challenge the current dogma of oncolytic virotherapy and show that *in vitro* permissiveness to an oncolytic virus is not necessarily an accurate predictor of oncolytic potency *in vivo*.

PMID:22341701

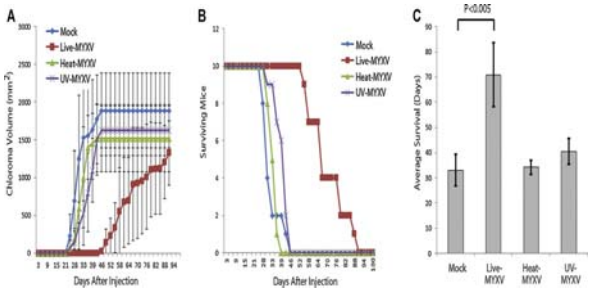

Keywords : Animal models; Bone marrow; Hematopoietic stem cell; Leukemia; Oncolytic virotherapy

Article 313

Artificial biosynthesis of phenylpropanoic acids in a tyrosine overproducing *Escherichia coli* strain

Microb Cell Fact. 11:153.

Kang SY, Choi O, Lee JK, Hwang BY, Uhm TB, Hong YS*

*Corresponding: hongsoo@kribb.re.kr
Chemical Biology Research Center

BACKGROUND: The phenylpropanoid metabolites are an extremely diverse group of natural products biosynthesized by plants, fungi, and bacteria. Although these compounds are widely used in human health care and nutrition services, their availability is limited by regional variations, and isolation of single compounds from plants is often difficult. Recent advances in synthetic biology and metabolic engineering have enabled artificial production of plant secondary metabolites in microorganisms.
RESULTS: We develop an *Escherichia coli* system containing an artificial biosynthetic pathway that yields phenylpropanoic acids, such as 4-coumaric acid, caffeic acid, and ferulic acid, from simple carbon sources. These artificial biosynthetic pathways contained a codon-optimized *tal* gene that improved the productivity of 4-coumaric acid and ferulic acid, but not caffeic acid in a minimal salt medium. These heterologous pathways extended in *E. coli* that had biosynthesis machinery overproducing tyrosine. Finally, the titers of 4-coumaric acid, caffeic acid, and ferulic acid reached 974 mg/L, 150 mg/L, and 196 mg/L, respectively, in shake flasks after 36-hour cultivation.
CONCLUSIONS: We achieved one gram per liter scale production of 4-coumaric acid. In addition, maximum titers of 150 mg/L of caffeic acid and 196 mg/L of ferulic acid were achieved. Phenylpropanoic acids, such as 4-coumaric acid, caffeic acid, and ferulic acid, have a great potential for pharmaceutical applications and food ingredients. This work forms a basis for further improvement in production and opens the possibility of microbial synthesis of more complex plant secondary metabolites derived from phenylpropanoic acids.

PMID:23206756

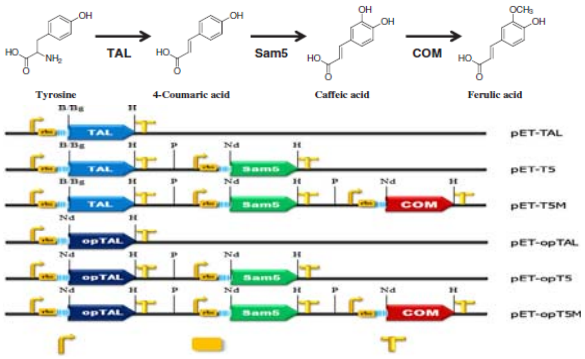

Keywords : Artificial biosynthetic pathway; *Escherichia coli*; Overproducing tyrosine; Phenylpropanoic acids; Phenylpropanoid metabolites

Article 314

Quercetin 3-rhamnoside exerts antiinfluenza A virus activity in mice

Phytother Res. 26(3):462-4.

Choi HJ, Song JH, Kwon DH*

*Co-corresponding: dhkwon@kribb.re.kr
Natural Medicine Research Center

Our previous report showed that quercetin 3-rhamnoside (Q3R) possessed antiviral activity against influenza A/WS/33 virus *in vitro*. The present study evaluated the effect of Q3R on influenza A/WS/33 virus infected mice. Mice orally treated with Q3R (6.25 mg/kg per dose) at 2 h before and once daily for 6 days after influenza virus infection showed significant decreases in weight loss, and decreased mortality. Lung virus titers of mice killed at 6 days after infection were about 2000 times lower than that of the placebo-treated control mice and about two times lower than that for the oseltamivir-treated mice. Furthermore, histological evaluation showed that administration of Q3R delayed the development and progression of pulmonary lesions. Therefore, Q3R could be an attractive lead for the development of antiviral agents against influenza virus.
PMID:21728202

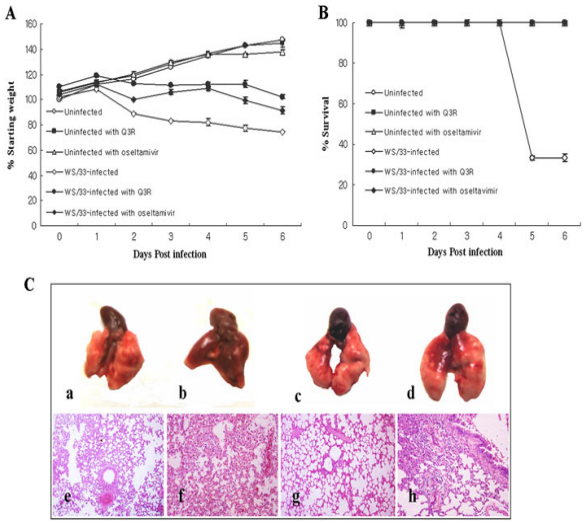

Keywords : Antiinfluenza A virus; Antiviral activity; Histological evaluation; Influenza; Mouse model; Quercetin 3-rhamnoside

Article 315

UBR2 of the N-end rule pathway is required for chromosome stability via histone ubiquitylation in spermatocytes and somatic cells

PLoS One. 7(5):e37414.

An JY, Kim E, Zakrzewska A, Yoo YD, Jang JM, Han DH, Lee MJ, Seo JW, Lee YJ, Kim TY, de Rooij DG, Kim BY*, Kwon YT

*Co-corresponding: bykim@kribb.re.kr
World Class Institute Center

The N-end rule pathway is a proteolytic system in which its recognition components (N-recognins) recognize destabilizing N-terminal residues of short-lived proteins as an essential element of specific degrons, called N-degrons. The RING E3 ligases UBR2 and UBR1 are major N-recognins that share size (200 kDa), conserved domains and substrate specificities to N-degrons. Despite the known function of the N-end rule pathway in degradation of cytosolic proteins, the major phenotype of UBR2-deficient male mice is infertility caused by arrest of spermatocytes at meiotic prophase I. UBR2-deficient spermatocytes are impaired in transcriptional silencing of sex chromosome-linked genes and ubiquitylation of histone H2A. In this study we show that the recruitment of UBR2 to meiotic chromosomes spatiotemporally correlates to the induction of chromatin-associated ubiquitylation, which is significantly impaired in UBR2-deficient spermatocytes. UBR2 functions as a scaffold E3 that promotes HR6B/UbcH2-dependent ubiquitylation of H2A and H2B but not H3 and H4, through a mechanism distinct from typical polyubiquitylation. The E3 activity of UBR2 in histone ubiquitylation is allosterically activated by dipeptides bearing destabilizing N-terminal residues. Insufficient monoubiquitylation and polyubiquitylation on UBR2-deficient meiotic chromosomes correlate to defects in double strand break (DSB) repair and other meiotic processes, resulting in pachytene arrest at stage IV and apoptosis. Some of these functions of UBR2 are observed in somatic cells, in which UBR2 is a chromatin-binding protein involved in chromatin-associated ubiquitylation upon DNA damage. UBR2-deficient somatic cells show an array of chromosomal abnormalities, including hyperproliferation, chromosome instability, and hypersensitivity to DNA damage-inducing reagents. UBR2-deficient mice enriched in C57 background die upon birth with defects in lung expansion and neural development. Thus, UBR2, known as the recognition component of a major cellular proteolytic system, is associated with chromatin and controls chromatin dynamics and gene expression in both germ cells and somatic cells.
PMID:22616001

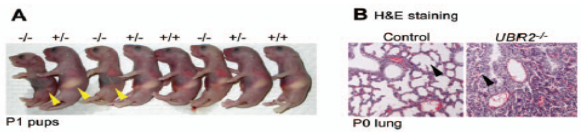

Keywords : Chromatin dynamics; Germ cells; Lung expansion; N-end rule pathway; UBR2 functions

Article 316

Cryptopleurine targets NF-κB pathway, leading to inhibition of gene products associated with cell survival, proliferation, invasion, and angiogenesis

PLoS One. 7(6):e40355.

Jin HR, Jin SZ, Cai XF, Li D, Wu X, Nan JX, Lee JJ*, Jin X

*Co-corresponding: jjlee@kribb.re.kr
Chemical Biology Research Center

BACKGROUND: Cryptopleurine, a phenanthroquinolizidine alkaloid, was known to exhibit anticancer activity; however, the underlying mechanism is poorly understood. Because the nuclear factor-κB (NF-κB) transcription factors control many physiological processes including inflammation, immunity, and development and progression of cancer, we investigated the effects of cryptopleurine on tumor necrosis factor alpha (TNF-α)-induced NF-κB activation pathway and on the expression of NF-κB-regulated gene products associated with many pathophysiological processes.
METHODOLOGY AND PRINCIPAL FINDING: MDA-MB231, MDA-MB435, MCF-7, HEK293, RAW264.7 and Hep3B cells were used to examine cryptopleurine's effect on the NF-κB activation pathway. Major assays were promoter-reporter gene assay, electrophoretic mobility shift assay (EMSA), *in vitro* immune complex kinase assay, real-time PCR, Western blot analysis, and Matrigel invasion assay. Experiments documenting cell proliferation and apoptosis were analyzed by MTT method and flow cytometry, respectively. The results indicated that cryptopleurine suppressed the NF-κB activation through the inhibition of IκB kinase (IKK) activation, thereby blocking the phosphorylation and degradation of the inhibitor of NF-κB alpha (IκBα) and the nuclear translocation and DNA-binding activity of p65. The suppression of NF-κB by cryptopleurine led to the down-regulation of gene products involved in inflammation, cell survival, proliferation, invasion, and angiogenesis.
CONCLUSIONS AND SIGNIFICANCE: Our results show that cryptopleurine inhibited NF-κB activation pathway, which leads to inhibition of inflammation, proliferation, and invasion, as well as potentiation of apoptosis. Our findings provide a new insight into the molecular mechanisms and a potential application of cryptopleurine for inflammatory diseases as well as certain cancers associated with abnormal NF-κB activation.
PMID:22768286

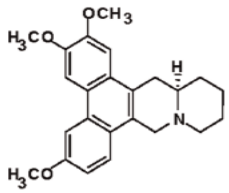

Keywords : Cryptopleurine; Flow cytometry; IKK; Inflammatory diseases; MTT method; NF-κB

Article 317

Convenient synthesis of an isoxazole compound, KRIBB3, as an anticancer agent

Synthetic Comm. 42(13):1890-4.

Lee HK, Yun E, Min JH, Yoon KS, Choung DH, Lee S*

*Co-corresponding: sangku@kribb.re.kr
Targeted Medicine Research Center

A diaryl isoxazole compound, KRIBB3, which exhibits strong antimigratory and antimitotic activities against cancer cells, was prepared in a practical synthetic way. The synthetic method may provide easy access to KRIBB3 analogs with various substituents at an aryl moiety for structure-activity relationships (SAR), as well as a large quantity of KRIBB3 for *in vivo* studies.

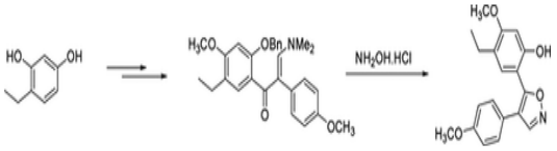

Keywords : Anticancer; Antimigratory; Antineoplastic agent; Cyclization; Isoxazole derivative

Article 318

K-RAS transformation in prostate epithelial cell overcomes H_2O_2-induced apoptosis via upregulation of gamma-glutamyltransferase-2

Toxicol In Vitro. 26(3):429-34.

Moon DO, Kim BY, Jang JH, Kim MO, Jayasooriya RG, Kang CH, Choi YH, Moon SK, Kim WJ, Ahn JS*, Kim GY

*Co-corresponding: jsahn@kribb.re.kr
Chemical Biology Research Center

The anti-apoptotic oncogene K-RAS is hypothesized to increase the antioxidant status of cells, thereby protecting them from generation of reactive oxygen species (ROS). Therefore, we examined whether K-RAS overcomes hydrogen peroxide (H_2O_2)-mediated apoptosis in the human fetal prostate epithelial cell 267B1. In this study, we found that treatment of 267B1 cells with H_2O_2 resulted in significant reduction of cell growth, which was associated with cytochrome-*c* release and caspase-3 activation. However, mutated K-RAS transformation (268B1/K-RAS) rendered 267B1 cells reduction of the resistance to H_2O_2-induced apoptosis through suppression of ROS generation. In addition, we analyzed profiling of gene expression in K-RAS transformation and found that gamma-glutamyltransferase 2 (GGT2) most highly expressed. Transient knockdown of K-RAS resulted in a significant downregulation of *GGT* gene expression. We also revealed that expression of *GGT2* gene is closely regulated by the ERK signal pathway in 267B1/K-RAS cells. In addition, the anti-apoptotic effect of mutated K-RAS was attenuated by treatment with GGT2 RNA interference through inhibition of ROS generation, suggesting that mutated K-RAS mediates resistance to H_2O_2-induced apoptosis through GGT2 activation. These results importantly provide mechanistic insights on the anti-apoptotic activity of mutated K-RAS.

PMID:22269385

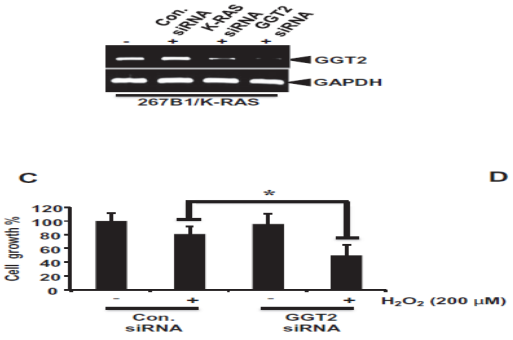

Keywords : Anti-apoptotic effect; K-RAS; Gamma-glutamyltransferase-2; Oxidative stress

Article 319

Updates on the genetic variations of norovirus in sporadic gastroenteritis in Chungnam Korea, 2009-2010

Virol J. 9:29.

Park K, Yeo S, Jeong H, Baek K, Kim D, Shin M, Song J, Lee S, Choi Y, Park J, Cho S*, Cheon D

*Co-corresponding: sungchan@kribb.re.kr
Targeted Medicine Research Center

Previously, we explored the epidemic pattern and molecular characterization of noroviruses (NoVs) isolated in Chungnam, Korea in 2008, and the present study extended these observations to 2009 and 2010. In Korea, NoVs showed the seasonal prevalence from late fall to spring, and widely detected in preschool children and peoples over 60 years of age. Epidemiological pattern of NoV was similar in 2008 and in 2010, but pattern in 2009 was affected by pandemic influenza A/H1N1 2009 virus. NoV-positive samples were subjected to sequence determination of the capsid gene region, which resolved the isolated NoVs into five GI (2, 6, 7, 9 and 10) and eleven GII genotypes (1, 2, 3, 4, 6, 7, 8, 12, 13, 16 and 17). The most prevalent genotype was GII.4 and occupied 130 out of 211 NoV isolates (61.6%). Comparison of NoV GII.4 of prevalent genotype in these periods with reference strains of the same genotype was conducted to genetic analysis by a phylogenetic tree. The NoV GII.4 strains were segregated into seven distinct genetic groups, which are supported by high bootstrap values and previously reported clusters. All Korean NoV GII.4 strains belonged to either VI cluster or VII cluster. The divergence of nucleotide sequences within VI and VII intra-clusters was > 3.9% and > 3.5%, respectively. The "Chungnam(06-117)/2010" strain which was isolated in June 2010 was a variant that did not belong to cluster VI or VII and showed 5.8-8.2%, 6.2-8.1% nucleotide divergence with cluster VI and VII, respectively.

PMID:22273062

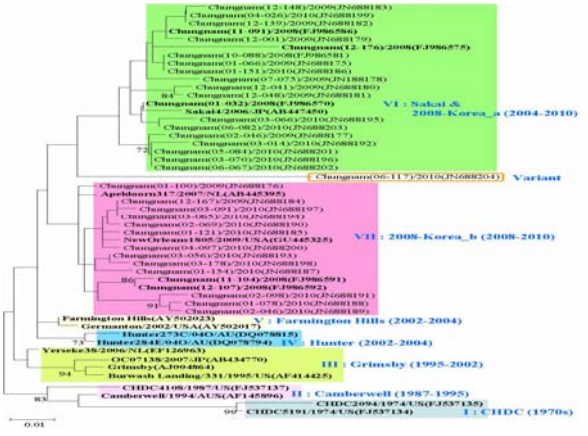

Keywords : Genetic analysis; Genetic variations; Noroviruses; Pandemic influenza A/H1N1 2009 virus

2012
KRIBB Article Abstracts : First or corresponding articles indexed in SCIE, Scopus, and PubMed

Jeonbuk Branch Institute

- Applied Microbiology Research Center
- Infection Control Material Research Center
- Bioindustrial Process Research Center

Korea Research Institute of Bioscience and Biotechnology

Article 320

Optimization of culture conditions for 1,3-propanediol production from glycerol using a mutant strain of *Klebsiella pneumoniae*

Appl Biochem Biotechnol. 166(1):127-37.

Oh BR, Seo JW, Heo SY, Hong WK, Luo LH, Kim S, Park DH, Kim CH*

*Corresponding: kim3641@kribb.re.kr
Applied Microbiology Research Center

In the present work, mutant strains of *Klebsiella pneumoniae* with deletions of the *als* gene encoding acetolactate synthase involved in synthesis of 2,3-butanediol, the *ldhA* gene encoding lactate dehydrogenase required for lactate synthesis, or both genes, were prepared. Production of 1,3-propanediol (1,3-PD) from glycerol was enhanced in the *ldhA* mutant strain (Δ*ldhA*), but lower in Δ*als* or Δ*als* Δ*ldhA* mutant strains compared to the parent strain, concomitant with a reduction in the glycerol consumption rate, indicating that deletion of *ldhA* alone was useful to improve 1,3-PD production. Fed-batch fermentation analysis revealed that, in the Δ*ldhA* mutant strain, 1,3-PD production was higher at low pH than at neutral pH; the reverse was true for the parent strain. Further optimization of culture conditions, by variation of aeration and glycerol feed rates, dramatically improved the production of 1,3-PD by the mutant strain. The maximum level attained was 102.7 g l^{-1} of 1,3-PD from glycerol.

PMID:22072138

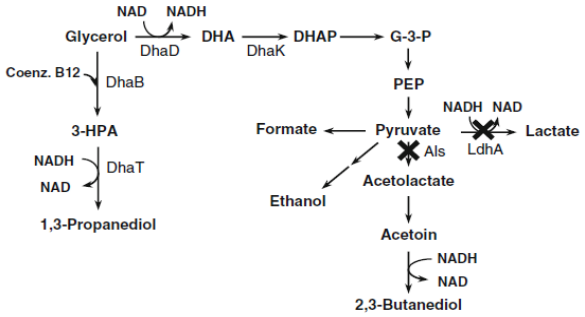

Keywords : 1,3-Propanediol; Culture conditions; Gene deletion; Glycerol; *Klebsiella pneumoniae*

Article 321

A rapid and simple method for preparing an insoluble substrate for screening of microbial xylanase

Appl Biochem Biotechnol. 167(4):677-84.

Ko KC, Han Y, Shin BS, Choi JH*, Song JJ*

*Co-corresponding: jhchoi@kribb.re.kr jjsong@kribb.re.kr
Applied Microbiology Research Center

Several types of enzymes, including cellulases and xylanases, are required to degrade hemicelluloses and cellulose, which are major components of lignocellulosic biomass. Such degradative processes can be used to produce various useful industrial biomaterials. Screening methods for detecting polysaccharide-degrading microorganisms include the use of dye-labeled substrates in growth medium and culture plate staining techniques. However, the preparation of screening plates, which typically involves chemical cross-linking to synthesize a dye-labeled substrate, is a complicated and time-consuming process. Moreover, such commercial substrates are very expensive, costing tenfold more than the natural xylan. Staining methods are also problematic because they may damage relevant microorganisms and are associated with contamination of colonies of desirable organisms with adjacent unwanted bacteria. In the present study, we describe a sonication method for the simple and rapid preparation of an insoluble substrate that can be used to screen for xylanase-expressing bacteria in microbial populations. Using this new method, we have successfully isolated a novel xylanase gene from a xylolytic microorganism termed Xyl02-KBRB and Xyl14-KBRB in the bovine rumen.

PMID:22585365

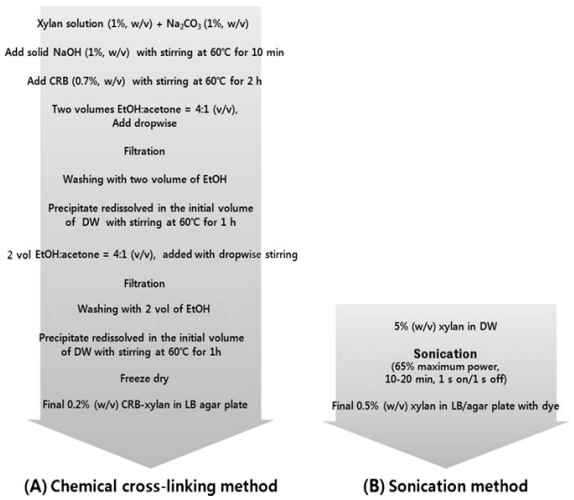

Keywords : Assay method; Dye substrate; Screening method; Sonication method; Xylanase

Article 322

Inhibition of LFA-1/ICAM-1-mediated cell adhesion by stilbene derivatives from *Rheum undulatum*

Arch Pharm Res. 35(10):1763-70.

Lee SW, Hwang BS, Kim MH, Park CS, Lee WS, Oh HM*, Rho MC*

*Co-corresponding: ohhm@kribb.re.kr rho-m@kribb.re.kr
Bioindustrial Process Research Center

Six stilbenes were isolated from the methanol extract of *Rheum undulatum* rhizomes by bioactivity-guided fractionation. The structures of the compounds were determined by spectroscopic analysis (^{1}H-, ^{13}C-NMR and MS), to be desoxyrhapontigenin (1), rhapontigenin (2), *trans*-resveratrol (3), piceatannol (4), piceatannol-3'-O-β-D-glucopyranoside (5) and isorhapontin (6). Compounds 1-4 inhibited the direct binding between sICAM-1 and LFA-1 of the THP-1 cells in a dose-dependent manner with IC_{50} values of 50.1, 25.4, 33.4 and 45.9 μM, respectively. On the other hand, the other compounds 5 and 6 with a glucose moiety in each molecule did not show any inhibitory activity in the cell adhesion assay (IC_{50} values of >100.0 μM). Compounds 2, 3 and 4 also had an inhibitory effect on direct binding between sVCAM-1 and VLA-4 of THP-1 cells. This suggests that the stilbenes from *Rheum undulatum* rhizomes are good candidates for therapeutic strategies towards inflammation.

PMID:23139127

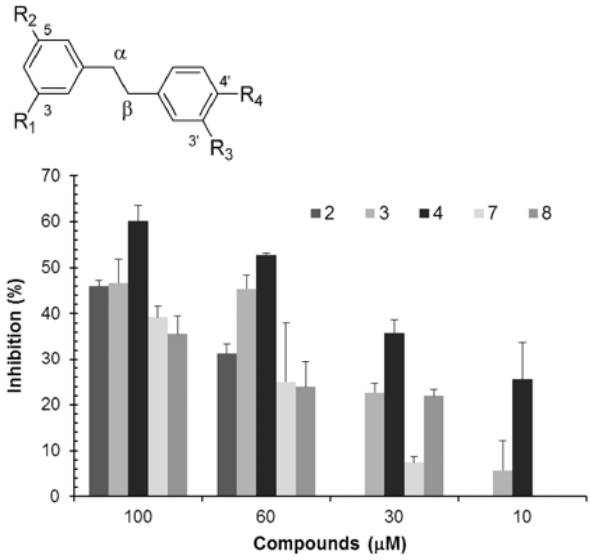

Keywords : Anti-inflammatory agents; Cell adhesion molecules; Intercellular adhesion molecule-1 (ICAM-1); Lymphocyte functionassociated antigen-1 (LFA-1); *Rheum undulatum*; Stilbenes

Article 323

Homoisoflavonoids from *Caesalpinia sappan* displaying viral neuraminidases inhibition

Biol Pharm Bull. 35(5):786-90.

Jeong HJ, Kim YM, Kim JH, Kim JY, Park JY, Park SJ, Ryu YB*, Lee WS*

*Co-corresponding: ybryu@kribb.re.kr wslee@kribb.re.kr
Infection Control Material Research Center

In this study, twelve neuraminidase (NA) inhibitory compounds 1-12 were isolated from heartwood of *Caesalpinia sappan* on the basis of their biological activities against three types of viral NAs. Of isolated homoisoflavonoids, sappanone A (2) showed the most potent NAs inhibitory activities with IC_{50} values of 0.7 μM [H1N1], 1.1 μM [H3N2], and 1.0 μM [H9N2], respectively, whereas saturated homoisoflavonoid (3) did not show significantly inhibition. This result revealed that α,β-unsaturated carbonyl group in A-ring was the key requirements for viral NAs inhibitory activity. In our enzyme kinetic study, all NA inhibitors screened were found to be reversible noncompetitive types.

PMID:22687418

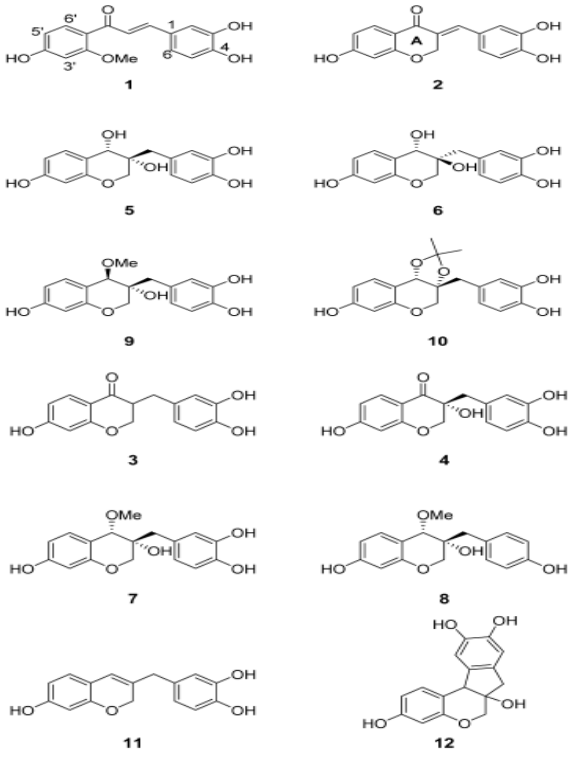

Keywords : α,β-unsaturated carbonyl; *Caesalpinia sappan*; Heartwood; Homoisoflavonoid; NA inhibitors; Viral neuraminidases

Article 324

Diarylheptanoids from *Alnus japonica* inhibit papain-like protease of severe acute respiratory syndrome coronavirus

Biol Pharm Bull. 35(11):2036-42.

Park JY, Jeong HJ, Kim JH, Kim YM, Park SJ, Kim D, Park KH, Lee WS*, Ryu YB*

*Co-corresponding: wslee@kribb.re.kr ybryu@kribb.re.kr
Infection Control Material Research Center

The papain-like protease (PL^{pro}), which controls replication of the severe acute respiratory syndrome coronavirus (SARS-CoV), has been identified as a potential drug target for the treatment of SARS. An intensive hunt for effective anti-SARS drugs has been undertaken by screening for natural product inhibitors that target SARS-CoV PL^{pro}. In this study, diarylheptanoids 1-9 were isolated from *Alnus japonica*, and the inhibitory activities of these compounds against PL^{pro} were determined. Of the isolated diarylheptanoids, hirsutenone (2) showed the most potent PL^{pro} inhibitory activity, with an inhibitory concentration (IC_{50}) value of 4.1 μM. Structure-activity analysis showed that catechol and α,β-unsaturated carbonyl moiety in the molecule were the key requirement for SARS-CoV cysteine protease inhibition.

PMID: 22971649

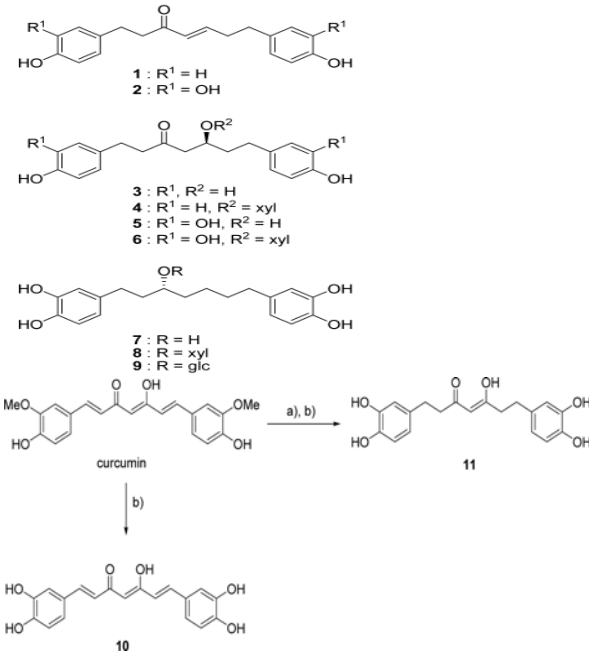

Keywords : *Alnus japonica*; Cysteine protease; Diarylheptanoid; Papain-like protease; Severe acute respiratory syndrome

Article 325

Selective and slow-binding inhibition of shikonin derivatives isolated from *Lithospermum erythrorhizon* on glycosyl hydrolase 33 and 34 sialidases

Bioorg Med Chem. 20(5):1740-8.

Kim JY, Jeong HJ, Park JY, Kim YM, Park SJ, Cho JK, Park KH, Ryu YB*, Lee WS*

*Co-corresponding: ybryu@kribb.re.kr wslee@kribb.re.kr
Infection Control Material Research Center

Sialidases are enzymes that catalyze the hydrolysis of sialic acid residues from various glycoconjugates, which are widely found in a number of viral and microbial pathogens. In this study, we investigated the biological evaluation of isolated six shikonins (1-6) and three shikonofurans (7-9) from *Lithospermum erythrorhizon*. The nine isolated compounds 1-9 showed strong and selective inhibition of glycosyl hydrolase (GH) 33 and -34 sialidases activities. In GH33 bacterial-sialidase inhibition assay, the inhibitory activities against GH33 siadliase of all shikonofuran derivatives (7-9) were greater than shikonin derivatives (1-6). Shikonofuran E (8) exhibited the most potent inhibitory activity toward GH33 sialidases (IC_{50}=0.24μM). Moreover, our detailed kinetic analysis of these species unveiled that they are all competitive and simple reversible slow-binding inhibitors. Otherwise, they showed different inhibitory capacities and kinetic modes to GH34 viral-sialidase activity. All the naphthoquinone derivatives (1-6) were of almost equal efficiency with IC_{50} value of 40μM and shikonofurans (7-9) did not show the significant inhibitory effect to GH34 sialidase. Kinetic analyses indicated that naphthoquinones acted via a noncompetitive mechanism.

PMID:22300884

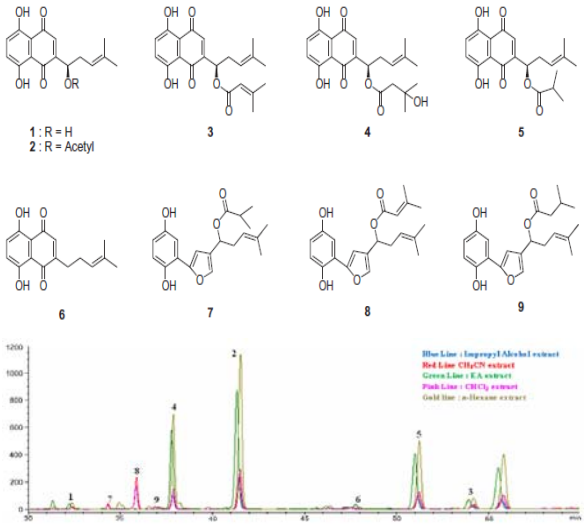

Keywords : Glycosyl hydrolase; Lithospermum erythrorhizon; Shikonin; Shikonofuran; Sialidase

Article 326

Cholinestrase inhibitory effects of geranylated flavonoids from *Paulownia tomentosa* fruits

Bioorg Med Chem. 20(8):2595-602.

Cho JK, Ryu YB*, Curtis-Long MJ, Ryu HW, Yuk HJ, Kim DW, Kim HJ, Lee WS, Park KH

*Co-first: ybryu@kribb.re.kr
Infection Control Material Research Center

Alzheimer's disease is rapidly becoming one of the most prevalent human diseases. Inhibition of human acetylcholinestrase (hAChE) and butyrylcholinestrase (BChE) has been linked to amelioration of Alzheimer's symptoms and research into inhibitors is of critical importance. Purification of the methanol extract of *Paulownia tomentosa* fruits yielded potent hAChE and BChE inhibitory flavonoids (1-9). A comparative activity screen indicated that a geranyl group at C6 is crucial for both hAChE and BChE. For example, diplacone (8) showed 250-fold higher efficacy than its parent eriodictyol (12). IC_{50}s of diplacone (8) were 7.2 μM for hAChE and 1.4 μM for BChE. Similar trends were also observed for 4'-O-methyldiplacone (4) (vs its parent, hesperetin 10) and mimulone (7) (vs its parent, naringenin 11). Representative inhibitors (1-8) showed mixed inhibition kinetics as well as time-dependent, reversible inhibition toward hAChE. The binding affinities of these compounds to hAChE were investigated by monitoring quenching of inherent enzyme fluorescence. The affinity constants (K_{SA}) increased in proportion to inhibitory potencies.

PMID:22445674

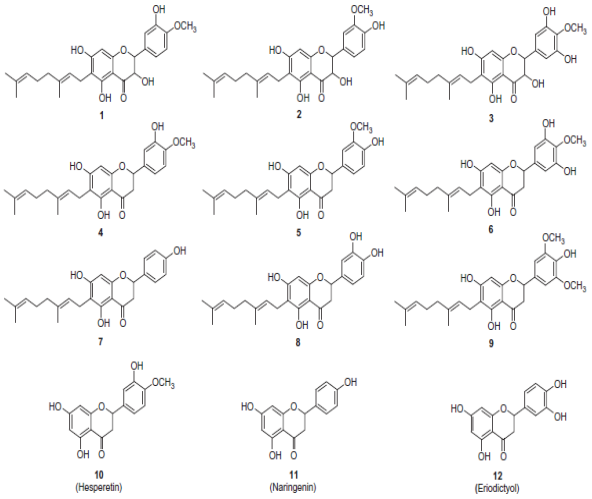

Keywords : Butyrylcholinesterase; Fluorescence quenching; Human acetylcholinesterase; *Paulownia tomentosa*; Time-dependent inhibitor

Article 327

Tanshinones as selective and slow-binding inhibitors for SARS-CoV cysteine proteases

Bioorg Med Chem. 20(19):5928-35.

Park JY, Kim JH, Kim YM, Jeong HJ, Kim DW, Park KH, Kwon HJ, Park SJ, Lee WS*, Ryu YB*

*Co-corresponding: wslee@kribb.re.kr ybryu@kribb.re.kr
Infection Control Material Research Center

In the search for anti-SARS-CoV, tanshinones derived from *Salvia miltiorrhiza* were found to be specific and selective inhibitors for the SARS-CoV $3CL^{pro}$ and PL^{pro}, viral cysteine proteases. A literature search for studies involving the seven isolated tanshinone hits showed that at present, none have been identified as coronaviral protease inhibitors. We have identified that all of the isolated tanshinones are good inhibitors of both cysteine proteases. However, their activity was slightly affected by subtle changes in structure and targeting enzymes. All isolated compounds (1-7) act as time dependent inhibitors of PL^{pro}, but no improved inhibition was observed following preincubation with the $3CL^{pro}$. In a detail kinetic mechanism study, all of the tanshinones except rosmariquinone (7) were identified as noncompetitive enzyme isomerization inhibitors. However, rosmariquinone (7) showed a different kinetic mechanism through mixed-type simple reversible slow-binding inhibition. Furthermore, tanshinone I (5) exhibited the most potent nanomolar level inhibitory activity toward deubiquitinating (IC_{50}=0.7 μM). Additionally, the inhibition is selective because these compounds do not exert significant inhibitory effects against other proteases including chymotrysin, papain, and HIV protease. These findings provide potential inhibitors for SARS-CoV viral infection and replication.

PMID: 22884354

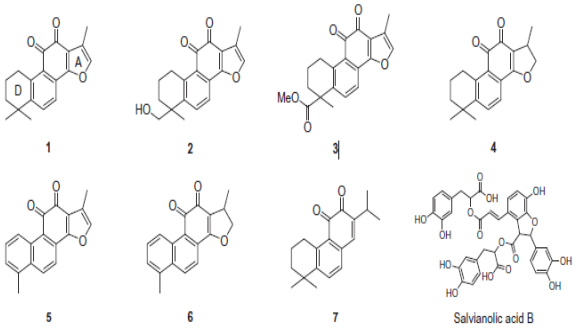

Keywords : 3CLpro; PLpro; SARS-CoV; Slow-binding inhibitor; Tanshinone

Article 328

Production of cellulase enzymes during the solid-state fermentation of empty palm fruit bunch fiber

Bioprocess Biosyst Eng. 35(1-2):61-7.

Kim S, Kim CH*

*Corresponding: kim3641@kribb.re.kr
Applied Microbiology Research Center

Penicillium verruculosum COKE4E is a fungal strain isolated from bituminous coal. The microorganism cultivated in a minimal medium supplemented with Avicel, carboxymethylcellulose, and oat spelt xylan produced cellulase enzymes as exhibiting carboxymethylcellulase (CMCase), Avicelase, xylanase, and cellobiosidase activities. In this study, the productivity of the extracellular enzymes in the strain was evaluated by using empty palm fruit bunch fiber (EPFBF), a lignocellulosic biomass, as a substrate for solid-state bioconversion. The highest cellulase activities were observed after 6 days of fermentation at pH 6.0 and 30 °C. The enzymes were secreted as cellulosomes for the degradation of EPFBF as a sole carbon source. Focused ion beam analysis showed that *P. verruculosum* COKE4E produced cellulolytic enzymes that were able to effectively biodegrade EPFBF during solid-state fermentation. In this process, 6.5 U of CMCase, 6.8 U of Avicelase, and 8.8 U of xylanase per gram of dry solid EPFBF were produced. These results demonstrate that EPFBF may be a potential raw material in solid-state fermentation for the production of cellulase enzymes to be used for biofuel production.
PMID: 22052232

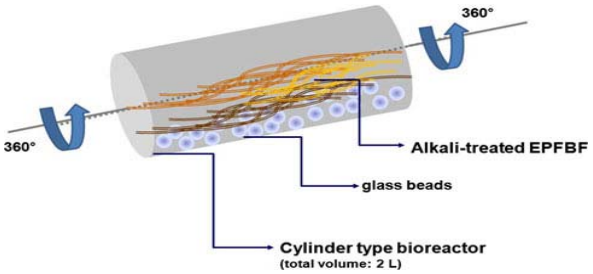

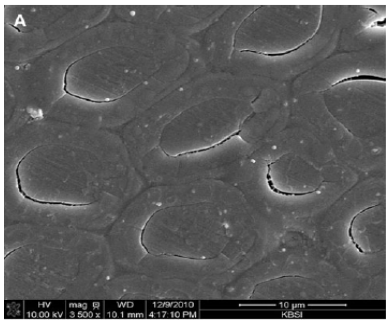

Keywords : Cellulase; Cellulosome; Empty palm fruit bunch fiber; Fungus; Lignocellulosic biomass; *Penicillium verruculosum*; Solid-state fermentation

Article 329

Growth of the oleaginous microalga *Aurantiochytrium* sp. KRS101 on cellulosic biomass and the production of lipids containing high levels of docosahexaenoic acid

Bioprocess Biosyst Eng. 35(1-2):129-33.

Hong WK, Kim CH, Rairakhwada D, Kim S, Hur BK, Kondo A, Seo JW*

*Co-corresponding: jwseo@kribb.re.kr
Applied Microbiology Research Center

We examined the growth of a novel oleaginous microalga, *Aurantiochytrium* sp. KRS101, using cellulosic materials as nutrients, and the resultant production of lipids containing high levels of docosahexaenoic acid (DHA). The microalgal strain could grow using either carboxymethylcellulose or cellobiose as a carbon source, and produced lipids containing high levels of DHA (49-58% of total fatty acids). In line with this growth behavior, carboxymethylcellulase and cellobiohydrolase activities were evident in both cell-free lysates and culture broths. Additionally, an industrial cellulosic biomass, palm oil empty fruit bunches (POEFB), a by-product of the palm oil industry, were utilized by the microalgal strain for cell growth and lipid production.
PMID: 21959581

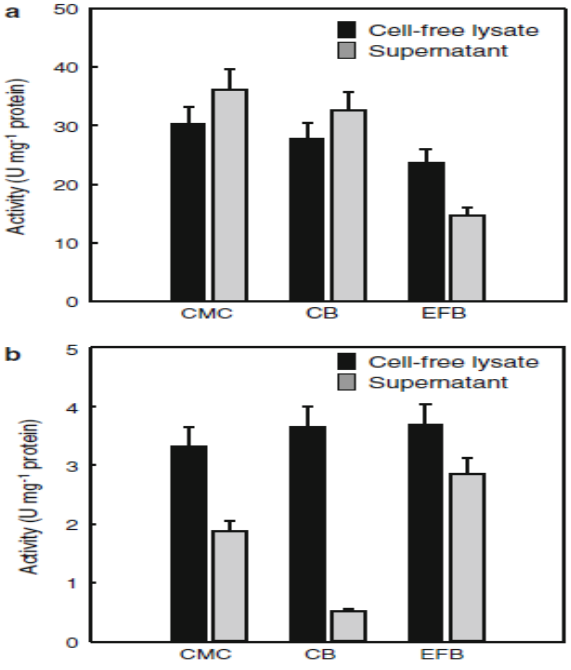

Keywords : *Aurantiochytrium*; Cellulose; Empty fruit bunch; Lipid; Microalga

Article 330

Fermentation strategies for 1,3-propanediol production from glycerol using a genetically engineered *Klebsiella pneumoniae* strain to eliminate by-product formation

Bioprocess Biosyst Eng. 35(1-2):159-65.

Oh BR, Seo JW, Heo SY, Hong WK, Luo LH, Son JH, Park DH, Kim CH*

*Corresponding: kim3641@kribb.re.kr
Applied Microbiology Research Center

We generated a genetically engineered *Klebsiella pneumoniae* strain (AK-VOT) to eliminate by-product formation during production of 1,3-propanediol (1,3-PD) from glycerol. In the present study, the glycerol-metabolizing properties of the recombinant strain were examined during fermentation in a 5 L bioreactor. As expected, by-product formation was completely absent (except for acetate) when the AK-VOT strain fermented glycerol. However, 1,3-PD productivity was severely reduced owing to a delay in cell growth attributable to a low rate of glycerol consumption. This problem was solved by establishing a two-stage process separating cell growth from 1,3-PD production. In addition, nutrient co-supplementation, especially with starch, significantly increased 1,3-PD production from glycerol during fed-batch fermentation by AK-VOT in the absence of by-product formation.
PMID: 21959580

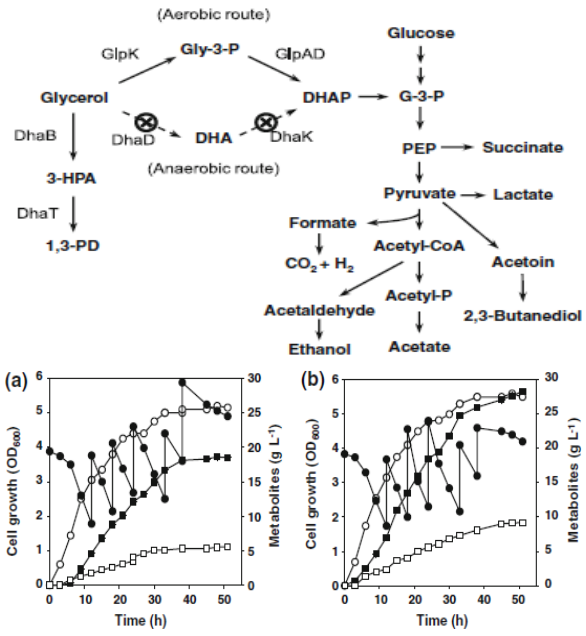

Keywords : 1,3-Propanediol; By-product formation; Glycerol; *Klebsiella pneumoniae*; Nutrient co-supplementation; Two-stage fermentation

Article 331

Production of 3-hydroxypropionic acid through propionaldehyde dehydrogenase PduP mediated biosynthetic pathway in *Klebsiella pneumoniae*

Bioresour Technol. 103(1):1-6.

Luo LH, Kim CH, Heo SY, Oh BR, Hong WK, Kim S, Kim DH, Seo JW*

*Corresponding: jwseo@kribb.re.kr
Applied Microbiology Research Center

The *pduP* gene encodes a propionaldehyde dehydrogenase (PduP) was investigated for the role in 3-hydroxypropionic acid (3-HP) glycerol metabolism in *Klebsiella pneumoniae*. The enzyme assay showed that cell extracts from a *pduP* mutant strain lacked measurable dehydrogenase activity. Additionally, the mutant strain accumulated the cytotoxic intermediate metabolite 3-hydroxypropionaldehyde (3-HPA), causing both cell death and a lower final 3-HP titer. Ectopic expression of *pduP* restored normal cell growth to mutant. The enzymatic property of recombinant protein from *Escherichia coli* was examined, exhibiting a broad substrate specificity, being active on 3-HPA. The present work is thus the first to demonstrate the role of PduP in glycerol metabolism and biosynthesis of 3-HP.
PMID: 22018749

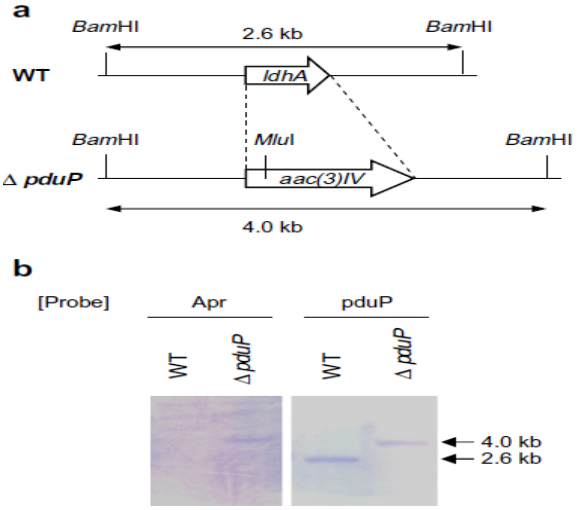

Keywords : 3-hydroxypropionic acid; Glycerol; *Klebsiella pneumoniae*; Propanediol utilization protein; Propionaldehyde dehydrogenase

Article 332

Sequential acid-/alkali-pretreatment of empty palm fruit bunch fiber

Bioresour Technol. 109:229-33.

Kim S, Park JM, Seo JW, Kim CH*

*Corresponding: kim3641@kribb.re.kr
Applied Microbiology Research Center

Pretreatment processes are key technologies for generating fermentable sugars based on lignocellulosic biomass. In this study, we developed a novel method for empty palm fruit bunch fiber (EPFBF) using sequential pretreatment with dilute acid and then alkali. Dilute sulfuric acid was used in the first step, which removed 90% of the hemicellulose and 32% of the lignin, but left most of the cellulose under the optimum pretreatment condition. Sodium hydroxide was then applied in the second step, which extracted lignin effectively with a 70% delignification yield, partially disrupting the ordered fibrils of the EPFBF and thus enhancing the enzyme digestibility of the cellulose. The sequentially pretreated biomass consisted of 82% cellulose, less than 1% hemicellulose, and 30% lignin content afterward. The pretreated biomasses morphologically revealed rough, porous, and irregularly ordered surfaces for enhancing enzyme digestibility. These results indicate that the sequentially acid/alkali-pretreated EPFBF could be broadly useful as a novel biomass.

PMID: 22306078

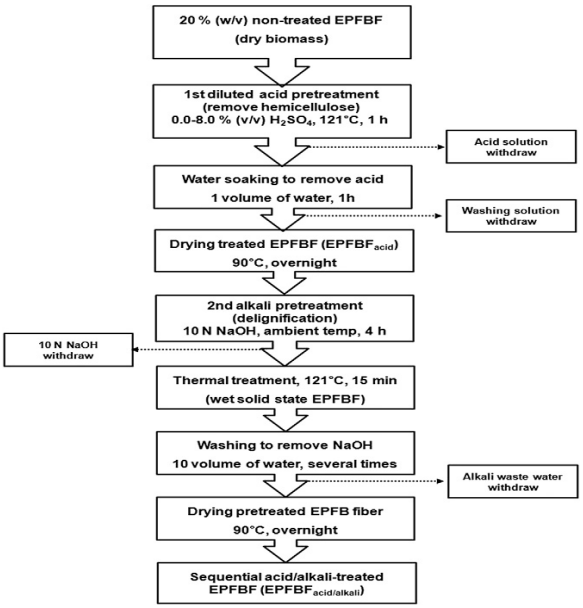

Keywords : Delignification; Diluted acid/alkaline pretreatment; Empty palm fruit bunch fiber; Enzyme hydrolysis; Sequential pretreatment

Article 333

Production of human papillomavirus type 33 L1 major capsid protein and virus-like particles from *Bacillus subtilis* to develop a prophylactic vaccine against cervical cancer

Enzyme Microb Technol. 50(3):173-80.

Baek JO, Seo JW, Kwon O, Park SM, Kim CH*, Kim IH

*Co-corresponding: kim3641@kribb.re.kr
Applied Microbiology Research Center

We developed a bacterial expression system to produce human papillomavirus (HPV) type 33 L1 major capsid protein and virus-like particles from a recombinant *Bacillus subtilis* strain. For the first time, we have isolated self-assembled virus-like particles (VLPs) of HPV type 33 from *B. subtilis*, a strain generally recognized as safe (GRAS). The gene encoding the major capsid protein L1 of HPV type 33 was amplified from viral DNA isolated from a Korean patient and expressed in *B. subtilis*; a xylose-induction system was used to control gene activity. HPV33 L1 protein was partially purified by 40% (w/v) sucrose cushion centrifugation and strong cation exchange column chromatography. Eluted samples exhibited immunosignaling in fractions of 0.5-1.0 M NaCl. The HPV33 L1 protein was shown to be approximately 56 kDa in size by SDS-PAGE and Western blotting; recovery and purity were quantified by indirect immuno-ELISA assay. The final yield and purity were approximately 20.4% and 10.3%, respectively. Transmission electron microscopic analysis of fractions immunoactive by ELISA revealed that the L1 protein formed self-assembled VLPs with a diameter of approximately 20-40 nm. Humoral and cellular immune responses provoked by the *B. subtilis*/HPV33 L1 strain were approximately 100- and 3-fold higher than those of the empty *B. subtilis* strain as a negative control, respectively. Development of a VLP production and delivery system using *B. subtilis* will be helpful, in that the vaccine may be convenient production as an antigen delivery system. VLPs thus produced will be safer for human use than those purified from Gram-negative strains such as *Escherichia coli*. Also, use of *B. subtilis* as a host may aid in the development of either live or whole cell vaccines administered by antigen delivery system.

PMID:22305172

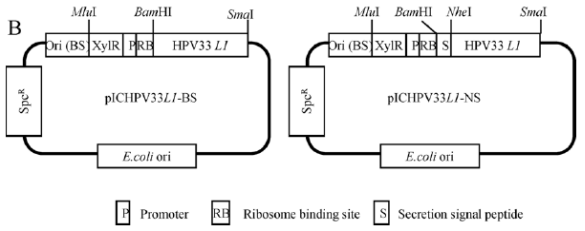

Keywords : Antigen delivery system; *Bacillus subtilis*; Cervical cancer; Human papillomavirus (HPV); Virus-like particle (VLP)

Article 334

Bacteroides thetaiotaomicron VPI-5482 glycoside hydrolase family 66 homolog catalyzes dextranolytic and cyclization reactions

FEBS J. 279(17):3185-91.

Kim YM*, Yamamoto E, Kang MS, Nakai H, Saburi W, Okuyama M, Mori H, Funane K, Momma M, Fujimoto Z, Kobayashi M, Kim D, Kimura A

*First: u9897854@kribb.re.kr
Infection Control Material Research Center

Bacteroides thetaiotaomicron VPI-5482 harbors a gene encoding a putative cycloisomaltooligosaccharide glucanotransferase (*BT3087*) belonging to glycoside hydrolase family 66. The goal of the present study was to characterize the catalytic properties of this enzyme. Therefore, we expressed *BT3087* (recombinant endo-dextranase from *Bacteroides thetaiotaomicron* VPI-5482) in *Escherichia coli* and determined that recombinant endo-dextranase from *Bacteroides thetaiotaomicron* VPI-5482 preferentially synthesized isomaltotetraose and isomaltooligosaccharides (degree of polymerization > 4) from dextran. The enzyme also generated large cyclic isomaltooligosaccharides early in the reaction. We conclude that members of the glycoside hydrolase 66 family may be classified into three types: (a) endo-dextranases, (b) dextranases possessing weak cycloisomaltooligosaccharide glucanotransferase activity, and (c) cycloisomaltooligosaccharide glucanotransferases.
PMID:22776355

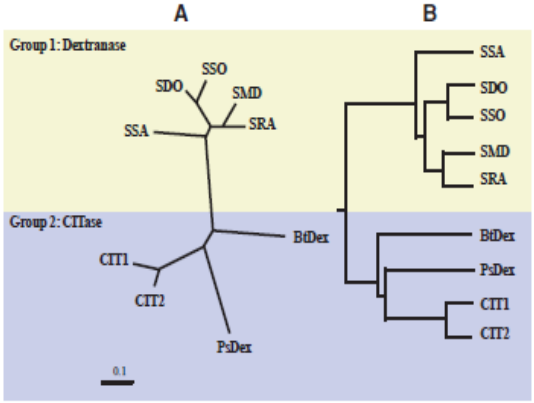

Keywords : *Bacteroides thetaiotaomicron* VPI-5482; Cycloisomaltooligosaccharide glucanotransferase; Endo-dextranase; Glycoside hydrolase family 66; Isomaltotetraose

Article 335

Azuki bean (*Vigna angularis*) extract inhibits the development of experimentally induced atopic dermatitis-like skin lesions in NC/Nga mice

Food Chem. 132(3):1269-75.

Collantes TM, Rho MC*, Kwon HJ, Jung BG, Alfajaro MM, Kim DS, Kim HJ, Hosmillo M, Park JG, Son KY, Park SI, Kang MI, Park SJ, Lee SW, Lee WS, Cho KO

*Co-first: rho-m@kribb.re.kr
Bioindustrial Process Research Center

The present study investigated the effects of azuki bean (*Vigna angularis*) extract (VAE) on the progress of atopic dermatitis (AD)-like skin lesions in NC/Nga mice induced by 1-chloro-2,4-dinitrobenzene. The efficacy of VAE in NC/Nga mice was determined by measuring gross and histological skin lesions, serum IgE levels, eosinophil ratio in peripheral leucocytes, and mRNA expression levels of interleukin (IL)-4, tumour necrosis factor (TNF)-α and interferon (IFN)-γ in splenocytes. Continuous ingestion of VAE inhibited the development of the AD-like skin lesions in a dose-dependent manner. In the VAE-treated mice, the numbers of mast cells in the skin, eosinophil ratio in peripheral leucocytes, relative mRNA expression of inflammatory cytokines in the spleen, and serum IgE levels were significantly reduced. Results suggest that VAE can inhibit the development of AD-like skin lesions in NC/Nga mice by regulating immune mediators and cells, and may be an effective alternative therapy for AD.

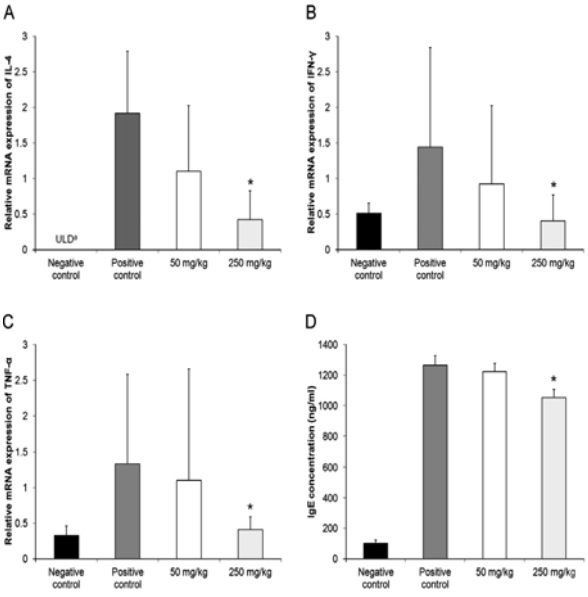

Keywords : Atopic dermatitis; Azuki bean; IgE; Immune cells; Inflammatory cytokines; NC/Nga mice

Article 336

Mass production of rubusoside using a novel stevioside-specific β-glucosidase from *Aspergillus aculeatus*

J Agric Food Chem. 60(24):6210-6.

Ko JA, Kim YM, Ryu YB, Jeong HJ, Park TS, Park SJ, Wee YJ, Kim JS, Kim D, Lee WS*

*Corresponding: wslee@kribb.re.kr
Infection Control Material Research Center

Rubusoside (R) is a natural sweetener and a solubilizing agent with antiangiogenic and antiallergic properties. However, currently, its production is quite expensive, and therefore, we have investigated nine commercially available glycosidases to optimize an economically viable R-production method. A stevioside (ST)-specific β-glucosidase (SSGase) was selected and purified 7-fold from *Aspergillus aculeatus* Viscozyme L by a two-step column chromatography procedure. The 79 kDa protein was stable from pH 3.0 to pH 7.0 at 50-60 °C. Hydrolysis of ST by SSGase produced R and steviol monoglucosyl ester as determined by (1)H and (13)C nuclear magnetic resonance (NMR). Importantly, SSGase showed higher activity toward ST than other β-linked glucobioses. The optimal conditions for R production were 280 μM ST and 16.6 μL of SSGase at pH 5.1 and 63 °C. This is the first discussion detailing the production of R by enzymatic hydrolysis of ST and is useful for the food additive and pharmaceutical industries.
PMID:22530920

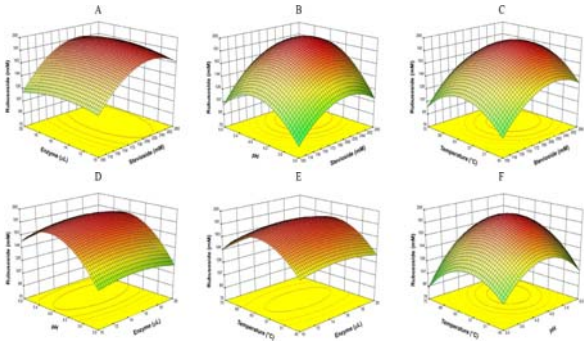

Keywords : *Aspergillus aculeatus*; β-glucosidase; Natural solubilizer; Rubusoside; Stevioside

Article 337

STAT3 protein interacts with Class O Forkhead transcription factors in the cytoplasm and regulates nuclear/cytoplasmic localization of FoxO1 and FoxO3a proteins in CD4(+) T cells

J Biol Chem. 287(36):30436-43.

Oh HM*, Yu CR, Dambuza I, Marrero B, Egwuagu CE

*First: ohhm@kribb.re.kr
Bioindustrial Process Research Center

An important feature of the adaptive immune response is its remarkable capacity to regulate the duration of inflammatory responses, and effector T cells have been shown to limit excessive immune responses by producing anti-inflammatory cytokines such as IL-10 and IL-27. However, how anti-inflammatory cytokines mediate their suppressive activities is not well understood. In this study, we show that STAT3 contributes to mechanisms that control the duration of T cell proliferation by regulating the subcellular location of FoxO1 and FoxO3a, two Class O Forkhead transcription factors that mediate lymphocyte quiescence and inhibit T cell activation. We show that active FoxO1 and FoxO3a reside exclusively in the nucleus of naïve T cells whereas inactive pFoxO1 and pFoxO3a were most abundant in activated T cells and sequestered in their cytoplasm in association with unphosphorylated STAT3 (U-STAT3) and 14-3-3. We further show that FoxO1/FoxO3a rapidly relocalized into the nucleus in response to pSTAT3 activation by IL-6 or IL-10, and the accumulation of FoxO1/FoxO3a in their nuclei coincided with increased expression of $p27^{Kip1}$ and $p21^{WAF1}$. STAT3 inhibitors completely abrogated cytokine-induced translocation of FoxO1/FoxO3a into the nucleus. In naïve or resting STAT3-deficient T cells, expression of pFoxO1/pFoxO3a was predominantly in the cytoplasm and correlated with defects in $p27^{Kip1}$ and $p21^{WAF1}$ expression, suggesting requirement of STAT3 for importation or retention of FoxO in the nucleus and attenuation of lymphocyte proliferation. Taken together, these results suggest that U-STAT3 collaborates with 14-3-3 to sequester pFoxO1/pFoxO3a in cytoplasm and thus prolong T cell activation, whereas pSTAT3 activation by anti-inflammatory cytokines would curtail the duration of TCR activation and re-establish lymphocyte quiescence by inducing nuclear localization of FoxO1/FoxO3a and FoxO-mediated expression of growth-inhibitory proteins.
PMID:22761423

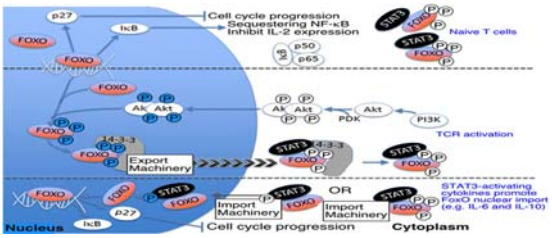

Keywords : Anti-inflammatory cytokines; Immune response; Inflammatory responses; STAT3 inhibitors

Article 338

Identification and characterization of a novel cold-adapted esterase from a metagenomic library of mountain soil

J Ind Microbiol Biotechnol. 39(5):681-9.

Ko KC, Rim SO, Han Y, Shin BS, Kim GJ, Choi JH*, Song JJ*

*Co-corresponding: jhchoi@kribb.re.kr jjsong@kribb.re.kr
Applied Microbiology Research Center

A novel lipolytic enzyme was isolated from a metagenomic library after demonstration of lipolytic activity on an LB agar plate containing 1% (w/v) tributyrin. A novel esterase gene (*estIM1*), encoding a lipolytic enzyme (EstIM1), was cloned using a shotgun method from a pFosEstIM1 clone of the metagenomic library, and the enzyme was characterized. The *estIM1* gene had an open reading frame (ORF) of 936 base pairs and encoded a protein of 311 amino acids with a molecular mass 34 kDa and a p*I* value of 4.32. The deduced amino acid sequence was 62% identical to that of an esterase from an uncultured bacterium (ABQ11271). The amino acid sequence indicated that EstIM1 was a member of the family IV of lipolytic enzymes, all of which contain a GDSAG motif shared with similar enzymes of lactic acid microorganisms. EstIM1 was active over a temperature range of 1-50°C, at alkaline pH. The activation energy for hydrolysis of *p*-nitrophenyl propionate was 1.04 kcal/mol, within a temperature range of 1-40°C. The activity of EstIM1 was about 60% of maximal even at 1°C, suggesting that EstIM1 is efficiently cold-adapted. Further characterization of this cold-adapted enzyme indicated that the esterase may be very valuable in industrial applications.

PMID: 22270890

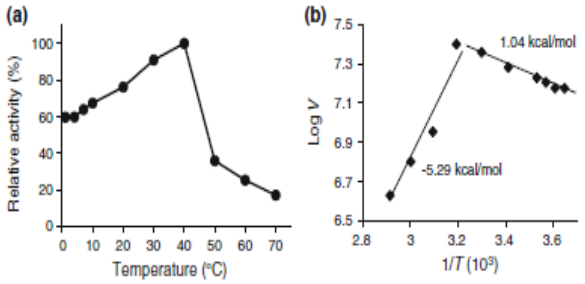

Keywords : Cloning; Cold-adapted esterase; Expression; Metagenomic library; Screening

Article 339

Large increase in *Leuconostoc citreum* KM20 dextransucrase activity achieved by changing the strain/inducer combination in an *E. coli* expression system

J Microbiol Biotechnol. 22(4):510-5.

Ko JA, Jeong HJ, Ryu YB, Park SJ, Wee YJ, Kim D, Kim YM*, Lee WS*

*Co-corresponding: u9897854@kribb.re.kr wslee@kribb.re.kr
Infection Control Material Research Center

A recombinant putative dextransucrase (DexT) was produced from *Leuconostoc citreum* KM20 as a 160 kDa protein, but its productivity was very low (264 U/l). For optimization, we examined enzyme activity in 7 *Escherichia coli* strains with inducer molecules such as lactose or IPTG. *E. coli* BL21-CodonPlus(DE3)-RIL exhibited the highest enzyme activity with lactose. Finally, DexT activity was remarkably increased by 12-fold under the optimized culture conditions of a cell density to start induction (OD_{600}) of 0.95, a lactose concentration of 7.5 mM, and an induction temperature of 17 degrees C. These results may effectively apply to the heterologous expression of other large DexT genes.

PMID: 22534298

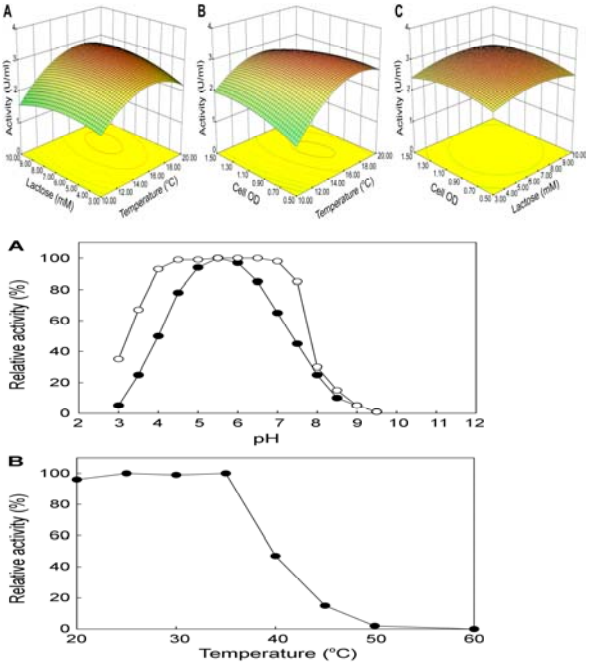

Keywords : Dextransucrase; Lactose; *Leuconostoc citreum* KM20; Optimization; Response surface methodology

Article 340

Biochemical characterization of thermophilic dextranase from a thermophilic bacterium, *Thermoanaerobacter pseudethanolicus*

J Microbiol Biotechnol. 22(5):637-41.

Park TS, Jeong HJ, Ko JA, Ryu YB, Park SJ, Kim D, Kim YM*, Lee WS*

*Co-corresponding: u9897854@kribb.re.kr wslee@kribb.re.kr
Infection Control Material Research Center

TPDex, a putative dextranase from *Thermoanaerobacter pseudethanolicus*, was purified as a single 70 kDa band of 7.37 U/mg. Its optimum pH was 5.2 and the enzyme was stable between pH 3.1 and 8.5 at 70 degrees C. A half-life comparison showed that TPDex was stable for 7.4 h at 70 degrees C, whereas *Chaetominum dextranase* (CEDex), currently used as a dextranase for sugar milling, was stable at 55 degrees C. TPDex showed broad dextranase activity regardless of dextran types, including dextran T2000, 742CB dextran, and alternan. TPDex showed the highest thermostability among the characterized dextranases, and may be a suitable enzyme for use in sugar manufacture without decreased temperature.

PMID:22561857

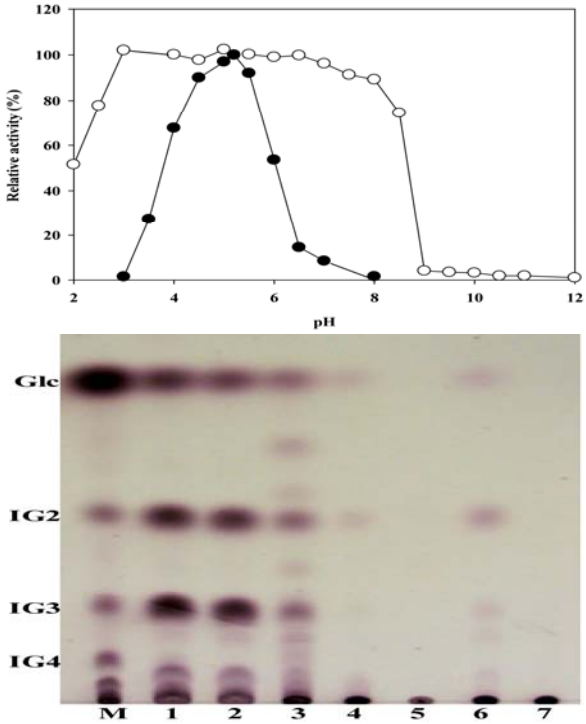

Keywords : Sugar processing; *Thermoanaereobacter*; Thermostability; Thermostable dextranase; TPDex

Article 341

Enzymatic synthesis of puerarin glucosides using *Leuconostoc* dextransucrase

J Microbiol Biotechnol. 22(9):1224-9.

Ko JA, Ryu YB, Park TS, Jeong HJ, Kim JH, Park SJ, Kim JS, Kim D, Kim YM*, Lee WS*

*Co-corresponding: u9897854@kribb.re.kr wslee@kribb.re.kr
Infection Control Material Research Center

Puerarin (P), an isoflavone derived from kudzu roots, has strong biological activities, but its bioavailability is often limited by its low water solubility. To increase its solubility, P was glucosylated by three dextransucrases from *Leuconostoc* or *Streptococcus* species. *Leuconostoc lactis* EG001 dextransucrase exhibited the highest productivity of puerarin glucosides (P-Gs) among the three tested enzymes, and it primarily produced two P-Gs with a 53% yield. Their structures were identified as alpha-D-glucosyl-(1-->6)-P (P-G) by using LC-MS or ^{1}H- or ^{13}C-NMR spectroscopies and alpha-D-isomaltosyl-(1-->6)-P (P-IG2) by using specific enzymatic hydrolysis, and their solubilities were 15- and 202-fold higher than that of P, respectively. P-G and P-IG2 are easily applicable in the food and pharmaceutical industries as alternative functional materials.

PMID: 22814496

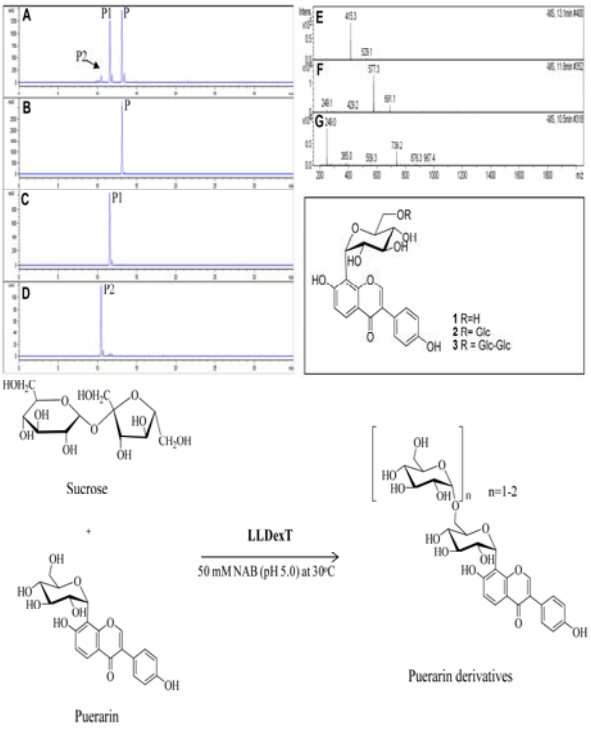

Keywords : Dextransucrase; Leuconostoc lactis; Puerarin; Transglucosylation; Water solubility

Article 342

Norkurarinol inhibits toll-like receptor 3 (TLR3)-mediated pro-inflammatory signaling pathway and rotavirus replication

J Pharmacol Sci. 118(2):161-70.

Oh HM, Lee SW, Park MH, Kim MH, Ryu YB, Kim MS, Kim HH, Park KH, Lee WS, Park SJ*, Rho MC*

*Co-corresponding: sjpark@kribb.re.kr rho-m@kribb.re.kr
Bioindustrial Process Research Center

This study examined the effect of norkurarinol on the toll-like receptor 3 (TLR3)-mediated signaling pathways and rotavirus replication. Norkurarinol, a lavandulylated flavanone, was isolated from the roots of *Sophora flavescens*, which has been shown to have anti-inflammatory activity. Norkurarinol suppressed the NF-κB and AP-1 inducible secreted embryonic alkaline phosphatase (SEAP) activity induced by poly(I:C), TLR3 ligand, in THP1-Blue-CD14 cells with IC_{50} values of 20.9 μM. Norkurarinol also significantly suppressed the mRNA expression of pro-inflammatory and adhesive molecules induced by poly(I:C) and rotavirus infection. Pretreatment of norkurarinol blocked the NF-κB and AP-1 signaling pathway and the phosphorylation of MAPKs induced by poly(I:C). On the other hand, norkurarinol increased the level of IRF3 phosphorylation and IFNβ expression in a dose-dependent manner. Moreover, norkurarinol inhibited the rotavirus-induced cytopathic effects. These results suggest that norkurarinol can modulate the TLR3-mediated inflammatory responses and rotavirus replication.

PMID:22293288

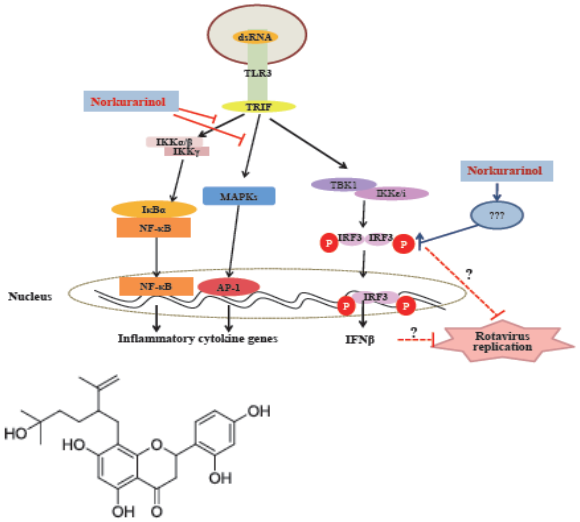

Keywords : dsRNA; Inflammatory response; Norkurarinol; Rotavirus; Toll-like receptor 3 (TLR3)

Article 343

Phenolic compounds isolated from *Psoralea corylifolia* inhibit IL-6-induced STAT3 activation

Planta Med. 78(9):903-6.

Lee SW, Yun BR, Kim MH, Park CS, Lee WS, Oh HM*, Rho MC*

*Co-corresponding: ohhm@kribb.re.kr rho-m@kribb.re.kr
Bioindustrial Process Research Center

Inhibiting interleukin-6 (IL-6) has been postulated as an effective therapy in the pathogenesis of several inflammatory diseases. In this study, seven flavonoids were isolated from the methanol extracts of *Psoralea corylifolia* by bioactivity-guided fractionation. The structures of bakuchiol (1), bavachinin (2), neobavaisoflavone (3), corylifol A (4), corylin (5), isobavachalcon (6), and bavachin (7) were determined by spectroscopic analysis (^{1}H-, ^{13}C- NMR and MS). We demonstrated that compounds 1-7 showed an inhibitory effect on IL-6-induced STAT3 promoter activity in Hep3B cells with IC_{50} values of 4.57 ± 0.45, 3.02 ± 0.53, 2.77 ± 0.02, 0.81 ± 0.15, 1.37 ± 0.45, 2.45 ± 0.13, and 4.89 ± 0.05 μM, respectively. These compounds also inhibited STAT3 phosphorylation induced by IL-6 in Hep3B cells. Overall, several flavonoids from *P. corylifolia* might be useful remedies for treating inflammatory diseases by inhibiting IL-6-induced STAT3 activation and phosphorylation.

PMID:22573369

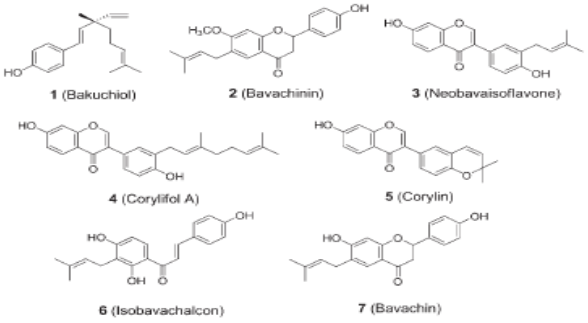

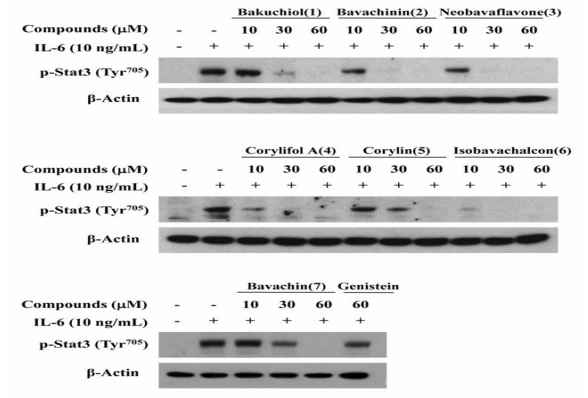

Keywords : Anti-inflammatory; Fabaceae; Flavonoids; IL-6; *Psoralea corylifolia* L.; STAT3

Article 344

Enhancement of ethanol production from glycerol in a *Klebsiella pneumoniae* mutant strain by the inactivation of lactate dehydrogenase

Process Biochem. 47(1):156-9.

Oh BR, Seo JW, Heo SY, Hong WK, Luo LH, Kim S, Kwon O, Sohn JH, Joe MH, Park DH, Kim CH*

*Corresponding: kim3641@kribb.re.kr
Applied Microbiology Research Center

Previously, using γ-irradiation treatment, we isolated a mutant strain of *Klebsiella pneumoniae* (named GEM167) that showed high-level ethanol production from glycerol. In the present study, in an effort to enhance ethanol production, we used a deletion of the lactate dehydrogenase gene to engineer a mutant strain incapable of lactate synthesis. In the Δ*ldhA* mutant of GEM167, the production of ethanol was significantly increased from 21.5 g/l to 28.9 g/l and from 0.93 g/(l h) to 1.2 g/(l h). Introduction of the *Zymomonas mobilis pdc* and *adhII* genes encoding pyruvate decarboxylase and aldehyde dehydrogenase, respectively, further improved the ethanol production level from glycerol to 31.0 g/l; this is the highest level reported to date.

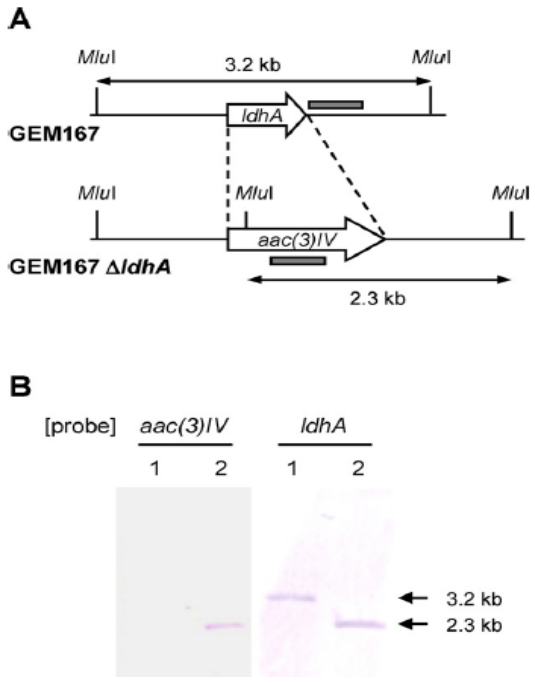

Keywords : Ethanol; Glycerol; *Klebsiella pneumoniae*; Lactate dehydrogenase genes; Mutant strain

Article 345

A nanosized Ag-silica hybrid complex prepared by γ-irradiation activates the defense response in *Arabidopsis*

Radiation Phys Chem. 81(2):180-4.

Chu H, Kim HJ, Kim J, Kim MS, Yoon BD, Park HJ, Kim CY*

*Corresponding: kimcy@kribb.re.kr
Infection Control Material Research Center

Silver nanoparticles have antimicrobial activity against many pathogenic microbes. Here, the preparation of a nanosized Ag-silica hybrid complex (NSS) prepared by γ-irradiation is described. The effects of both NSS and reduced Ag nanoparticles (Ag^0) on the growth of the model plant *Arabidopsis thaliana* were tested. The application of 1-10ppm NSS complex improved *Arabidopsis* growth in soil, whereas 100ppm NSS resulted in weakly curled leaves. In addition, supplementation of Murashige and Skoog (MS) growth medium with 1ppm NSS promoted the root growth of *Arabidopsis* seedlings, but root growth was inhibited by supplementation with 10ppm NSS. To investigate whether the NSS complex could induce plant defense responses, the expression of pathogenesis-related (*PR*) genes that are implicated in systemic acquired resistance (SAR) in *Arabidopsis* plants was examined. *PR1, PR2* and *PR5* were significantly up-regulated by each application of 10ppm NSS complex or Ag^0 to the rosette leaves. Furthermore, pretreatment with the NSS complex induced more pathogen resistance to the virulent pathogen *Pseudomonas syringae* pv. *tomato* DC3000 (*Pst*) compared to water treatment in *Arabidopsis* plants.

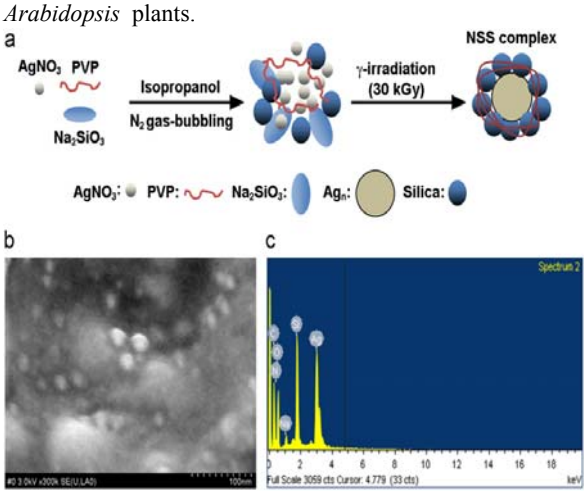

Keywords : *Arabidopsis*; Defense response; γ-irradiation; Pathogenesis-related genes; Silver nanoparticles; Systemic acquired resistance

Article 346

Antiviral activity of *Alpinia katsumadai* extracts against rotaviruses

Res Vet Sci. 92(2):320-3.

Kim HH, Kwon HJ, Ryu YB, Chang JS, Cho KO, Hosmillo MD, Rho MC, Park SJ*, Lee WS*

*Co-corresponding: sjpark@kribb.re.kr wslee@kribb.re.kr
Infection Control Material Research Center

In vitro anti-rotavirus activity of *Alpinia katsumadai* (AK) extracts were evaluated against bovine G8P[7] and porcine G5P[7] rotaviruses in two different assay strategies, a mixed treatment assay and a post treatment assay. In the mixed treatment assay, six AK extracts [AK-1 (EtOH extract), AK-3 (H_2O layer), AK-5 (40% methanol fraction), and AK-9-11 (H_2O extract, polysaccharide fraction, supernatant fraction)] exhibited inhibitory activities against G5P[7] rotavirus with the EC_{50} values ranging from 0.7±0.4 to 33.7±6.5 μg/mL. Extracts AK-1, AK-3, and AK-5 inhibited rotavirus infection against G8P[7] rotavirus, the with EC_{50} values of 8.4±2.2 μg/mL, 6.5±0.8 μg/mL and 8.4±5.0 μg/mL, respectively. By hemagglutination inhibition (HI) assay, six AK extracts completely inhibited viral adsorption onto human RBCs in both strains of rotaviruses at less than 11 μg/mL. However, in the post treatment assay, there was no anti activity shown against both strains of rotaviruses. As a result, six AK extracts were attributed mainly to having a strong interaction with hemagglutinin protein on the outer surface of rotavirus, resulting to blockage of viral adsorption.

PMID:21196021

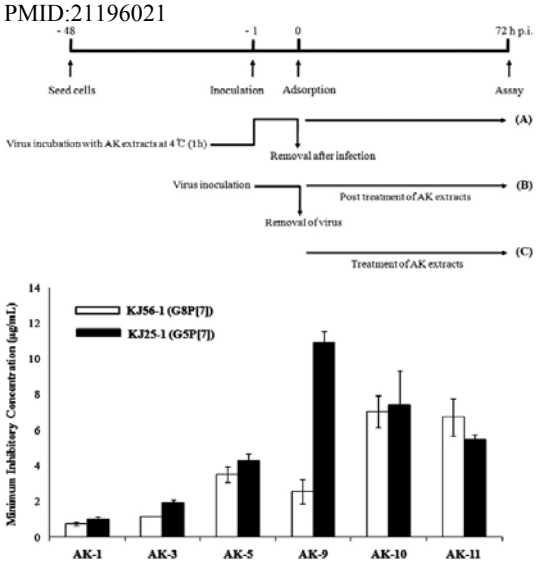

Keywords : *Alpinia katsumadai*; AK extracts; Anti-rotavirus; Hemagglutination inhibition; Viral adsorption

Article 347

Detection and molecular characterization of porcine type 3 orthoreoviruses circulating in South Korea

Vet Microbiol. 157(3-4):456-63.

Kwon HJ, Kim HH, Kim HJ, Park JG, Son KY, Jung J, Lee WS, Cho KO, Park SJ*, Kang MI

*Co-corresponding: sjpark@kribb.re.kr
Infection Control Material Research Center

Orthoreoviruses infect virtually all mammalian species, causing systemic infections including mild gastrointestinal and respiratory illnesses. However, little is known about the prevalence or genetic diversity of porcine orthoreoviruses in South Korea. We examined 237 diarrheic fecal samples collected from 78 pig farms around the country. RT-PCR utilizing primers specific for the L1 gene of mammalian orthoreoviruses showed that 45 (19.0%) samples were positive. The 10 strains isolated from orthoreovirus-positive samples formed typical perinuclear cytoplasmic inclusion bodies and had an atypical hemagglutination pattern; these are characteristics of type 3 orthoreovirus. Phylogenetic analysis of the S1 gene in these 10 Korean and other strains showed that type 3 orthoreoviruses could be divided into four lineages; the 10 Korean strains were included in porcine lineage IV, along with T3/porcine/Sichuan/2006. Sequence analysis showed that strains in lineage IV had nucleotide identities of 97.0-98.1% and deduced amino acid identities of 96.4-98.2%. Sequence analysis of the σ1 protein, a viral attachment protein, revealed that the amino acid sequences associated with neurotropism (amino acids 198-204, 249I, 350D, and 419E) were highly conserved among the Korean strains, confirming that neural tropism was present. In conclusion, our findings suggest that porcine orthoreovirus infections are endemic in pig farms in South Korea and that the 10 novel Korean porcine orthoreoviruses belong to porcine lineage IV of type 3 orthoreovirus. In addition, sequence analysis of S1 genes encoding the σ1 protein showed that the 9 of 10 Korean porcine orthoreoviruses exhibited neural tropism.

PMID:22265235

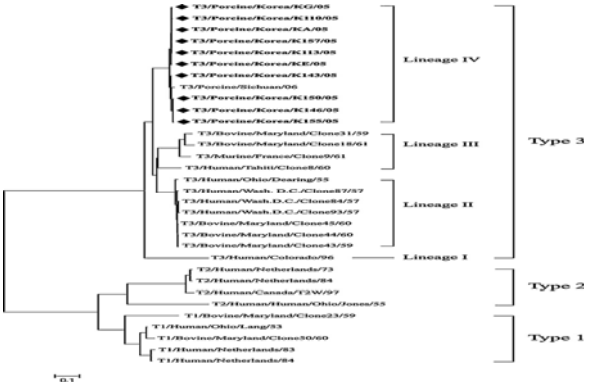

Keywords : Genetic diversity; Orthoreovirus; Phylogenetic analysis; Porcine; Prevalence; RT-PCR


KRIBB
www.kribb.re.kr

2012
KRIBB Article Abstracts : First or corresponding articles indexed in SCIE, Scopus, and PubMed

Indexes

Korea Research Institute of Bioscience and Biotechnology

Author Index

Journal Index

Keyword Index

한국생명공학연구원
Korea Research Institute of Bioscience and Biotechnology

305-806 대전광역시 유성구 과학로 125
Tel. 042)860-4114 Fax. 042)861-1759 http://www.kribb.re.kr